

# **Experimental Investigation for Quality Evaluation and Concurrent Design Principles Applied to CNC Turning**

## **THESIS**

Submitted in partial fulfillment  
of the requirements for the degree of  
**DOCTOR OF PHILOSOPHY**

by

**C PHANEENDRA KIRAN**

Under the Supervision of  
**Dr. Shibu Clement**



**BIRLA INSTITUTE OF TECHNOLOGY AND SCIENCE  
PILANI (RAJASTHAN) INDIA**

**2012**

**BIRLA INSTITUTE OF TECHNOLOGY AND SCIENCE  
PILANI (RAJASTHAN)**

**CERTIFICATE**

This is to certify that the thesis entitled “**Experimental Investigation for Quality Evaluation and Concurrent Design Principles Applied to CNC Turning**” and submitted by **C Phaneendra Kiran** ID No. **2004PHXF449G** for award of Ph. D. Degree of the Institute embodies original work done by him/her under my supervision.

Signature in full of the Supervisor: \_\_\_\_\_

Name in capital block letters: **Dr. SHIBU CLEMENT**

Designation: **Assistant Professor  
(Mechanical Engineering)**

Date:

## **Acknowledgement**

I wish to record my sincere gratitude to Dr. Shibu Clement, my research supervisor, for his role in shaping my thought process. His knowledge, keen interest, constant encouragement, help, constructive criticism and endless patience have contributed greatly to making this doctoral study a successful and enjoyable journey. Words would not suffice to express my deep gratitude and respect to Prof. V.P. Agrawal for not only guiding me on the thesis, but also for sharing with me some precious pearls of wisdom on career-related aspects and life in general. I hold close to my heart several of his statements and analogies which I will cherish always.

I am grateful to Prof. B. N. Jain, Vice Chancellor, Prof. L.K. Maheswari, Ex-Vice Chancellor and Advisor to Chancellor, and Prof. A. K. Das, Dean, Research and Consultancy Division, BITS Pilani, for granting me an opportunity to conduct research at this renowned institute and also for assuring the availability of necessary infrastructure and facilities to carry out my work. I wish to offer my sincere thanks to Prof. K. E. Raman, Director, BITS-Pilani, K. K. Birla Goa Campus, for his constant encouragement and support. Sincere thanks are also due to Late Prof. T. C. Goel, former Director, BITS-Pilani, K. K. Birla Goa Campus, for his valuable motivation and for inspiring me to work toward my PhD degree.

Special thanks are due to Dr. P.M. Singru, Head, Department of Mechanical Engineering, BITS-Pilani, K. K. Birla Goa Campus, for his encouragement and for sharing with me thoughts on matters beyond my imagination. My special thanks to Prof. B.J.C. Babu and Dr. D.M. Kulkarni for their role in shaping this work. I would also like to fondly acknowledge their generosity in sharing with me their ideas and inputs on issues beyond the academic world and for their company on so many occasions, all of which have gone a long way in forging a great working relationship. I record my gratitude to Dr. S.D. Manjare, Faculty In-charge, Research and Consultancy and Education Development Division, BITS Pilani- K. K. Birla Goa Campus, for his valuable inputs on this research and dissertation.

Warm thanks are also due to Prof. A.P. Koley, Dr. Neena Goveas, Prof. Suresh Ramaswamy, Prof. Dibakar Chakraborty for their continuous encouragement, support and also for taking personal interest in making life more comfortable and enjoyable.

I am thankful to Savio Cavalho (Director) and Jose Maria (senior engineer) TURBOCAM International, Goa, India for providing the turbine blade material samples.

I am also thankful to the Director, NCAOR, Goa, and Prof. Gauthama, IIT, Kanpur for permission to use the SEM/EDX facilities located in their campus.

This work is incomplete without acknowledging Dr. Saby John, for spending her valuable time in proof reading the thesis.

I wish to express my heart-felt gratitude to my “peer-mentors” — Dr. Abhishek Kumar and Dr. Sachin Waigoankar, who has spent long hours listening to and helping me sort through, the numerous ideas that coursed through my mind while working on this thesis and making valuable comments.

I wish to thank Mr. G. J. Desai and Mr. Vijay Suryavamshi, workshop superintendent, for their immense and continuous help in words and deeds, especially during course of experimental work. Special thanks are due to Aneet S. Raj, research practice student, who helped me in preparing the specimens for micro structural analysis. My sincere gratitude to Anoop, Prasad, Vrishabh, Viraj, Abhijeet and all the workshop staff of our institute who helped me a lot during the experimental work.

The role of my friends in cheering me on and helping me face life with equanimity can never be overstated. Varinder, Vikas, Mohanty, A.C. Kulkarni, Kiran Mali, Prasad, P. V. Rao, Raghu, Sreedhar, Ramkumar, Dr. Saroj Baral, Dr. Ranjan Dey and Dr. Hemanth have provided more than their share of emotional support.

My wife Sravani Prabha and son Tanmay have been instrumental in motivating me from time to time. I am indebted to them for giving me a happy and joyous environment at home and for their silent sacrifices.

I would forever be indebted to my parents for their constant love, confidence, prayers, strong support and good wishes. Also, thanks are due to my sister, brother, brother-in-law whose blessings and good wishes were always with me. I owe it all to them.

**C Phaneendra Kiran**

## **ABSTRACT**

The sophistication which has more recently been possible through increasingly powerful processing devices and heightened software skills has resulted in an increasing trend towards the development of embedded CNC machines involving a combination of mechanics, electronics, and software. During the initial stages of design it is essential to consider quality and x-abilities related issues in evaluation of different materials for machining.

In this work, quality, performance, decision making, and concurrent engineering based mathematical tools in modeling, analysis, evaluation, ranking and selection of a material for CNC turning were developed. The focus was on quality, x-abilities and optimal selection related issues, which would be of great value for the manufacturing industry to thrive in the current, highly competitive market scenario. The experimental investigation was carried out to address the quality issues related to CNC turning for steam turbine blade materials.

A new direction for quality modeling and analysis of a CNC turning center was proposed. The quality of a machined material on a CNC turning center is decided by its conformance to requirements. The voice of the customer should be translated to technical requirements and these should be satisfied/met at different levels i.e. subsystem, sub-subsystem up to component level. In the process of implementing quality at subsystem level, quality interactions among the sub systems are also important. A mathematical model which considers subsystems along with their interactions simultaneously was proposed. A quality graph for a CNC turning center was developed and was translated into quality matrix and finally a variable permanent function was obtained. To evaluate the quality interactions between the subsystems, experimental data was considered. A new performance measure, quality index, was defined, which would be useful for quality based evaluation and selection of CNC turning center. A step-by-step procedure useful for the designer as well as manufacturing engineers during conceptual and manufacturing stages of CNC turning center was proposed. The implementation of the proposed methodology was demonstrated.

In selection of a material, a designer should consider product lifecycle issues as well as design and manufacturing strategies simultaneously at conceptual design stage without missing

any of the information. The proposed methodology concurrently considered all the x-abilities/design aspects along with interactions without missing any information and hence would lead to a high quality product. A methodology which amalgamates concurrent design concepts, graph theory, matrix algebra and permanent multinomial was proposed. Eight x-abilities namely miniaturization, intelligence, integration, environment, quality, reliability, manufacturing and assembly for concurrent design and decision making of a material for CNC turning were identified. A colored graph useful for visual analysis was proposed. The derived concurrent design index was useful for researcher and designer in evaluating the alternatives. The proposed step-by-step procedure would be useful for developing a new algorithm for software coding. The uniqueness of this approach is that it considers design aspects and interactions between the design aspects simultaneously. The proposed methodology was applied to concurrent evaluation of three turbine blade materials ST 12TE, ST T17/13W and ST17-PH for CNC turning operation.

A MADM(Multi Attribute Decision Making)- TOPSIS (Technique for Order Preference by Similarity to Ideal Solution) based methodology for evaluation, ranking and selection of a material for CNC turning was developed. An exhaustive list of attributes which influence the structure and performance of a material were identified. An attribute based coding scheme for identification and differentiation of materials was developed. A three stage selection procedure was proposed for optimal selection of a material for CNC turning. In the first stage, large numbers of available materials were converged to a manageable number using elimination search. In the second stage, a matrix for storing all the information pertaining to a material was proposed. In the third stage, all the materials were ranked according to the Euclidian distance from best possible and worst solutions. Two visual methods namely linear graph and spider chart were proposed for ranking of materials for CNC turning. Evaluation, ranking and selection of a material suitable for turbine blade for CNC turning among the five materials (9SMnPb28k,42CrMo steel, ST 12TE, ST T17/13W and ST17-PH) was demonstrated. This methodology would be useful for industries in selection of an optimal material for the given machining operation.

An experimental investigation for surface quality evaluation of three types of turbine blade materials (ST 12TE, ST 17-4PH and ST17/13W) with different combination of cutting parameters in a CNC turning process was carried out. The central composite design was used for the design of experiments and 20 experiments for each material were designed and conducted.

The trends in the responses were analyzed and interpreted using metallurgical reasoning, ANNOVA and different graphical tools. The regression equations between response and input variables were formulated and verified by conducting the confirmatory experiments. This investigation showed that ST 12TE had the best surface quality and ST 17-4PH had the highest surface roughness. These results were in good agreement with the results obtained using MADM and Design for X concepts.

Finally, it was concluded that the proposed methodology for quality and concurrent engineering based modeling is a virtual integration of design, manufacturing and optimal selection of materials for CNC turning in an interactive manner at conceptual stage or product development stage and would lead to the development of alternative feasible solutions. The proposed methodologies would be useful to the end customer in optimal selection from a set of alternative materials available.

# Table of Contents

Acknowledgement .....	i
Abstract.....	iii
Table of contents.....	vi
List of Tables .....	x
List of Figures.....	xii
List of Acronyms .....	xvi
<b>Chapter 1 Introduction.....</b>	<b>1</b>
1.1    CNC turning .....	1
1.2    Turbine blade materials and manufacturing methods .....	2
1.3    Measurement of quality for CNC turning .....	3
1.4    Need for an integrated approach .....	4
1.5    Scope and objectives of present work .....	5
1.6    Organization of thesis.....	6
<b>Chapter 2 Literature Review .....</b>	<b>8</b>
2.1    Classification on the basis of identified categories .....	8
2.1.1    CNC turning to meet quality features .....	8
2.1.2    CNC machining for turbine blade materials .....	11
2.1.3    Metallurgical changes during machining .....	13
2.1.4    Concurrent engineering and X-abilities .....	16
2.2.5    Graph theory and its applications.....	20
2.1.6    MADM-TOPSIS approach .....	21
2.1.7    Design of experiments and CNC turning process .....	22
2.2    Analysis and gaps in existing literature.....	26
<b>Chapter 3 Quality modeling and analysis of CNC turning.....</b>	<b>29</b>
3.1    Introduction .....	29
3.2    Identification of quality subsystems and interactions .....	29



3.3	Quality Digraph (QD) .....	31
3.4	Matrix representation of QD .....	34
3.5	Variable Permanent Quality Function (VPQF).....	34
3.6	CNC machine quality index (QI) .....	36
3.7	Quality analysis .....	37
3.8	Coefficient of similarity and dissimilarity .....	40
3.9	Step-by-step procedure.....	43
3.10	Experimental evaluation of interactions.....	43
3.11	Summary .....	57
<b>Chapter 4 Design for x-abilities of CNC turning .....</b>		<b>59</b>
4.1	Introduction .....	59
4.2	Design for X aspects .....	59
4.2.1	Identification of x-abilities.....	59
4.2.2	Graph theory based design methodology .....	65
4.2.2.1	Concurrent design digraph (CDD) .....	66
4.2.2.2	Adjacency matrix.....	68
4.2.2.3	Concurrent design matrix .....	69
4.2.2.4	Concurrent Design Multinomial (CDM) .....	70
4.2.2.5	Evaluation of nodes ( $N_i$ ) and interactions ( $e_{ij}$ ).....	77
4.3	Evaluation of CDI for CNC turning operation.....	78
4.4	Summary .....	88
<b>Chapter 5 Material selection for CNC turning using MADM approach. ....</b>		<b>89</b>
5.1	Introduction .....	89
5.2	Identification of attributes .....	89
5.3	Coding Scheme .....	91
5.4	Three-stage selection procedure.....	94
5.4.1	Stage 1- Elimination search .....	95
5.4.2	Stage 2- MADM-TOPSIS based evaluation and ranking procedure .....	96

5.4.3	Stage 3- Decision making .....	101
5.5	Graphical methods.....	102
5.5.1	Linear graph representation .....	102
5.5.2	Spider diagram representation .....	103
5.5.3	Graphical representation of bench mark material .....	104
5.5.4	Coefficient of similarity (COS).....	104
5.6	Step-by-step procedure.....	105
5.7	Evaluation of Turbine blade materials for CNC turning.....	105
5.8	Summary .....	112
<b>Chapter 6 Experimental investigation for surface quality of turbine blade materials for CNC turning .....</b>		<b>114</b>
6.1	Introduction .....	114
6.1.1	Plan of experiments.....	115
6.1.2	Materials used .....	116
6.1.3	Cutting inserts and holder .....	118
6.1.4	Experimental setup and measuring instruments.....	119
6.2	Results and discussion.....	120
6.2.1	ANOVA .....	129
6.2.2	Contour plots and response surface graphs .....	135
6.2.3	Interaction plots.....	139
6.2.4	Confirmatory experiments .....	142
6.3	Summary .....	142
<b>Chapter 7 Conclusions.....</b>		<b>144</b>
7.1	Conclusions .....	144
7.2	Recommendations for the future work.....	148
References.....		149
Appendix A.....		170
Appendix B .....		172
Appendix C.....		174

Publication based on Present work .....	193
Brief Biography of the Candidate .....	194
Brief Biography of the Supervisor .....	194

## List of Tables

Table 2. 1 Tool condition monitoring sensing methods .....	10
Table 2. 2 Literature on DOE based CNC turning process optimization .....	25
Table 3. 1 Distribution of terms in VPQF.....	38
Table 3. 2 Factorial design input parameters and the dynamic response of accelerometer in cutting direction (Chelladurai et al, 2008) .....	45
Table 3. 3 Factorial design input parameters and the dynamic response of accelerometer in feed direction (Chelladurai et al, 2008) .....	46
Table 3. 4 Factorial design input parameters and the dynamic response of strain gauge bridge (Chelladurai et al, 2008) .....	47
Table 3. 5 ANOVA for effect of machining parameters w.r.t. dynamic response of accelerometer in cutting direction .....	48
Table 3. 6 ANOVA for effect of machining parameters w.r.t. dynamic response of accelerometer in feed direction .....	48
Table 3. 7 ANOVA for effect of machining parameters w.r.t. dynamic response of strain gauge bridge .....	49
Table 3. 8 Values of FR and DOC for calculating interaction effect .....	52
Table 3. 9 Values of FR and DOC for calculating interaction effect .....	53
Table 3. 10 Interaction effect for different sensor outputs.....	53
Table 3. 11 Values range for quantifiable quality factors.....	54
Table 3. 12 Values range for unquantifiable quality factors.....	54
Table 3. 13 Numerical quality values of a CNC turning center.....	55
Table 4. 1 Critical design parameters for concurrent design of a MPS .....	63

Table 4. 2 Normalization of cutting parameters for different materials .....	80
Table 4. 3 Different costs considered for each material in manufacturing of turbine blade.....	84
Table 4. 4 CDI indices of the considered materials .....	87
Table 5. 1 Example coding scheme for machining of ST-174PH on CNC machine.....	92
Table 5. 2 Compact coding scheme for machining of ST-174PH on CNC machine .....	95
Table 5. 3 Pertinent attributes of turning operation and alternatives for the turbine blade material .....	106
Table 5. 4 Ranking of alternative materials for CNC turning process.....	112
Table 6. 1 Material properties of commercially available turbine blade materials .....	114
Table 6. 2 Design layout for the experiments .....	116
Table 6. 3 Chemical composition in % weight of the materials .....	116
Table 6. 4 SEM/EDS weight and atomic percentages at the selected location of the specimen	117
Table 6. 5 Mechanical properties of the turbine blade materials .....	118
Table 6. 6 Geometry of insert and the tool holder .....	118
Table 6. 7 Levels of independent variables .....	119
Table 6. 8 Experimental results Ra in ( $\mu\text{m}$ ).....	127
Table 6. 9 Analysis of Variance for the regression model of ST 17-4PH .....	129
Table 6. 10 Analysis of Variance for the regression model of ST 12TE.....	130
Table 6. 11 Analysis of Variance for the regression model of ST T17/13W .....	130
Table 6. 12 ANOVA for the coefficients in regression equation .....	131
Table 6. 13 Confirmatory experiment results for all the three materials .....	142

## List of Figures

Fig 1. 1 Typical HP and LP turbine rotor (James et al., 2010) .....	2
Fig 1. 2 Typical compression blade of HP turbine ( <a href="http://www.cblade.it/steam-turbine-blades.html">http://www.cblade.it/steam-turbine-blades.html</a> ).....	3
Fig 2. 1 Images of a rhomboidic HP blade from the 3DS TM series with a total length of $\approx 100$ mm (left) and an LP blade with integral shroud and snubber made of titanium with a total length of $\approx 1200$ mm (right) Ritcher (2003) .....	12
Fig 2. 2 Surface and subsurface integrity after machining Brinksmeier eta al (2004) .....	15
Fig 3. 1 General framework for tool condition monitoring .....	30
Fig 3. 2 Quality hierarchical tree of CNC turning centre .....	31
Fig 3. 3 Quality interaction block diagram of CNC turning centre .....	31
Fig 3. 4 Quality digraph of CNC turning centre .....	32
Fig 3. 5 Analysis of grouping of terms in VPQF .....	39
Fig 3. 6 Comparison of dyads and loops in VPQF of six and five subsystem CNC machines ....	40
Fig 3. 7 Step-by-step procedure for quality modeling of a CNC machine .....	44
Fig 3. 8 Interaction plot of machining parameters for the response of accelerometer mounted in cutting direction .....	50
Fig 3. 9 Interaction plot of machining parameters for the response of accelerometer mounted in feed direction .....	51
Fig 3. 10 Interaction plot of machining parameters for the response of strain gauge bridge .....	51
Fig 3. 11 Control panel of GILDMEISTER CTX 400 Serie2 lathe .....	57
Fig 4. 1 Concurrent engineering design cycle of a MPS .....	67
Fig 4. 2 Colored concurrent design graph of a MPS.....	68
Fig 4. 3 Graphical representation of first group of terms in CDM .....	72
Fig 4. 4 Graphical representation of third group of terms in CDM .....	73
Fig 4. 5 Graphical representation of fourth group of terms in CDM.....	73
Fig 4. 6 Graphical representation of fifth group of terms in CDM.....	74

Fig 4. 7 Graphical representation of sixth group of terms in CDM.....	74
Fig 4. 8 Graphical representation of seventh group of terms in CDM .....	75
Fig 4. 9 Graphical representation of eighth group of terms in CDM.....	76
Fig 4. 10 Graphical representation of ninth group of terms in CDM .....	77
Fig 4. 11 Turbine blades manufactured at Turbocam, Goa (ref: <a href="http://www.turbocam.com/blades">http://www.turbocam.com/blades</a> ) .....	78
Fig 5. 1 Two-attribute representation of an alternative in two dimensional space .....	101
Fig 5. 2 Line graph for 'n' number of attributes .....	103
Fig 5. 3 Spider diagram for 'n' attributes.....	103
Fig 5. 4 Line graph and area plot for the weighted normalized matrix .....	110
Fig 5. 5 Spider diagram polygon for weighted normalized matrix.....	111
Fig 6. 1 SEM/EDS spectrum results for the material ST 17 4-PH .....	117
Fig 6. 2 Experimental setup and the flow of work.....	120
Fig 6. 3 Trend in results of different material.....	121
Fig 6. 4 Shaeffler diagram- modified (after Schneider (1960)).....	122
Fig 6. 5 Favorable and unfavorable conditions for sacrificial film formation (Gwidon and Andrew, 2005) .....	123
Fig 6. 6 The relationship between corrosivity and lubricating effect of some EP lubricants (Heshmat and Dill, 1992).....	124
Fig 6. 7 Photograph of indentation observed under microscope for the material ST 17-4PH...	124
Fig 6. 8 SEM microstructure of material ST 17-4PH.....	125
Fig 6. 9 SEM microstructure of material ST 12TE.....	126
Fig 6. 10 SEM microstructure of material ST 17/13W.....	126
Fig 6. 11 Normal probability plot for the Ra response of St 17-4PH material .....	132
Fig 6. 12 Residual vs Fits for the Response Ra of St 17-4PH .....	133
Fig 6. 13 Normal probability plot for the Ra response of material ST 12TE .....	133

Fig 6. 14 Residual plot for the Ra response of material ST 12TE.....	134
Fig 6. 15 Normal probability plot for the Ra response of material ST T17/13W.....	134
Fig 6. 16 Residual plot for the Ra response of material ST T17/13W.....	135
Fig 6. 17 Contour and 3D surface graphs of speed and feed vs surface roughness for the materials.....	137
Fig 6. 18 Contour and 3D surface graphs of feed and depth of cut vs surface roughness for the materials.....	138
Fig 6. 19 Contour and 3D surface graphs of speed and depth of cut vs surface roughness for the materials.....	139
Fig 6. 20 Interaction effect of cutting parameters on Ra for the material ST 17-4PH.....	140
Fig 6. 21 Interaction effect of cutting parameters on Ra for the material ST 12TE.....	141
Fig 6. 22 Interaction effect of cutting parameters on Ra for the material ST T17/13W.....	141
Fig 7. 1 Detailed step-by-step procedure.....	147



## List of Acronyms

CNC	Computer Numerical Control
ANOVA	Analysis of Variance
ATC	Automatic Tool Changer
CCD	Central Composite Design
CDI	Concurrent Design Index
CDM	Concurrent Design Multinomial
CDVPM	Concurrent Design Variable Permanent Matrix
COS	Coefficient of Similarity
CS	Cutting Speed
DF	Degrees of Freedom
DFA	Design for Assembly
DFC	Design for Cost
DFE	Design for Environment
DFIN	Design for Integration
DFINCE	Design for Intelligence
DFM	Design for Manufacturing
DFMI	Design for Miniaturization
DFQ	Design for Quality
DFR	Design for Reliability
DFX	Design For X abilities
DOC	Depth of Cut
EDX	Energy Dispersive X-ray spectroscopy
FPGA	Field Programmable Gate Array
FR	Feed Rate
FW	Flank Wear
HP	High Pressure
HRC	Rockwell C Hardness
IT	Information Technology
LP	Low Pressure
MADM	Multi Attribute Decision Making
MRR	Material Removal Rate
PC	Power Consumption
PLC	Programmable Logic Controller
QD	Quality Digraph
QI	Quality Index
RSM	Response Surface Method
SEM	Scanning Electron Microscope
SWOT	Strengths Weakness Opportunities Threats
TC	Tool Cost

TCM	Tool Condition Monitoring
TOPSIS	Technique for Order Preference by Similarity to Ideal Solution
VPQF	Variable Permanent Quality Function
VPQM	Variable Permanent Quality Matrix

# CHAPTER 1

## INTRODUCTION

### 1.1 CNC turning

CNC turning is an important and widely used machining processes in engineering industries. With the rapid advancement of information technology associated with NC technology, the manufacturing environment has changed significantly since the last decade. High speed machining, high precision machining, and multi-axis machining have extensively enhanced the productivity and quality of manufacturing. Furthermore, advanced internet technology has introduced a new paradigm of e-manufacturing, in which the so-called DABA (Design-Anywhere-Build-Anywhere) system can be realized via the collaborated scheme of a distributed manufacturing system (Suh et al, 2006).

Turning involves the use of a tool to remove material from the surface of a less resistant body, through relative movement and application of force. The material removed, called chip, slides on the face of tool, known as tool rake face, subjecting it to high normal and shear stresses and, moreover, to a high coefficient of friction during chip formation (Shaw et al, 1951). Most of the mechanical energy used in forming the chip is released as heat, which generates high temperatures in the cutting region. The higher the tool temperature, the faster it wears. The main goal of using cutting fluids in machining processes is the reduction of the cutting temperature either through lubrication, reducing friction wear, or through cooling by conduction of heat. However, the advantages of using cutting fluids have been questioned lately, due to the several negative effects they cause (Aggarwal et al, 2008). When inappropriately handled, cutting fluids may pollute oil and water resources, causing serious damage to the environment which is of grave concern. Therefore, the handling and disposal of cutting fluids must conform to the rigid rules laid down by regulatory bodies governing environmental protection. In turning, the cutting conditions such as cutting speed, feed rate, depth of cut, features of tools and work piece materials, affect process efficiency and performance characteristics (Ahinlan et al, 2012).

## 1.2 Turbine blade materials and manufacturing methods

Power generation in thermal stations relies on large steam turbines; a typical high pressure (HP) and low pressure (LP) rotor set is shown in Fig 2.1. Blades are the heart of a steam turbine, as they are the principal elements that convert the thermal energy into kinetic energy. The efficiency and reliability of a turbine depend on the proper design of the blades. In the HP turbine, the blades are short and operate under the maximum steam temperature (Llewellyn and Hudd, 2004), i.e. 565°C. The creep strength of 12% Cr steels is not adequate to operate at such temperatures and therefore the first few rows of blades at the HP inlet are generally manufactured from Nimonic 80A. In the LP turbine, the blades are long, and in large turbines the exhaust blades can exceed a length of one meter. Such blades generate high centrifugal forces. The 12% Cr steels are not strong enough to cope with the conditions to which these turbines are exposed. In such situations, precipitation-strengthened steel may be employed (Llewellyn and Hudd, 2004).



Fig 1. 1 Typical HP and LP turbine rotor (James et al, 2010)

Among the different materials typically used for blades are 403 stainless steel, 422 stainless steel, A-286, Haynes Stellite Alloy Number 31 and titanium alloy. The 403 stainless steel is essentially the industry's standard blade material and, on impulse steam turbines, it is probably found on over 90% of all the stages. It is used because of its high yield strength, endurance limit, ductility, toughness, erosion and corrosion resistance, and damping. It is used within a Brinell hardness range of 207 to 248 to maximize its damping and corrosion resistance. The 422 stainless steel material is applied only

on high temperature stages (between 700 and 900°F or 371 and 482°C), where its higher yield, endurance, creep and rupture strengths are required.

In general, HP blades are machined on CNC machine and LP blades are manufactured using different methods like casting, forging, powder metallurgy etc. The generalized steps involved in machining the HP blade as shown in the Fig 1.2 involves facing, turning the shaft, size milling, size grinding, root bottom width milling, neck milling, total length milling, convex profile, concave profile, pitch milling, pitch grinding, finishing and surface hardening. In this work, different commercially available materials are evaluated for the CNC turning process.



**Fig 1. 2 Typical compression blade of HP turbine (<http://www.cblade.it/steam-turbine-blades.html>)**

### **1.3 Measurement of quality for CNC turning**

Surface quality is an important parameter to evaluate the performance of machine tools as well as machined components. Hence, achieving the desired surface quality is of great importance for the functional behavior of the mechanical parts (Benardos and Vosniakos, 2003). Surface roughness is used as the critical quality indicator for the machined surfaces and influences several properties such as wear resistance, fatigue strength, coefficient of friction, lubrication, wear rate and corrosion resistance of the machined parts (Feng and Wang, 2002). In today's manufacturing industry, special attention is given to dimensional accuracy and surface finish. Thus, measuring and characterizing the surface finish can be considered as the predictor of the machining performance (Reddy and Rao, 2005).

Surface roughness describes the geometry of the machined surface combined with surface texture. The formation of surface roughness mechanism is very complicated and mainly depends on machining process ( Benardos and Vosniakos, 2003; Petropoulos et al., 2006). Hence, it is very difficult to determine the surface roughness through analytical equations. Surface finish can be characterized by two main parameters, average roughness ( $R_a$ ) and maximum peak to valley height ( $R_t$ ). Theoretical models have been proposed to estimate these parameters and are given as ( Shaw, 1984; Boothroyd and Knight, 1989):

$$R_a = \frac{1000f^2}{32r} \quad (1.1)$$

$$R_t = \frac{1000f^2}{8r} \quad (1.2)$$

Where  $f$  is the feed rate (mm/rev) and  $r$  is the tool nose radius (mm).

However, the above theoretical models do not take into account any imperfections in the process such as tool vibration or chip adhesion (Diniz and Micaroni, 2002). Further, these models do not reflect the effect of other process parameters on surface roughness (Davim et al, 2001). It has been shown that cutting speed and feed rate also play important roles on surface quality of finished component (Davim, 2008). Surface roughness can be affected by many other factors like built-up-edge, tool vibrations etc. This indicates that there are many other factors and their interactions which need to be taken into consideration in calculating the surface roughness.

#### **1.4 Need for an integrated approach**

Most of the engineering applications or physical processes encountered in the real world comprise of multiple responses. Unfortunately, only the simplest of systems can be modeled with single-response optimization and the bulk of physical processes are too complex to be categorized into individual responses. In true quality sense, a customer usually considers several correlated quality characteristics of a product for product quality. Accordingly, variability of a product's response has to be reduced and the mean must be brought close to the target. The optimal parameters for CNC turned parts may include surface roughness, material removal rate,

tool wear, tool life, cutting force, power consumption, etc. While evaluating materials for these optimal parameters, one has to consider relative importance between these parameters and the concurrent interactions between them. There are several mathematical tools and techniques available in the literature, namely graph theory (Deo, 2004), decision making models (Hwang and Yoon, 1982), fuzzy logic (Zadeh et al., 1996), artificial neural networks (Davim, 2008), and design of experiments in modeling of such complex decision making situations.

### **1.5 Scope and objectives of present work**

The present work involves the application of systems quality, graph theory, concurrent engineering, decision making and design of experiments approaches for evaluation of turbine blade materials for CNC turning operation. The objectives of the present work are:

1. To develop a quality model for assessing the overall quality of CNC turning using graph theory as a tool. Taking into consideration the quality of interactions between the subsystems simultaneously, an overall quality index may be derived. The quality index should help the user in optimal selection and also in monitoring quality at different stages of design and manufacturing. The interaction quality can then be quantified using experimental results. This in turn may be employed in evaluating the overall quality of CNC turning center.
2. To develop a mathematical model for concurrent engineering based design approach to reduce design and development time. This mathematical model should factor in multi-functional design aspects (i.e. X-abilities) by considering significant interactions/interdependence between them. Also there is a need for identification of design specifications under each x-ability in determining the turned surface quality. Thus, using the design specifications, the designer can select an optimal turbine blade material.
3. To derive a methodology by which coding, evaluation and selection of a turbine blade material for CNC turning can be made easy. A unique coding scheme which helps the designer and expert system in differentiating between the alternatives at conceptual stage is required. There is a requirement for a simple methodology which helps designer,

manufacturer and the end user for evaluation and selection of alternatives. The functioning and utility of the attributes-based evaluation system developed should be illustrated for commercial materials.

4. To validate the decision making approaches in the previous objectives by experimental investigation. In order to withstand cyclic loading, the turbine blade materials require high surface quality. Surface quality depends on the machining operations and the basic parameters like speed, feed and depth of cut. A regression equation correlating these variables and surface quality would be of great value to industry. The interactions between the input variables are highly significant for the system based modeling approach.

## **1.6 Organization of thesis**

The research work is presented in 7 chapters. The logical order is as follows:

Chapter 1 is an introduction to CNC turning, its quality measurements, and turbine blade materials. It also gives an idea of the organization of content for the better understanding of the scope and objectives of the research work.

Chapter 2 reviews literature in the field of quality evaluation and concurrent design aspects with reference to decision making studies pertaining to material selection for a CNC turning operation of turbine blade material. Literature is collected on the fields like quality performance measures of a CNC turning, steam turbines and its blade materials, concurrent engineering, systems approach, graph theoretic approach, design for 'X', decision making methods (MADM, and TOPSIS), and design of experiments. The literature emphasizes on requirement of integrated evaluation and decision making approach which appraises the design aspects and the interactions to carry out further research studies. Finally, based on the literature review the pertinent gaps are identified.

In Chapter 3, a quality based mathematical model for a CNC turning center is proposed. This model considers subsystems and their interaction quality. A method for quantification of interaction quality is proposed. From the proposed quality model a quality index is obtained. The



interactions are obtained based on the experimental results. The derived methodology is applied in evaluation of a CNC turning center.

Chapter 4 provides a new way of combining various design aspects in evaluation of a blade material for X-abilities. The pertinent X-abilities which are essential are identified. In this methodology, every design aspect along with the interactions between the design aspects, without missing any information is considered. The present work utilizes concurrent engineering principles in developing a new methodology which utilizes all the design aspects simultaneously. The proposed methodology is derived using graph theory, matrix algebra and permanent. The obtained concurrent design index is useful for evaluation, comparison and final decision making among the alternative materials for CNC turning. The proposed methodology is applied for concurrent evaluation of three materials ST 12TE, ST T17/13W and ST17-PH for CNC turning.

Chapter 5 introduces a methodology for coding, evaluation, ranking and optimal selection of alternative materials for CNC turning. Based on the literature several attributes are identified. A unique coding scheme and the evaluation procedure useful to the designer are proposed. MADM-TOPSIS approach is used for evaluation, ranking and selection of a material from the number of alternatives available. Line graph and spider diagrams are proposed for evaluation, comparison, ranking and benchmarking purposes. The proposed three stage selection procedure is applied in evaluation of turbine blade materials, which is in continuation with the previous chapter.

In Chapter 6, experimental investigation of turned surface quality of turbine blade materials on a CNC lathe is presented. The experiments are designed using central composite method for turning of three different turbine blade materials. The results obtained from the experiments are analyzed and interpreted using ANOVA and different graphical representations. Regression equation is formulated between the response and input variables. Confirmatory experiments are conducted for verifying the regression equations.

In Chapter 7, the outcome of this work and suggestions for the future scope are presented.

## **CHAPTER 2**

### **LITERATURE REVIEW**

#### **2.1 Classification on the basis of identified categories**

To develop a methodology for quality based modeling, evaluation and selection of a material for CNC turning process, systems approach, design for 'X' principles, graph theory, matrix algebra, multi attribute decision making approaches, and design of experiments are employed. In view of this, the literature survey is classified into following categories:

- CNC turning to meet quality features
- CNC turning for turbine blade materials
- Concurrent engineering and X-abilities
- Graph theory and its applications
- MADM-TOPSIS approach
- Design of experiments and CNC turning process

##### **2.1.1 CNC turning to meet quality features**

In the current scenario, mechatronic features have become product differentiators in the traditional mechanical systems. One of the best examples is the CNC turning center which was derived from the conventional lathe over a period of time. This is further accelerated by higher performance to price ratio in electronics, increasing market demand for innovative products with smart features, and reducing the production cost by incorporating mechatronic elements (Robert, 2002). In the past, quality was a product differentiator, but in the current market scenario with cut-throat competition, quality is essential, from the customer point of view, in all the components manufactured on a CNC machine. To meet these expectations, industry should focus on the quality characteristics of CNC machine and the materials to be machined.

Turning is an important and widely used machining processes in engineering industries. In turning, the cutting conditions such as cutting speed, feed rate, depth of cut, features of tools and work piece materials, affect process efficiency and performance characteristics (Shaw, 1984; Boothroyd and Knight, 1989). Performance evaluation of CNC turning is based on performance

characteristics like surface roughness, material removal rate, tool wear, tool life, cutting force and power consumption. Cutting parameters are determined based on experience or by use of a handbook, which does not guarantee optimal performance (Groover, 1996). Thermally induced errors can account for as much as 70% of dimensional errors of a work piece (Du et al, 2002). Accuracy of the machined part cannot always be achieved using design techniques. The use of error compensation technique is a viable alternative . Developing a system-independent error compensation equation is a huge challenge for the researcher.

It is necessary to select the most appropriate machining settings in order to improve cutting efficiency, process at low cost and produce high-quality products (Kopak and Sali, 2001; Ishan et al, 2004; Xavious and Adithan, 2009). Another way of achieving quality is by part-to-part dimensional control of the parts produced. This kind of integration can be reached by using devices commonly known as touch trigger probes attached to machine tools (Guerra and Coelho, 2006). These devices assure the immediate detection of dimensional errors, reduce scrap, prevent the scrapping of a full batch of pieces, and reducing cost due to part rework.

Another reason for the poor surface quality of a machined work piece is the condition of the cutting tool i.e. tool wear, tool breakage etc. To anticipate the problems in time and to avoid the catastrophic failure of the cutting tool, condition monitoring of the cutting tool is suggested in the literature. Cutting tool condition monitoring can help in online realization of tool wear, tool breakage and surface roughness (Chaudhury and Bajapi, 2005). In the literature various sensing techniques have been used to detect edge chipping, fracture, and surface roughness. In general tool condition monitoring (TCM) is done by two methods (Chelladurai, 2008): direct and indirect sensing (Table 2.1).

Acoustic emission (AE) is the spontaneous release of localized strain energy in stressed material. The elastic waves are recorded by piezoelectric sensors on the material surface. The obtained electrical signal is parameterized and/or stored, and analyzed with an AE system. AE signals can be of burst or continuous type. AE feature parameters are typically defined for burst signals (but some of them can be extended for continuous signals). In machining, AE is produced by many sources such as: plastic deformation during cutting (in the workpiece and chip), friction (tool rake and chip, tool flank and workpiece), work material and chip breaking, tool fracture,

and collisions between chip and tool. Both continuous and burst emissions are produced depending on the sources. It has even been proved that there exists a strong correlation between AE and torque while assessing the deep hole drilling tool (Hienemann and Hinduja, 2008) and drilling tool condition (Gómez et al, 2010).

**Table 2.1 Tool condition monitoring sensing methods**

<b>Direct method</b>	Optical methods, resistance measurement, radioactive, contact sensing
<b>Indirect method</b>	Acoustics and vibration emission, strain measurement, temperature measurement, force measurement

It has been widely established that variation in cutting force can be correlated with tool wear. In practice, application and interpretation of cutting force parameter has been diverse, with more effort concentrated on studying the dynamic characteristic of the cutting force signal and interpreting its relation to tool wear levels. This can largely be attributed to the fact that force becomes important in worn tool conditions as a result of the variations produced due to friction between cutting tool flank and the workpiece (Ko and Cho, 1994; Dornfeld, 1994). Experiments (Remdana and Regal, 2006) have shown that the three components of the cutting force respond differently to the various forms of wear occurring on the tool. For example, the feed force may be insensitive to crater wear whereas the feed and radial forces may be influenced more by tool wear than the main cutting force.

Vibrations are produced by cyclic vibrations in dynamic components of cutting force. Usually, these vibrational motions start as a small chatter responsible for serrations on the finished surface and chip thickness irregularities. The nature of vibration signal arising from metal cutting process is such that it incorporates the facets of free, force, periodic and random type of vibrations. Direct measurement of vibration is difficult because its determining characteristic feature, the vibration mode, is frequency-dependent. Hence, related parameter acceleration is measured and the characteristics of vibrations are obtained from the patterns obtained. Choudhury and Rath (2000) proposed an accurate relationship between tool wear tangential cutting forces with 8% error. Another analysis showed that the static force was the

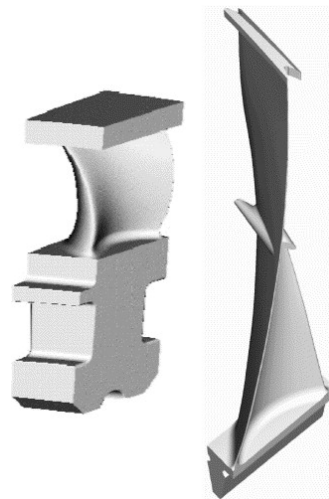
most sensitive indicator of cutting condition changes such as DOC and feed-rate while the dynamic sensors were good at tracking changes in the sensors from accrued wear (Dimla and Lister, 2000).

Cutting force is generally considered one of the most significant variables in the turning process (Sick, 2002). It has been widely recognized that variation in the cutting force can be correlated with tool wear, as a result of the variations produced by friction between cutting tool flank and workpiece ( Dimla, 2000; Coudhury and Kishore, 2002). Tool dynamometers are commonly used to record these cutting forces (Rehorn, 2005). However, dynamometers are not suitable instruments for shop floor use due to their high cost, negative impact on machining system rigidity, geometric limitations and lack of overload protection (O'Donnell, 2001). Therefore, a low-cost system for measuring cutting forces is necessary. In the past, Scheffer and Heyns(2004) used a simple sensor-integrated tool holder using strain gauges, and Audy (2006) also presents an overview of techniques and equipment used for measuring cutting forces using a strain gauge-based system. Chelladurai et al (2008) have carried out regression analysis for cutting tool vibration (accelerometer in cutting and feed direction, strain gauge) with respect to input parameters (flank wear, speed, feed and depth of cut).

### **2.1.2 CNC machining for turbine blade materials**

Following the steam path through a turbine, the environment for the converging blades varies strongly and, as a consequence, so do the mechanical requirements. These requirements have a strong influence on the choice of material and the design with respect to temperature, wetness and cleanliness of medium, acting forces as well as other factors such as hardenability and oxidation. Therefore, different blade families exist which can be categorized according to their use in the primary three turbine modules as high, intermediate and low pressure blades (HP, IP and LP). The first two turbine modules, HP and IP, are characterized (Richter, 2003) by high temperatures and they contain comparably small blades that have to sustain small centrifugal forces but large steam-induced bending forces due to relatively high static pressure differences and impulse changes at the stage. They are equipped mostly with statically determinate T-roots assembled in tangential grooves around the rotor. The blades are tightly bound to each other by integral roots and shrouds that ensure high stiffness of the blade row and also introduce frictional

damping to the structure. Of course, the integral shrouds also serve to seal the blade and hence reduce the aerodynamic leakage losses. Fig 1.1 (left) shows an example of a rhombic and integrally shrouded HP blade taken from the recent Siemens 3DS™ blading family. The 3DS™ blade is characterized by a fully three-dimensional airfoil shape aimed at reducing the secondary flow losses that are dominant in the front stages of HP and IP turbine components.



**Fig 2.1 Images of a rhomboidic HP blade from the 3DS™ series with a total length of  $\approx 100$  mm (left) and an LP blade with integral shroud and snubber made of titanium with a total length of  $\approx 1200$  mm (right), Ritcher (2003)**

There are three basic properties (Couchman et al, 1997) namely strength, ductility and toughness expected in turbine blade materials. Strength to withstand the stresses imposed on it, as no material is perfect, it must possess sufficient toughness to tolerate reasonable level of imperfections without fracturing. Despite taking precautions, during forging and casting of materials, there exist common defects like forging tear, shrinkage, porosity, etc. Besides, the material should have resistance to cracks due to foreign material left in the steam path. In addition to these there are many other supplementary characteristics or properties required of a material such as machinability, surface finish, corrosion resistance, metallurgical stability, cost, fretting resistance, hardness, erosion resistance, weldability, damping, density, etc.

In the literature related to manufacturing of turbine blades, several types of manufacturing methods are discussed. Generally HP blades are machined on CNC turning followed by CNC milling machine (Lim et al, 2002). Lu et al (2011) reported direct laser forming (DLF) of turbine

blade using the metal powder. Their paper describes the fabrication of the steam turbine blade from 316L powders by DLF. The influence of laser specific energy, scanning speed and powder feeding rate on the forming characteristics of elementary units is also systematically investigated. The limitation of DLF method is that the average surface roughness obtained was much higher (10 to 26  $\mu\text{m}$ ) and hence needs a finishing process to obtain a good surface finish. James et al. (2010) studied the effect of shot-peening at fir tree roots of the blades for the residual stresses and found that the blades roughness was still high and there was no discernible effect from fatigue loading when the mean stress was set at 600 MPa.

Different types of steels are used in manufacturing turbine blades which includes 17-4PH (Yao et al., 2007), 13%Cr steel (Xu et al, 2007), AISI 430 (Bruschi and Ghiotti, 2008), 12CrNiMo martensite steel with Din number 1.4939 (James et al, 2010) 316L (Lu et al, 2011), etc. The 17-4PH has been used to make steam turbine blades in light water reactors (LWRs) and pressurized water reactors (PWRs), due to its excellent combination of mechanical properties and corrosion resistance. These materials have to serve for over a very long period during the whole life-span of the power plants. With increasing requirements on life-span and security of steam turbines, the quality of turbine blades becomes more and more important. So there is a need to improve the surface qualities, such as surface hardness and wear resistance (Hsiao et al, 2002; Lo et al, 2003; Wang and Zou, 2006). Yao et al (2007) studied the CO<sub>2</sub> laser based alloying of 17-4PH material and found that the hardness of the surface is double than the substrate and the surface finish has been improved.

### **2.1.3 Metallurgical changes during machining**

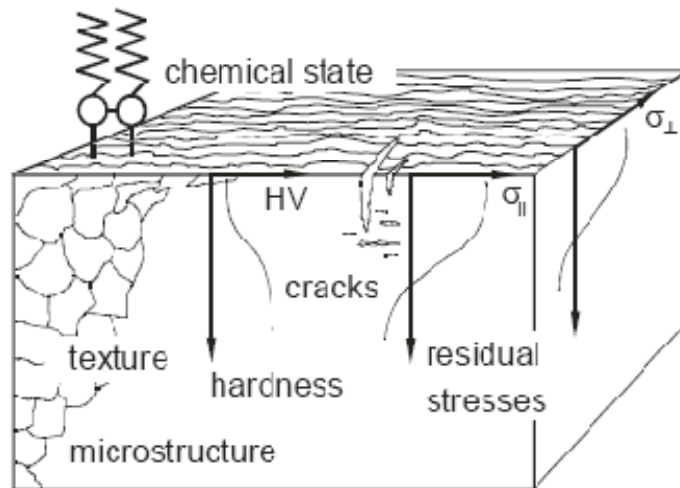
The tool-chip interaction on the tool rake face is extremely important in metal cutting and the situation is often further complicated by the presence of a third body. The phenomena occurring on the tool face depend on the local conditions of stress, velocity, temperature, the local properties of tool and workpiece material, and the third body or the interfacial media including the cutting fluid. Under extreme conditions of pressure and temperature, chemical and physical reactions between the three components may occur which may change the known properties of the partner materials significantly. The influence of even minor changes in the tool shape due to wear, have an immediate effect on workpiece dimensions or surface roughness and the integrity

of the subsurface layer (van Luttervelt et al., 1998). A fundamental understanding of the interaction between the cutting tool and workpiece during machining is also essential for determining the tool life. New tool materials such as ceramics, including cubic boron nitride (CBN), and new technology such as tool coatings have improved the cutting efficiency and tool life in high speed machining of difficult-to-cut materials. The efficient utilization of new tool materials and technology requires further understanding of cutting mechanisms either on macro or micro-scales. In machining studies, there have been fewer theoretical analysis of the secondary deformation zone compared with studies of the primary deformation zone. This is mainly due to the lack of fundamental understanding of the basic mechanisms of the interactions of cutting tool and work material (van Luttervelt et al., 1998). In the secondary deformation zone, the material flow depends on inadequately understood conditions in the flow zone and the material properties of the workpiece. The latter is not a constant but varies, since it is temperature, strain and strain-rate dependent, as well as being affected by micro-structural variations and possible phase transformations, like austenitisation(Helle, 1995).

Several kinds of layers have been reported in metal cutting processes (Helle, 1995; Katayama and Hashimura, 1995; Karagöz and Fischmeister, 1996; Sidjaninand Kovac, 1997; Qi and Mills, 2000). These include layers of inclusions from the workpiece, oxide layers due to chemical reaction between the chip-tool and third medium (e.g. coolant), plastic deformation layers on the tool and material transfer layers (MTL) or built-up layers (BUL) or stagnant layers. Bletton et al. (1990) investigated the influence of the nature of the oxide on the machinability of 316L stainless steels and showed that the low melting point of anorthitic oxide inclusions in the steel made them more malleable at the cutting temperatures. These inclusions were finely elongated in the shear zone. Scanning electron microscope observations showed an oxide layer in the tool crater.

The influence of metalworking fluids on machining processes has been extensively studied over the last 50 years. Much of this work focused on the characterization of the effects of metalworking fluids and their influence on the workpiece. For many years subsurface damage caused by machining was characterized with respect to detrimental changes in texture, microstructure, hardness, residual stresses and cracks. Progress in chemical surface analyses over the last few years has enabled a broader definition of surface integrity as shown in Fig 2.2.





**Fig 2.2 Surface and subsurface integrity after machining Brinksmeier et al (2004)**

Metalworking fluids should ideally be formulated to meet both cooling and lubrication requirements. Most metalworking fluids consist of a basic fluid, enhanced with other products such as anti-wear, anti-corrosion or emulsifying agents (Brinksmeier et al, 2004). Polar active substances (synthetic esters, fatty acids), extreme-pressure (EP) additives (sulfur carriers), AW (anti-wear) additives (phosphorus compounds) and others (anti-corrosion additives, anti-mist additives, anti-oxidants, emulsifiers) are all used as additives.

Some of the authors focused on correlating the microstructure and metallurgical effects after machining the steel. Chou (2002) investigated how to increase the surface hardness by combining machining and heat treatment process simultaneously. The attempt was to utilize wear land rubbing, together with mechanical loading, to achieve hardening mechanism at machined surfaces. In the preliminary investigation, soft AISI 4340 steel bars machined with 1.2 mm flank wear land (VB), showed roughly 30  $\mu\text{m}$  deep hardened layer (49 HRC versus 28 HRC). Furthermore, the machined surface had about 7 volume% austenite, an evidence of phase transformation. These results suggest the possibility of utilizing machining to surface harden steel parts. This process will increase the surface finish which is one of the requirements from the industry.

Duan and Wang (2005) studied about adiabatic shear bands and white layers induced during high speed cutting of 30CrNi<sub>3</sub>MoV steel. This was investigated by using scanning electron

microscopy, X-ray diffraction and transmission electron microscopy. The results showed that some non-diffusional martensitic phase transformation and dynamic recrystallization might take place in the adiabatic shear bands and white layers within the chips.

Martin et al (2011) worked on the evaluation of Hydrogen-assisted fracture of AISI type 304 steel with a special focus on the strain-induced martensite produced below the specimen surface during a standard turning operation. Two different surface conditions were investigated: one containing martensite, resulting from the machining process, and a martensite-free state which was obtained after a proper heat treatment. Additionally, the chemical composition and thickness of oxide layers, occurring in both studied cases, were analyzed by secondary ion mass spectrometry. These two different conditions were tested at room temperature in air (ambient pressure) and in hydrogen gas (40 MPa) atmosphere, respectively. Experimental results revealed a detrimental effect of machining-induced martensite on AISI type 304 steel performance in hydrogen, leading to major differences in relative reduction of area (RRA) between the as-machined and the heat-treated state for the same material. In this context, an operating mechanism based on hydrogen diffusion was discussed.

A few researchers like Modelin et al (2011) have studied the surface integrity of turned precipitated hardened steel 15-5PH. In this study, a numerical model was implemented for the prediction of surface integrity after turning. It has been shown that the thermal kinetics does not allow a significant austenite formation even if the maximal reached temperature were clearly higher than the austenization start temperature. The good adequacy between calculated and measured residual stress profiles confirms that austenization does not occur.

#### **2.1.4 Concurrent engineering and X-abilities**

Concurrent engineering (Ashley, 1992) is a systematic approach to integrated product development that emphasizes the response to customer expectations. It embodies team values of cooperation, trust, and sharing in such a manner that decision making proceeds with large intervals of parallel working by all life-cycle perspectives early in the process synchronized by comparatively brief exchanges to produce consensus.

In the sequential design of a CNC, mechanical components are designed first, in which emphasis is given to geometry. The electrical and electronic components are designed next in their respective domains, and the dynamic behavior of the system is considered in control system design. Finally, the programming part is designed in the software engineering domain. Sequential design has several drawbacks such as lack of integration and compatibility among the components, longer time-to-market and additional efforts as well as costs required in achieving the required specifications.

The advantages of considering concurrent design principles to a CNC turning include:

- Cost effectiveness
- Time-to-market
- Ease of integration
- Increased efficiency
- Increased subsystem compatibility
- Increased quality and reliability
- Added functionalities, etc.

In an effort to implement concurrent engineering, industry has begun to focus on design for manufacturing (DFM) where constraints in manufacturing and design goals are taken into consideration simultaneously at the design stage (Bralla, 1986; O'Driscoll, 2002) and design for assembly (DFA), which considers assembly constraints i.e. methods and costs, during the design stage (Boothroyd and Atling, 1992; Boothroyd et al., 2002). Later, researchers have focused mainly on reducing product life cycle cost, so areas such as design for life cycle (Alting, 1995; Glazebrooke et al., 2000), design for environment (Lee and Xu, 2005; Jesweit and Hauschild, 2008), design for recycling (Masanet and Horvath, 2007), etc. were developed. Design study based on these areas is known as Design for X (DFX). There exist interactions/interdependence between the x-abilities, for example, a design parameter (assembly time) under DFA may depend on the design parameter (tolerances) in DFM.

Despite the progress, most of the currently developed systems focus on modeling and manipulation of geometric information, such as solid modeling, CNC machining path generation, rapid prototyping, reverse engineering, and so on. Modeling of non-geometric design information, such as design requirements, conceptual design candidates and other product

development life-cycle considerations, is not well understood and studied for developing these computer-based systems (Xue and Yang, 2004). In concurrent design of a CNC system (Portilla-Flores, 2011) for manufacturing, mechanical elements are more expensive (i.e., a gear pinion must be built by a CNC machine) than controller implementation, it is better to have a large set of controller gains, maintaining a constant size of mechanical elements. Therefore, from the design engineer's point of view, solutions in the mentioned area represent a smaller investment on the final prototype. Fang Li et al (2010) proposed a CNC model based integrated framework (CNCMIF) in concurrent design of a controller for CNC machine.

Concurrent engineering is not only important in design of a CNC machine but also in simultaneous selection of process and materials. Gopalakrishnan and Pandiarajan (1991) discussed aspects relating to the selection of work materials and suitable processes required to manufacture the product which has been designed in the domain of concurrent engineering. The optimal selection of work materials and manufacturing processes impact production costs considerably, which are committed largely during the preliminary and detail design stages of the product, based mostly on product functionality rather than manufacturing considerations. A methodology to select work materials and their processing techniques in the light of manufacturability considerations, during the preliminary and detail product design stages was proposed. Expert systems technology was used to build the models with appropriate interfaces to algorithms and data bases, for performing the quantitative measurements pertaining to manufacturability.

Thurston et al (1994) proposed a method for integrating environmental considerations directly into the material selection process. They used a design hierarchy to perform concurrent multi-attribute material evaluation on the basis of cost, physical properties and customer preferences. A proof-of-concept case study of material selection for beverage containers was presented. The results of a consumer survey were reported. Trade-offs between aluminium, glass and plastic containers were analyzed. The price reduction necessary to make plastic competitive with aluminium for a particular market niche was calculated.

Chan et al (1998) proposed an approach to an emerging concept, Meta Planning, which brings manufacturing issues upstream by generating timely and appropriate feedback to design

engineers. While a product or feature was being designed, all feasible downstream manufacturing processes can be compared. A meta planner was integrated into existing CAD/CAPP/CAM systems to automate high-level process planning such that heterogeneous processes can be organized into a coherent plan. COMPASS (Computer Oriented Materials, Processes, and Apparatus Selection System), developed as a meta- planner, had the basic framework to provide essential information regarding production cost, cycle time, and product quality for all of the candidate processes. This tool helped design engineers to identify potential manufacturing problems in the earlier stages of product development. Three different hole-making process models were implemented in COMPASS to illustrate the mechanism that analyzes and compares different manufacturing processes. Close interaction between design parameters and manufacturing performance for selected processes was demonstrated through a detailed case study involving a single feature.

Zha (2005) proposed a work of selecting suitable manufacturing processes and materials in concurrent design for manufacturing environment. In this work a fuzzy knowledge-based decision support method was proposed for multi-criteria decision-making in evaluating and selecting possible manufacturing process/material combinations in terms of the total production cost. Based on the proposed method, a prototype Web-based knowledge-intensive manufacturing consulting service system (WebMCSS) with the client-knowledge server architecture was developed to help designers/users find good processes and materials while still at the conceptual level of design. The system, as one of the important parts of an advanced design for manufacturing tool, was a concept level process and material selection tool that could be used both as a stand-alone application and as a Java applet freely available via the Web. Interlinked with Web pages of tutorials, and reference pages explaining the facets, fabrication processes and material choices, the system performed reasoning and calculations using the process capability and material property data retrieved from the remote Web-based database and knowledge base that was maintained and updated via the Internet. The use of the system was illustrated with an example. McDowell et al (2011) proposed a simulation tool for concurrent design of materials and processes in managing the design complexity.

Albiñana and Vila (2012) proposed a framework for integrated materials and process selection in product design. Following an in-depth review of existing studies and the factors that

influence decision-making, the flow of reasoning in the process was defined and the relations among the parameters of the whole life cycle to be considered in the conceptual design phase were established. This analysis was then used to define a workflow that breaks the work down into stages and gates, and specified how the preliminary selection was to be performed.

### **2.1.5 Graph theory and its applications**

Graph theory has a wide range of applications like biology-biological networks (Girvan and Newman, 2002), computer science- finding the clustering of data quality (Schaeffer, 2007), electric networks-in preventive control of power systems (Maharana and Swarup, 2010), chemistry-in analyzing the nets of crystal chemistry (Delgado-Friedrichs and O'Keeffe, 2005), etc. Graph theory, along with the matrix algebra, is applied in technical areas like structural analysis of automobile vehicle (Venkatasamy and Agrawal, 1995), failure and root cause analysis of a hydraulic system (Gandhi and Agrawal, 1996), analyzing parametric influences in torsional vibrations (Sreeram, 2005), functional perspectives based conceptual design of grippers, clutches, flywheels etc. (Al-Hakim et al., 2000), representation of function and feature relation at detailed design stage (Feng et al., 1996), structural modeling of electroplating system (Kumar and Agrawal, 2008), quality modeling of composite material system (DuraiPrabhakaran et al., 2006a), evaluation, comparison and selection of a power plant (Gerg et al., 2006), structure based reliability analysis of a hydraulic system (Gandhi et al., 1991), composite system (DuraiPrabhakaran et al., 2006c), DFX based graph theoretic design of RTM products (DuraiPrabhakaran et al., 2006b), selection of a material for an engineering component (Rao, 2006), analyzing the fundamental challenges in applying graph transformations in design context (Campbell et al., 2007), graph based design and analysis of dynamic software architecture (Bruni et al., 2008), development of interactive similarity metrics in graph based design model (Anandan and Summers, 2006), etc.

A limited number of articles are available on modeling of a CNC machine using graph theory. Diaz-Calderon et al. (2000) proposed a system graph for modeling of physical systems. In this, the system graph contained the collection of terminal graphs, and the mathematical relation between the terminals represented the physical characteristics. The developed methodology was explained using the example of a missile seeker. The other contributions are

on using bond graphs in modeling of mechatronic application(CNC) systems (Amerongen, 2003; Malik and Khurshid, 2003; Kayani and Malik, 2007), but bond graph is completely different from the graph theory, it is very touse in modeling and is a symbols based modeling tool. To the best of my knowledge, graph theory and matrix algebra based modeling and evaluation of a CNC machine has not been reported in the literature so far.

### **2.1.6 MADM-TOPSIS approach**

Often a design engineer has to make a decision based on a unique situation, for example, optimal selection of a suitable material for CNC turning. In such a situation, the designer has to make decision based on large group of attributes which are significant in the particular application. The mathematical tools that aid this kind of decision making are referred to as multi attribute decision making (MADM). One of the tools is TOPSIS (Technique for Order Priority by Similarity to Ideal Solution), based on the concept that the chosen alternative should have shortest Euclidean distance from the ideal solution and farthest from the worst solution in an n-dimensional attribute space (Hwang and Yoon, 1982).

Attributes can be either quantitative or qualitative in nature. Decision making processes like selection of a material for a CNC operation with a combination of these attributes is a complex task. MADM methodology is suitable for selection of a product or process based on complex set of attributes. MADM methodology is being applied in wide range of areas like selection of plant layout (Yang and Hung, 2007), selection of electroplating system (Abhishek and Agrawal, 2009), optimal selection of robot grippers (Agrawal and Rao, 1987), coding, evaluation and selection of an automotive vehicle (Venkatasamy and Agrawal, 1994), x-abilities based computer network selection (Balaji and Agrawal, 2008), selection of a supplier (Li *et al.*, 2007) based on different constraints, etc.

The selection of optimal material for an engineering design from among two or more alternative materials on the basis of two or more attributes is a multiple attribute decision making problem. The selection decisions are complex, as material selection is more challenging today. There is a need for simple, systematic, and logical methods or mathematical tools to guide decision makers in considering a number of selection attributes and their interrelations. The objective of any material selection procedure is to identify appropriate selection attributes, and

obtain the most appropriate combination of attributes in conjunction with the actual requirement. Thus, efforts need to be extended to identify those attributes that influence material selection for a given engineering design to eliminate unsuitable alternatives, and to select the most appropriate alternative using simple and logical methods (Rao and Patil, 2010).

Various approaches had been proposed in the past to help address the issue of material selection. Ashby et al. (2004) provided a comprehensive review of the strategies or methods for materials selection, from which three types of material selection methodologies had been identified such as (a) free searching based on quantitative analysis, (b) checklist/questionnaire based on expertise capture, and (c) inductive reasoning and analog procedure. For the free-searching method, there are already a number of well-documented methods, the most famous being the graphical engineering selection method or the ranking method (Ashby, 1995) and (Ashby, 2002). Edwards (2005) developed a checklist/questionnaire method to improve the likelihood of achieving an optimal design solution. Some knowledge based systems developed by researchers for materials selection include that of Sapuan (2001), Amen and Vomacka(2001), Zha (2005) and Jalham (2006). However, these systems and methods are complex and knowledge- intensive.

### **2.1.7 Design of experiments and CNC turning process**

Quality and productivity improvement are most effective when they are an integral part of the product and process development cycle (Montgomery, 2007). The experimental design methodology plays a key role at early stages of the development cycle, where new products are designed, existing product designs are improved and manufacturing processes optimized, leading to product success. Design of experiments (DOE) is based on the effective use of sound statistical tools that can lead to products that are easy to manufacture and have high reliability, enhanced field performance as well as troubleshooting activities. DOE has been established in many industries like electronics and semiconductors, aerospace, automotive, medical devices, food and pharmaceuticals, manufacturing, chemical, and process industries.

The most used DOE methods are factorial experiments, Taguchi method and response surface methodology. In a factorial experiment, all possible combinations of the factors are represented for each complete replication of the experiment. The number of treatment is equal to



the product of the number of factor levels and can therefore become large when either the factors or levels are numerous (Amitava, 2008). The advantage of factorial experiments is that interaction effects are also considered as an evaluation factor. The Taguchi method seeks to minimize the effects of noise and to determine the optimal level of important controllable factors based on the concept of robustness (Dehnad, 1989; Nair, 1992). In this method, signal-to-noise ratio is given as the performance evaluation of the experiments. The disadvantage of Taguchi orthogonal array design is that the alias structure is not readily apparent from the actual design. It leads to inaccurate conclusions because an inference on the significance of main effect depends on the interaction effect. The factorial experiments used for process characterization i.e. identifying the most important factor which affect the process. Once this objective is fulfilled the next objective is process optimization or finding the set of operating conditions for the process variables that result in the best process performance. Response surface methodology (RSM) is a collection of mathematical and statistical technique that is useful for modeling and analysis in applications where optimization of response is the main objective.

The analysis of the data during manufacturing by using suitable statistical designs is of great importance for precise evaluation to be obtained from the process. Design and methods such as factorial design, RSM and Taguchi methods are widely used in place of one-factor-at-a-time experimental approach which is time consuming and expensive (Noordin et al, 2004).

The literature on DOE applied to CNC turning process can be classified based on the measured responses like tool wear in terms of a sensor (accelerometer, strain gauge, acoustic emission, temperature, ultra sonic emission, and wear area), surface roughness, tool life, cutting forces (Kannatey and Dornfeld, 1981; Lan and Dornfeld, 1984; Braschdorff et al, 1993; Zhang et al, 1995; Rahman et al, 1995; Tarnng et al, 1995), spindle/drive (Bikramjit et al, 2002; Tarnng et al, 1999), chip reflectance (Yeo et al, 2000), and power or current.

The recent literature on turning of different materials is given in Table 2.2. Lalwani et al (2008) studied the effect of cutting parameters in turning on cutting forces and surface finish. A number of experiments based on RSM have been carried out and the linear and quadratic models have been formed to explain the relation between the parameters. Most of the authors (Young, 2005, Anselmo, 2008; Esteves and Paulo, 2011; İlhan and Harun, 2011; İlhan et al, 2012) have

considered speed, feed and depth of cut as basic parameters and some authors considered one additional parameter like flank wear (Chelladurai et al, 2008), hardness (Tamizharasan et al, 2006), tool geometry like rake angle, nose radius, etc. (Pawade et al, 2007; Aman et al, 2008; Suleyman, 2011). The responses measured in most of the above mentioned literature is surface roughness, tool wear, cutting forces and tool life. There are very few reports on researches which studied the power consumption (Aman et al, 2008), material removal rate (Tian and Ming, 2003) and effect of coolant (Joseph et al, 2008) during cutting operation.

**Table 2.2 Literature on DOE based CNC turning process optimization**

Author	Year	Work piece material	Tool material (insert)	Responses	Methodology
Young Huang	2005	AISI 52100 HRC=62	CBN (KD050)	Tool life	RSM
Tamizharasan et al	2006	Engine crank pin HRC >45	PCBN (A,B,C grades) insert	Tool life, MRR, MR	18 experiments
Pawade et al	2007	Inconel 718	PCBN(3 types fo chamfers)	cutting force, feed force, radial force, surface roughness	27 experiments
Chelladurai	2008	EN8 Steel	DNMG 150608 (carbide) insert	accelerometer, strain gauge	Factorial design (27*5=135)
D I Lalwani	2008	MDN 250 steel (18Ni(250) marraging steel) HRC=50	CBN insert, chamfers	cutting force, feed force, radial force, surface roughness	RSM (28 experiments)
Aman et al	2008	AISI P-20 tool steel (32-36 HRC)	CNMG 120404, 08	Power consumption (Watt)	30 Taguchi, RSM
Anselmo	2008	AISI 4340 steel with 56 HRC	CBN 7020 with chamfer	Tool life	100min or tool end
Paulo Davim	2011	AISI 1045 (207 HB)	wiper inserts (CNMG 120404,08)	Surface roughness	9 experiments
Suleyman	2011	AISI 1040	CNMG 120404	Surface roughness	L27 Taguchi, RSM
İlhan and Harun	2011	AISI 1040, (32HRC)	Carbide insert WNMG 080408	Surface roughness	27 experiments
İlhan and Suleman	2012	AISI 304 austenitic stainless steel	Carbide inserts (SNMG 120408-PP)	Surface roughness ( $R_a$ & $R_z$ )	27 experiments

## 2.2 Analysis and gaps in existing literature

In most of the literature surface finish of the machined surface is considered as the quality indicator and different parameters like cutting parameters, tool geometry, cutting forces, tool wear as input parameters, and accelerometers, acoustic sensors, strain gauges, optical methods, temperature measurement etc. are the measuring sensors. Though they seem to act independently, there exist interactions between the different subsystems of CNC and the sensors and electronic components. Quantification of interaction quality between different subsystems of a CNC machine is lacking in the literature. A few authors (Athani and Vinod, 1986; Altinatas and Munasinghe, 1994; Park and Kim, 1997; Bahar et al, 2001 ;Omirou and Barouni, 2005; Suh et al,2006; Yeung, 2006; Ma et al, 2007; Wang et al, 2007 Vichara et al, 2009; Li et al, 2010; ) have attempted to consider CNC machine as a system. Reports on research in which the CNC machine is considered as a system in quality evaluation, while factoring in the interaction quality between the subsystems, are lacking in the literature.

The design of a CNC system also has to overcome the limitations of mechanical system such as friction, lack of accuracy, vibrations, windup error, dimensional error, poor performance, less productivity, low reliability, low quality, less user friendliness, etc. To overcome these limitations proper selection of structural quality constituents and consideration of environmental interactions, human interactions, etc. are important during the design phase. To achieve this, the designer should have a thorough understanding of structure of a CNC turning center and the interactions between the subsystems and with the other systems. Thus an integrated approach, which considers the subsystems quality along with the interactions, is necessary. Quantitative structure activity relationship (QSAR) and Quantitative structure properties relationship (QSPR) which is more established in drug industry for the design of molecular structure (Hall and Keir, 2001) reveals that the overall structural quality of a system is a function of subsystems quality and their interactions quality.

The manufacturing methods in the literature conclude that HP turbine blades are manufactured on multi axis machining and the LP turbine blades can be manufactured using different manufacturing techniques like casting, forgings, powder metallurgy, rapid prototyping etc. The limitation with these methods is getting high surface finish as machining process by

retaining the strength. Reports on researches that investigate the evaluation of materials based on the CNC turning for surface roughness while considering different interactions, are lacking in the literature.

During the design phase selection of a material for CNC turning, the designer has to consider several x-abilities simultaneously to meet the requirements of a customer. The x-abilities may include manufacturability, quality, reliability, cost, environment, etc. In the literature, the x-abilities are considered independently. It was proved that over 70% of the production cost of a product is determined during the conceptual design stage. However, the design phase itself accounts for only 6% of the total development cost (Hundal, 1993). Sehab and Abdulla (2001) considered design to cost, an x-ability, in estimating the cost of a product based on the geometry, material to be used etc. Some studies on simultaneous selection of materials and processes (Chan et al, 1998; Zha, 2005; Albiñana and Vila, 2012) are at the abstract level and application of these to a specific process is vague. A methodology which incorporates 'X' abilities and their interactions simultaneously in selection of a turbine blade material for a CNC turning process is lacking in literature.

Though there exists a lot of literature (Rao, 2006; Shanian et al, 2008; Thakker et al, 2008; Gupta, 2011; Chauhan and Vaish, 2011; Jahan, 2011; Albiñana and Vila, 2012;) on material selection based on MADM approaches, an MADM approach which is useful in selection of a turbine blade material for CNC turning is missing in the literature.

After analyzing the literature on DOE of materials for machining, we found that a methodology which compares different commercially available turbine blade materials like ST 17-4PH, ST 17/13W and ST 12TE for CNC turning to get the best surface quality is lacking.

Based on the above literature review the following pertinent gaps are identified:

- There is a need to develop a methodology for determination and evaluation of quality of CNC machine during design stage, while considering subsystems and the interactions. An experimental means is required to evaluate the interaction quality.
- A methodology which considers different 'X' abilities and their interactions concurrently in evaluating turbine blade materials for CNC turning process is required.

- There is a need to identify different attributes influencing the machining of turbine blade materials on a CNC turning center. Based on the identified attributes a decision making model needs to be developed.
- An experimental investigation for surface quality in turning operation of steam turbine blade materials on CNC turning center is lacking.

Hence, the motivation for this work stems directly from the needs of a designer, manufacturer and end user, who wish to consider the interrelationship or interaction or interdependence among several design aspects of product development to reduce product development time, life cycle costs, improve the quality of a CNC turning for different materials.

## **CHAPTER 3**

### **QUALITY MODELING AND ANALYSIS OF CNC TURNING**

#### **3.1 Introduction**

In the current scenario, quality of mechatronic features has become product differentiators in the traditionally mechanical, electrical, hydraulic or thermal systems. To achieve six sigma standards the systems approach is best suited for complex multi-domain systems like CNC.

System based quality evaluation is emphasized in different areas like improving the quality of a manufacturing system by ergonomic interventions (Erdinc and Vayavay, 2008), measuring and improving the quality of a software system (Amuthakkannan et al., 2008), and impact of a system's quality on another system (Dedeke and Huang, 2010). Some of the contributions are Taguchi (Lan and Wang, 2009; Ahialn et al., 2012) based quality modeling of turning, adaptive fuzzy petrinet (kasirolvalad et al., 2006) based control etc. From the literature survey, it is concluded that less research is done for a systems based approach in modeling and analysis of a CNC turning center.

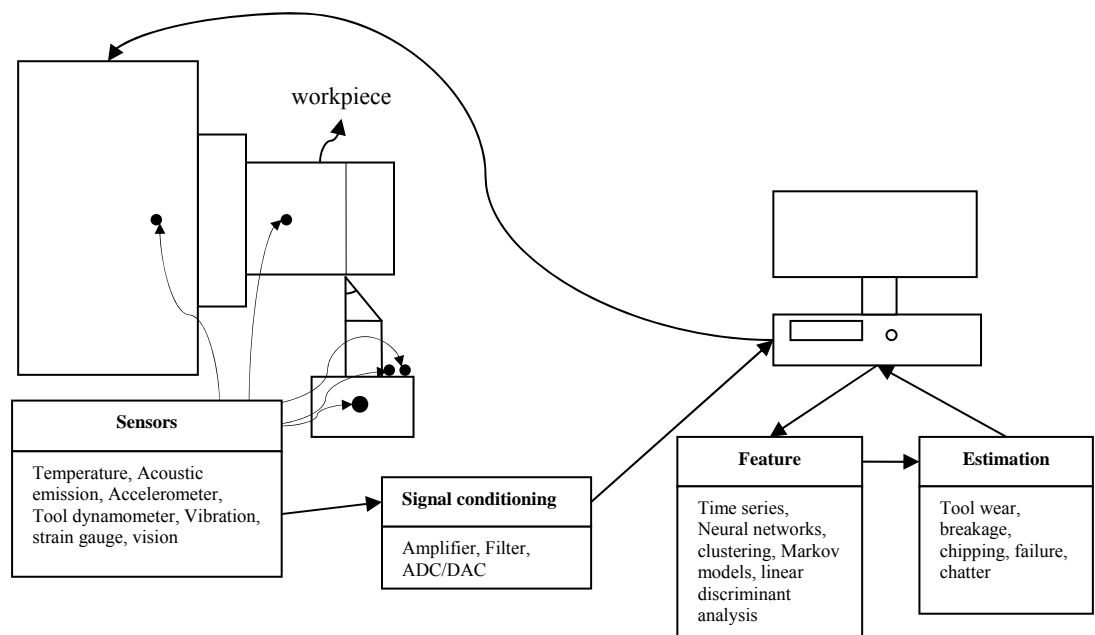
In view of this, a mathematical model is proposed for the quality evaluation of a CNC machine. It helps the industry in achieving six sigma standards in turning a product on CNC.

#### **3.2 Identification of quality subsystems and interactions**

The primary objective of the CNC turning center is to get high dimensional accuracy with mirror like surface finish on machined parts. This can only be achieved when the quality and performance of structural components is high. Uninterrupted machine operation and minimal human supervision are still partially solved problems for the machining industry. One of the important techniques for maintaining the quality of a CNC machine tool is condition monitoring of cutting tool wear state, tool breakage and work piece surface roughness.

There are two ways, direct and indirect, for tool condition monitoring (TCM). The direct methods are basically optical methods, which are difficult to monitor because most of the time the tool is in contact with the work piece and the coolant is in between. The indirect methods are

most frequently used and are related to the following parameters: acoustic emissions, tool temperature, cutting forces (static and dynamic), vibrations signature (acceleration signals), strain (strain gauge) and so on. The framework of TCM is shown in Fig 3.1. In this framework, indirect information in the form of temperature, vibrations, forces, acceleration and strain is collected using different sensors like strain gauge, tool dynamometer, accelerometer, etc. The collected information is processed using a signal conditioning device and the processed information is passed to a PC or a complex decision making system (microcontroller, microprocessor etc.) for feature extraction and estimation of the tool condition. A feedback is given to the automatic tool changer (ATC) based on the status of the tool.



**Fig 3. 1 General framework for tool condition monitoring**

The quality of the components produced on a CNC turning centre depends on the functional quality of the different subsystems. The quality of structural components of a CNC turning centre are identified and shown in Fig 3.2. This quality hierarchical tree of a CNC turning centre has six subsystems at level 0. In general, the quality hierarchical tree may have  $n+1$  levels as shown below:

- LEVEL 0     Whole CNC turning center
- LEVEL 1     Subsystems (s-systems)
- LEVEL 2     Sub-subsystems (ss-systems)
- LEVEL 3     Sub-sub-subsystems (sss-systems)



LEVEL n      Component level (component)

The quality hierarchical tree is useful in identifying components at each level and analyzing the quality of subsystems. For quality evaluation of CNC turning center, not only is the subsystem's quality important, but also, the quality of interactions between the subsystems is too.

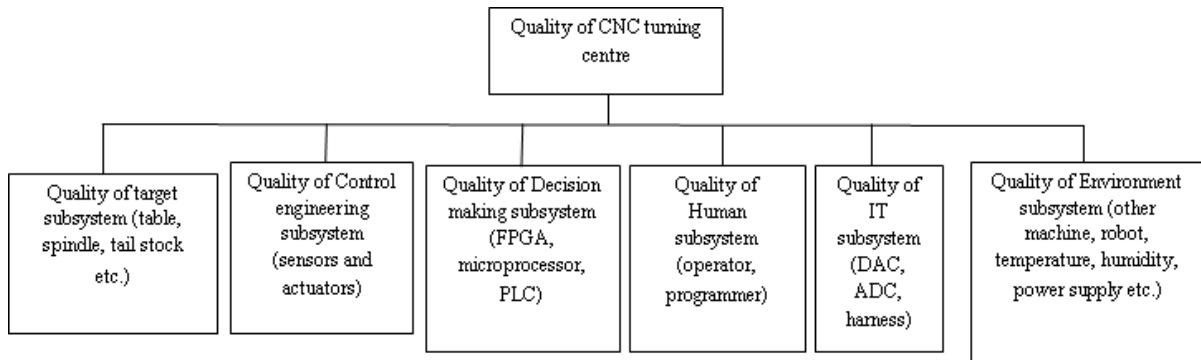


Fig 3. 2 Quality hierarchical tree of CNC turning centre

For this case, some of the interactions between the subsystems are identified and presented using a block diagram as shown in Fig 3.3. This block diagram is not a mathematical entity.

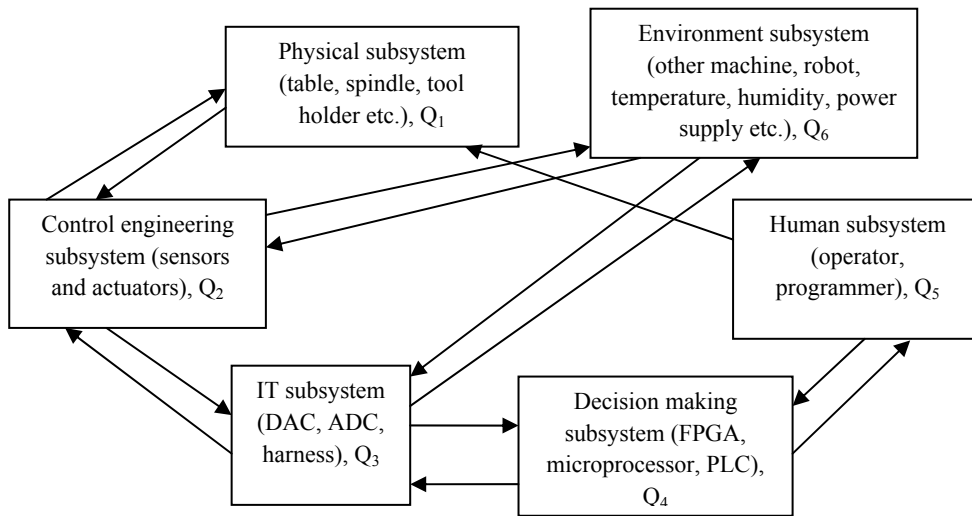


Fig 3. 3 Quality interaction block diagram of CNC turning centre

### 3.3 Quality Digraph (QD)

To translate the block diagram into a mathematical entity, a quality digraph (QD) is developed (Fig 3.4). In this digraph, each vertex is assigned to a subsystem and the

corresponding name can be referred from Fig 3.3. The quality digraph (QD)  $G = [V, E]$ , consists of a set of nodes or vertices  $V = [v_1, v_2, v_3, \dots, v_n]$ ; and set of edges  $E = [e_{12}, e_{21}, e_{31}, \dots]$ . The vertex  $v_i$  represents the quality of subsystem and the edge  $e_{ij}$  represents the quality of interaction between the corresponding subsystems. The interactions between the subsystems are represented by directed lines and are labeled according to the origin of interaction. For example,  $q_{12}$  denotes that the interaction is originating from  $Q_1$  and terminating at  $Q_2$ . The QD is useful for visual inspection of the quality of subsystems and interactions. The visual analysis of quality interactions are as follows:

**$q_{12}$ :** Two accelerometers and a strain gauge mounted on the cutting tool collect information about the cutting tool condition. The quality of the control engineering subsystem depends on the quality of the information interacted with the cutting tool.

**$q_{21}$ :** The accuracy in tool changing time of ATC (Automatic Tool Changer) depends on the accuracy of signals received by the control engineering subsystem.

**$q_{23}$  and  $q_{32}$ :** The quality of analog\digital input signal influence the quality of digital\analog output from the ADC\DAC.

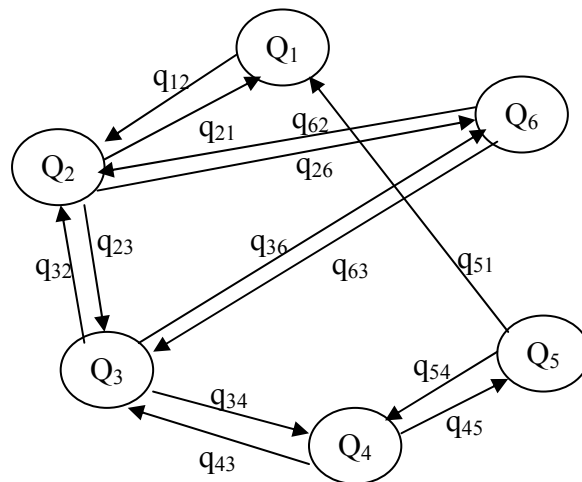


Fig 3. 4 Quality digraph of CNC turning centre

**$q_{26}$ :** The quality of signal received by the other system like robot depends on the quality of information with the control engineering subsystem

***q<sub>62</sub>***: The functional quality of the control engineering subsystem depends on quality of the information about the environment subsystem (temperature, humidity etc.). For instance, sometimes, the temperature at the sensor location is lower than that at other places.

***q<sub>34</sub>***: The quality of the decision made by the PLC, FPGA, or microprocessor depends on the quality of interfacing or interconnecting elements like bus or harness.

***q<sub>43</sub>***: The quality of the signal received from the PLC, FPGA, or microprocessor depends on the quality of the interconnecting elements transmitting information.

***q<sub>36</sub>***: The quality of the signal received by the environment (machine, robot etc.) depends on the amount of signal loss (quality) in the data bus carrying the information.

***q<sub>63</sub>***: The performance quality of the interfacing connections depends on the surrounding temperature, humidity and fluctuations in the power supply.

***q<sub>45</sub>***: The efficiency of the complex decision making subsystem depends on the quality of the programmer interacting or programming it.

***q<sub>54</sub>***: The quality of the graphical user interface of the complex decision making subsystem depends upon the skill of the operator using it.

***q<sub>51</sub>***: The quality of the physical system depends on the quality of the operator performing offsetting and referencing operations.

Fig 3.4 represents the quality digraph of a CNC machine. The quality of a CNC machine is considered as a system, and the quality of subsystems are represented as nodes in the quality digraph. Quality digraphs can be obtained at each hierarchical level, for example, in the subsystem level digraph, the sub-subsystems are represented by nodes. The quality digraph gives a basic understanding of quality of a CNC machine. Quality improvement is possible by inspecting the strength of interactions. The shortcoming of a quality digraph is that it is not computation friendly, and thus storage and retrieval of data from the computer is hardly possible.

### 3.4 Matrix representation of QD

To develop a computational friendly quality model for CNC machine, quality digraph is represented in the form of a matrix named Variable Permanent Quality Matrix (VPQM) and is given in equation (3.1). The size of VPQM is  $N \times N$ , where ‘N’ represents the number of nodes in a QD. In this work, six subsystems are considered for developing QD, so the size of the VPQM is  $6 \times 6$ . In this matrix, the diagonal elements represent the quality of the subsystem and the off-diagonal elements represent the quality of interactions/interdependencies between subsystems.

$$VPQM_{CNCturningcenter} = \begin{matrix} & \begin{matrix} 1 & 2 & 3 & 4 & 5 & 6 & \text{vertices} \end{matrix} \\ \begin{matrix} Q_1 & q_{12} & 0 & 0 & 0 & 0 \end{matrix} & \begin{matrix} 1 \\ 2 \\ 3 \\ 4 \\ 5 \\ 6 \end{matrix} \end{matrix} \quad (3.1)$$

In this matrix, the diagonal elements,  $Q_i$ ,  $i=1,2,..,6$  represents the quality of CNC turning center subsystems and the off-diagonal elements  $q_{ij}$  represent quality interaction of  $i^{th}$  subsystem with  $j^{th}$  subsystem.

This is the complete representation of a CNC machine quality and its interdependencies. This VPQM representation can be extended to sub-subsystems, and in that case, the diagonal elements of that new matrix would represent the quality information of sub-subsystems and the remaining elements of the matrix represent the interactions among the sub-subsystems. Even though VPQM is the complete representation of a CNC machine, it is not a unique way of representing the CNC machine. VQPM may vary by interchanging the labeling of vertices.

### 3.5 Variable Permanent Quality Function (VPQF)

From the VPQM, two characteristic functions can be obtained based on the type of mathematical operation being used. They are the permanent and the determinant, both of which are multinomial. They are often used in combinatorial mathematics (Marcus and Minc, 1965; Jurkat and Ryser 1966). In the determinant, when numerical values of  $Q_i$  and  $q_{ij}$  are substituted, some of the quality information is lost due to the presence of positive and negative signs between

the terms. This is a shortcoming of using the determinant as a characteristic equation. To overcome this, the quality of a CNC machine is modeled using the permanent multinomial, where all the terms are positive and no is negative sign present. The permanent for quality modeling of a CNC machine is defined as Variable Permanent Quality Function (VPQF). This VPQF is obtained from the matrix VPQM and is given in the equation (3.2).

$$\text{VPQF} = \text{Per}(\text{VPQM})$$

$$\begin{aligned} & \prod_{i=1}^6 Q_i + \left[ \sum_i \sum_j \sum_k \sum_l \sum_m \sum_n (q_{ij}q_{ji}) Q_k Q_l Q_m Q_n \right] + \left[ \sum_i \sum_j \sum_k \sum_l \sum_m \sum_n (q_{ij}q_{jk}q_{ki}) Q_l Q_m Q_n \right] \\ & + \left[ \sum_i \sum_j \sum_k \sum_l \sum_m \sum_n (q_{ij}q_{ji})(q_{kl}q_{lk}) Q_m Q_n + \sum_i \sum_j \sum_k \sum_l \sum_m \sum_n (q_{ij}q_{jk}q_{kl}q_{li}) Q_m Q_n \right] \\ & + \left[ \sum_i \sum_j \sum_k \sum_l \sum_m \sum_n (q_{ij}q_{jk}q_{ki})(q_{lm}q_{ml}) Q_n + \sum_i \sum_j \sum_k \sum_l \sum_m \sum_n (q_{ij}q_{jk}q_{kl}q_{lm}q_{mi}) Q_n \right] \quad (3.2) \\ & + \left[ \sum_i \sum_j \sum_k \sum_l \sum_m \sum_n (q_{ij}q_{ji})(q_{kl}q_{lk})(q_{mn}q_{nm}) + \sum_i \sum_j \sum_k \sum_l \sum_m \sum_n (q_{ij}q_{jk}q_{ki})(q_{lm}q_{mn}q_{nl}) \right. \\ & \left. + \sum_i \sum_j \sum_k \sum_l \sum_m \sum_n (q_{ij}q_{jk}q_{kl}q_{li})(q_{mn}q_{nm}) + \sum_i \sum_j \sum_k \sum_l \sum_m \sum_n (q_{ij}q_{jk}q_{kl}q_{lm}q_{mn}q_{ni}) \right] \end{aligned}$$

In expanded expression, the equation (3.2) contains  $6! = 720$  terms. The VPQF shown in the equation (3.2) represents the systematic arrangement of the terms in different groups. Each group of terms is shown within square brackets and the groups are arranged in descending order of the number of  $Q_i$ 's in the group. In these groups of terms,  $Q_i$  is the quality of an unconnected subsystem. The portion of a term,  $(q_{ij}q_{ji})$  represent the two subsystem quality dyad,  $(q_{ij}q_{jk}q_{ki})$  represent the three subsystem quality loop and  $(q_{ij}q_{jk}q_{kl} \dots q_{xi})$  represent the x-subsystems quality loop. For convenience, a new nomenclature is introduced, a dyad  $(q_{ij}q_{ji})$  is represented by  $Q_{ij}$ , and x-subsystem loop  $q_{ij}q_{jk}q_{kl} \dots q_{xi}$  is represented by  $Q_{ij \dots x}$ . Thus, a term in VPQF may have combination of subsystem quality  $Q_i$ 's and dyad  $Q_{ij}$  and/or loop  $Q_{ij \dots x}$ . Using the new notation the equation (3.2) is rewritten as:

$$\text{VPQF} = \text{Per}(\text{VPQM})$$

$$\prod_{i=1}^6 Q_i + \left[ \sum_i \sum_j \sum_k \sum_l \sum_m \sum_n (Q_{ij}) Q_k Q_l Q_m Q_n \right] + \left[ \sum_i \sum_j \sum_k \sum_l \sum_m \sum_n (Q_{ijk}) Q_l Q_m Q_n \right] \quad (3.3)$$

$$\begin{aligned}
& + \left[ \sum_{i,j,k,l,m,n} (\mathcal{Q}_{ij}\mathcal{Q}_{kl})\mathcal{Q}_m\mathcal{Q}_n + \sum_{i,j,k,l,m,n} (\mathcal{Q}_{ijkl})\mathcal{Q}_m\mathcal{Q}_n \right] \\
& + \left[ \sum_{i,j,k,l,m,n} (\mathcal{Q}_{ijk}\mathcal{Q}_{lm})\mathcal{Q}_n + \sum_{i,j,k,l,m,n} (\mathcal{Q}_{ijklm})\mathcal{Q}_n \right] \\
& + \left[ \sum_{i,j,k,l,m,n} (\mathcal{Q}_{ij}\mathcal{Q}_{kl}\mathcal{Q}_{mn}) + \sum_{i,j,k,l,m,n} (\mathcal{Q}_{ijk}\mathcal{Q}_{lmn}) \right] \\
& + \left[ \sum_{i,j,k,l,m,n} (\mathcal{Q}_{ijkl}\mathcal{Q}_{mn}) + \sum_{i,j,k,l,m,n} (\mathcal{Q}_{ijklmn}) \right]
\end{aligned}$$

Terms in the multinomial expressed in equation (3.2) and (3.3) are arranged into N+1 groups, where N is the number of subsystems, and here N is 6. The first group has only N number of  $Q_i$ 's and there is no  $Q_i$  in the last group. In general, the  $i^{\text{th}}$  subsystem has (N+1-1) number of independent subsystem quality  $Q_i$  and the remaining are the quality interactions. It is well verified that, the structural quality component in any term or terms in any group are distinct. The equation (3.2) is easy to understand once the physical meaning of all the terms is understood. The equations (3.2) and (3.3) are invariant of CNC machine, so it is the characteristic equation. Both the equations are exactly the same and have the same capability for quality considerations. The derived expression is an efficient tool for quality analysis of a CNC machine. The equations (3.2) and (3.3) are abbreviated representations of the quality of a CNC machine.

### 3.6 CNC machine quality index (QI)

VPQF is a function of the quality of subsystems namely, target subsystem, complex decision making subsystem, control engineering subsystem, IT subsystem, human subsystem and environment subsystem as well as the quality of interactions between them. After substituting the values of quality parameters in VPQF expression, it becomes a single valued index named as QI (Quality Index). This index forms a basis for the optimal selection of a CNC machine, in evaluation of alternatives at the design stage and in monitoring the continuous quality of a CNC machine. VPQF could also be helpful in obtaining the QI of a positively benchmarked (best) system and negatively benchmarked (worst) system. QI can be calculated from either of the equations (3.2) and (3.3). The VPQF and QI are derived for a CNC machine up to subsystem

level only. For obtaining the complete QI, one has to repeat this procedure up to the component level. Even the optimized quality of a CNC machine may be obtained by varying the quality level of different parameters in the VPQF.

A quality comparison between two CNC machines could be carried out based on their QI. The higher the value of the QI, the higher would be the rank given to particular CNC machine. This tool would be useful to the designer in selection of the best CNC machine based on quality, at initial stages of design.

### 3.7 Quality analysis

Each term of the VPQF expression yields a useful test for quality analysis, if a term is considered as a set of CNC machine quality subsystems forming a complex system. If the VPQF of a CNC machine has  $N$  number of terms, then quality analysis can be conducted in  $N$  distinct ways. It ensures that the CNC machine is tested and analyzed in all possible way, and it can be constructed from quality structural constituents. The quality analysis of a CNC machine is carried out as follows:

- The first term (group) represents a set of quality of  $N$  unconnected subsystems as

$$/Q_1 / Q_2 / Q_3 / \dots / Q_N /$$

The notation ‘/’ represent a separation mark between two entities.

- The second group is absent in general due to absence of interactions with self.
- Each term of the third group represents quality of 2-subsystem dyad,  $Q_{ij}$ , and quality of the remaining  $(N-2)$  unconnected subsystems  $Q_x$ ,  $x \neq i, j$  as

$$/Q_{12} / Q_3 / Q_4 / \dots / Q_N /$$

- Each term of the fourth group represents a set of the quality of 3-subsystems loop (i-j-k),  $Q_{ijk}$ , and the quality of  $(N-3)$  unconnected subsystems,  $Q_x$ ,  $x \neq i, j, k$  as

$$/Q_{123} / Q_4 / Q_5 / \dots / Q_N /$$

- Each term in the first sub group of the fifth group represents a set of the quality of two 2-subsystem dyads ( $Q_{ij}$ ,  $Q_{kl}$ ) and the quality of the remaining  $(N-4)$  unconnected subsystems,  $Q_x$ ,  $x \neq i, j, k$  and  $l$  as

$$/Q_{12} / Q_{34} / Q_5 / \dots / Q_N /$$

- Each term in the second sub group of the fifth grouping represents a set of the quality of 4-subsystem loop ( $Q_{ijk}$ ) and the quality of the remaining (N-4) unconnected subsystems,  $Q_x$ ,  $x \neq i, j, k$  and  $l$  as

$$/Q_{1234} / Q_5 / Q_6 / \dots / Q_N /$$

Likewise the other terms could be considered.

From the above analysis, it is clear that there exist several structural quality components in the multinomial VPQF, and they need the attention of a designer, manufacturer and maintenance personnel in a quality based evaluation and analysis. At the conceptual design stage, the designer can compare different QI by altering the quality levels of the subsystem, which give scope to optimize the overall quality of a CNC machine. This expression would also be helpful to the designer in evaluating subsystems which need more attention in improving its quality.

The distribution of quality terms in VPQF for a six subsystem CNC machine is tabulated (Table 3.1). It is clearly evident that the second subgroup of sixth group has the maximum number of terms i.e.162 terms.

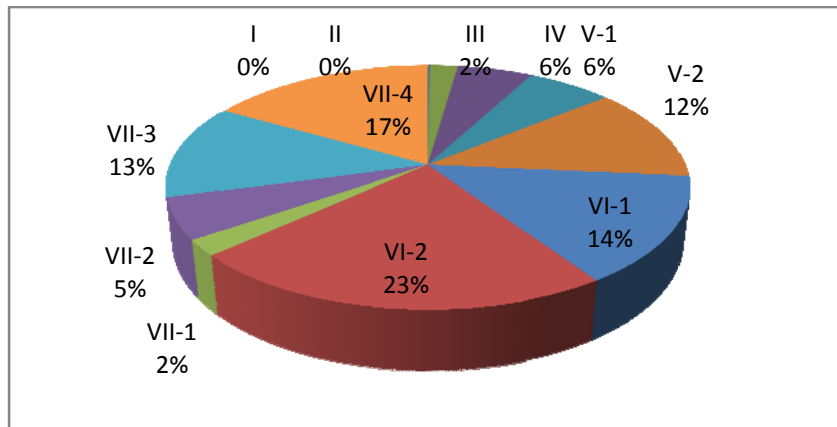
**Table 3. 1 Distribution of terms in VPQF**

Group/sub group	Number of terms
I	1
II	0
III	15
IV	40
V-1	45
V-2	90
VI-1	102
VI-2	162
VII-1	15
VII-2	39
VII-3	91
VII-4	120



From Fig 3.5, it is also clear that 80% of the total terms are from the V-2, VI-1,VI-2,VII-3,and VII-4 subgroups, so the designer should focus more on these terms. The designer could prioritize the areas of quality improvements by arranging the groups according to the number of terms and concentrate more on the subgroup/group with the maximum number of terms.

The complexity of analyzing the quality of a CNC machine depends upon the number of terms in each group as well as on the number of dyads, and M-subsystem loops present, where M=3,4,5,6. As the number of subsystems reduces, the complexity of analysis also reduces. For example, consider a comparison of terms in each group/subgroup of VPQF for CNC machines with five subsystems and six subsystems. The comparison is given by a bar chart (Fig 3.6). It is clear that the number of terms in each subgroup of a CNC machine with six subsystems has increased by 6 to 8 times. Hence the complexity of analysis also increases proportionally.



**Fig 3. 5 Analysis of grouping of terms in VPQF**

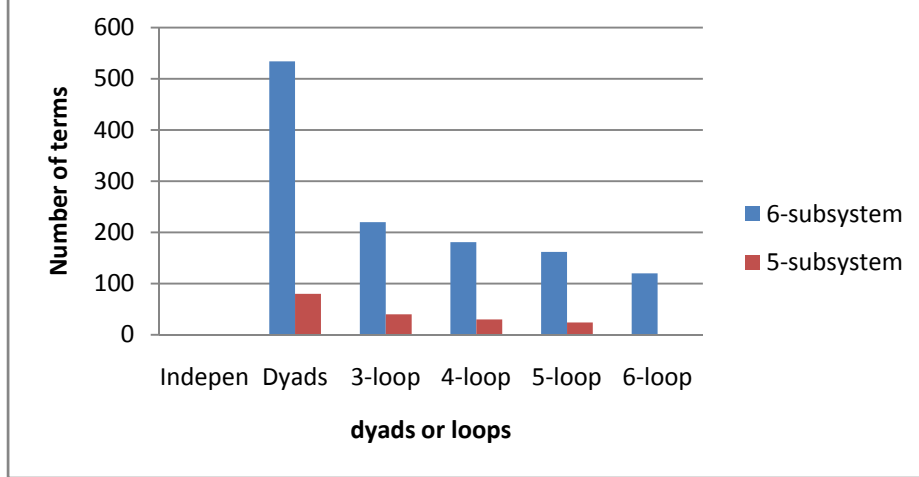


Fig 3. 6 Comparison of dyads and loops in VPQF of six and five subsystem CNC machines

From the above statement, it is clear that the quality of a CNC machine depends not only on the combination of subsystems but also on the combination of dyads, loops and independent quality subsystems. The developed methodology is helpful in carrying out the cause and effect analysis for poor quality performing subsystems. This methodology would also be useful in checking the quality compatibility between in-house components and the off-the-shelf components.

### 3.8 Coefficient of similarity and dissimilarity

In general, no two CNC machines are isomorphic from the quality point of view. For quality comparison between two CNC machines, they should have topologically similar configurations. The coefficient of similarity or dissimilarity for a CNC machine is derived based on the VPQF multinomial. This comparison is useful for determination of similarity or dissimilarity between two CNC machines based on the quality and structural considerations.

If the number of distinct terms in the  $j^{\text{th}}$  sub group of the  $i^{\text{th}}$  group of two VPQFs are represented by  $M_{ij}$  and  $M'_{ij}$ , the coefficient of dissimilarity is defined as:

Criterion 1

$$C_{d-1} = \frac{1}{Z_1} \sum_i \sum_j \psi_{ij} \quad (3.4)$$

where  $Z_1 = \text{Maximum} \left[ \sum_i \sum_j M_{ij} \text{ and } \sum_i \sum_j M'_{ij} \right]$

If subgroups are absent,  $M_{ij} = M_i$  and  $M'_{ij} = M'_i$ . Also  $\psi_{ij} = M_{ij} - M'_{ij}$ , when subgroups exist and  $\psi_{ij} = M_i - M'_i$ , when subgroups are absent.

Criterion 1 is based on the sum of the differences in the number of terms in the VPQF of two CNC machines. Using criterion 1 there might arise a situation where, though the qualities of two CNC machines differ, similarity could still be inferred by observing the similarity coefficient. This would be due to cancellation of sum of the positive and negative terms in  $\psi_{ij}$ . In order to avoid this situation, a new criterion is defined:

Criterion 2

$$C_{d-2} = \frac{1}{Z_2} \sum_i \sum_j \psi_{ij} \quad (3.5)$$

Where  $\psi_{ij} = |M_{ij} - M'_{ij}|$  when sub groups exist and  $\psi_{ij} = |M_i - M'_i|$  when subgroups are absent and  $Z_2$  is similar to criterion 1. To improve the differentiating power of the coefficient, two more criteria are proposed.

Criterion 3

This criterion is based on the sum of the differences between the squares of subgroups of two MVPQFs. The criterion is defined as:

$$C_{d-3} = \frac{1}{Z_3} \sum_i \sum_j \psi_{ij} \quad (3.6)$$

Where  $\psi_{ij} = |(M_{ij})^2 - (M'_{ij})^2|$  when subgroups exist and  $\psi_{ij} = |(M_i)^2 - (M'_i)^2|$  when subgroups are absent and  $Z_3$  is expressed as follows:

$$Z_3 = \text{Maximum} \left[ \sum_i \sum_j (M_{ij})^2 \text{ and } \sum_i \sum_j (M'_{ij})^2 \right]$$

If subgroups are absent,  $M_{ij} = M_i$  and  $M'_{ij} = M'_i$ .

Criterion 4:

Criterion 4 is based on the root of the sum of the difference squares in the number of terms in different subgroups and groups of two VPQF of the two systems. Criterion 4 is defined as:

$$C_{d-4} = \sqrt{\frac{1}{Z_4} \sum_i \sum_j \psi_{ij}} \quad (3.7)$$

Where  $\Psi$  is defined as  $\psi_{ij} = (M_{ij} - M'_{ij})^2$  when sub groups are present and  $\psi_{ij} = (M_i - M'_i)^2$  when subgroups are absent.  $Z_4$  is the same as  $Z_3$ .

From the expressions (3.4), (3.5), (3.6) and (3.7), the coefficients of similarity for four criteria are expressed as below:

$$C_{s-1} = 1 - C_{d-1} \quad (3.8)$$

$$C_{s-2} = 1 - C_{d-2} \quad (3.9)$$

$$C_{s-3} = 1 - C_{d-3} \quad (3.10)$$

$$C_{s-4} = 1 - C_{d-4} \quad (3.11)$$

Where,  $C_{s-1}$ ,  $C_{s-2}$ ,  $C_{s-3}$  and  $C_{s-4}$  are the quality-based coefficient of similarity of two proposed CNC machine systems and are derived from criteria 1, 2, 3 and 4. From the expressions (3.8), (3.9), (3.10) and (3.11) it is clear that the coefficient of similarity range from 0 to 1. If the coefficient of similarity is '1' or the coefficient of dissimilarity is '0', then the quality of both the CNC machine systems is identical. If the coefficient of similarity is '0' or coefficient of dissimilarity is '1' then the quality of one CNC machine is completely different from that of the other based on the structural quality comparison.

The value of the coefficient of similarity is useful for dividing the CNC machines into different groups. A quality-based coefficient of similarity index is also helpful in comparing the proposed CNC machine's design specifications with the benchmarked CNC machine's

specifications. This index is also helpful in comparing the quality of a proposed CNC machine with similar products available in the market.

### **3.9 Step-by-step procedure**

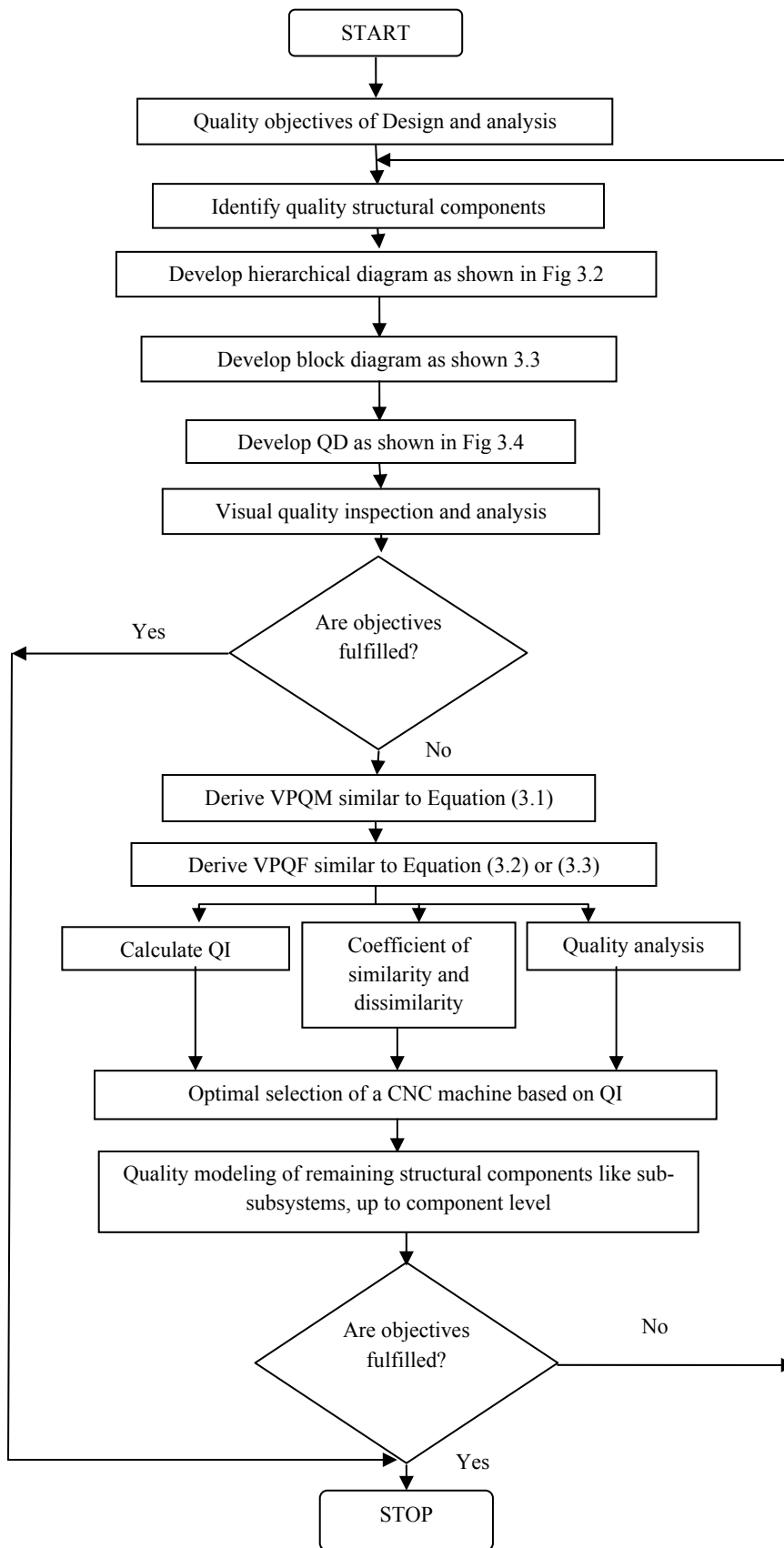
The methodology developed for quality modeling and analysis for a CNC machine is compiled as a step-by-step procedure and is presented as a flow chart as shown in Fig 3.7.

The proposed step-by-step procedure is flexible but comprehensive in the hands of designer and manufacturer to develop a competitive CNC machine that works effectively and efficiently under different situations. This methodology is capable of meeting the requirements of the manufacturing industry.

### **3.10 Experimental evaluation of interactions**

The quality of a CNC turning center depends on the quality of the subsystems like target subsystem (spindle, headstock, motor, etc.), control engineering subsystem (accelerometer signal, strain gauge signal etc.), etc. and the interactions between these subsystems. To quantify the interactions, pertinent parameters are input (cutting speed, feed rate, depth of cut and flank wear) corresponding to target subsystem and the responses received by the control engineering subsystem (accelerometer and strain gauge) are taken into consideration. To quantify the quality of interactions between the structural components of CNC machine, the experimental data is taken from the literature (Chelladurai et al, 2008). The experiments were conducted on an EN-8 steel tool with DNMG 150608 insert and Seco tool holder, on a CNC turning center without cutting fluid. Three sensors, one accelerometer in cutting direction mounted on tool holder, another accelerometer in feed direction mounted on turret and strain gauge is mounted on cutting tool, were used. The accelerometer data was taken to an FFT analyzer and the voltage induced due to strain was measured using a Wheatstone half bridge circuit using Labview software.

The experiments were conducted using  $3^k$  full factorial design, where the number of levels are low (-1), intermediate (0), and high (1). The independent variables taken in this study were cutting speed (CS), feed rate (FR), and depth of cut (DOC). Artificial flank wear was the fourth independent variable, maintained at five different levels ranging from 0 to 0.5. The responses for different sensors are shown in Table 3.2 – 3.4 respectively.



**Fig 3. 7 Step-by-step procedure for quality modeling of a CNC machine**

**Table 3. 2 Factorial design input parameters and the dynamic response of accelerometer in cutting direction (Chelladurai et al, 2008)**

Experimental conditions				Amplitude of acceleration, g for different levels of flank wear				
Ex no	CS	FR	DOC	0.5 FW	0.4 FW	0.3 FW	0.2 FW	0.1 FW
1	500	500	5	0.233	0.158	0.0298	0.0091	0.0107
2	500	500	4	0.0528	0.0079	0.0131	0.0043	0.0026
3	500	500	3	0.0456	0.0196	0.0026	0.0009	0.002
4	500	300	5	0.0759	0.0298	0.0132	0.0113	0.007
5	500	300	4	0.0389	0.0079	0.005	0.0058	0.0012
6	500	300	3	0.0348	0.0035	0.0047	0.0023	0.0014
7	500	100	5	0.0492	0.0033	0.0019	0.0028	0.0061
8	500	100	4	0.031	0.0029	0.0019	0.002	0.0031
9	500	100	3	0.0238	0.0013	0.0003	0.0006	0.0005
10	350	500	5	0.275	0.233	0.105	0.0199	0.0111
11	350	500	4	0.2	0.02	0.0219	0.0053	0.0036
12	350	500	3	0.0316	0.0111	0.0038	0.003	0.0034
13	350	300	5	0.253	0.0456	0.0247	0.0128	0.0083
14	350	300	4	0.154	0.0187	0.009	0.0085	0.0061
15	350	300	3	0.0275	0.0052	0.0074	0.0043	0.0016
16	350	100	5	0.189	0.0348	0.0105	0.0066	0.0064
17	350	100	4	0.0691	0.0115	0.0097	0.0009	0.0039
18	350	100	3	0.0107	0.0008	0.0026	0.0011	0.0009
19	200	500	5	0.265	0.265	0.232	0.0345	0.0153
20	200	500	4	0.232	0.0585	0.0241	0.009	0.0095
21	200	500	3	0.176	0.0065	0.0092	0.0087	0.0052
22	200	300	5	0.241	0.0621	0.0261	0.0442	0.0132
23	200	300	4	0.163	0.0389	0.011	0.0098	0.0091
24	200	300	3	0.158	0.0076	0.0058	0.0045	0.0019
25	200	100	5	0.106	0.0613	0.0145	0.0129	0.0112
26	200	100	4	0.0613	0.0186	0.0098	0.0092	0.0053
27	200	100	3	0.0186	0.0042	0.0077	0.0051	0.0037

**Table 3. 3 Factorial design input parameters and the dynamic response of accelerometer in feed direction (Chelladurai et al, 2008)**

Experimental conditions				Amplitude of acceleration, g for different levels of flank wear				
Ex no	CS	FR	DOC	0.5 FW	0.4 FW	0.3 FW	0.2 FW	0.1 FW
1	500	500	5	0.267	0.245	0.0103	0.0089	0.0068
2	500	500	4	0.237	0.0883	0.0065	0.0058	0.0037
3	500	500	3	0.157	0.0277	0.0035	0.0025	0.0017
4	500	300	5	0.0939	0.0638	0.0071	0.0061	0.004
5	500	300	4	0.0448	0.0191	0.0049	0.0051	0.0031
6	500	300	3	0.0239	0.0087	0.0024	0.0017	0.0025
7	500	100	5	0.0457	0.0229	0.004	0.0033	0.0033
8	500	100	4	0.0408	0.0059	0.0028	0.0028	0.0024
9	500	100	3	0.0191	0.0065	0.0015	0.0007	0.0019
10	350	500	5	0.248	0.237	0.021	0.0136	0.0077
11	350	500	4	0.245	0.0389	0.0086	0.0061	0.0054
12	350	500	3	0.164	0.011	0.0054	0.0033	0.0044
13	350	300	5	0.249	0.0627	0.01	0.007	0.0054
14	350	300	4	0.19	0.0122	0.0066	0.0058	0.0034
15	350	300	3	0.143	0.0057	0.0033	0.0021	0.0027
16	350	100	5	0.0929	0.0264	0.005	0.0053	0.0037
17	350	100	4	0.0264	0.0055	0.0036	0.0029	0.0028
18	350	100	3	0.0249	0.0045	0.0031	0.0007	0.0025
19	200	500	5	0.271	0.121	0.0226	0.0194	0.0083
20	200	500	4	0.264	0.0239	0.0123	0.0094	0.0067
21	200	500	3	0.169	0.0017	0.0085	0.0037	0.0051
22	200	300	5	0.233	0.0408	0.0159	0.0125	0.0061
23	200	300	4	0.147	0.0063	0.012	0.0084	0.0041
24	200	300	3	0.131	0.0039	0.0062	0.0045	0.0034
25	200	100	5	0.192	0.0167	0.0127	0.0064	0.0049
26	200	100	4	0.133	0.0249	0.0089	0.0033	0.0032
27	200	100	3	0.0601	0.0044	0.0081	0.001	0.0028



**Table 3. 4 Factorial design input parameters and the dynamic response of strain gauge bridge (Chelladurai et al, 2008)**

Experimental conditions				Amplitude of acceleration, g for different levels of flank wear				
Ex no	CS	FR	DOC	0.5 FW	0.4 FW	0.3 FW	0.2 FW	0.1 FW
1	500	500	5	7.4488	4.2373	0.0141	0.02108	0.00135
2	500	500	4	0.0274	0.1118	0.0013	0.00566	0.000378
3	500	500	3	0.01	0.0017	0.0006	0.00229	0.000234
4	500	300	5	0.8566	0.021	0.0025	0.00736	0.001245
5	500	300	4	0.0224	0.0031	0.0011	0.00174	0.000166
6	500	300	3	0.0017	0.0011	0.0002	0.00053	0.00002
7	500	100	5	0.05	0.3906	0.0007	0.00004	0.000749
8	500	100	4	0.0141	0.0079	0.0003	0.00056	0.000148
9	500	100	3	0.0015	0.001	0.0003	0.00009	0.000138
10	350	500	5	13.972	5.7864	0.394	0.02123	0.2695
11	350	500	4	0.594	0.0141	0.0727	0.01852	0.001401
12	350	500	3	0.1176	0.0045	0.0061	0.01562	0.000265
13	350	300	5	1.0856	1.8221	0.1274	0.01791	0.013886
14	350	300	4	0.3371	0.0104	0.0241	0.00196	0.000343
15	350	300	3	0.0727	0.0017	0.0159	0.00108	0.000159
16	350	100	5	0.0637	0.0797	0.0014	0.00014	0.000803
17	350	100	4	0.0485	0.01	0.0012	0.00064	0.000286
18	350	100	3	0.027	0.0012	0.0007	0.00096	0.000002
19	200	500	5	14.168	13.972	12.848	0.65594	0.36703
20	200	500	4	4.2373	0.3184	5.6611	0.01325	0.01556
21	200	500	3	0.3217	0.0727	0.0168	0.00064	0.006222
22	200	300	5	2.4882	2.4882	0.4354	0.02416	0.019056
23	200	300	4	0.4334	0.0141	0.0322	0.00437	0.01244
24	200	300	3	0.1361	0.0036	0.0199	0.00038	0.004686
25	200	100	5	0.145	0.0985	0.011	0.00303	0.000729
26	200	100	4	0.0943	0.0284	0.0011	0.0008	0.001429
27	200	100	3	0.0286	0.0017	0.0009	0.00049	0.000128

For these responses, the analysis of variance (ANOVA) was done at 95% confidence intervals (Table 3.5 to 3.7). In these tables the parameters having values of  $P \leq 0.05$  are significant

and are marked with a ‘\*’ symbol. This analysis was conducted using a software, MINITAB 15.0. In Table 3.5 the P value of cutting speed (CS), feed rate (FR), depth of cut (DOC) and flank wear (FW) are significant. In addition to these, the interactions between these independent parameters (For example, CS and DOC) were also found to be significant. This has not been reported in an earlier study (Chelladurai et al, 2008).

**Table 3. 5 ANOVA for effect of machining parameters w.r.t. dynamic response of accelerometer in cutting direction**

Source	DF	Seq SS	Adj SS	Adj MS	F	P
CS	2	0.0264233	0.0264233	0.0132117	22.86	0.000*
FR	2	0.0476122	0.0476122	0.0238061	41.18	0.000*
DOC	2	0.0802331	0.0802331	0.0401166	69.40	0.000*
FW	4	0.2352414	0.2352414	0.0588103	101.74	0.000*
CS*FR	4	0.0054097	0.0054097	0.0013524	2.34	0.076
CS*DOC	4	0.0074328	0.0074328	0.0018582	3.21	0.025*
CS*FW	8	0.0248704	0.0248704	0.0031088	5.38	0.000*
FR*DOC	4	0.0292265	0.0292265	0.0073066	12.64	0.000*
FR*FW	8	0.0407017	0.0407017	0.0050877	8.80	0.000*
DOC*FW	8	0.0525433	0.0525433	0.0065679	11.36	0.000*
CS*FR*DOC	8	0.0009924	0.0009924	0.0001240	0.21	0.986
CS*FR*FW	16	0.0113624	0.0113624	0.0007102	1.23	0.300
CS*DOC*FW	16	0.0205464	0.0205464	0.0012841	2.22	0.027*
FR*DOC*FW	16	0.0275549	0.0275549	0.0017222	2.98	0.004*
Error	32	0.0184973	0.0184973	0.0005780		

**Table 3. 6 ANOVA for effect of machining parameters w.r.t. dynamic response of accelerometer in feed direction**

Source	DF	Seq SS	Adj SS	Adj MS	F	P
CS	2	0.0035165	0.0035165	0.0017582	14.22	0.000*
FR	2	0.0543179	0.0543179	0.0271589	219.69	0.000*
DOC	2	0.0333204	0.0333204	0.0166602	134.77	0.000*
FW	4	0.3913171	0.3913171	0.0978293	791.35	0.000*
CS*FR	4	0.0075929	0.0075929	0.0018982	15.35	0.000*
CS*DOC	4	0.0003271	0.0003271	0.0000818	0.66	0.623

CS*FW	8	0.0262597	0.0262597	0.0032825	26.55	0.000*
FR*DOC	4	0.0073883	0.0073883	0.0018471	14.94	0.000*
FR*FW	8	0.0827171	0.0827171	0.0103396	83.64	0.000*
DOC*FW	8	0.0390739	0.0390739	0.0048842	39.51	0.000*
CS*FR*DOC	8	0.0013672	0.0013672	0.0001709	1.38	0.242
CS*FR*FW	16	0.0205260	0.0205260	0.0012829	10.38	0.000*
CS*DOC*FW	16	0.0037037	0.0037037	0.0002315	1.87	0.064
FR*DOC*FW	16	0.0242301	0.0242301	0.0015144	12.25	0.000*
Error	32	0.0039559	0.0039559	0.0001236		

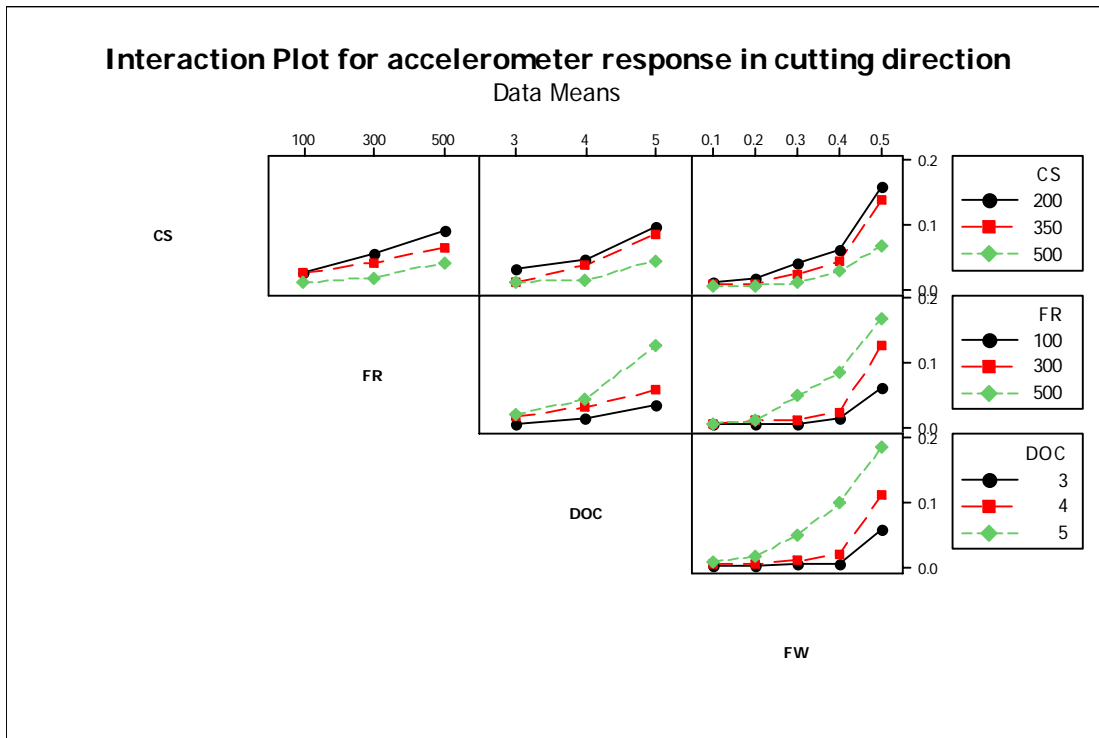
**Table 3. 7 ANOVA for effect of machining parameters w.r.t. dynamic response of strain gauge bridge**

Source	DF	Seq SS	Adj SS	Adj MS	F	P
CS	2	25.297	25.297	12.648	10.53	0.000*
FR	2	95.811	95.811	47.905	39.88	0.000*
DOC	2	91.280	91.280	45.640	38.00	0.000*
FW	4	57.305	57.305	14.326	11.93	0.000*
CS*FR	4	36.437	36.437	9.109	7.58	0.000*
CS*DOC	4	21.454	21.454	5.363	4.47	0.006*
CS*FW	8	20.081	20.081	2.510	2.09	0.067
FR*DOC	4	123.492	123.492	30.873	25.70	0.000*
FR*FW	8	74.850	74.850	9.356	7.79	0.000*
DOC*FW	8	82.925	82.925	10.366	8.63	0.000*
CS*FR*DOC	8	29.086	29.086	3.636	3.03	0.012*
CS*FR*FW	16	35.730	35.730	2.233	1.86	0.066
CS*DOC*FW	16	21.162	21.162	1.323	1.10	0.394
FR*DOC*FW	16	109.099	109.099	6.819	5.68	0.000*
Error	32	38.435	38.435	1.201		

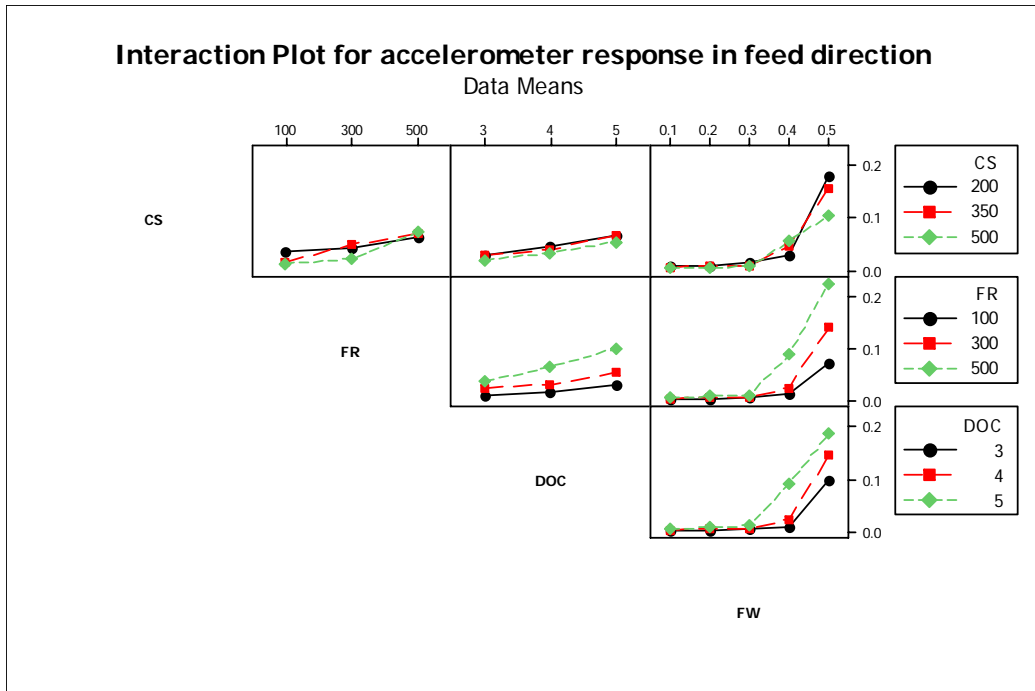
To analyze the interactions between these parameters, the interactions plots for all the three sensor responses were plotted as shown in Fig. 3.9 to 3.10. In Fig 3.8 the interaction plot for the accelerometer (cutting direction) was plotted with respect to different parameters CS, FR, DOC and FW. This figure shows that the amplitude of vibration increases with feed rate which results in increased dynamic force. With increased dynamic force, the stiffness of the tool will decrease. In each box, the lines representing the parameters at different levels are intersecting

with each other. This shows that the response of the accelerometer varies when both the parameters are varied simultaneously. Hence, there exists an interaction between those parameters, and requires attention during design of subsystems.

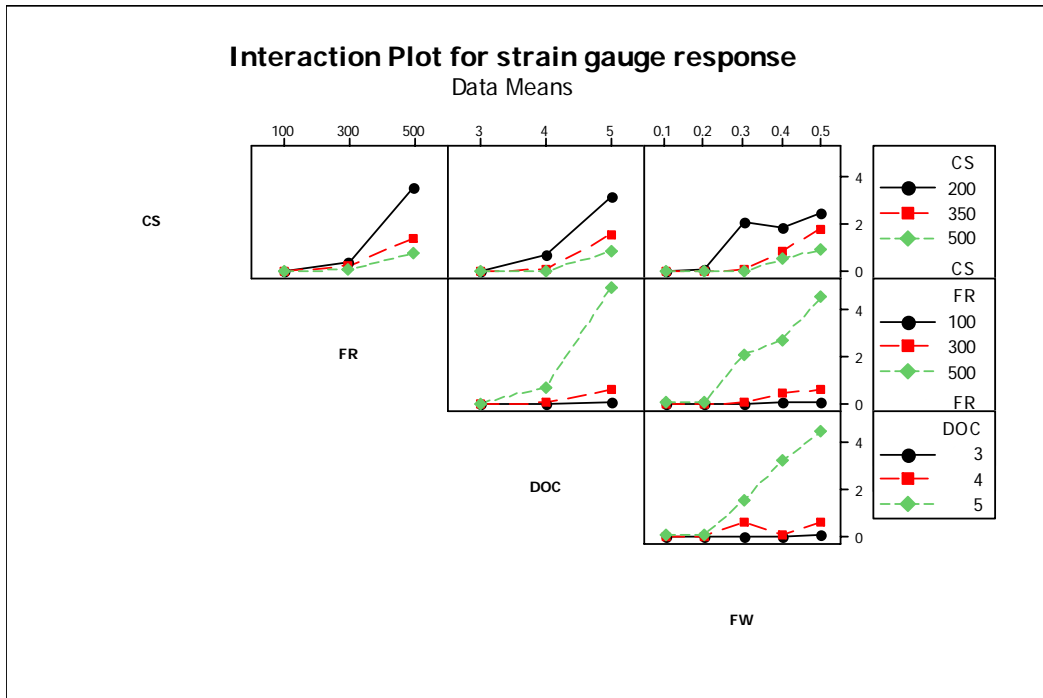
In Fig 3.9, the response of the accelerometer (feed direction) is plotted with respect to the combination of parameters FR, CS, DOC and FW. In this analysis, it was observed that the maximum amplitude of acceleration was observed for the combination of high FW, low CS, high FR, and high depth of cut. In Fig 3.10, the increase in micro strain was low up to intermediate level of the parameters FR, DOC and high up to intermediate levels of CS and low at high speeds. The increase in strain was moderate up to 0.2 FW and high for the higher FW. The increase in strain rate was due to increase in the dynamic force.



**Fig 3. 8 Interaction plot of machining parameters for the response of accelerometer mounted in cutting direction**



**Fig 3. 9 Interaction plot of machining parameters for the response of accelerometer mounted in feed direction**



**Fig 3. 10 Interaction plot of machining parameters for the response of strain gauge bridge**

The quantification of this interaction effect was a significant achievement of the present work. The interaction effect could be quantified (Sung, 1996) as follows:

$$\text{Interaction effect} = \frac{1}{2} \left[ \begin{array}{l} \text{effect of one factor at high level of the other factor-} \\ \text{effect of the same factor at low level of the other factor} \end{array} \right]$$

For example, FR and DOC are two factors, each kept at three levels. The interaction effect (FR x DOC) for the response 'amplitude of vibration in cutting direction' was given by:

$$\text{FR x DOC} = \frac{1}{2} [\text{effect of FR at high level of DOC} - \text{effect of FR at low level of DOC}]$$

From the experimental data and from Fig 3.8, the parameters FR and DOC interaction effect was found to be significant when the CS and FW were at their minimum (200 and 0 respectively). Hence, the interaction effect for the FR and DOC for the signal amplitude of vibration in cutting direction could be calculated (Table 3.8).

**Table 3. 8 Values of FR and DOC for calculating interaction effect**

FR	DOC	Accelerometer response
500	5	0.0153
500	3	0.0052
100	5	0.0112
100	3	0.0037

$$\text{FR x DOC} = \frac{1}{2} [(0.0153 - 0.0112) - (0.0052 - 0.0037)] = 0.0013$$

From the Fig 3.8, it is clear that the variation of accelerometer (cutting direction) response at lower and middle level values of the FR is low irrespective of DOC levels. When the FR is at a high level, there is considerable variation in response for the different levels of DOC. The three response lines for FR vs DOC are not parallel to each other. Therefore there exists an interaction between these two parameters. This interaction is nothing but  $q_{12}$  shown in Fig 3.3. The interaction effect between cutting speed (CS) and flank wear (FW) could be derived from Fig 3.8. The levels of CS and FW considered are shown in Table 3.9 and the calculated value of interaction effect was 0.0042 which is higher than the previous interaction.

**Table 3. 9 Values of FR and DOC for calculating interaction effect**

CS	FW	Accelerometer response
500	0.5	0.0238
500	0.1	0.0005
200	0.5	0.0186
200	0.1	0.0037

$$CS \times FW = \frac{1}{2} [(0.0238 - 0.0186) - (0.0005 - 0.0037)] = 0.0042$$

The three lines representing accelerometer response for the three levels of CS are not parallel and they intersect at lower levels of FW (0.1, 0.2, and 0.3). This shows that there exists an interaction effect on the response. The calculated value of this interaction effect was higher than the previous interaction and this shows that this interaction is stronger than the previous one. In the same way other interaction effects were calculated for different sensor responses (Table 3.10). These values could be substituted in the QI to obtain the accurate results.

**Table 3. 10 Interaction effect for different sensor outputs**

Interaction effect	Accelerometer (cutting direction)	Accelerometer (feed direction)	Strain gauge
CS x FR	0.0001	-0.001	-0.003
CS x DOC	-0.0039	-0.00035	0.0005
CS x FW	0.0042	-0.2905	-0.1035
FR x DOC	0.0013	0.0005	0.1801
FR x FW	0.0779	0.0533	0.1435
DOC x FW	0.0399	-0.0116	0.0579

### ***Quality index (QI)***

The QI of CNC turning center would be obtained by substituting the values of  $Q_i$ 's and  $q_{ij}$ 's into the equation (3.2). In this case quality of  $Q_i$ 's and  $q_{ij}$ 's were classified into quantifiable (measurable) factors and unquantifiable factors in the following manner. The quantifiable

(measurable) quality factors were divided into five ranges and each range was assigned a value. For example, the quality of the complex decision making subsystem ( $Q_4$ ) depends on how fast the feedback loop is updated. For a 1-2 axes CNC machines the feedback loop update time ranges from 31 $\mu$ sec to 62 $\mu$ sec. The assignment of values to this quantity is shown in the Table 3.11. In this case, the lower the feedback time, the better the performance. In some cases, the higher the quality factor, the better the performance.

The unquantifiable quality factors like operator skill, a relative quantity, are important in evaluating the quality interaction  $q_{54}$ . In this case, the opinion of the experts was taken and the quality interaction was divided into a range (Table 3.12). For this unquantifiable interaction ( $q_{54}$ ), the operator with the greatest skill was assigned the highest numerical value, 5, in 1-5 scale and the operator with the lowest skill was assigned the lowest value, 1 in the scale. The interactions like  $q_{12}$  were calculated based on the experiments and e normalized in the scale (1-5).

**Table 3. 11 Values range for quantifiable quality factors**

<b>Feedback loop update time</b>	<b>Value assigned</b>
31 $\mu$ sec-37.2 $\mu$ sec	5
37.3 $\mu$ sec-43.4 $\mu$ sec	4
43.5 $\mu$ sec-49.6 $\mu$ sec	3
49.7 $\mu$ sec-55.8 $\mu$ sec	2
55.9 $\mu$ sec-62 $\mu$ sec	1

**Table 3. 12 Values range for unquantifiable quality factors**

<b>Operator skill</b>	<b>Value assigned</b>
Very high	5
High	4
Moderate	3
Less	2
Very less	1



Similarly the rest of the quality factors were quantified. The range of values or the scale (1-5) was maintained uniform for all the quality factors. For the purpose of illustration, numerical values within the range of scale were assigned and the values were tabulated (Table 3.12).

**Table 3. 13 Numerical quality values of a CNC turning center**

Subsystem\interaction	Q <sub>1</sub> , Q <sub>2</sub> , Q <sub>3</sub> , Q <sub>4</sub> , Q <sub>5</sub> , Q <sub>6</sub>	q <sub>12</sub> , q <sub>21</sub>	q <sub>23</sub> , q <sub>32</sub>	q <sub>26</sub> ,q <sub>62</sub>	q <sub>34</sub> ,q <sub>43</sub>	q <sub>36</sub> ,q <sub>63</sub>	q <sub>45</sub> , q <sub>54</sub>	q <sub>51</sub>
Quantity (1-5)	5, 4, 3, 4, 5, 3	3, 2	4, 5	3, 4	5, 4	2, 4	2, 3	4

The respective numerical values for all the subsystems and the quality interactions from the Table 3.13 were substituted in equations (3.2) and (3.3) and the quality index (QI) obtained for a CNC turning center was as follows:

$$VPQM_{CNCturningcenter} = \begin{matrix} & \begin{matrix} 1 & 2 & 3 & 4 & 5 & 6 \end{matrix} & \text{vertices} \\ \begin{bmatrix} 5 & 3 & 0 & 0 & 0 & 0 \\ 2 & 4 & 4 & 0 & 0 & 3 \\ 0 & 5 & 3 & 5 & 0 & 2 \\ 0 & 0 & 4 & 4 & 2 & 0 \\ 4 & 0 & 0 & 3 & 5 & 0 \\ 0 & 4 & 4 & 0 & 0 & 3 \end{bmatrix} & & \end{matrix} \quad (3.12)$$

$$QI_{CNC turning center} = 52612$$

For interpreting this index, industry should set its bench mark positive and negative indices by substituting the maximum and minimum possible quality. In this case, the positive benchmark or maximum possible QI and negative benchmark or minimum possible QI were

$$\begin{aligned}
& \begin{matrix} 1 & 2 & 3 & 4 & 5 & 6 & \text{vertices} \end{matrix} \\
(VPQM_{CNCturningcenter})_{MAX} &= \begin{bmatrix} 5 & 5 & 0 & 0 & 0 & 0 \\ 5 & 5 & 5 & 0 & 0 & 5 \\ 0 & 5 & 5 & 5 & 0 & 5 \\ 0 & 0 & 5 & 5 & 5 & 0 \\ 5 & 0 & 0 & 5 & 5 & 0 \\ 0 & 5 & 5 & 0 & 0 & 5 \end{bmatrix} \begin{matrix} 1 \\ 2 \\ 3 \\ 4 \\ 5 \\ 6 \end{matrix}
\end{aligned} \tag{3.13}$$

$$(QI_{CNC \text{ turning center}})_{MAX}=3,28,125$$

$$\begin{aligned}
& \begin{matrix} 1 & 2 & 3 & 4 & 5 & 6 & \text{vertices} \end{matrix} \\
(VPQM_{CNCturningcenter})_{MIN} &= \begin{bmatrix} 1 & 1 & 0 & 0 & 0 & 0 \\ 1 & 1 & 1 & 0 & 0 & 1 \\ 0 & 1 & 1 & 1 & 0 & 1 \\ 0 & 0 & 1 & 1 & 1 & 0 \\ 1 & 0 & 0 & 1 & 1 & 0 \\ 0 & 1 & 1 & 0 & 0 & 1 \end{bmatrix} \begin{matrix} 1 \\ 2 \\ 3 \\ 4 \\ 5 \\ 6 \end{matrix}
\end{aligned} \tag{3.14}$$

$$(QI_{CNC \text{ turning center}})_{MIN}=21$$

Hence, the QI of the CNC lathe with similar structure varies between 21 to 3,28,125. Using these benchmark indices the areas of quality improvement can be identified and corrective action can be taken. For example, if the value of the quality interaction  $q_{54}$  is improved from the existing value of 3 to 5, then the percentage change in QI as compared to the original is 10.5%. This shows that a lot of corrective actions can be taken to improve the quality of a CNC machine based on the QI. The interaction  $q_{54}$  is between CNC interface and the operator. The existing control panel for the GILDMEISTER CTX 400 Serie2 lathe is shown in Fig 3.11. The design variables available are letter size, button size, button color, letter color, background color, button shape, touch panel operations label, and number of buttons. When the control panel is designed for 3-factorial experiments for the eight design variables, it gives 18 experimental arrangements. A customer preference is needed for the preference metric. One way to do this is to show the panels to the customers and have them rank order the control panels in terms of how well they like them. This

ranks each trial into a numbering scheme from 1 to 18, best to worst. This can be replicated with many customers, and so a replicated set of data may be developed and ANOVA on the data could be applied to analyze the data. Using this method the best control panel could be chosen for a given application and the quality of the interaction would be improved.



**Fig 3. 11 Control panel of GILDMEISTER CTX 400 Serie2 lathe**

It is quite logical that a CNC turning center with high quality subsystems and high quality interactions will have high overall quality. This index is useful to the industry in evaluating the quality of a CNC machine in the design phase, pre-procurement phase, and in commissioning after the procurement. The methodology is demonstrated up to subsystem level only. It is recommended that one should apply this methodology up to component level.

### **3.11 Summary**

In this chapter, a systems based approach for quality modeling of a CNC machine was presented. A graph theory, matrix algebra and permanent based mathematical model was developed. The developed quality digraph is useful for visual inspection of a CNC machine, the developed matrices are useful for higher computational purpose, and the permanent is the unique way of representing structural quality in the form of a multinomial. An experimental method was presented for quantification of quality interactions between the subsystems.

The proposed methodology was applied by substituting the numerical values. From the experiments conducted, the interaction between feed rate and depth of cut was obtained and the value was 0.0013. The quality of the subsystems and their interactions were obtained in the scale of 1 to 5. After substituting the values, the obtained quality index for this CNC (GILDMEISTER CTX 400 Serie2) was 52,612. To compare the quality index of the CNC lathe the positive and negative benchmark quality indices were obtained - 3,28,125 and 21. Using this methodology the

areas of improvement for the quality can be identified and improved. For example, if you improve the interaction value of  $q_{54}$  from 3 to 5 then the quality index improves by 10.50% as compared to the original. The methods for quality improvement are suggested.

The designer may use this methodology during the conceptual stage for quality based evaluation and optimal selection of a CNC machine from a set of alternatives. The manufacturer may choose the optimal manufacturing process based on the desirable quality derived using this methodology. The maintenance engineer may monitor the health of a CNC machine and can take a corrective action based on the real-time QI of a CNC machine. The developed coefficient of similarity and dissimilarity would be helpful for comparison and ranking between available candidates. With the help of the proposed methodology, the intermediate specifications derived during the design phase can be verified for a quality index and the corrective action may be taken for improving the quality. The proposed methodology is highly flexible, comprehensive and gives a new direction to industry to achieve high quality CNC turning center.

## CHAPTER 4

### DESIGN FOR X-ABILITIES OF CNC TURNING

#### 4.1 Introduction

This chapter describes the concurrent design of CNC turning using a graph theory based approach. That takes into consideration the x-abilities with different interactions. A concurrent design graph shows the x-abilities and the interactions between them. This was converted to matrix form and finally to a permanent index. This index is useful to decide the overall design acceptability of a material for CNC turning.

#### 4.2 Design for X aspects

Designing a CNC turning for integration, complexity, reliability, quality, intelligence, manufacturing, assembly, environment, recyclability, etc. is critical in obtaining a good surface finish product. System engineering is useful in meeting the above requirements during the design stage. Another recommendation involves a shift from the traditional sequential design process to a concurrent engineering design process. It has been claimed that the concurrent design approach will reduce life cycle costs greatly and this is becoming essential in the current competitive environment. As a first step in the proposed methodology, design for X (DFX) aspects, useful at the conceptual design stage, were identified.

##### 4.2.1 Identification of x-abilities

Based on the literature, eight x-abilities were chosen for use in this work. Provisions have been made to give flexibility to the manufacturer, the designer, and the end user in choosing the x-abilities according to their functional needs. For example, in the design of a machine tool, there is little scope for miniaturization of the complete machine for machining the same work piece, so in that case, the designer can give less importance to the miniaturization x-ability.

##### *Design for Integration (DFIN)*

Design for integration of a CNC turning center, a mechatronic application, involves two types of integration (Isermann, 1996) - one is component integration (hardware integration), and another is integration by information processing (software integration). In the process of

integrating electronic components, actuators, sensors and control unit with the mechanical components, issues like working condition of mechanical components (i.e. vibration, heat, dirt etc.) need to be taken into consideration. Some important parameters that should be considered in integration include sampling frequency of sensors, real time control of mechanical components behavior, compatibility of multidisciplinary or intra-disciplinary components, compatibility of in-house and off-the-shelf components.

The software has no physical border conditions i.e. no friction, no corrosion, etc, but it comprises a complete system complexity since it is used as an integration platform as well as a functional carrier with high flexibility.

### ***Design for miniaturization (DFMI)***

The last decade has shown a progressive interest in higher precision and miniaturization in a wide range of manufacturing activities. The methods available for manufacturing micro-sized components are photolithography and micromachining. Limitations of photolithography on silicon substrate include a low aspect ratio and quasi 3D structure (Lim et al., 2002). Micromachining involves the use of micro turning, milling and grinding processes wherein the conventional material removal process has been miniaturized (Rahman et al., 2005). Since a solid tool is used for machining the work piece, a definite 3D shape can be obtained. The limitations of micro turning include machining force influence on machining accuracy and the machinable size limit. In micromachining, industry should factor in design for miniaturization during initial stages of the design. Reducing the size of mechanical components by retaining strength and functionality is a critical task. The increasing processing speed to size ratio and robustness of microelectronic components, enable greater scope for miniaturization. Current leakage, resistance heat dissipation, electrical noise and power loss are crucial design constraints in miniaturization of electronic components. Miniaturization of sensors with increased performance and reduced cost is a key area for research in this field (Alting et al., 2003).

### ***Design for manufacturing (DFM)***

Design for manufacture (DFM) indicates the design for ease of manufacture (O'Driscoll, 2002). As an integral part of DFM, the designer has to select a perfect combination of material and process at the early stages of design. In DFM based concurrent design, the parameters that should be considered at early stages include product-life volume, permissible tooling expenditure

levels, possible part shape categories and complexity levels, appearance factors, accuracy factors etc. DFM deals with structure, property, processibility characteristics of materials chosen. The main benefits of implementing DFM are simplification of products, reduced manufacturing costs, less time-to-market, and improved quality.

### ***Design for Assembly (DFA)***

Design for assembly (DFA) is the ease with which parts or sub assemblies can be assembled together. DFA not only saves on assembly cost but also overall production cost, reduces the inventory, improves the material inflow, production inflow etc. For the assembly of product, the minimum requirement in the assembly equipment is automatic alignment, joining, and quality check with the help of sensors, actuator, controller and software component. Integration of product need to be assembled and production system is the method of choice (Reinhart and Angerer, 2002) to save assembly time. The critical parameters to be considered under this category are number of parts, ease of handling the parts, ease of insertion and fastening, number of fasteners, adhesives and lubricants, assembly sequence, assembly time, assembly method, etc.

### ***Design for intelligence (DFINCE)***

The dream of performing intelligent control on a CNC turning center has never been realized due to low level (G-code) information manipulation, where minimum amount of optimization is possible (Xu and Newman, 2006). The high level intelligent activities which can be performed on a CNC turning center includes- automatic part setup, automatic tool path generation, accurate machining status and results feedback, complete collision avoidance, optimal machining operation sequence, adaptive control and on-machine inspection, etc. Tools like STEP-NC, expert system, inference engine, genetic algorithm, neural networks, fuzzy logic, intelligent agent etc., are helpful to the designer in achieving intelligence in a CNC turning center. The new standard available in design for intelligence of a CNC turning center is ISO 14649 (ISO 14649-1, 2003; ISO 14649-10, 2003; ISO 14649-11, 2003; ISO 14649-111, 2001; ISO/DIS 14649-12, 2003; ISO/DIS 14649-121, 2003).

### ***Design for environment (DFE)***

Environmental requirements are driven by political and public awareness concerning increasingly unpredictable climate change, depletion of natural resources, increasing challenge of waste disposal and water pollution. The need to consider the potential impact of a design in the early stage of its development would be beneficial in terms of time and cost (Zahari et al., 2010). The aim of the product design engineer is to assess the environment impact of each design feature (holes, chamfer, surface finish etc.), based on the minimum information available at embodiment design phase. The total equivalent CO<sub>2</sub> emission can be assessed based on the power consumption of the machine, lubricant and oil consumption and amount of chip removed during the machining process.

### ***Design for reliability (DFR)***

The reliability of a CNC turning center has become an important concern with increasing number of multidisciplinary components like sensors, actuators, electrical connections, electronic circuits, mechanical components etc. and interactions among them. Hence, considering design for reliability of a CNC turning center at the initial design stages leads to lower life cycle cost, reduced down time, reduced unexpected failure, higher safety, etc. The critical parameters influencing reliability of electronic components include the effect of vibrations, dirt in the working environment, thermal stresses and thermo-mechanical stresses. For the mechanical components, stresses (tensile, compression, bending, torsion), fracture strength, fatigue strength, creep resistance and corrosion resistance are the critical parameters. The location of faults in the software is closely related to the complexity characteristics (Munson, 1996). Critical parameters in the software domain include variability in functional complexity, operational complexity, complexity of code/programmer's skill ratio etc. The designer has to consider these parameters in an integrated manner to achieve the best results.

### ***Design for quality (DFQ)***

The quality of a CNC turning operation is judged not only on the basis of the quality of its structural components, but also on the surface finish of the machined work piece. Surface quality is an important performance index to evaluate the productivity of the machine tool and as well as the machined components (Shaw, 1984; Davim, 2001). The quality of surface finish also depends on the feed, cutting and thrust forces, tool wear, tool life, tool temperature, etc. In the



case of certain components, quality cannot be tested directly, but it can be assessed by testing some related visible factors. These factors include functionality (correctness, usability, reliability, and integrity), engineering (efficiency, testability, strength, user-friendliness, operating conditions, and intelligence) and adaptability (flexibility, maintainability, recyclability, eco-friendliness, reusability). Consideration of these factors at the initial stage of design is vital in achieving a high quality.

Under the eight design x-abilities chosen, the design parameters corresponding to each x-ability were identified (Table 4.1). In this Table, each design parameter is given a code depending upon the x-ability under which it is listed. The generalized code is  $X_iDP_j$ , where  $i=1,2..8$ , and  $j=1,2..n$ , 'n' is the number of design parameters under  $i^{th}$  x-ability.

**Table 4. 1 Critical design parameters for concurrent design of CNC turning**

<p>DFIN(DFX<sub>1</sub>)</p> <ul style="list-style-type: none"> <li>• Working condition of mechanical components (Heat, dirt, vibration)- <math>X_1DP_1</math></li> <li>• Sampling frequency of sensors- <math>X_1DP_2</math></li> <li>• Real time control- <math>X_1DP_3</math></li> <li>• Compatibility of components- <math>X_1DP_4</math></li> <li>• Data transfer rate- <math>X_1DP_5</math></li> </ul>
<p>DFMI(DFX<sub>2</sub>)</p> <ul style="list-style-type: none"> <li>• Software portability- <math>X_2DP_1</math></li> <li>• Size/processing speed- <math>X_2DP_2</math></li> <li>• Size/weight ratio of physical structure- <math>X_2DP_3</math></li> <li>• Electric noise due to miniaturization of microelectronics- <math>X_2DP_4</math></li> <li>• Current leakage due to miniaturization of microelectronics- <math>X_2DP_5</math></li> <li>• Power loss due to miniaturization of microelectronics- <math>X_2DP_6</math></li> <li>• Resistance heat dissipation due to miniaturization of microelectronics- <math>X_2DP_7</math></li> </ul>
<p>DFM(DFX<sub>3</sub>)</p> <ul style="list-style-type: none"> <li>• Product-life volume - <math>X_3DP_1</math></li> <li>• Permissible tooling expenditure- <math>X_3DP_2</math></li> <li>• Possible part shape category - <math>X_3DP_3</math></li> <li>• Complexity level- <math>X_3DP_4</math></li> <li>• Appearance factor- <math>X_3DP_5</math></li> <li>• Accuracy factor- <math>X_3DP_6</math></li> <li>• Tolerances- <math>X_3DP_7</math></li> <li>• Cost- <math>X_3DP_8</math></li> <li>• Cutting parameters- <math>X_3DP_9</math></li> <li>• Material characteristics- <math>X_3DP_{10}</math></li> </ul>
<p>DFA(DFX<sub>4</sub>)</p> <ul style="list-style-type: none"> <li>• Number of components and sub assemblies- <math>X_4DP_1</math></li> </ul>

<ul style="list-style-type: none"> <li>• Ease of handling the parts- <math>X_4DP_2</math></li> <li>• Ease of insertion and fastening- <math>X_4DP_3</math></li> <li>• Number of fastener- <math>X_4DP_4</math></li> <li>• Adhesives and lubricants- <math>X_4DP_5</math></li> </ul>
<p>DFINCE(DFX<sub>5</sub>)</p> <ul style="list-style-type: none"> <li>• Self-adaption- <math>X_5DP_1</math></li> <li>• Self-organization- <math>X_5DP_2</math></li> <li>• Evolutionary learning- <math>X_5DP_3</math></li> <li>• Decision making capacity- <math>X_5DP_4</math></li> <li>• Positional accuracy- <math>X_5DP_5</math></li> </ul>
<p>DFE(DFX<sub>6</sub>)</p> <ul style="list-style-type: none"> <li>• Material removal rate- <math>X_6DP_1</math></li> <li>• Energy consumption- <math>X_6DP_2</math></li> <li>• Coolant consumption- <math>X_6DP_3</math></li> <li>• Toxicity on product disposal- <math>X_6DP_4</math></li> <li>• Recycling potential- <math>X_6DP_5</math></li> <li>• Cost estimation of recycling- <math>X_6DP_6</math></li> <li>• Toxicity of the manufacturing process disposals- <math>X_6DP_7</math></li> </ul>
<p>DFR(DFX<sub>7</sub>)</p> <p><i>Electronic components</i></p> <ul style="list-style-type: none"> <li>• Effect of vibrations, dirt- <math>X_7DP_1</math></li> <li>• Thermal and thermo-mechanical stresses- <math>X_7DP_2</math></li> </ul> <p><i>Mechanical components</i></p> <ul style="list-style-type: none"> <li>• Stresses- <math>X_7DP_3</math></li> <li>• Fracture strength- <math>X_7DP_4</math></li> <li>• Fatigue strength- <math>X_7DP_5</math></li> <li>• Creep resistance- <math>X_7DP_6</math></li> <li>• Corrosion resistance- <math>X_7DP_7</math></li> </ul> <p><i>Software</i></p> <ul style="list-style-type: none"> <li>• Functional complexity- <math>X_7DP_8</math></li> <li>• Operational complexity- <math>X_7DP_9</math></li> <li>• Ratio of complexity to programmer skill ratio- <math>X_7DP_{10}</math></li> </ul>
<p>DFQ(DFX<sub>8</sub>)</p> <p><i>Functionality</i></p> <ul style="list-style-type: none"> <li>• Correctness- <math>X_8DP_1</math></li> <li>• Usability- <math>X_8DP_2</math></li> <li>• Integrity- <math>X_8DP_3</math></li> <li>• Response time- <math>X_8DP_4</math></li> <li>• Dimensional accuracy- <math>X_8DP_5</math></li> </ul> <p><i>Engineering</i></p> <ul style="list-style-type: none"> <li>• Efficiency- <math>X_8DP_6</math></li> <li>• Testability- <math>X_8DP_7</math></li> <li>• Strength- <math>X_8DP_8</math></li> </ul>

- User friendliness-  $X_8DP_9$
- Operating conditions-  $X_8DP_{10}$
- Surface quality-  $X_8DP_{11}$
- Different forces-  $X_8DP_{12}$
- Tool wear-  $X_8DP_{13}$
- Tool life-  $X_8DP_{14}$

*Adaptability*

- Flexibility-  $X_8DP_{15}$
- Maintainability-  $X_8DP_{16}$
- Recyclability-  $X_8DP_{17}$
- Eco-friendliness-  $X_8DP_{18}$
- Reusability-  $X_8DP_{19}$

The methodology followed at the initial design stage in the conventional concurrent engineering design approach, is shown in Fig 4.1. In this methodology all the eight x-abilities  $DFX_i$ ,  $i=1,2,\dots,8$  are considered parallel to obtain a CNC turning operation with high quality and exceptional design characteristics.

In the conventional methodology, the interaction among the x-abilities  $DFX_1$  to  $DFX_8$  are not taken into consideration, where interactions among these x-abilities are most significant in design and development of a CNC turning. In order to address this limitation, a methodology, based on the use of graph theory is proposed.

#### 4.2.2 Graph theory based design methodology

An integrated systems approach, which considers all the x-abilities and interactions, is required for design and development of a CNC turning center. CNC turning with integrated x-abilities was represented by  $[M, I]$  where the x-abilities/design aspects were represented as a design set  $\{M\}=\{M_1, M_2,\dots,M_n\}$  and interactions or interdependence were represented by a set  $\{I\}=\{I_1, I_2,\dots,I_n\}$ , where  $M_i$  represents  $i^{\text{th}}$  x-ability and the associated design parameters and  $I_j$  represents  $j^{\text{th}}$  interactions between the two corresponding design aspects/x-abilities. In general, the graph was represented mathematically by  $G = \{N, E\}$ ; let  $N$  represent nodes/vertices of the graph  $\{N\}=\{N_1, N_2,\dots,N_n\}$  and  $E$  represent the edges connecting these nodes  $\{E\}=\{e_1, e_2,\dots,e_m\}$ . In order to represent a CNC turning center mathematically, all the eight design aspects/x-abilities were denoted by eight nodes and corresponded to the set  $\{N\}$ , and the interactions between the design aspects were represented by the set  $\{E\}$ . Depending on the type

of interaction between the nodes, the design graph was shown as a directional if the edges were directional and a non-directional otherwise.

#### 4.2.2.1 Concurrent design digraph (CDD)

In order to consider life cycle issues in the process of CNC turning center design, eight design aspects or x-abilities were considered concurrently i.e. integration (DFX<sub>1</sub>), miniaturization (DFX<sub>2</sub>), manufacturability (DFX<sub>3</sub>), assembly (DFX<sub>4</sub>), intelligence (DFX<sub>5</sub>), environment (DFX<sub>6</sub>), quality (DFX<sub>7</sub>), and reliability (DFX<sub>8</sub>). To develop the design digraph, eight x-abilities {DFX<sub>1</sub>, DFX<sub>2</sub>, DFX<sub>3</sub>, DFX<sub>4</sub>, DFX<sub>5</sub>, DFX<sub>6</sub>, DFX<sub>7</sub>, DFX<sub>8</sub>} were represented by eight nodes {N<sub>1</sub>, N<sub>2</sub>, N<sub>3</sub>, N<sub>4</sub>, N<sub>5</sub>, N<sub>6</sub>, N<sub>7</sub>, N<sub>8</sub>} respectively, i.e. DFX<sub>i</sub> is represented by N<sub>i</sub>. The interaction between any two x-abilities say DFX<sub>i</sub> and DFX<sub>j</sub> i.e. N<sub>i</sub> and N<sub>j</sub> was represented by e<sub>ij</sub>. If the interaction between the design aspects/x-abilities had directional characteristics then the graph theory representation for this was e<sub>ij</sub> ≠ e<sub>ji</sub>. This means that i<sup>th</sup> node influence on j<sup>th</sup> node is not equal to j<sup>th</sup> node influence on i<sup>th</sup> node. The proposed colored digraph is shown in Fig 4.2.

In this colored digraph, the interactions are differentiated by a color. A color was assigned to an interaction based on the node from which it originated. For example, the interaction originating from node 1 i.e. N<sub>1</sub> is represented by red color. The color differentiation reduces the complexity involved in reading the graph. For the purpose of demonstrating the methodology some of the interactions were not considered in the digraph shown in Fig 4.2. For example, DFX<sub>7</sub> may need interaction information from DFX<sub>6</sub>, but interaction information from DFX<sub>7</sub> to DFX<sub>6</sub> may be weaker and therefore be ignored. The graph representation is helpful for visual inspection and understanding, but the graph is not computational friendly for storage and retrieval of data and also for further mathematical operations.

#### 4.2.2.2 Adjacency matrix

In order to store and retrieve the data from the graph and for further mathematical operations, the matrix algebra was used. The digraph shown in Fig 4.2 could easily be converted into a matrix representation using the graph theory and Boolean algebra. A digraph with 'm' nodes will lead to m<sup>th</sup> order matrix, having values (0,1).

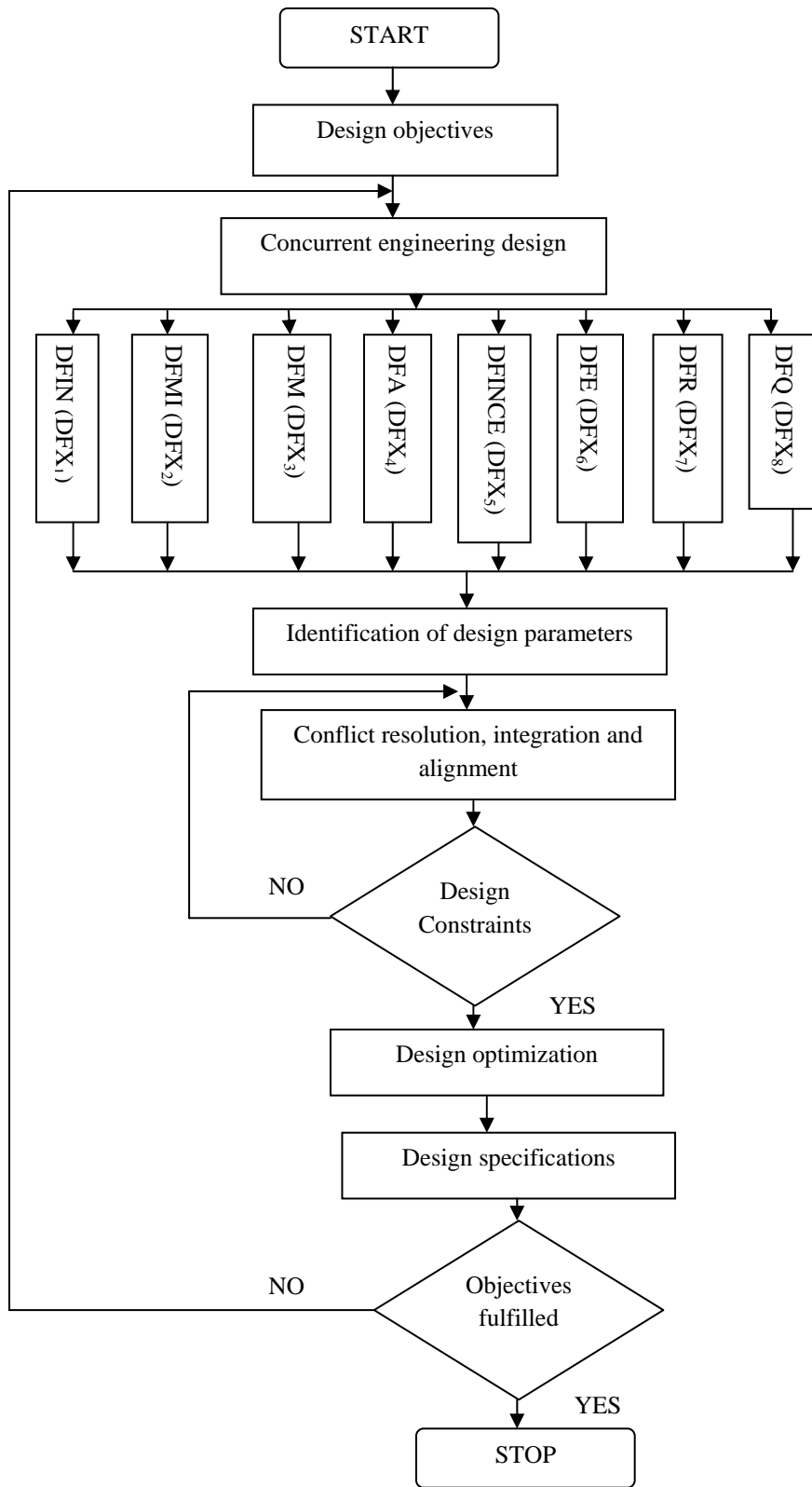


Fig 4. 1 Concurrent engineering design cycle

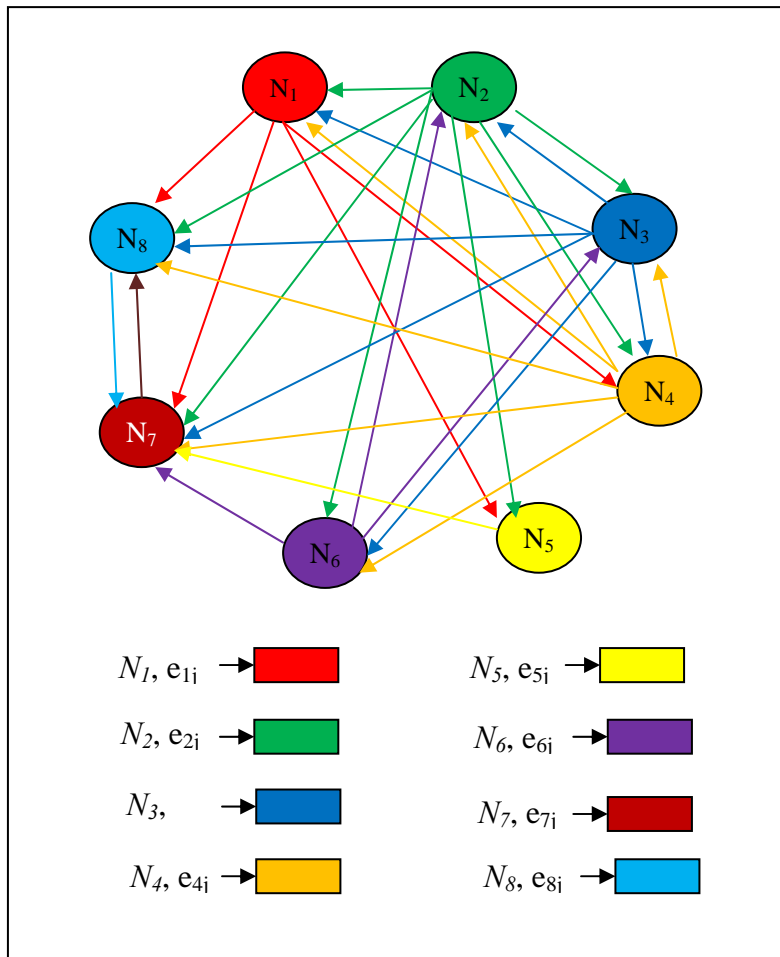


Fig 4. 2 Colored concurrent design graph of CNC turning

The rows and columns in this matrix represent the eight design aspects shown in the digraph. The design adjacency matrix  $A = [e_{ij}]$ , where

$e_{ij} = 1$ , if  $i^{\text{th}}$  design aspect interacts with  $j^{\text{th}}$  design aspect

$= 0$ , otherwise

The design adjacency matrix for the digraph is written as:

$$\begin{matrix}
& N_1 & N_2 & N_3 & N_4 & N_5 & N_6 & N_7 & N_8 & \text{vertices} \\
A = & \begin{bmatrix}
0 & 0 & 0 & 1 & 1 & 0 & 1 & 1 \\
1 & 0 & 1 & 1 & 1 & 1 & 1 & 1 \\
1 & 1 & 0 & 1 & 0 & 1 & 1 & 1 \\
1 & 1 & 1 & 0 & 0 & 1 & 1 & 1 \\
0 & 0 & 0 & 0 & 0 & 0 & 1 & 0 \\
0 & 1 & 1 & 0 & 0 & 0 & 1 & 0 \\
0 & 0 & 0 & 0 & 0 & 0 & 0 & 1 \\
0 & 0 & 0 & 0 & 0 & 0 & 1 & 0
\end{bmatrix} & \begin{matrix}
N_1 \\
N_2 \\
N_3 \\
N_4 \\
N_5 \\
N_6 \\
N_7 \\
N_8
\end{matrix}
\end{matrix} \quad (4.1)$$

#### 4.2.2.3 Concurrent design matrix

To store and retrieve the data from the graph and for further mathematical operations, matrix algebra was chosen. The graph shown in Fig 4.2 was translated into a permanent matrix as discussed in chapter 3. A generalized concurrent design variable permanent matrix (CDVPM<sub>G</sub>) was developed and given below

$$\begin{matrix}
& 1 & 2 & \dots & i & \dots & n & \text{vertices} \\
CDVPM_G = & \begin{bmatrix}
N_1 & e_{12} & \dots & e_{1i} & \dots & e_{1n} \\
e_{21} & N_2 & & & & \\
\vdots & & \ddots & & & \\
e_{i1} & & & N_i & & e_{in} \\
\vdots & & & & \ddots & \\
e_{n1} & \dots & \dots & e_{ni} & \dots & N_n
\end{bmatrix} & \begin{matrix}
1 \\
\vdots \\
i \\
\vdots \\
n
\end{matrix}
\end{matrix} \quad (4.2)$$

The equation (4.2) is a generalized form for ‘n’ number of x-abilities. The value for ‘n’ is decided by the design engineer depending on the application product. For example, the CDVPM for the CDD shown in Fig 4.2 was derived as follows:

$$\begin{matrix}
& 1 & 2 & 3 & 4 & 5 & 6 & 7 & 8 & \text{Vertices} \\
CDVPM = & \begin{bmatrix}
N_1 & 0 & 0 & e_{14} & e_{15} & 0 & e_{17} & e_{18} \\
e_{21} & N_2 & e_{23} & e_{24} & e_{25} & e_{26} & e_{27} & e_{28} \\
e_{31} & e_{32} & N_3 & e_{34} & 0 & e_{36} & e_{37} & e_{38} \\
e_{41} & e_{42} & e_{43} & N_4 & 0 & e_{46} & e_{47} & e_{48} \\
0 & 0 & 0 & 0 & N_5 & 0 & e_{57} & 0 \\
0 & e_{62} & e_{63} & 0 & 0 & N_6 & e_{67} & 0 \\
0 & 0 & 0 & 0 & 0 & 0 & N_7 & e_{78} \\
0 & 0 & 0 & 0 & 0 & 0 & e_{87} & N_8
\end{bmatrix} & \begin{matrix}
1 \\
2 \\
3 \\
4 \\
5 \\
6 \\
7 \\
8
\end{matrix}
\end{matrix} \quad (4.3)$$

In equation (4.3) the eight design aspects are diagonal elements i.e.  $N_1, N_2, \dots, N_8$ , and the off-diagonal elements represents the interactions between the design aspects. This model of expression considers all the quantitative values of the design aspects and interactions, without any loss of information in multinomial representation. The CDVPM is not a unique representation, however, because by interchanging rows and columns the matrix may change.

#### 4.2.2.4 Concurrent Design Multinomial (CDM)

To develop a unique and comprehensive design model, an expression named permanent which is frequently used in combinatorial mathematics was derived, (Marcus and Minc, 1965). A permanent multinomial was derived based on equation (4.3), and a design index is obtained. The design index decides whether the overall design and development of a CNC turning is acceptable according to the design aspects and the interactions. The multinomial is a unique representation obtained by considering the design for X-abilities together in a single attempt. When the actual values of each term are substituted in the multinomial, the final value after the algebraic addition gives a design index, which can be used to compare conceptual design alternatives. The multinomial derived from the equation (4.3) is as follows:

$$\begin{aligned}
\text{CDM} &= \text{per}(\text{CDVPM}) = \\
& \prod (Group I) + \sum (Group III) + \sum (Group IV) + \sum (Group V) + \sum (Group VI) \\
& + \sum (Group VII) + \sum (Group VIII) + \sum (Group IX) \\
& = \prod_1^8 N_i + \left[ \sum_{i=1}^7 \sum_{j=i+1}^8 \sum_{k=1}^3 \sum_{l=k+1}^4 \sum_{m=l+1}^5 \sum_{n=m+1}^6 \sum_{o=n+1}^7 \sum_{p=o+1}^8 \sum_{k,l,m,n,o,p=pnu}^8 (e_{ij}e_{ji}) N_k N_l N_m N_n N_o N_p \right] + \\
& \left[ \sum_{i=1}^6 \sum_{j=i+1}^7 \sum_{k=j+1}^8 \sum_{l=1}^4 \sum_{m=l+1}^5 \sum_{n=m+1}^6 \sum_{o=n+1}^7 \sum_{p=o+1}^8 \sum_{k,l,m,n,o,p=pnu}^8 (e_{ij}e_{jk}e_{ki} + e_{ik}e_{kj}e_{ji}) N_l N_m N_n N_o N_p \right] + \\
& \left[ \sum_{i=1}^5 \sum_{j=i+1}^7 \sum_{k=i+1}^8 \sum_{l=i+1}^8 \sum_{m=1}^5 \sum_{n=m+1}^6 \sum_{o=n+1}^7 \sum_{p=o+1}^8 \sum_{k,l,m,n,o,p=pnu}^8 (e_{ij}e_{jk}e_{kl}e_{li} + e_{il}e_{lk}e_{kj}e_{ji}) N_m N_n N_o N_p \right] \\
& + \left[ \sum_{i=1}^5 \sum_{j=i+1}^8 \sum_{k=i+1}^7 \sum_{l=i+2}^8 \sum_{m=1}^5 \sum_{n=m+1}^6 \sum_{o=n+1}^7 \sum_{p=o+1}^8 \sum_{k,l,m,n,o,p=pnu}^8 (e_{ij}e_{ji})(e_{kl}e_{lk}) N_m N_n N_o N_p \right]
\end{aligned} \tag{4.4}$$



$$\begin{aligned}
& + \left[ \sum_{i=1}^4 \sum_{j=i+1}^7 \sum_{k=i+1}^8 \sum_{l=i+1}^8 \sum_{m=j+1}^8 \sum_{n=1}^6 \sum_{o=n+1}^7 \sum_{p=o+1}^8 \sum_{k,l,m,n,o,p=pnu} \left( e_{ij} e_{jk} e_{kl} e_{lm} e_{mi} + e_{im} e_{ml} e_{lk} e_{kj} e_{ji} \right) N_n N_o N_p \right. \\
& + \left. \sum_{i=1}^4 \sum_{j=i+1}^7 \sum_{k=i+1}^8 \sum_{l=1}^7 \sum_{m=l+1}^8 \sum_{n=1}^6 \sum_{o=n+1}^7 \sum_{p=o+1}^8 \sum_{k,l,m,n,o,p=pnu} \left( e_{ij} e_{jk} e_{ki} + e_{ik} e_{kj} e_{ji} \right) (e_{lm} e_{ml}) N_n N_o N_p \right] \\
& + \left[ \sum_{i=1}^3 \sum_{j=i+1}^7 \sum_{k=i+1}^8 \sum_{l=i+1}^8 \sum_{m=i+1}^8 \sum_{n=j+1}^8 \sum_{o=1}^7 \sum_{p=o+1}^8 \sum_{k,l,m,n,o,p=pnu} \left( e_{ij} e_{jk} e_{kl} e_{lm} e_{mn} e_{ni} + e_{in} e_{nm} e_{ml} e_{lk} e_{kj} e_{ji} \right) N_o N_p \right. \\
& + \sum_{i=1}^3 \sum_{j=i+1}^7 \sum_{k=i+1}^8 \sum_{l=j+1}^7 \sum_{m=1}^8 \sum_{n=m+1}^7 \sum_{o=1}^7 \sum_{p=o+1}^8 \sum_{k,l,m,n,o,p=pnu} \left( e_{ij} e_{jk} e_{kl} e_{li} + e_{il} e_{lk} e_{kj} e_{ji} \right) (e_{mn} e_{nm}) N_o N_p \\
& + \sum_{i=1}^3 \sum_{j=i+1}^7 \sum_{k=j+1}^8 \sum_{l=1}^6 \sum_{m=l+1}^7 \sum_{n=m+1}^8 \sum_{o=1}^7 \sum_{p=o+1}^8 \sum_{k,l,m,n,o,p=pnu} \left( e_{ij} e_{jk} e_{ki} + e_{il} e_{lk} e_{ki} \right) (e_{lm} e_{mn} e_{nl} + e_{ln} e_{nm} e_{ml}) N_o N_p \\
& + \left. \sum_{i=1}^3 \sum_{j=i+1}^8 \sum_{k=j+1}^7 \sum_{l=1}^8 \sum_{m=l+1}^7 \sum_{n=m+1}^8 \sum_{o=1}^7 \sum_{p=o+1}^8 \sum_{k,l,m,n,o,p=pnu} \left( e_{ij} e_{ji} \right) (e_{kl} e_{lk}) (e_{mn} e_{nm}) N_o N_p \right] + \\
& \left[ \sum_{i=1}^2 \sum_{j=i+1}^7 \sum_{k=i+1}^8 \sum_{l=i+1}^8 \sum_{m=i+1}^8 \sum_{n=i+1}^7 \sum_{o=j+1}^7 \sum_{p=1}^8 \sum_{k,l,m,n,o,p=pnu} \left( e_{ij} e_{jk} e_{kl} e_{lm} e_{mn} e_{no} e_{oi} + e_{io} e_{on} e_{nm} e_{ml} e_{lk} e_{kj} e_{ji} \right) N_p \right. \\
& + \sum_{i=1}^2 \sum_{j=i+1}^7 \sum_{k=i+1}^8 \sum_{l=i+1}^8 \sum_{m=j+1}^7 \sum_{n=1}^8 \sum_{o=n+1}^7 \sum_{p=1}^8 \sum_{k,l,m,n,o,p=pnu} \left( e_{ij} e_{jk} e_{kl} e_{lm} e_{mi} + e_{im} e_{ml} e_{lk} e_{kj} e_{ji} \right) (e_{mn} e_{nm}) N_p \\
& + \sum_{i=1}^2 \sum_{j=i+1}^7 \sum_{k=i+1}^8 \sum_{l=j+1}^6 \sum_{m=1}^7 \sum_{n=m+1}^7 \sum_{o=n+1}^8 \sum_{p=1}^8 \sum_{k,l,m,n,o,p=pnu} \left( e_{ij} e_{jk} e_{kl} e_{li} + e_{il} e_{lk} e_{kj} e_{ji} \right) (e_{mn} e_{no} e_{om} + e_{mo} e_{on} e_{nm}) N_p \\
& + \left. \sum_{i=1}^2 \sum_{j=i+1}^7 \sum_{k=i+1}^8 \sum_{l=1}^7 \sum_{m=l+1}^8 \sum_{n=1}^7 \sum_{o=n+1}^8 \sum_{p=1}^8 \sum_{k,l,m,n,o,p=pnu} \left( e_{ij} e_{jk} e_{ki} + e_{ik} e_{kj} e_{ji} \right) (e_{lm} e_{ml}) (e_{no} e_{on}) N_p \right] \\
& + \left[ \sum_{i=1}^1 \sum_{j=i+1}^7 \sum_{k=i+1}^8 \sum_{l=i+1}^8 \sum_{m=i+1}^8 \sum_{n=i+1}^8 \sum_{o=i+1}^8 \sum_{p=j+1}^8 \sum_{k,l,m,n,o,p=pnu} \left( e_{ij} e_{jk} e_{kl} e_{lm} e_{mn} e_{no} e_{op} e_{pi} + e_{ip} e_{po} e_{on} e_{nm} e_{ml} e_{lk} e_{kj} e_{ji} \right) \right. \\
& + \sum_{i=1}^1 \sum_{j=i+1}^7 \sum_{k=i+1}^8 \sum_{l=i+1}^8 \sum_{m=i+1}^8 \sum_{n=j+1}^7 \sum_{o=1}^7 \sum_{p=o+1}^8 \sum_{k,l,m,n,o,p=pnu} \left( e_{ij} e_{jk} e_{kl} e_{lm} e_{mn} e_{ni} + e_{in} e_{nm} e_{ml} e_{lk} e_{kj} e_{ji} \right) (e_{op} e_{po}) \\
& + \left. \sum_{i=1}^1 \sum_{j=i+1}^7 \sum_{k=i+1}^8 \sum_{l=i+1}^8 \sum_{m=j+1}^6 \sum_{n=1}^7 \sum_{o=n+1}^8 \sum_{p=o+1}^8 \sum_{k,l,m,n,o,p=pnu} \left( e_{ij} e_{jk} e_{kl} e_{lm} e_{mi} + e_{im} e_{ml} e_{lk} e_{kj} e_{ji} \right) (e_{no} e_{op} e_{pn} + e_{np} e_{po} e_{on}) \right]
\end{aligned}$$

$$\begin{aligned}
& + \sum_{i=1}^1 \sum_{j=i+1}^7 \sum_{k=i+1}^8 \sum_{l=j+1}^8 \sum_{m=1}^5 \sum_{n=m+1}^6 \sum_{o=n+1}^7 \sum_{p=o+1}^8 \sum_{k,l,m,n,o,p=pnu}^8 (e_{ij}e_{jk}e_{kl}e_{li} + e_{il}e_{lk}e_{kj}e_{ji})(e_{mn}e_{no}e_{op}e_{pm} + e_{mp}e_{po}e_{on}e_{nm}) \\
& + \sum_{i=1}^1 \sum_{j=i+1}^7 \sum_{k=j+1}^8 \sum_{l=1}^6 \sum_{m=l+1}^7 \sum_{n=m+1}^8 \sum_{o=1}^7 \sum_{p=o+1}^8 \sum_{k,l,m,n,o,p=pnu}^8 (e_{ij}e_{jk}e_{ki} + e_{il}e_{lk}e_{ki})(e_{lm}e_{mn}e_{nl} + e_{ln}e_{nm}e_{ml})(e_{op}e_{po}) \\
& + \left. \sum_{i=1}^3 \sum_{j=i+1}^8 \sum_{k=j+1}^7 \sum_{l=1}^8 \sum_{m=l+1}^7 \sum_{n=m+1}^8 \sum_{o=1}^7 \sum_{p=o+1}^8 \sum_{k,l,m,n,o,p=pnu}^8 (e_{ij}e_{ji})(e_{kl}e_{lk})(e_{mn}e_{nm})(e_{op}e_{po}) \right]
\end{aligned}$$

In the equation (4.4), pnu represents a previously not used subscript. In a generalized permanent expression for the equation (4.3), without any zero off-diagonal elements may contain 8! i.e.40320 terms. After substituting zero in some of the off-diagonal elements, the number of terms became reduced. These terms in the multinomial were grouped into M+1(M number of x-abilities) groups for unique representation and interpretation. The multinomial consists of different combinations of x-abilities and interaction components, for instance unconnected vertices N<sub>is</sub>, dyads e<sub>ijeji</sub>, three node loop e<sub>ijejkeki</sub>, four node loop e<sub>ijejkekleli</sub>, etc.. The terms in the multinomial were arranged in descending order of the number of nodes in a term; the last term did not contain any unconnected node. Each term in the CDM provided information required for comparing compatibility and analysis. The permanent function had terms in different groups as follows:

- The first group contained only one term, which was a set of eight unconnected nodes N<sub>is</sub>. The graphical representation of the first group of terms is shown in Fig 4.3. The first group of terms indicated that all the x-abilities should be considered individually while, at the same time, a complete understanding of the CNC turning was required for achieving the optimal.

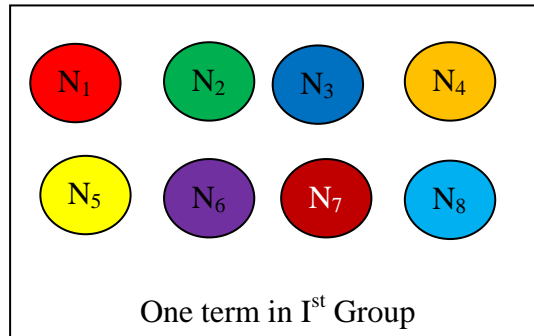


Fig 4. 3 Graphical representation of first group of terms in CDM

- The second group was absent, because the x-abilities cannot connect or influence itself.
- The third group was a combination of dyad  $e_{ij}e_{ji}$ , and the remaining six unconnected nodes  $N_i$ s, for example  $(e_{12}e_{21})(N_3N_4N_5N_6N_7N_8)$ . In this  $/e_{12}e_{21}/$ , represented a dyad between the x-abilities integration and miniaturization. In consideration of this entity, the analyst would be able to determine the factors and causes attributing to it, in conjunction with other entities of the term. The graphical representation of the third group of terms is shown in Fig 4.4.

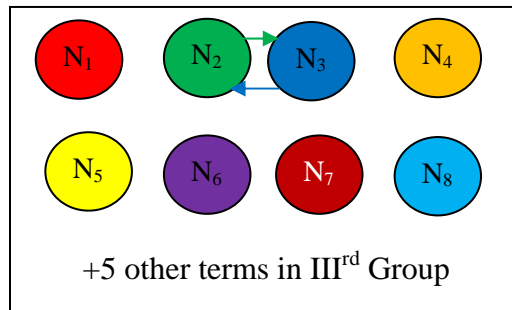


Fig 4. 4 Graphical representation of third group of terms in CDM

- The fourth group consisted of a three node loop  $e_{ij}e_{jk}e_{ki}$ , and five unconnected nodes  $N_i$ s. For example, the part of the term  $(e_{12}e_{23} e_{31})( N_4N_5N_6N_7N_8)$ ,  $/e_{12}e_{23} e_{31}/$  represented a loop between the x-abilities integration, miniaturization and manufacturing. In-depth analysis of this would be likely to reveal how these characteristic combination are contributing to the robustness of the design in association with other entities of the terms. The graphical representation of fourth group of terms is shown in Fig 4.5.

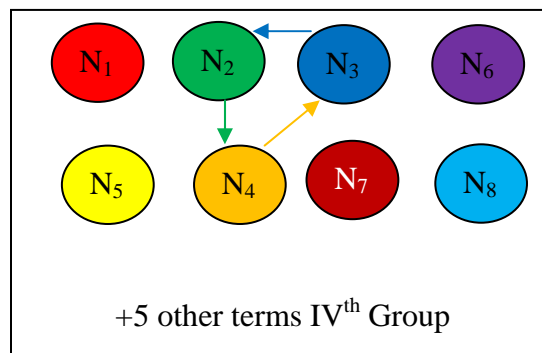


Fig 4. 5 Graphical representation of fourth group of terms in CDM

- The fifth group consisted of two sub groups, the first subgroup had four node loop i.e  $e_{ij}e_{jk}e_{kl}e_{li}$ , and the four unconnected nodes  $N_i$ s, and the second subgroup had two dyads and four unconnected nodes. If the numerical value of the four node loop  $/e_{ij}e_{jk}e_{kl}e_{li}/$  or

the two dyads  $/ e_{ij}e_{ji} // e_{kl}e_{lk} /$  was on the higher side, then more attention would be required by the designer in considering these four x-abilities together along with the remaining four independent x-abilities. The graphical representation of the fifth group of terms is shown in Fig 4.6.

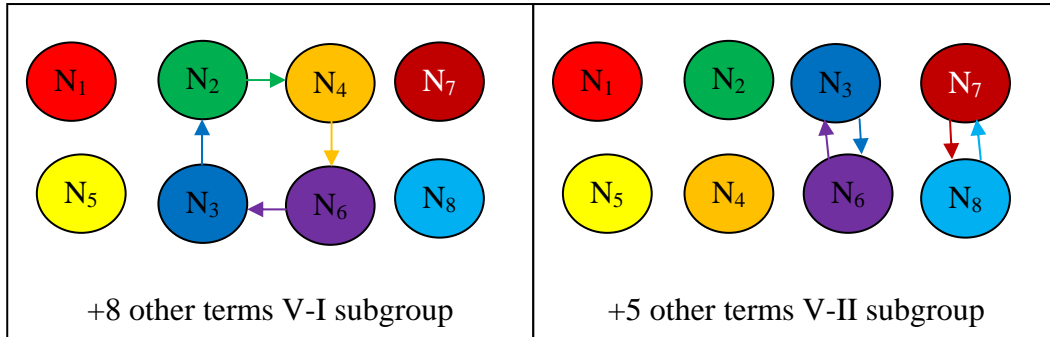


Fig 4. 6 Graphical representation of fifth group of terms in CDM

- The sixth group consisted of two subgroups, the first subgroup consisting of a five node loop ( $e_{ij}e_{jk}e_{kl}e_{lm}e_{mi}$ ) and three unconnected nodes, and second subgroup consisting of a dyad ( $e_{ij}e_{ji}$ ), three node loop ( $e_{kl}e_{lm}e_{mk}$ ), and three unconnected nodes. If the numerical value of the connected x-abilities were found to be on the higher side, then more attention should be given to this loop and dyed along with unconnected x-abilities for design of best CNC turning. The graphical representation of the sixth group of terms is shown in Fig 4.7.

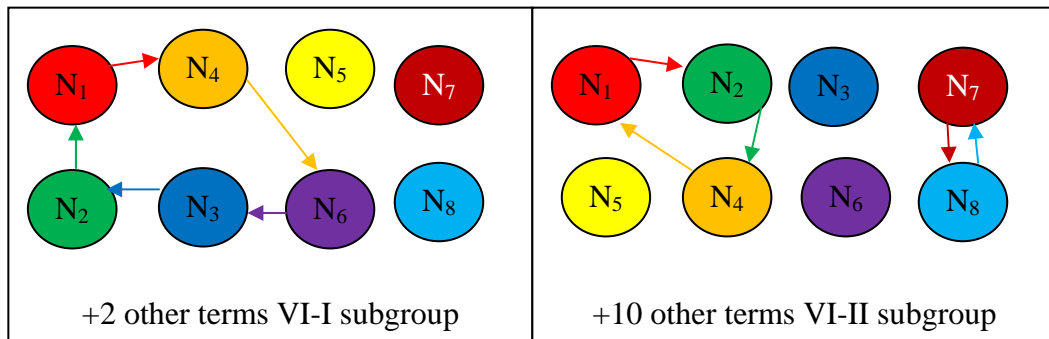
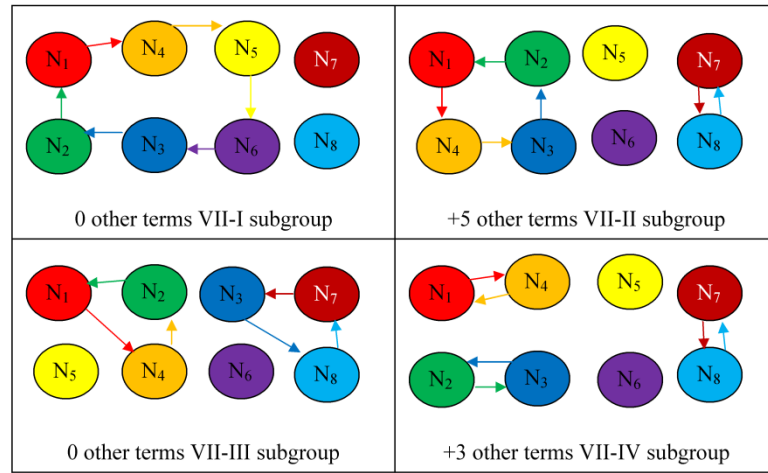


Fig 4. 7 Graphical representation of sixth group of terms in CDM

- The seventh group consisted of four subgroups, the first subgroup consisting of six node loop ( $e_{ij}e_{jk}e_{kl}e_{lm}e_{mn}e_{ni}$ ) and two unconnected nodes, the second subgroup consisting of a dyad, a four node loop, and two unconnected nodes, the third subgroup consisting of

three node loops two in number and two unconnected nodes, and the fourth subgroup having three dyads and two unconnected nodes. The subgroup with the highest numerical value should be given greater attention. The corresponding loop characteristics along with the independent x-abilities would be significant in concurrent design of a CNC turning. The graphical representation of the seventh group of terms is shown in Fig 4.8.



**Fig 4. 8 Graphical representation of seventh group of terms in CDM**

- The eighth group of terms consisted of three subgroups, the first subgroup had a five node loop, a dyad and a unconnected node, the second subgroup had a three node loop, a four node loop and a unconnected node, the third subgroup had two dyads, a three node loop and a unconnected node. For example, if the numerical value of the first group was on the higher side, then the characteristics of loop /  $e_{14}e_{46}e_{63}e_{32}e_{21}$  / and dyad /  $e_{78}e_{87}$  / along with the integration x-ability would be significant in the concurrent design of CNC turning. The graphical representation of the eighth group of terms is shown in Fig 4.9.
- The ninth group of terms did not have any unconnected nodes and they were divided into seven subgroups, the first subgroup consisting of an eight node loop, the second subgroup containing a dyad and a five node loop, the third subgroup consisting of a three node loop and a four node loop, the fourth subgroup consists of four node loops two in number, the fifth subgroup had two dyads and a four node loop, the sixth subgroup contained three node loops, two in number, and a dyad, and the seventh subgroup consisted of four dyads. If the numerical values of this group were on the higher side as

compared to other groups, then it implies that all the x-abilities along with respective interactions would be significant in the concurrent design. The graphical representation of ninth group of terms is shown in Fig 4.10.

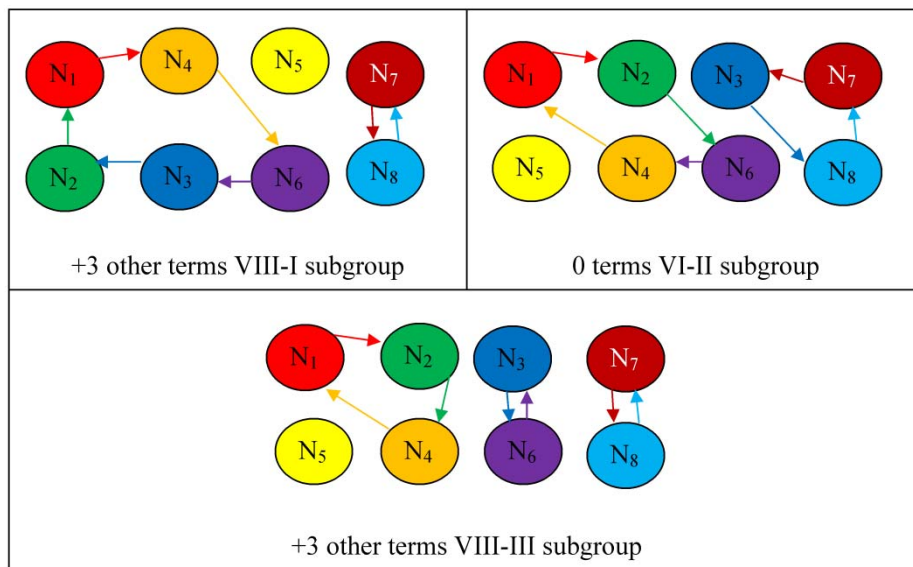
The CDM expression derived integrated all the design aspects using the systems approach. The expression considered all the design aspects, attributes and interactions between them. The terms in CDM expression were a combination of nodes along the diagonal and loops of off-diagonal elements with different sizes. From the multinomial defined in the equation (4.4), a unique numerical index named Concurrent Design Index (CDI) was derived and was defined as

$$CDI = per(E) \text{ (after substituting numerical values in the matrix } E) \quad (4.5)$$

During the conceptual design, say ‘n’ materials were shortlisted based on CNC machining, and the best needed to be evaluated and ranked. In that case, the design index for each material would be obtained and the *n* indices arranged in the descending order of their numerical values. To illustrate, if five materials were chosen and their indices were arranged in descending order and the following result emerged:

$$CDI_3 > CDI_1 > CDI_4 > CDI_2 > CDI_5$$

Then, since  $CDI_3$  is the highest among the five indices, the third material is the best amongst these five based on eight x-abilities and the interactions between them.



**Fig 4.9 Graphical representation of eighth group of terms in CDM**

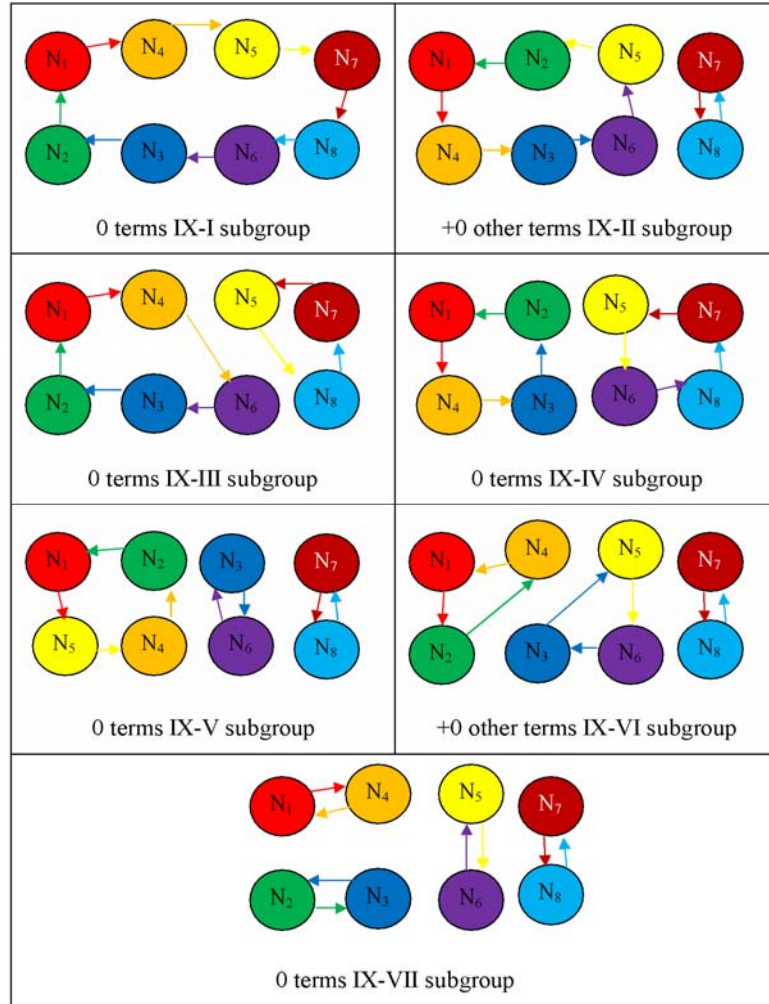


Fig 4. 10 Graphical representation of ninth group of terms in CDM

#### 4.2.2.5 Evaluation of nodes ( $N_i$ ) and interactions ( $e_{ij}$ )

Nodes ( $N_i$ ) and interactions ( $e_{ij}$ ) play a vital role in evaluation of CDM and CDI. The x-abilities along with the design parameters under each x-ability were considered simultaneously in developing digraph, design matrix and CDI. The developed procedure in the previous sections was applied to each x-ability ( $DFX_i$ ) and a  $CDM_i$  was developed for each x-ability. In deriving  $CDM_i$  of  $i^{th}$  x-ability, design parameters under that x-ability were considered as nodes and the interactions between them, as edges of the digraph. Table 4.1 shows the critical design parameters  $X_iDP_j$  under each x-ability. Using this, a separate digraph or matrix or index could be derived for each node or x-ability as shown in the Fig 4.2. The design index would represent the

design development and implementation time. If no interaction existed among the x-abilities, only one term would remain in the CDI i.e  $N_1N_2N_3..N_8$ . This would result in a CDI with the smallest value.. It would indicate that very little time would be required for design, development and implementation of this type of product or process.. In a real time situation, such products or processes are rare.

### 4.3 Evaluation of CDI for CNC turning operation

Turbine blades (Fig 4.11) are highly stressed components, demanding very precise manufacturing methods. The blade shafts are finish turned on a CNC lathe to obtain accurate profiles and the required surface finish. The dimensional accuracy of the blades and the radius joining at the intersections of two surfaces should be smooth and without under cuts. During the design phase of turbine blades, it is desirable to have a single numerical index for evaluation of manufacturing. The derivation of this numerical index, known as concurrent design index (CDI), this has been presented in the previous sections. Based on this concept, the CDI was derived for evaluation of the turning process for three different materials (ST 17-4PH, ST 12TE, and ST T17/13W) used in the manufacturing of turbine blades. In deriving this CDI, different x-abilities like DFM, DFQ, DFE and Design for cost (DFC) were used.

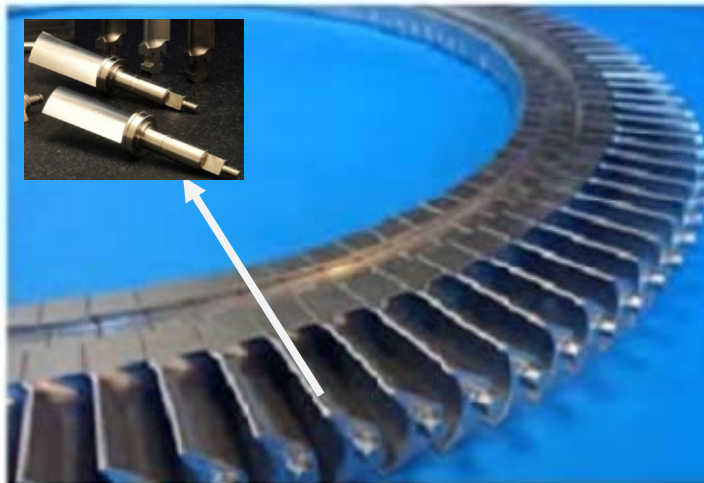


Fig 4. 11 Turbine blades manufactured at Turbocam, Goa (ref:<http://www.turbocam.com/blades>)

### Design for manufacturing (DFM)

Machining is the most widespread metal shaping process in mechanical manufacturing industry. Machining operations such as turning, milling, boring, drilling and shaping, waste a



large amount of raw material as well as time, and consume a large amount of global money annually (Childs et al, 2001). Out of these machining processes, turning remains the most important operation used to shape metals because in turning, the conditions of operation are most varied. Increasing productivity and reducing manufacturing cost have always been critical to successful business (Trent and Wright, 2000). In turning, higher values of cutting parameters offer opportunities for increasing productivity but it also involves a greater risk of deterioration in surface quality and tool life (Childs et al, 2001; Ueda et al, 2006). Optimal combinations of turning parameters are required to obtain the best surface on the work pieces. The basic turning parameters in deciding the quality of the turbine shafts are speed ( $V$ ), feed ( $f$ ) and depth of cut ( $a$ ). Other factors which influence manufacturability include tool geometry and materials. All the cutting parameters would come under design parameter  $X_3DP_9$  shown in Table 4.1 The methodology is applied in evaluation of turbine blade materials for CNC turning. In this, geometry was maintained constant for turning of all the three materials. The optimal combination of the basic parameters obtained using central composite design (CCD) method in Chapter 6 were substituted here to obtain the DFM index of each material. The DFM permanent matrix was defined as:

$$\text{DFM} = \begin{bmatrix} V & e_{12} & e_{13} \\ e_{21} & f & e_{23} \\ e_{31} & e_{32} & a \end{bmatrix} \quad (4.6)$$

Where  $V$ =speed,  $f$ =feed, and  $a$ =depth of cut, and  $e_{ij}$  represents the interaction between these parameters. The units and dimensions of the diagonal elements in DFM were different for different parameters. To make them non-dimensional numbers, individual parameters were divided with the maximum value considered in the experiment. For example, in all the experiments, the maximum speed considered was 209 m/min, so the non-dimensional velocity component for the material 1 was  $V/209$ . The interactions between different cutting parameters were obtained from the experiments conducted in the chapter 6. To bring the interaction values into a single range, all the values were normalized. In the experimental results, the interactions obtained were symmetric about the diagonal i.e.  $e_{ij}=e_{ji}$ . The optimum parameter combination to obtain maximum surface quality for the materials and the normalized values are listed in Table 4.2.

**Table 4. 2 Normalization of cutting parameters for different materials**

Materials Parameters	ST 12TE	ST T17/13W	ST 17-4 PH
Speed ( $V$ ) m/min	175	209	175
Feed ( $f$ ) mm/min	200	150	100
Depth of cut ( $a$ ) mm	0.500	0.875	0.500
$V/V_{max}(=209)$	0.837	1	0.837
$f/f_{max}(=234)$	0.854	0.640	0.427
$a/a_{max}(1.5)$	0.330	0.580	0.330
$e_{12}(V*f)$	0.005	0.582	1
$e_{13}(V*a)$	0.156	0.030	1
$e_{23}(f*a)$	1	0.145	0.016

After substituting the normalized values of cutting parameters and the interaction values into the equation (4.6), an index for each material was obtained as follows:

$$DFM_{ST12TE} = \begin{bmatrix} 0.837 & 0.005 & 0.156 \\ 0.005 & 0.854 & 1 \\ 0.156 & 1 & 0.33 \end{bmatrix} = 1.095 \quad (4.7)$$

$$DFM_{ST T17/13W} = \begin{bmatrix} 1 & 0.582 & 0.030 \\ 0.582 & 0.64 & 0.145 \\ 0.030 & 0.145 & 0.58 \end{bmatrix} = 0.5943 \quad (4.8)$$

$$DFM_{ST 17-4PH} = \begin{bmatrix} 0.837 & 1 & 1 \\ 1 & 0.427 & 0.016 \\ 1 & 0.016 & 0.333 \end{bmatrix} = 0.913 \quad (4.9)$$

A high value of the index indicates that a particular material is highly suited for a manufacturing process.

### **Design for Quality (DFQ)**

Surface finish of a turbine blade is an important parameter in the turning process. It is a characteristic that could influence the performance of the finished product and production costs. Various failures, sometimes catastrophic, leading to high costs have been attributed to the

surface finish of the components in question [Paulo Davim, 2001]. Also cutting forces are critically important in turning operations because cutting force correlate strongly with cutting performance such as surface accuracy, tool wear, tool breakage, cutting temperature, self-excited and forced vibrations, etc. The resultant cutting force is generally resolved into three components, namely, feed force, cutting force and thrust force. In this case the dimensional accuracy ( $X_8DP_5$ ) of turned steel depends on factors like surface finish ( $R_a$ ) cutting force ( $f_c$ ), thrust force ( $f_T$ ) and tool wear ( $T_w$ ). Hence, these four parameters were considered under the x-ability DFQ. The DFQ permanent matrix was written as below:

$$DFQ = \begin{bmatrix} \frac{R_a}{(R_a)_{\max}} & e_{12} & e_{13} & e_{14} \\ e_{21} & \frac{f_c}{(f_c)_{\max}} & e_{23} & e_{24} \\ e_{31} & e_{32} & \frac{f_T}{(f_T)_{\max}} & e_{34} \\ e_{41} & e_{42} & e_{43} & \frac{T_w}{(T_w)_{\max}} \end{bmatrix} \quad (4.10)$$

The parameters considered under DFQ are the responses; hence it is not possible to find the interactions using DOE. Each interaction was thus assigned with either 1 or 0 depending on whether the interaction existed or not. The value of  $R_a$  depends on the  $f_c$ ,  $f_T$ , and  $T_w$ , so the interaction between them ( $e_{12}$ ,  $e_{13}$  and  $e_{14}$ ) was taken as 1. The cutting forces are independent of each other, hence interaction between them ( $e_{23}$ ) was considered as 0. The tool wear depends on the rest of three factors, so these interactions ( $e_{14}$ ,  $e_{24}$  and  $e_{34}$ ) were considered as 1. In the permanent DFQ matrix, it was assumed that interactions are symmetric about the diagonal i.e.  $e_{ij}=e_{ji}$ . The DFQ indices for different materials were calculated as follows:

$$DFQ_{ST12TE} = \begin{bmatrix} 0.388 & 1 & 1 & 1 \\ 1 & 1 & 0 & 1 \\ 1 & 0 & 0.76 & 1 \\ 1 & 1 & 1 & 0.4 \end{bmatrix} = 9.78 \quad (4.11)$$

$$DFQ_{ST\ T17/13W} = \begin{bmatrix} 1 & 1 & 1 & 1 \\ 1 & 0.86 & 0 & 1 \\ 1 & 0 & 0.8 & 1 \\ 1 & 1 & 1 & 1 \end{bmatrix} = 12.06 \quad (4.12)$$

$$DFQ_{ST\ 17-4PH} = \begin{bmatrix} 0.787 & 1 & 1 & 1 \\ 1 & 0.767 & 0 & 1 \\ 1 & 0 & 1 & 1 \\ 1 & 1 & 1 & 0.2 \end{bmatrix} = 9.39 \quad (4.13)$$

All the diagonal elements of DFQ were found to have a negative effect on the quality of the turned product. Hence, the higher the values of DFQ index, the lower the quality of turned work piece.

### **Design for environment (DFE)**

As the importance of minimizing the environmental burden of each process is becoming more and more evident and essential, it is imperative that these effects be considered during the design phase. The basic parameters effecting the environment include machine tool electricity power consumption (PC), the material removal rate (MRR) and the coolant consumption.

The power consumption of a machine tool for a turning operation depends on different motors like servo motor, spindle motor, spindle coolant circulating motor, coolant pump, chip conveyer, auto tool changing motor, tool magazine, and machine tool standby power consumption. The power consumption of peripheral devices for this operation is measured using the operation duration time and the power rating of particular device in kWh.

In case of water-miscible cutting fluid, water is generally used to enhance the performance and is circulated in machine tools by coolant pumps until replaced. During this period, some coolants are eliminated by adhering to metal chips and extra coolant is supplied to compensate this. The reduction in dilution fluid (water) due to vapor must also be considered (Hirohisha and Hirio, 2009) in estimating total coolant.

The amount of material removed is equal to amount of raw material wasted. A lot of resources are wasted in preparing the raw material billets like furnaces used for processing raw material, transportation cost, inventory cost, etc. The removed chip wastes energy by carrying

the lubricant, heat (proportional to electricity), tool wear, build up edge, etc. Hence, the MRR is considered as one of the parameter in calculating the DFE index. The permanent matrix of DFE was written as follows:

$$DFE = \begin{bmatrix} \frac{MRR}{(MRR)_{\max}} & e_{12} & e_{13} \\ e_{21} & \frac{PC}{(PC)_{\max}} & e_{23} \\ e_{31} & e_{32} & \frac{CC}{(CC)_{\max}} \end{bmatrix} \quad (4.14)$$

In the above expression MRR=material removal rate cm<sup>3</sup>/min, PC=Power consumption kWh, and CC=coolant consumption in cc. All the diagonal elements were normalized to make them units free and also to bring them in a common scale. In the off-diagonal elements, the MRR interacted with PC and CC (increase in MRR will increase PC and CC), therefore the value considered for this interaction was 1. There will be no direct interaction between PC and CC so this interaction value was considered as 0. The DFE index for different materials were calculated as follows:

$$DFE_{ST12TE} = \begin{bmatrix} 0.625 & 1 & 1 \\ 1 & 0.7 & 0 \\ 1 & 0 & 0.75 \end{bmatrix} = 1.778 \quad (4.15)$$

$$DFE_{ST T17/13W} = \begin{bmatrix} 1 & 1 & 1 \\ 1 & 1 & 0 \\ 1 & 0 & 0.875 \end{bmatrix} = 2.75 \quad (4.16)$$

$$DFE_{ST 17-4PH} = \begin{bmatrix} 0.5625 & 1 & 1 \\ 1 & 0.6 & 0 \\ 1 & 0 & 1 \end{bmatrix} = 1.937 \quad (4.17)$$

All diagonal elements of the DFE have a negative effect on the environment. Hence, the higher the values of DFE index, the greater the impact on the environment.

## Design for cost (DFC)

Cost is an important criterion in production of a turbine blade. Therefore, it is required to consider different costs at the design phase. The non-dimensional cost components taken into consideration for development of DFC matrix were:

- Raw material cost ratio ( $C_R$ )
- Tooling cost ratio ( $C_T$ )
- Processing cost ratio ( $C_P$ )
- Labor cost ratio ( $C_L$ )

The material costs were obtained from vendors/supplier of the material, while the other costs could be estimated by the manufacturer by taking into account factors like machine utilization cost, machines capability to produce number of components over its useful life, cost of operating the CNC lathe, overall labor charges, etc. In the present analysis, the overhead cost and profits have not been considered.

The work reported in the previous chapter indicates that near net shaped casting is the best alternative for the machining of these steels. Hence, the cost of near net shaped casting was taken as the benchmarking cost for production of turbine blade. The relative cost ratio was obtained by dividing the total cost of benchmarked product by individual cost component of the product. It should be noted that cost components were calculated per unit/product basis. It was evident that individual cost components  $C_R$ ,  $C_T$ ,  $C_P$  and  $C_L$  were maximized when the individual cost components were minimized. This corroborates the idea that minimizing the cost components leading to minimizing the total cost. The costs of different materials are presented in Table 4.3.

**Table 4. 3 Different costs considered for each material in manufacturing of turbine blade**

Material	Cost/ kg (INR)	Mass of turbine blade(kg)	Raw material cost INR(1.5xmass of blade)	Tooling cost, INR	Processing cost, INR	Labor cost, INR	Total cost, INR
ST 12TE	150	3	675	100	148	29.6	952.6
ST T17/13W	155	3.5	814	90	162	32.4	1098.4
ST 17-4PH	168	2.8	705	120	153	30.6	1008.6

### ***Raw material cost ratio ( $C_R$ )***

The raw material cost ratio is based on the mass of the final turbine blade multiplied by the factor 1.5 (Sachin, 2010). This factor accounts for wastage of material in the machining. The cost of the steel was taken from the vendors based on the prices of the steel on the day of study. The cost ratio of raw material is defined as:

$$C_R = \frac{\text{Toatal cost of near net shaped product}}{\text{Cost of the raw material}} \quad (4.18)$$

### ***Tooling cost ratio ( $C_T$ )***

The tooling cost of a turbine blade includes the partial cost of the tool insert used in turning, partial cost of finishing tool, and the partial cost of milling tool if any used in the process. The term partial cost indicates that if the tool insert is used for ten work pieces and the cost of each insert is INR 100, then partial cost of the tool insert is INR 10 for each work piece. The tooling cost ratio is defined as

$$C_T = \frac{\text{Toatal cost of near net shaped product}}{\text{Cost of the tooling}} \quad (4.19)$$

### ***Processing cost ratio ( $C_P$ )***

The processing cost of a turbine blade includes cost of the auxiliary processes applied on the product. For example, heat treatment of the product, die penetration test for finding out the surface defects, etc. The power consumption for each work piece is also counted in this cost. The processing cost ratio is defined as follows

$$C_P = \frac{\text{Toatal cost of near net shaped product}}{\text{Cost of the tooling}} \quad (4.20)$$

### ***Labor cost ratio ( $C_L$ )***

The labor cost is assumed as 20% of the processing cost per component. With increase in the number of auxiliary processes the labor cost also increases. The labor cost ratio is defined as

$$C_L = \frac{\text{Toatal cost of near net shaped product}}{\text{Cost of the Labor}} \quad (4.21)$$

After calculating the cost ratios from the equations 4.18-4.21, the values were substituted in the design for cost matrix defined as follows:

$$DFC = \begin{bmatrix} C_R & e_{12} & e_{13} & e_{14} \\ e_{21} & C_T & e_{23} & e_{24} \\ e_{31} & e_{32} & C_P & e_{34} \\ e_{41} & e_{42} & e_{43} & C_L \end{bmatrix} \quad (4.22)$$

In this matrix diagonal elements represents the cost ratios of each material and off-diagonal elements represent the interactions between the costs. As the cost ratios are independent of each other, the values of  $e_{ij}$  are substituted as zeroes. The DFC matrix for each material is defined as follows

$$DFC_{ST12TE} = \begin{bmatrix} 1.04 & 0 & 0 & 0 \\ 0 & 7 & 0 & 0 \\ 0 & 0 & 4.73 & 0 \\ 0 & 0 & 0 & 23.65 \end{bmatrix} = 814.374 \quad (4.23)$$

$$DFC_{ST T17/13W} = \begin{bmatrix} 0.86 & 0 & 0 & 0 \\ 0 & 7.78 & 0 & 0 \\ 0 & 0 & 4.32 & 0 \\ 0 & 0 & 0 & 21.6 \end{bmatrix} = 624.332 \quad (4.24)$$

$$DFC_{ST 17-4PH} = \begin{bmatrix} 0.99 & 0 & 0 & 0 \\ 0 & 5.83 & 0 & 0 \\ 0 & 0 & 4.58 & 0 \\ 0 & 0 & 0 & 22.88 \end{bmatrix} = 604.819 \quad (4.25)$$

All the diagonal elements of DFC matrix were larger-the-better parameters. Hence, it could be concluded that DFC should be maximized for the production of best turbine blade at optimal cost.

### Design for X (DFX)

The calculated indices of different x-abilities namely DFM, DFQ, DFE and DFC were substituted in the overall DFX matrix to obtain the CDI. In substituting the values of DFQ and DFE, the reciprocals were used in order to minimizing the effects. The DFX matrix is defined as



$$DFX = \begin{bmatrix} DFM & 0 & 0 & 0 \\ 0 & \frac{1}{DFQ} & 0 & 0 \\ 0 & 0 & \frac{1}{DFE} & 0 \\ 0 & 0 & 0 & DFC \end{bmatrix} \quad (4.26)$$

The permanent function of the DFX matrix would yield a single index called concurrent design index (CDI). Table 4.4 shows the different design indices values and the CDI in the last column.

**Table 4. 4 CDI indices of the considered materials**

Material	DFM	1/DFQ	1/DFE	DFC	CDI
ST 12TE	1.095	0.102	0.562	814.374	51.12
ST T17/13W	0.5943	0.083	0.364	624.332	11.21
ST 17-4PH	0.913	0.106	0.516	604.819	30.2

## Results and discussion

The CDI considered for each material was a contribution of separate design parameters. A high value of the CDI would indicate a better choice of material for the CNC machining of turbine blade. In the overall ST 12TE obtained, the highest CDI equaled 51.12. For the individual indices, ST 12TE had the highest indices for DFM, DFE and DFC. The material ST17-4PH had highest index for the quality. This can be attributed to high surface finish for the specified combination of cutting parameters, and low cutting and thrust forces. Otherwise, ST17-PH was found to be a harder material to machine than the others. Material ST T17/13W had the lowest value of DFX as compared to others. This material had the lowest surface finish at the highest speed as compared to the other materials. In general at higher speed the surface finish would be higher due to large amount of material removal rate. The lower DFX index of this material could also be attributed to consistently lower values of DFM and DFC and higher values of DFE and DFQ.

#### **4.4 Summary**

In this chapter a methodology was proposed whereby the manufacturing industry could consider all design for x-abilities simultaneously, for evaluating CNC turning. This methodology assist the design engineer at the conceptual design stage in evaluation and selection of best CNC turning device by taking into consideration all the design for X-aspects simultaneously. Designing a CNC turning operation by factoring in manufacturability, miniaturization, integration, quality, reliability etc. is a huge task for a designer. The outcome of this work was a new mathematical model which considered all the design aspects in a unified systems approach without losing any useful information. The proposed model considered interactions/interdependence between the X-abilities in concurrent design of a CNC turning operation. The proposed design graph would be useful for visual inspection of interdependencies between the design aspects. The permanent function derived was a unique representation of all the design parameters of x-abilities and the interactions. The developed concurrent design index would be a handy tool to the designer in evaluating the CNC turning suitability for different materials.

The proposed methodology was applied for DFX based evaluation of three materials viz. ST 12TE, ST T17/13W and ST17-PH in turning of turbine blades. Four x-abilities viz. DFM, DFQ, DFE and DFC were simultaneously considered in the evaluation. The CDI obtained from this evaluation proved that ST 12TE was the more suitable material for machining of turbine blades and the next one was ST 174-PH and then ST T17/13W. Though several other design parameters were also considered, the DFX based results showed that ST 12TE was the most suitable material among those considered. This could be attributed to lower surface roughness, less cutting and thrust forces, low machining costs and less environmental impact. The DFX methodology thus allows the users/designers to analyze the different parameters impartially and arrive at an unbiased conclusion.

## **CHAPTER 5**

### **MATERIAL SELECTION FOR CNC TURNING USING MADM APPROACH**

#### **5.1 Introduction**

The optimal selection of a material for a CNC turning process, bearing in mind influencing factors like process parameters, surface roughness, environmental effect, material removal rate, etc. is a difficult task for the manufacturing industry. Industries require a mathematical tool for the selection of a material for the CNC turning operation.

There are several reports in the literature regarding the selection of a specific material for a specific application. Sandstorm (1985) suggested a two stage selection procedure which includes discriminating and optimizing stages to minimize the number of quality decisions. Ashby (1989) proposed material property charts for mechanical and thermal properties, which defines the correlation between the properties in the selection of materials. Rao (2006) has proposed a graph theory and matrix algebra based approach in selection of a material for a particular application. In one of the attempts (Rao and Davim, 2008), a material selection procedure was suggested based on the combination of two methods. To the best of my knowledge, a material selection procedure specific to CNC turning is lacking in the literature.

In this chapter a 3-stage selection procedure is described for the decision-making process. TOPSIS (technique for order preference by similarity to ideal solution)-an MADM tool as well as graphical methods, namely line graph and spider graph, are used in quality evaluation of materials by considering all responsible attributes in totality. The methodology is applied in quality evaluation and selection of turbine blade material for the CNC turning process.

#### **5.2 Identification of attributes**

As discussed in the previous chapter, the surface roughness of turbine blade materials for CNC turning process is critical. Surface roughness cannot be controlled as accurately as geometrical form (Karyel, 2009) and dimensional quality as it fluctuates according to many factors such as machine tool structural parameters, cutting tool geometry, workpiece and cutting tool materials,

environment, etc. In other words, surface quality is affected by the machining process, for instance by changes in the conditions of either the workpiece, tool or machine tool. Surface roughness changes over a wide range in response to these parameters. Many authors (Fand and Safi-Zahanshaki, 1997; Hongxiang et al, 2002) have proposed an empirical relation between surface quality and the machining parameters-speed, feed and depth of cut.

Several attributes of the material and CNC which influence the turning operation, were identified on the basis of the reports in the literature. The attributes identified under each category are listed below:

**I. Cutting parameters**

1. Speed
2. Feed
3. Depth of cut

**II. Tool geometry**

4. Nose radius
5. End relief angle
6. Side relief angle
7. Back rake angle
8. Side rake angle
9. Side cutting edge angle
10. End cutting edge angle

**III. Materials**

11. Microstructure
12. Grain size
13. Impurities
14. Weight composition of alloying elements

**IV. Mechanical properties**

15. Hardness
16. Tensile strength
17. Yield strength
18. Impact strength
19. Young's modulus
20. Density
21. Fracture toughness
22. Fatigue strength

**V. Coolant**

23. Type
24. Specific heat

25. Coolant pump capacity
26. Position of the coolant jet
27. Reactive constituents
28. Thermal conductivity
29. Viscosity
30. Non corrosive properties
31. Toxicity

**VI. Tool insert**

32. Shape
33. Life
34. Built-up-edge
35. Reaction with coolant
36. Flank wear
37. Insert material

**VII. Accuracy**

38. Machine co-ordinates
39. Axis alignment of machine and work piece
40. Tool compensation
41. Spindle speed
42. Uniformity in material properties

**VIII. Performance**

43. Power consumption
44. Setup time
45. Machining time
46. Heat carried by the coolant
47. Heat carried by chip
48. Cost
49. Material removal rate
50. Type of chip

### **5.3 Coding Scheme**

To simplify the identification and characterization of a material for CNC turning and to make this procedure user and computation friendly, a coding scheme was developed. This alphanumeric coding scheme was a unique representation of a material alternative based on the chosen attributes. The developed coding scheme for turning of ST 17-4PH steel on compact CNC turning center manufactured by ASKAR, India is illustrated in Table 5.1. In this table, the first column corresponds to the block number of an attribute, the second column corresponds to the name of the attribute, the third column represents information about the attribute in a

particular application, and the last column represents alphanumeric code based on the type of attribute; it could be either quantitative or qualitative.

**Table 5.1 Example coding scheme for machining of ST-174PH on CNC machine**

<b>Block. No.</b>	<b>Attribute</b>	<b>Information</b>	<b>Code</b>
<b>Cutting parameters</b>			
1	Speed	rpm	2
2	Feed	mm/min	3
3	Depth of cut	mm	3
<b>Tool geometry</b>			
4	Nose radius	mm	4
5	End relief angle	Degrees	4
6	Side relief angle	Degrees	3
7	Back rake angle	Degrees	3
8	Side rake angle	Degrees	4
9	Side cutting edge angle	Degrees	4
10	End cutting edge angle	Degrees	3
<b>Materials</b>			
11	Weight composition of alloying elements	C, Si, Mn, P, S, Cr, Ni, Mo, V, W, Ta, Ti, Nb, Cu	-
12	Microstructure	-	0
13	Grain size	-	0
14	Impurities	Type and %	0
<b>Mechanical properties</b>			
15	Hardness	HRB	4
16	Tensile strength	MPa	4
17	Yield strength	MPa	4
18	Impact strength	MPa	0
19	Young's modulus	MPa	0
20	Density	Kg/m <sup>3</sup>	0
21	Fracture toughness	K <sub>IC</sub>	0
22	Fatigue strength	Number of cycles	0

<b>Coolant</b>			
23	Type	<u>D</u> ry, <u>W</u> ater, <u>M</u> ineral oil, <u>A</u> ctive oil, <u>S</u> ynthetic, <u>G</u> as	W
24	Specific heat	J/kg K	0
25	Coolant pump capacity	m <sup>3</sup> /min	4
26	Position of the coolant jet	-	0
27	Reactive constituents	<u>S</u> ulphur, <u>P</u> hosphorous, <u>C</u> lorine, <u>N</u> one	N
28	Thermal conductivity	W/m K	0
29	Viscosity	N.s/m <sup>2</sup>	0
30	Non corrosive properties	-	0
31	Toxicity	<u>H</u> igh(or) <u>A</u> verage(or) <u>L</u> ow	L
<b>Tool insert</b>			
32	Shape	C(80 <sup>o</sup> ), D (55 <sup>o</sup> ), S (90 <sup>o</sup> ), T(60 <sup>o</sup> ), V(35 <sup>o</sup> )	C
33	Life	Hrs	0
34	Built-up-edge	<u>H</u> igh(or) <u>A</u> verage(or) <u>L</u> ow	0
35	Reaction with coolant	<u>H</u> igh(or) <u>A</u> verage(or) <u>L</u> ow	0
36	Flank wear	<u>H</u> igh(or) <u>A</u> verage(or) <u>L</u> ow	1
37	Insert material	<u>C</u> arbide, <u>D</u> iamond Tip, <u>C</u> eramic	Ca
<b>Accuracy</b>			
38	Machine co-ordinates	mm	0
39	Axis alignment of machine and work piece	Degree	0
40	Tool compensation	-	0
41	Spindle speed	rpm	0
42	Uniformity in material properties	-	0
<b>Performance</b>			
43	Power consumption	kW	4
44	Setup time	Sec	0
45	Machining time	Min	0
46	Heat carried by the coolant	Joule	4
47	Heat carried by chip	Joule	0
48	Cost	Rs	0
49	Material removal rate	gm/min	0
50	Type of chip	<u>C</u> ontinuous or <u>D</u> iscontinuous	C

A compact 50-digit electronic coding scheme for the above application is given in Table 5.2. A material for CNC turning could, thus, be characterized using the coding scheme developed in a similar manner.

In this code (Table 5.2) each attribute was given a box and all the boxes were arranged in block number sequence. The code within the box was in the format  $b_i/a_i$ ,  $i=1, \dots, n$ , where  $b_i$  was the block number and  $a_i$  was the alphanumeric code given to a particular attribute.

A numerical value was allotted to quantitative attribute and an alphabet based code was allotted to each qualitative attribute. Attributes with no information available were assigned a numerical value of '0'. Numerical values of the quantitative attributes were allotted in the scaled range 0-5. For example, the spindle speed ( $N$ ) of the CNC turning center in r.p.m was used with an interval scale of 0-5. In this scale, '0' implied unavailable information from manufacturer,  $4000 < N < 5000$  was assigned the code '5',  $4000 < N < 3000$  was assigned the code '4',  $2000 < N < 3000$  was assigned the code '3',  $1000 < N < 2000$  was assigned the code '2', and  $N < 1000$  was assigned the code '1'. Similarly, the remaining attributes were also given values according to the range within which the particular attribute fit.

In brief, the proposed coding schemes had two sets of information- first, the box number corresponding to the block number of the attribute, and second the alphanumeric code representing either the value range of an attribute (quantitative) or the short form of information (qualitative). It was proposed that for a manufacturing industry, an integrated team should establish the value of the attribute either analytically, experimentally or by experience. The developed coding scheme would be useful for storage and retrieval of different materials for CNC turning from the database, whenever needed.

#### **5.4 Three-stage selection procedure**

In this section a three-stage selection procedure for evaluation, ranking and selection of a material for CNC turning process is presented. In the first stage, the unmanageable numbers of alternatives were reduced to a manageable number based on the threshold value of the pertinent attributes. In the second stage, the TOPSIS method was used for attribute based evaluation of a material for CNC turning. In the last stage, the final decision was made with the help of a preference list developed at second stage.



**Table 5.2 Compact coding scheme for machining of ST-174PH on CNC machine**

<b>Cutting parameters</b> Block No. 1-3	1/2	2/3	3/3						
<b>Tool geometry</b> Block No. 4-10	4/4	5/4	6/3	7/3	8/4	9/4	10/3		
<b>Materials</b> Block No. 11-14	11/0	12/0	13/0	14/0					
<b>Mechanical properties</b> Block No.15-22	15/4	16/4	17/4	18/4	19/0	20/0	21/0	22/0	
<b>Coolant</b> Block No.23-31	23/W	24/0	25/4	26/0	27/N	28/0	29/0	30/0	31/L
<b>Tool insert</b> Block No.32-37	32/C	33/0	34/0	35/0	36/1	37/Ca			
<b>Accuracy</b> Block No.38-42	38/0	39/0	40/0	41/0	42/0				
<b>Performance</b> Block No.43-50	43/4	44/0	45/0	46/4	47/0	48/0	49/0	50/C	

**5.4.1 Stage 1- Elimination search**

In the previous section, 55 attributes were identified for selection of a material for CNC turning. Evaluation of *m* number of alternatives using these attributes is economically not viable. All the attributes are not equally important for different applications. For example, in evaluation and selection of materials for turbine blades corrosion resistance is more significant, whereas in

some other application it may not be so significant. The pertinent attributes were identified and the large number of alternatives was reduced to a manageable number, which could then be evaluated using all the relevant attributes. These few, ‘pertinent attributes’, important to the specific application, would be sufficient for selection process. Threshold values for these pertinent attributes could be assigned by a team of experts in that particular application. Thereafter the methodology would focus primarily on the pertinent attributes, leaving out the rest. A large number of available materials could be reduced to a manageable number based on the threshold values of these pertinent attributes. This could be achieved by scanning the database for pertinent attributes, one at a time, and eliminating alternatives with one or more pertinent attribute value(s) falling short of the threshold values. To facilitate this search an identification code was assigned to each alternative based on the procedure developed in the previous section.

#### **5.4.2 Stage 2-MADM-TOPSIS based evaluation and ranking procedure**

The use of TOPSIS, a multi-attribute decision making procedure, proposed by Hwang and Yoon (1982), was illustrated with the help of the following step-by-step procedure:

##### **Evaluation procedure**

A manageable number of feasible mechatronic alternatives as result of ‘elimination search’ had to be further filtered to obtain an optimal number of materials. Hence alternatives had to be ranked in preference order to select an optimal one.

##### ***Decision matrix***

As a first step, all information about the pertinent attributes was expressed in a matrix form and the matrix was named as decision matrix,  $D$ , a mathematical expression defined to incorporate the information pertaining to attributes of shortlisted alternatives. Matrix  $D$  was expressed as follows:

$$D = [d_{ij}]_{m \times n}, i=1, \dots, m; j=1, \dots, n \quad (5.1)$$

Where ‘m’ represented the number of alternatives and ‘n’, the number of pertinent attributes. Each element of the matrix  $d_{ij}$  represented the value of the  $j^{\text{th}}$  attribute corresponding to

the  $i^{\text{th}}$  alternative, along with the units. Elements in each column of this matrix had different units and scales. Hence this was a non-normalized form of a matrix.

### ***Normalized matrix***

The decision matrix could contain qualitative or quantitative attributes, and the units of measurement or assessment and their values could vary widely. These values had to be brought down to a common scale using a normalization procedure.

To convert the elements of matrix  $D$  into a scale and unit-independent quantity, it was normalized. The normalized decision making matrix,  $R$ , was obtained from the decision matrix  $D$  and each element of this matrix  $r_{ij}$ , was expressed as:

$$r_{ij} = \frac{d_{ij}}{\sqrt{\left(\sum_{i=1}^m d_{ij}^2\right)}} \text{ where } i = 1, \dots, m \text{ and } j = 1, \dots, n \quad (5.2)$$

The normalization procedure reduced the values of attributes on 0-1 scale. This value would indicate the standing of particular attribute magnitude when compared to the whole range of the magnitudes for all possible alternatives.

### ***Relative importance matrix***

Information about the pair-wise comparison of attributes was stored in a matrix,  $A$ , the relative importance matrix. The size of the relative importance matrix was  $n \times n$  and each element in this matrix,  $a_{ij}$ , was defined as:

$$a_{ij} = \frac{\text{importance of } i^{\text{th}} \text{ attribute}}{\text{importance of } j^{\text{th}} \text{ attribute}} \quad (5.3)$$

The relative importance of attributes could be obtained from a multi domain team of experts specialized in a particular application. Matrix,  $A$ , would yield information regarding the pair-wise comparison of attributes for a typical physical situation. Normalization would be meaningful when, after the weight of each attribute was determined, the cumulative sum of the weights of all attributes would be unity.

### **Weight matrix**

In order to determine the weight of all the attributes, Eigen value formulation was used and was expressed as:

$$A W = \lambda W \quad (5.4)$$

Where  $W = [w_1, w_2, \dots, w_n]^T$ , a weight matrix and  $\lambda$  is the Eigen value/variable.

Equation (5.4) could be expressed as:

$$(A - \lambda I) W = 0 \quad (5.5)$$

In equation (5.5),  $\lambda$  is the Eigen value of the matrix  $A$  and  $W$  is the Eigen vector (Strang and Strang, 1980). For  $[A]_{n \times n}$  there would be  $n$  Eigen values  $\lambda_i$ , for  $i=1 \dots n$ , and corresponding to  $\lambda_i$ , there would be  $n$  Eigen vectors  $W_i$ , for  $i=1 \dots n$ . To avoid trivial solution, it was assumed that  $W \neq 0$  and equation (5.5) became:

$$(A - \lambda I) = 0 \quad (5.6)$$

The solution of equation (5.6) yielded a set of 'n' Eigen values ( $\lambda_1, \lambda_2, \dots, \lambda_i, \dots, \lambda_n$ ), out of which the maximum Eigen value (Hwang and Yoon, 1982),  $\lambda_{\max}$ , was selected to obtain the weight matrix. The expression used to determine the weight vector was:

$$(A - \lambda_{\max} I) W = 0 \quad (5.7)$$

The solution of equation (5.7) yielded the weight vector.  $W = [w_1, w_2, \dots, w_n]^T$ , was the weight matrix. This matrix should satisfy the condition:

$$\sum_{i=1}^n w_i = 1 \quad (5.8)$$

In case the written program did not support this feature, the normalized weight vector could be obtained by using:

$$w_i = \frac{w_i}{\alpha}, \text{ where } \alpha = \sum_{i=1}^n (w_i)_{\lambda_{\max}} \quad (5.9)$$

The weight matrix would be meaningful if applied to the normalized matrix.

### ***Weighted normalized decision matrix***

To make the weight matrix more meaningful, weight information was incorporated into the normalized matrix,  $\mathbf{R}$ , and a new matrix weighted normalized decision matrix,  $\mathbf{Q}$ , was defined. Each element of this weighted normalized matrix  $q_{ij}$  was defined as:

$$Q = [q_{ij}] = [r_{ij}] * [w_j], \quad i=1,2,\dots,m; j=1,2,\dots,n. \quad (5.10)$$

$$Q = \begin{bmatrix} q_{11} & q_{12} & \cdot & \cdot & \cdot & q_{1n} \\ q_{21} & \cdot & \cdot & \cdot & \cdot & \cdot \\ \cdot & \cdot & \cdot & \cdot & \cdot & \cdot \\ \cdot & \cdot & \cdot & \cdot & \cdot & \cdot \\ \cdot & \cdot & \cdot & \cdot & \cdot & \cdot \\ q_{m1} & q_{m2} & \cdot & \cdot & \cdot & q_{mn} \end{bmatrix} = \begin{bmatrix} w_1 r_{11} & w_2 r_{12} & \cdot & \cdot & \cdot & w_n r_{1n} \\ w_1 r_{21} & \cdot & \cdot & \cdot & \cdot & \cdot \\ \cdot & \cdot & \cdot & \cdot & \cdot & \cdot \\ \cdot & \cdot & \cdot & \cdot & \cdot & \cdot \\ \cdot & \cdot & \cdot & \cdot & \cdot & \cdot \\ w_1 r_{m1} & w_2 r_{m2} & \cdot & \cdot & \cdot & w_n r_{mn} \end{bmatrix} \quad (5.11)$$

Each row in the equation (5.11) corresponded to the weighted normalized values of attributes for the  $m^{\text{th}}$  alternative.

### ***Ranking procedure***

The ranking of  $m$  alternatives was carried out using TOPSIS. The weighted normalized matrix  $\mathbf{Q}$  was used to obtain the hypothetical positive and negative benchmarks among available alternatives. The positive benchmark would have the best values for the attributes and the negative benchmark would have the worst attribute values. TOPSIS ranked the alternatives based on the distance from the alternative to the positively and negatively benchmarked solutions. The highest ranked alternative would have the shortest distance from the positively benchmarked solution and farthest distance from the negatively benchmarked solution.

### ***Positive ideal and negative ideal solution***

The values of the positive ideal solution ( $R^*$ ) and negative ideal solution ( $R^-$ ) could be obtained from the following expressions:

$$R^* = \{q_1^*, q_2^*, \dots, q_j^*, \dots, q_n^*\} \quad (5.12)$$

$$= \left\{ \left( \max_i q_{ij} \mid j \in J \right), \left( \min_i q_{ij} \mid j \in J', i = 1, 2, \dots, m \right) \right\}$$

$$\begin{aligned}
R^- &= \{q_1^-, q_2^-, \dots, q_j^-, \dots, q_n^-\} \\
&= \left\{ \left( \min_i q_{ij} \mid j \in J \right), \left( \max_i q_{ij} \mid j \in J', i = 1, 2, \dots, m \right) \right\}
\end{aligned} \tag{5.13}$$

Where set ‘J’ was associated with benefit attributes like larger-the-better type and set ‘J’ was associated with cost attributes like smaller-the-better type.

### ***Determination of separation measures***

The basic principle of the TOPSIS technique is that the selected alternative should be nearest to the positive ideal solution and farthest from the negative ideal solution in n-dimensional Euclidian space, where ‘n’ is the number of attributes.

The separation of each alternative from positive ideal solution  $R^*$ , is expressed as:

$$S_i^* = \sqrt{\sum_{i=1}^n (q_{ij} - q_j^*)^2}, i = 1, \dots, m \tag{5.14}$$

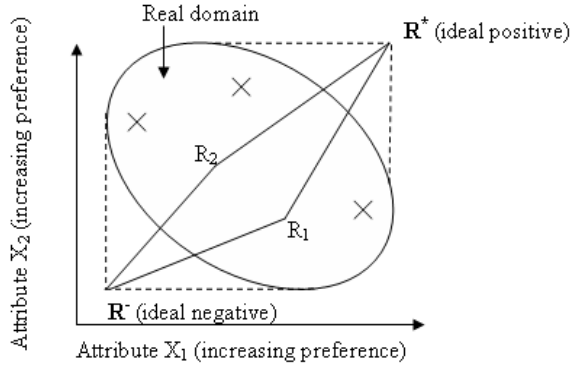
In the same way, separation measure for negative ideal solution is expressed as:

$$S_i^- = \sqrt{\sum_{i=1}^n (q_{ij} - q_j^-)^2}, i = 1, \dots, m \tag{5.15}$$

$S^*$  and  $S^-$  are two hypothetical benchmark solutions for comparison.

### ***Relative closeness to positive benchmark index***

The concept of Euclidian distance is shown in Fig 5.1 for two attributes in a two attribute Euclidian space. In this figure ordinate and abscissa represent the two attributes  $x_2$  and  $x_1$  and elliptical area represents the real domain. Two points  $R^*$  and  $R^-$  represents ideal positive and negative values. Two straight lines  $R^*R_1$  and  $R^-R_1$  represent the straight line distance of a real attribute of alternative 1 from the ideal positive and ideal negative values respectively.



**Fig 5.1**Two-attribute representation of an alternative in two dimensional space

Ranking of an optimal alternative by visual inspection of n-attribute Euclidian space is a difficult job. To make it simple an index named relative closeness to positive benchmark index,  $C^*$ , is defined and expressed as below

$$C^* = \frac{S_i^-}{S_i^* + S_i^-}, i = 1, \dots, m. \quad (5.16)$$

Where,  $0 \leq C^* \leq 1$

From the equation (5.16) and Fig 5.3 it is clear that if:

$$R_1 = R^* \text{ then } S_i^* = 0 \text{ and } S_i^- = 1 \text{ so } C^* = 1. \quad (5.17)$$

$$\text{and if } R_1 = R^- \text{ then } S_i^- = 0 \text{ and } S_i^* = 1 \text{ so } C^* = 0 \quad (5.18)$$

From the equation (5.17) and (5.18), it is clear that the alternative with highest value of  $C^*$  is closest to the ideal solution and farthest from negative solution. All the alternatives can be arranged in a descending value order of  $C^*$  to obtain the preference order of alternatives.

### 5.4.3 Stage 3- Decision making

Selection of an optimum material suitable to a CNC turning could be carried out on the basis of the preference order generated in the earlier section in the light of other attributes and business manufacturing strategies. The proposed methodology is user and computational friendly in optimal selection of a material. The only inputs required for this procedure are decision matrix, D, and relative importance matrix, A.

## 5.5 Graphical methods

In the previous section TOPSIS based evaluation of a material was discussed. An in depth understanding of the TOPSIS procedure is a difficult job for a novice customer. To enhance the understanding capability of a novice customer and minimize the complexity of the involved mathematics, two graphical methods namely linear graph and spider diagram were used.

### 5.5.1 Linear graph representation

The key matrices i.e. decision matrix ( $D$ ), normalized matrix ( $A$ ) and weighted normalized matrix ( $Q$ ) identified in the earlier section contain information regarding alternative material. The magnitude of information, stored in these matrices could be represented on a linear graph by plotting attribute magnitude on ordinate and attribute types on the abscissa at unit interval. In this graph, the magnitude of larger-the-better (benefit) attributes would be retained as is and reciprocal values for smaller-the-better (cost) attributes would be used in order to maintain consistency.

The values of different alternatives could be plotted as a separate poly line. These poly lines would be useful in comparison of alternative materials. The area under these poly lines as shown in Fig 5.2 would be useful in quantification, to compare alternative materials, and to define a positive bench mark material.

Line graphs could be plotted based on the information of attributes available in any of the matrices  $D$ ,  $R$  and  $Q$ . Allowing that the horizontal width between two vertical axes be unity and assigning  $d_{ij}$ ,  $m_{ij}$ , and  $q_{ij}$  as the elements of matrices  $D$ ,  $R$  and  $Q$  respectively,  $AQ^i$  would be the area under line graph of an  $i^{\text{th}}$  alternative based on a  $Q$  matrix. This area could be determined as follows:

$$AQ_i^L = (q_{i,1} + 2(q_{i,2} + \dots + q_{i,n-1}) + q_{i,n})/2 \quad (5.19)$$

Similarly, the area under linear graphs constructed based on the information of matrices  $D$  and  $R$  could be determined as  $AD_i^L$  and  $AR_i^L$  respectively.



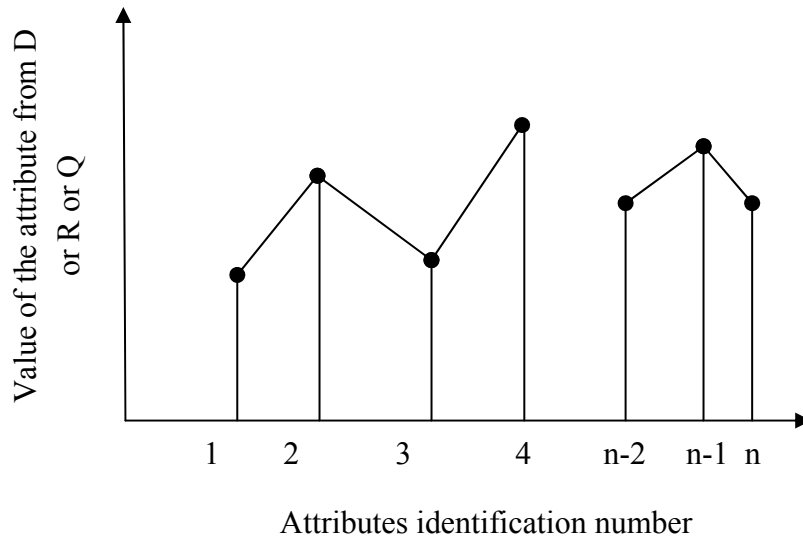


Fig 5.2 Line graph for 'n' number of attributes

### 5.5.2 Spider diagram representation

In this diagram n-number of permanent attributes divide  $360^\circ$  two dimensional polar space with 'n' number of lines. The angle between two attributes ' $\theta$ ' can be calculated as  $\theta = \frac{360}{n}$ . Separate spider diagrams can be plotted for information stored in the matrices D, R, and Q. Fig 5.3 is an example plotted based on the matrix, Q, information.

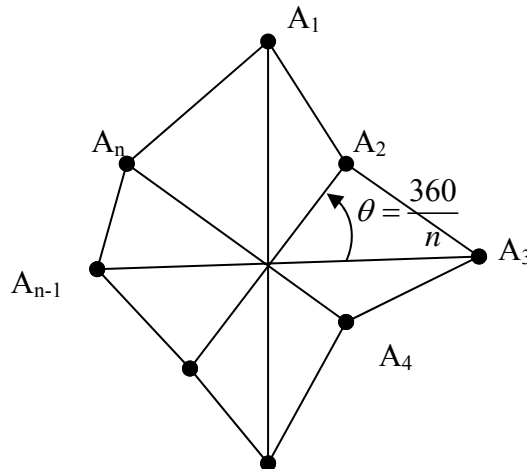


Fig 5.3 Spider diagram for 'n' attributes

A polygon was formed by joining attribute value locations identified on the attribute lines. The area of this polygon represented the capability of an alternative material. The enclosed polygon area of the  $i^{\text{th}}$  alternative could be calculated as follows:

Let  $q_{ij}$  represent the weighted normalized value of the  $j^{\text{th}}$  attribute in the  $i^{\text{th}}$  alternative along  $\theta_i$ . The area of spider diagram  $AQ_i^S$ , plotted based on the information of matrix  $Q$ , was calculated as:

$$AQ_i^S = \frac{\sin \theta}{2} \sum_{i=1}^n q_{ij} q_{i,j+1}; \text{ where } q_{i,n+1} = q_{i,1} \quad (5.20)$$

The areas  $AD_i^S$  and  $AR_i^S$  enclosed by the polygons could be similarly plotted based on values corresponding to matrices  $D$  and  $R$  respectively.

### 5.5.3 Graphical representation of bench mark material

A positive bench marked material is one having best magnitudes of attributes. The areas of positive bench marked material under the line graph ( $AQ_i^L, AD_i^L$  and  $AR_i^L$ ) and the spider diagram ( $AD_i^S, AR_i^S$  and  $AQ_i^S$ ) are calculated based on the best magnitude of attributes. Materials for CNC turning could be compared with the bench mark for evaluation purpose. This evaluation process would determine the suitability of the material for a particular application.

### 5.5.4 Coefficient of similarity (COS)

The index coefficient of similarity (COS) is defined as the ratio of the area enclosed under the line diagram or within the polygon by an alternative material to the area enclosed by corresponding positive bench marked material. The value of the COS would be a fraction ( $0 \leq \text{COS} \leq 1$ ) and its value, a measure of relative closeness of the alternative to the positive benchmark material. Alternatives with highest value of COS would be preferable for an application.

COS of a material based on the matrix  $Q$  is:

$$\text{COS}_i^Q = AQ_i / AQ_B \quad (5.21)$$

$AQ_i$  for  $i^{\text{th}}$  material was based on either linear graph or spider diagram method. Similarly, the COS for the alternatives could be calculated based on matrices  $D$  and  $R$ . The values of COS

calculated for all the materials based on both graphical methods i.e. linear graph and spider diagram would give a basic understanding and an insight about the process of evaluation and comparison. In the above discussion, only pertinent i.e. critical attributes would be considered for the development and illustration of the methodology. This would also be necessary to save cost, efforts and time. But each of the 50 attributes identified would be important and would need to be considered during design, optimization, or manufacturing stages. The overall performance of the material for CNC turning would depend on all the 50 attributes.

### **5.6 Step-by-step procedure**

- 1) Based on the application, select attributes and develop coding scheme with a degree of inheritance from the proposed list or updated list with more attributes.
- 2) Separate out pertinent/ critical attributes for computation purpose and to be considered directly. The remaining attributes may be considered indirectly to save time and effort.
- 3) Follow TOPSIS procedure for attribute based evaluation, comparison and ranking of feasible alternatives.
- 4) In the final stage of selection (stage 3), consider all aspects which have not been factored in during the evaluation and ranking procedure, such as non- technical issues, market dynamics, government policies and different other strategies.

### **5.7 Evaluation of Turbine blade materials for CNC turning**

The methodology derived in the previous section was applied in the selection of turbine blade material for CNC turning process.. The manufacturer would like to select the most suitable material for turning of a turbine blade, based on the multiple attributes, while considering all pertinent attributes simultaneously. In DFX based evaluation the interaction between the parameters are considered as the off-diagonal elements. It is also important to consider the relative importance of attributes. In the MADM approach the evaluation and selection is done based on the attributes and their relative importance.

#### *Stage 1-Elimination search*

In order to reduce a huge list of materials to a manageable number, only steels available in the inventory were considered. These materials were filtered to a manageable number by

machining at the following conditions and retaining only those materials that had surface roughness less than 5.5  $\mu\text{m}$ .

- 1) Speed = 75 m/min
- 2) Feed= 100 mm/min
- 3) Depth of cut= 0.5 mm
- 4) Coolant should be present
- 5) Tool insert is CNMG 120408MN
- 6) Machined length of the work piece is 30 mm
- 7) Minimum Chromium percentage 15%

Following the elimination search, the few alternatives that remained were further evaluated. Before proceeding for TOPSIS, the pertinent attributes for the selection process were identified and are listed in Table 5.3.

**Table 5.3 Pertinent attributes of turning operation and alternatives for the turbine blade material**

Material	Ra (micro meter)	Fc (N)	Ft (N)	PC (W)	MRR (cm <sup>3</sup> /min)	TC (INR)
ST 12TE (A1)	1.54	48.23	109.5	1280	1.5	952
ST 17/13W(A2)	1.203	56.73	106.34	1350	1.4	1098.4
ST 17-4PH (A3)	2.13	61.5	120.17	1560	1.3	900
9SMnPb28k (A4)	3.59	80.17	150	1650	2.5	1200
42CrMo steel (A5)	2.5	65.2	124.21	1580	2.1	1108

### *Stage 2-TOPSIS based evaluation and selection procedure*

#### *Decision matrix:*

The decision matrix for the alternative materials was formulated from the Table 5.3 and is given in equation (5.22).

$$D = \begin{matrix} A_1 \\ A_2 \\ A_3 \\ A_4 \\ A_5 \end{matrix} \begin{bmatrix} 1.54 & 48.23 & 109.50 & 1280 & 1.5 & 952 \\ 1.20 & 56.73 & 106.34 & 1350 & 1.4 & 1098.4 \\ 2.13 & 61.50 & 120.17 & 1560 & 1.3 & 900 \\ 3.59 & 80.17 & 150.00 & 1650 & 2.5 & 1200 \\ 2.50 & 65.20 & 124.21 & 1580 & 2.1 & 1108 \end{bmatrix} \quad (5.22)$$

This matrix could contain real values of the attributes with different units. Each row in the matrix  $D$  represented the attribute values of a particular alternative.

#### *Normalized matrix*

Each element of the matrix was processed according to the equation (5.2) to obtain a normalized matrix  $R$ .

$$R = \begin{bmatrix} 0.2937 & 0.3410 & 0.3981 & 0.3840 & 0.3686 & 0.4026 \\ 0.2294 & 0.4011 & 0.3866 & 0.4050 & 0.3440 & 0.4646 \\ 0.4062 & 0.4348 & 0.4369 & 0.4680 & 0.3195 & 0.3806 \\ 0.6847 & 0.5668 & 0.5453 & 0.4949 & 0.6143 & 0.5075 \\ 0.4768 & 0.4610 & 0.4515 & 0.4740 & 0.5160 & 0.4686 \end{bmatrix} \quad (5.23)$$

In the above matrix the values of attributes are reduced to uniform scale ranges from 0 to 1.

#### *Relative importance matrix*

Based on equation (5.3) the relative importance matrix  $A$  for this application was derived and is as follows:

$$A = \begin{bmatrix} 1 & 1 & 1 & 1.5 & 1 & 1 \\ 1 & 1 & 1 & 1 & 0.5 & 1 \\ 1 & 1 & 1 & 1 & 0.5 & 1 \\ 0.67 & 1 & 1 & 1 & 0.5 & 1 \\ 1 & 2 & 2 & 2 & 1 & 1 \\ 1 & 1 & 1 & 1 & 1 & 1 \end{bmatrix} \quad (5.24)$$

In the above expression diagonally symmetric values were taken reciprocal to each other. Based on the importance of one attribute over the other, the values of off-diagonal elements were assigned. For example, element  $a_{14}$  was assigned a value 1.5. This means that the first attribute is 1.5 times important than the fourth attribute. The diagonally opposite element i.e.  $a_{21}$  was assigned reciprocal of  $a_{12}$ , 0.67. Similarly, other values were also assigned.

*Weight vector*

The Eigen spectrum of relative importance matrix  $A$  was determined based on the equation (5.6) and was written as:

$$(A - \lambda I) = \begin{bmatrix} 1-\lambda & 1 & 1 & 1.5 & 1 & 1 \\ 1 & 1-\lambda & 1 & 1 & 0.5 & 1 \\ 1 & 1 & 1-\lambda & 1 & 0.5 & 1 \\ 0.67 & 1 & 1 & 1-\lambda & 0.5 & 1 \\ 1 & 2 & 2 & 2 & 1-\lambda & 1 \\ 1 & 1 & 1 & 1 & 1 & 1-\lambda \end{bmatrix} = 0 \quad (5.25)$$

Solving the equation (5.25) for  $\lambda$  yielded:

$$\lambda = (6.0841, -0.0429 + 0.6667i, -0.0429 - 0.6667i, 0.0008 + 0.2465i, 0.0008 - 0.2465i, -0.0000)$$

Using the maximum Eigen value and the equation (5.7):

$$(A - \lambda_{\max} I)W = \begin{bmatrix} -5.0841 & 1 & 1 & 1.5 & 1 & 1 \\ 1 & -5.0841 & 1 & 1 & 0.5 & 1 \\ 1 & 1 & -5.0841 & 1 & 0.5 & 1 \\ 0.67 & 1 & 1 & -5.0841 & 0.5 & 1 \\ 1 & 2 & 2 & 2 & -5.0841 & 1 \\ 1 & 1 & 1 & 1 & 1 & -5.0841 \end{bmatrix} \begin{bmatrix} w_1 \\ w_2 \\ w_3 \\ w_4 \\ w_5 \\ w_6 \end{bmatrix} = 0 \quad (5.26)$$

Calculating weights for each attributes using the equation (5.26) and based on equation (5.8) and (5.9):

$$w_1 = 0.1755; w_2 = 0.1451; w_3 = 0.1451; w_4 = 0.1356; w_5 = 0.2344; w_6 = 0.1644$$

*Weighted normalized decision matrix*

After substituting the values of  $R$  and  $W$  in the equation (5.10), the obtained weighted normalized decision matrix  $Q$  was as follows:

$$Q = \begin{bmatrix} 0.0515 & 0.0495 & 0.0578 & 0.0521 & 0.0864 & 0.0662 \\ 0.0403 & 0.0582 & 0.0561 & 0.0549 & 0.0806 & 0.0764 \\ 0.0713 & 0.0631 & 0.0634 & 0.0635 & 0.0749 & 0.0626 \\ 0.1202 & 0.0822 & 0.0791 & 0.0671 & 0.144 & 0.0834 \\ 0.0837 & 0.0669 & 0.0655 & 0.0643 & 0.1210 & 0.0770 \end{bmatrix} \quad (5.27)$$

### *Ranking procedure*

#### *Positive ideal and negative ideal solutions*

The values of Positive ideal and negative ideal solution for each attribute after following the equations (5.12) and (5.13) were found to be:

$$P^* = (0.0403, 0.0495, 0.0561, 0.0521, 0.144, 0.0626) \quad (5.28)$$

$$P^- = (0.1202, 0.0822, 0.0791, 0.0671, 0.0749, 0.0834) \quad (5.29)$$

#### *Determination of separation measures*

Separation measures for the four alternatives were calculated based on the method described in equation (5.14), (5.15), (5.28) and (5.29). The separation measures obtained were:

$$S_1^* = 0.0588 \quad S_2^* = 0.0655 \quad S_3^* = 0.0781 \quad S_4^* = 0.0930 \quad S_5^* = 0.0562 \quad (5.30)$$

$$S_1^- = 0.083 \quad S_2^- = 0.0879 \quad S_3^- = 0.0587 \quad S_4^- = 0.0691 \quad S_5^- = 0.0627 \quad (5.31)$$

#### *Relative closeness to positive benchmark indices*

The relative closeness to positive benchmark indices were calculated based on the equation (5.16) discussed earlier. Indices for all the four alternatives were:

$$C_1^* = 0.5853 \quad C_2^* = 0.5730 \quad C_3^* = 0.4291 \quad C_4^* = 0.4263 \quad C_5^* = 0.5273 \quad (5.32)$$

This index is a measure of suitability of the material for a particular machining operation.

#### *Graphical methods*

Line graph and spider diagram were plotted based on the weighted normalized matrix  $Q$ . The Line graph and area plot for this application is shown in Fig 5.4 and the Spider diagram is shown in Fig 5.5. The COS of two graphs was calculated based on these two diagrams.

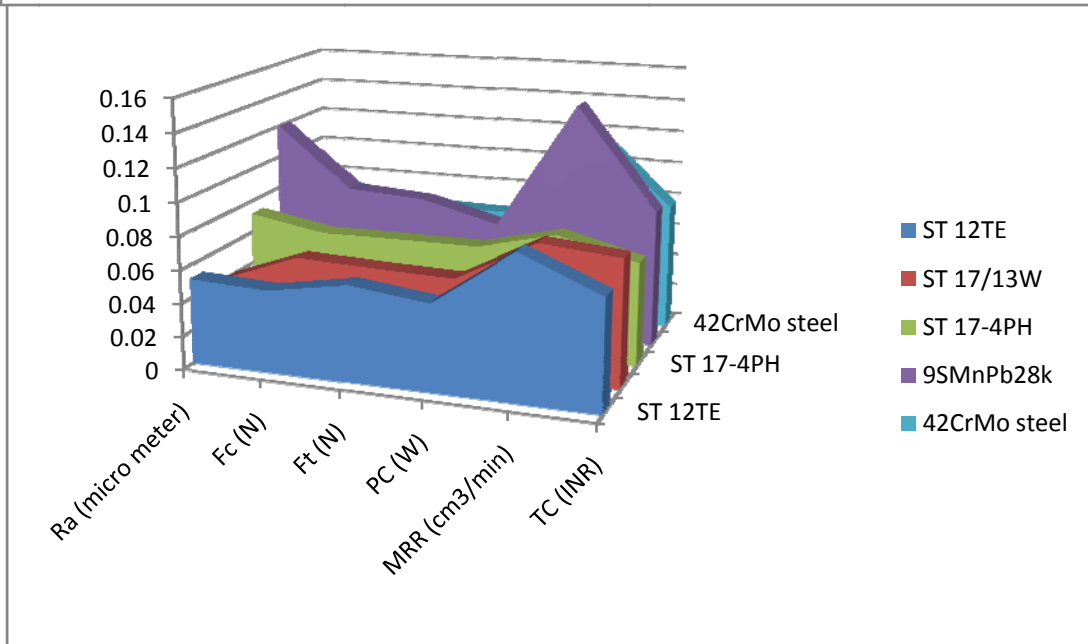
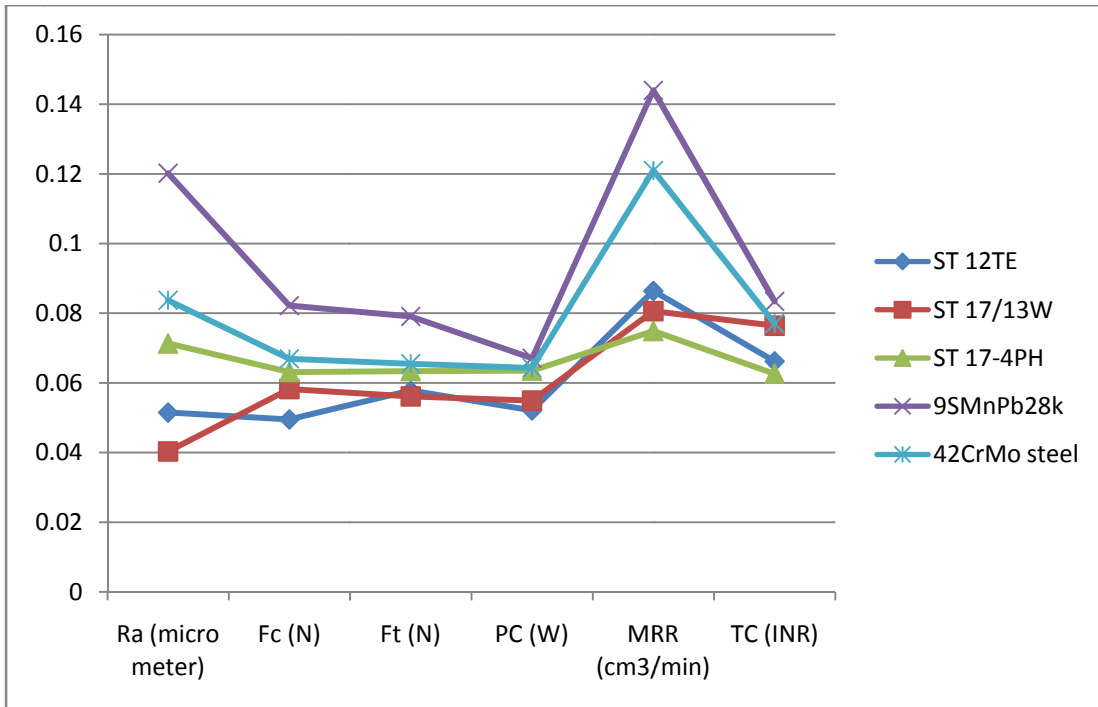


Fig 5.4 Line graph and area plot for the weighted normalized matrix



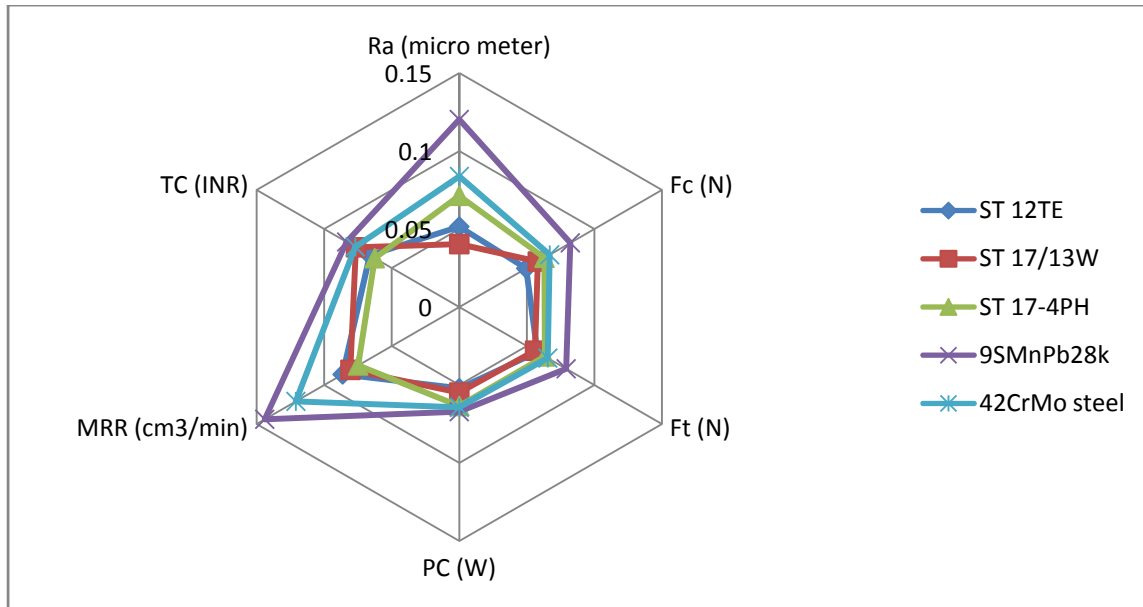


Fig 5.5 Spider diagram polygon for weighted normalized matrix

### Stage 3 – Ranking and final decision making

The ranking was carried out based on the values of relative closeness to benchmark indices. The alternative with the highest value of  $C^*$  was assigned the first rank and the lowest value was assigned the last rank. For the linear graph and spider plot, the lowest value was assigned the first rank. Ranking of all the six alternatives based on the three methods visually TOPSIS, line graph, and spider diagram are listed in Table 5.4. A minor discrepancy was observed in the rankings as obtained by linear and spider plot and that obtained from the TOPSIS analysis. This may be attributed to the fact that in calculating the area below the linear and spider chart most of the attributes were smaller-the-better and one attribute was larger-the-better. The area under the larger-the-better attribute was maximum-the-better and area under smaller-the-better attribute is minimum-the-better, but the areas given in Table 5.4 do not distinguish between these two.

All the three methods showed that the optimum material was ST 12TE based on the pertinent attributes and the relative importance matrix supplied by the customer. Though all the three methods showed almost similar ranking order, the TOPSIS method was found to be most accurate. This is because, in TOPSIS, the ranking ensures that the highest ranked alternative is closest to the ideal and farthest from the worst solution. Graphical methods ensure that the solution is closer to the ideal solution, but do not ensure that it is farthest from the worst solution.

As compared with graphical methods, TOPSIS differentiates the larger-the-better and smaller-the-better attributes.

**Table 5.4 Ranking of alternative materials for CNC turning process**

	TOPSIS Relative closeness to bench mark system, $C_i^*$	Rank based on $C_i^*$	COS based on Line Graph $COS_i^{QL}$	Rank based on $COS_i^{QL}$	COS based on spider diagram $COS_i^{QS}$	Rank based on $COS_i^{QS}$
ST 12TE (A1)	0.5853	1	0.3188	1	0.0099	1
ST 17/13W(A2)	0.573	2	0.327	2	0.01	2
ST 17-4PH (A3)	0.4291	4	0.3438	3	0.0119	3
9SMnPb28k (A5)	0.4263	5	0.4883	5	0.0241	5
42CrMo steel (A6)	0.5273	3	0.4125	4	0.017	4

The first rank status of ST 12TE can be attributed to its low surface roughness which ensures high machinability, low cutting forces, low power consumption, high material removal rate and low total cost. The best suited material, ST 12TE, is an austenitic steel having high corrosion resistance and machinability. This result also corroborates with the ranking derived in chapter 4 based on DFX. Hence, in this study, ST 12TE was identified and recommended as the best suited material for the turbine blade CNC turning application.

## 5.8 Summary

In this chapter a methodology for evaluation and optimal selection of a material for CNC turning was presented. The attributes for evaluation, ranking and selection of a material for CNC turning were identified based on different parameters. A unique coding scheme for identifying and differentiating alternative materials was also proposed. This coding scheme would be useful for characterization of a material. A 3-stage procedure for evaluation and optimal selection of a material was followed. This procedure employed TOPSIS-an MADM tool - for ranking of alternative materials. The ranking of alternatives was carried out based on the distance from the positive and negative benchmark solutions. Two graphical methods were also employed in ranking the alternatives. For all these tools the only inputs required were the decision matrix and

the relative importance matrix. This methodology would be useful in selection of a material with good quality and high performance for CNC turning.

The methodology devised was applied in the evaluation, ranking and selection of a material suitable for manufacture of a turbine blade. From the results, it was found that ST 12TE obtained the highest  $C_i^*$  index value of 0.6989. This implied that this alternative had the optimal surface finish, cutting and thrust forces, power consumption, and tool cost as compared to the others tested. The material ST 12TE was found to be the best ranked material among the five materials tested, using MADM-TOPSIS also. Hence, this material was identified as the recommended material for the CNC turning process.

## CHAPTER 6

### EXPERIMENTAL INVESTIGATION FOR SURFACE QUALITY OF TURBINE BLADE MATERIALS FOR CNC TURNING

In the previous chapters, theoretical modeling for the material selection for a CNC turning process was described. This chapter describes how the results obtained from modeling studies were verified experimentally.

#### 6.1 Introduction

A number of blades are used in steam turbines ranging from a few centimeters in height in high pressure (HP) turbines, to almost one meter long low pressure (LP) turbines. The causes of failure in HP and LP turbines include high cyclic fatigue caused by number of factors, centrifugal forces, steady and dynamic stresses, fracture propagation, etc. These failures may be avoided by thorough inspection of raw material and defect-free manufacturing of turbine blades. In general, high alloy steels with high chromium content are used in the manufacture of turbine blades. The machinability of these materials is poor and therefore these components are invariably produced directly as net-shaped products by the shell-mould-investment casting method. Achieving dimensional accuracy is one of the main challenges of investment casting, on account of shrinkage allowances. Hence, turbine blades are machined using turning, milling and finishing operations.

There are basically three groups of steam turbine blade materials used by turbine manufacturers. These are various grades of 12 to 13 percent chromium (Cr) steels with addition of Mo, W, Cb, V, Cu, Al, Ta, Ti and Nb. Higher chromium precipitation hardening steels such as 17-4PH and Titanium alloys are also very popular. The commercially available materials for the turbine materials are S41000, S41005, S41428, S42225, S41041, and S17400 (ASTM A1028, 2003). The properties of these materials are presented in the Table 6.1.

**Table 6. 1 Material properties of commercially available turbine blade materials**

Properties	Tensile strength ,min, MPa	Yield strength, min, MPa, 0.2%offset	Elongation in 50 mm, min, %	Reduction of area, min, %	Impact strength, min, N-m	Hardness, max, Brinell
------------	-------------------------------	---	--------------------------------	------------------------------	------------------------------	---------------------------

<b>Range</b>	689-1103	482-827	13-20	30-60	10-40	255-371
--------------	----------	---------	-------	-------	-------	---------

This chapter describes the study of three commercially available turbine blade materials St 17-4PH, St 12TE, and St 17/13W (TURBOCAM International, Goa, India) for machinability, surface roughness and other characteristics. The experimental conditions, instrumentations and measurements and the procedure adopted for the experiments were as follows:

### 6.1.1 Plan of experiments

To plan the experiments, the response surface method (RSM) was used. The parameters considered based on the literature were speed ( $V$ ), feed ( $f$ ) and depth of cut ( $a$ ). RSM is a collection of statistical and mathematical methods that are useful for modeling engineering problems. The main objective of this technique is to optimize the response surface that is influenced by various process parameters. RSM quantifies the relation between the controllable parameters and the response (Montgomery, 2007).

The design procedure of RSM (Joseph et al., 2008; Noordin et al., 2004) is as follows:

1. Design a series of experiments for adequate and reliable measurement of the response.
2. Find the optimal set of parameters that produce maximum or minimum value of response.
3. Analyze the results using two or three dimensional plots like contour, direct effect, surface plots, interaction effects, residual plots, etc.

Rotatable central composite design (CCD), a sub category of RSM was used to determine the number of experiments. The total number of experiments under this method were 20, which included  $2^3$  (3 factors at two levels) cube points, 6 axial points of the cube and central point (average point) of the cube repeated 6 times to calculate the pure error. The value of spatial choice  $\alpha = (F)^{1/4}$  where  $F$  is the number of points in the factorial part of design, in this case the value of  $\alpha$  was 1.683. The design layout for all the three materials was considered as common and is shown in Table 6.2. 20 cutting trials were performed on each material and a new insert with four cutting edges was used for each material. Each experiment was repeated twice, and the surface roughness was measured at three places on the work piece. As far as possible, experiments were conducted in random fashion.

**Table 6. 2 Design layout for the experiments**

Std. Order	Blocks	Speed-V (m/min)	Depth of cut -a (mm)	Feed-f (mm/min)
1	1	75	0.5	100
2	1	175	0.5	100
3	1	75	1.25	100
4	1	175	1.25	100
5	1	75	0.5	200
6	1	175	0.5	200
7	1	75	1.25	200
8	1	175	1.25	200
9	1	40.91	0.875	150
10	1	209.09	0.875	150
11	1	125	0.244	150
12	1	125	1.506	150
13	1	125	0.875	65.91
14	1	125	0.875	234.09
15	1	125	0.875	150
16	1	125	0.875	150
17	1	125	0.875	150
18	1	125	0.875	150
19	1	125	0.875	150
20	1	125	0.875	150

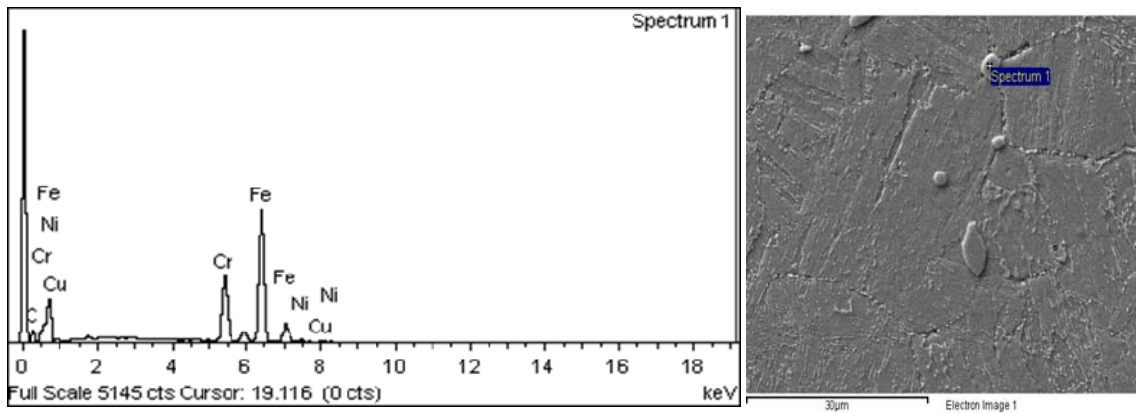
### 6.1.2 Materials used

Three types of stainless steels St 17-4PH, St T17/13 W, and St 12TE in the form of round bars were used for the experiments. The chemical composition of the materials in percentage weight was as shown in Table 6.3. From the Table 6.3, it is evident that all the three materials had a high percentage of chromium to ensure corrosion resistance. The material St 17-4PH was used for the applications requiring high strength and corrosion resistance. High strength is maintained up to 316°C. This versatile material is widely used in aerospace, chemical, petrochemical, food processing and general metal working industries.

**Table 6. 3 Chemical composition in %weight of the materials**

Material	C	Si	Mn	P	S	Cr	Ni	Mo	V	W	Ti	Nb	Ta	Cu
St 17-4PH	0.0 24	0.47	0.67	0.01 9	0.00 1	15.19	4.48	0.06	--	--	--	0.25	0.25	3.0 3
St T17/13 W	0.1 5	0.8	1.0	0.04 5	0.03 0	15.5- 18.0	13- 16	0.5	--	2.5 - 4.0	1.0	--	--	--
St 12TE	0.2- 0.2 6	0.50	0.80	0.02 5	0.02 0	11-12.5	0.30 - 0.80	0.80 - 1.20	0.25- 0.35	--	---	--	--	--

The material composition of ST 17-4PH was verified using scanning electron microscope (SEM) and energy-dispersive X-ray spectroscopy (EDS) analyses. The sample results are shown in Fig 6.1 and Table 6.4. The average value of the results obtained at different locations on the sample was found to be in good agreement with the compositions given by the industry (Turbocam India, Goa).



**Fig 6. 1 SEM/EDS spectrum results for the material ST 17 4-PH**

**Table 6. 4 SEM/EDS weight and atomic percentages at the selected location of the specimen**

Element	Weight%	Atomic%
C K	14.20	43.16
Cr K	19.08	13.39
Fe K	63.78	41.68
Ni K	1.52	0.95
Cu K	1.42	0.81
Totals	100.00	

The mechanical properties of these three materials are presented in Table 6.4. The tensile strength of St 17-4PH was found to be the highest among the three materials and the percentage reduction in area was much higher than the other two. The yield strength of the material St T17/13W was the lowest as compared to other two materials, but its impact strength was the highest as compared to the others. The properties of St 17-4PH and St 12TE were very similar.

The hardness of all the materials was not available, hence experiments were conducted to determine the hardness and the values are presented later in this chapter.

**Table 6. 5 Mechanical properties of the turbine blade materials**

Properties	Tensile strength, min, N/mm <sup>2</sup>	Yield strength, min, MPa, 0.2%offset	Elongation longitudinal, min, %	Reduction of area, min, %	Impact strength, min, J	Fracture toughness, MPa (m) <sup>1/2</sup>
St 17-4PH	1034	760	11	45	--	76
St T17/13 W	780	440	20	12	50	--
St 12TE	950	700	13	--	25	--

### 6.1.3 Cutting inserts and holder

In this experiment, carbide tools insert (Tin, TiCN and TiC coated) with ISO code CNMG 120408MN was used. The tool holder of ISO coding PCLNL 2020K12 D6I was used for holding this insert. The Tin coating on the insert reduced the possibility of built-up edge. The geometry of the insert cutting edges provided minimized cutting forces and longer tool life. The tool geometry of the insert and the tool holder were as follows:

**Table 6. 6 Geometry of insert and the tool holder**

Feature	Value
Insert shape	Diamond 80° 
Insert clearance angle	0°
Tolerance	±0.002 mm
Nose radius	0.4 mm
Holder style	Offset shank 5 SCEA
Insert clearance angle	0
Shank length	20 mm
Shank width	20 mm
Tool holder length	125 mm
Cutting edge length	25 mm



#### 6.1.4 Experimental setup and measuring instruments

The turning experiments were carried out in the presence of coolant (water oil emulsion) using ASKAR compact turning center. The flow of the coolant was maintained in such a way that tool temperature was always maintained at room temperature (27-32°C). The maximum speed of the lathe was 4000 rpm and the maximum spindle power was 7 kW. The materials selected fall in the lower range of hard turning materials (HRC 33 to 36) and accordingly the range of the speed, feed, and depth of cut were taken. In general, in hard turning the speed considered is in the range of 75-200 m/min, feed is taken in the range of 0.08-0.24 mm/rev, and the depth of cut in the range of 0.25-0.8 mm. Since the hardness of materials (*St 17-4PH*, *St T17/13 W*, and *St 12TE*) was in the lower range of hard turning, a higher side of feed and depth of cut were considered. The levels of cutting parameters considered in the experiments are shown in the Table 6.7.

Table 6. 7 Levels of independent variables

Parameter	Unit	Low Level (-1)	High level (+1)
Speed -V	m/min	75	175
Feed rate-f	mm/min	100	200
Depth of cut-a	mm	0.5	1.25

The surface roughness of the turned surface was measured and assessed using the values of central line average ( $R_a$ ). After turning the predetermined length and depth of cut the work piece was removed and the values of  $R_a$  were measured using Mitutoyo SJ-301 surface roughness tester. The experimental setup and flow of work are shown in Fig 6.2

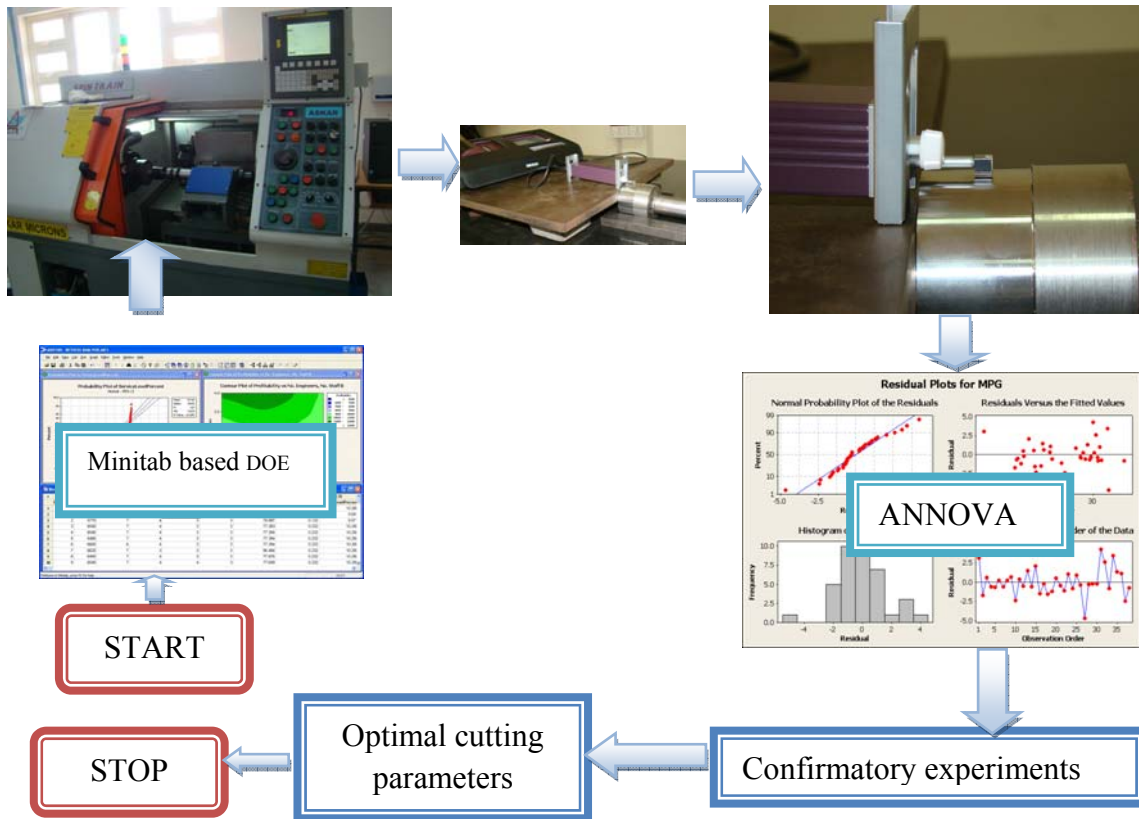
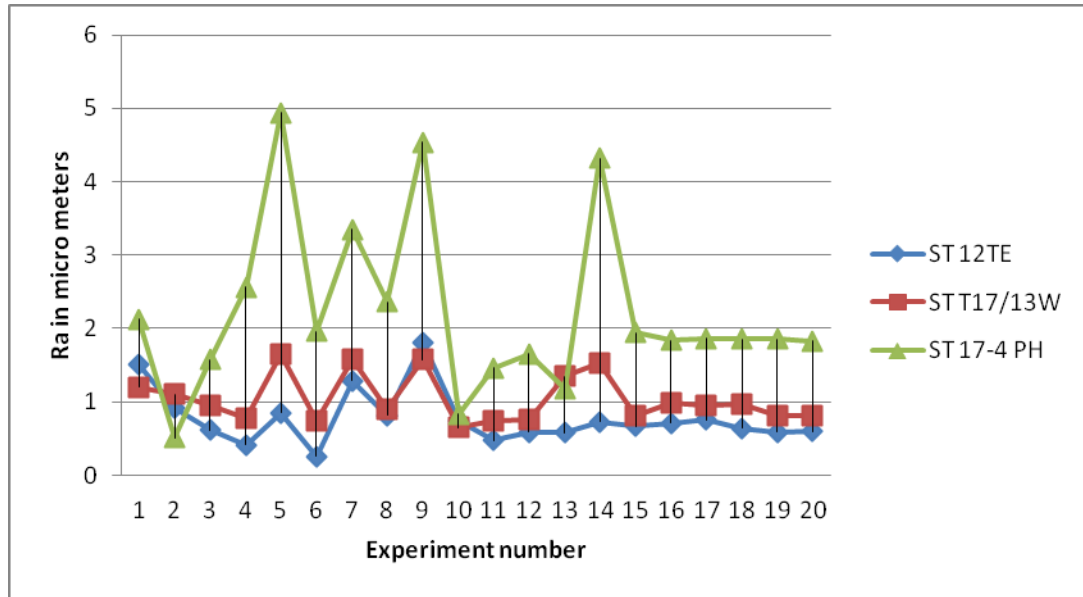


Fig 6. 2 Experimental setup and the flow of work

## 6.2 Results and discussion

The responses obtained from the machining process as per the design layout are shown in Table 6.8. The results obtained were given as input to the MINITAB 15.0 software without any transformation on the response fit. The model summary showed that the obtained results were statistically significant. Hence, this could be used for further analysis. The trend in the results for the three materials is shown in Fig. 6.3. It can be seen that they are comparable.



**Fig 6. 3 Trend in results of different material**

The Figure 6.3 shows that material ST 17-4PH is more sensitive to variation in the parameters as compared to the other two materials. For example, the highest roughness obtained for this material is 4.942 µm and for the other two materials it is less than 2 µm. After analyzing the results of ST 17-4PH material the derived reasons for the high surface roughness were:

- Carbon steel on cooling transforms from Austenite to a mixture of ferrite and cementite. With austenitic stainless steel, the high chrome and nickel content suppress this transformation keeping the material fully austenite on cooling (The Nickel maintains the austenite phase on cooling and the Chrome slows the transformation down so that a fully austenitic structure can be achieved with only 8% Nickel). This material has less than 8% Nickel, thus preventing austenite structure formation and leading to formation of martensitic like structure and causing an increase in hardness. The formation of martensitic like structure can also be conformed from the Schneider (1960) diagram as shown in Fig. 6.4. In this diagram, the percentage of chromium and Nickel equivalent can be calculated using the following equations and the percentages given in Table 6.3.

$$\text{Cr equivalent} = (\text{Cr}) + (2\text{Si}) + (1.5\text{Mo}) + (5 \text{ V}) + (5.5\text{Al}) + (1.75\text{Nb}) + (1.5\text{Ti}) + (0.75\text{W})$$

$$\text{Ni equivalent} = (\text{Ni}) + (\text{Co}) + (0.5\text{Mn}) + (0.3\text{Cu}) + (25\text{N}) + (30\text{C})$$

In these equations, all percentages are given on weight basis. After calculation, the coordinates for the ST 17-4PH comes out to be (Cr 16.65, Ni 6.44) which also conforms the presence of martensite in the microstructure.

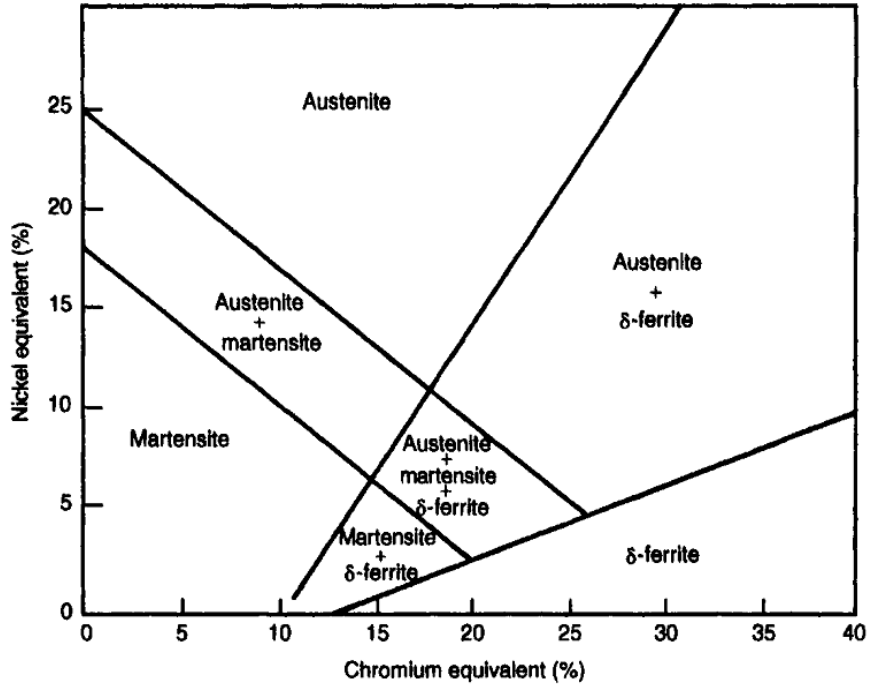
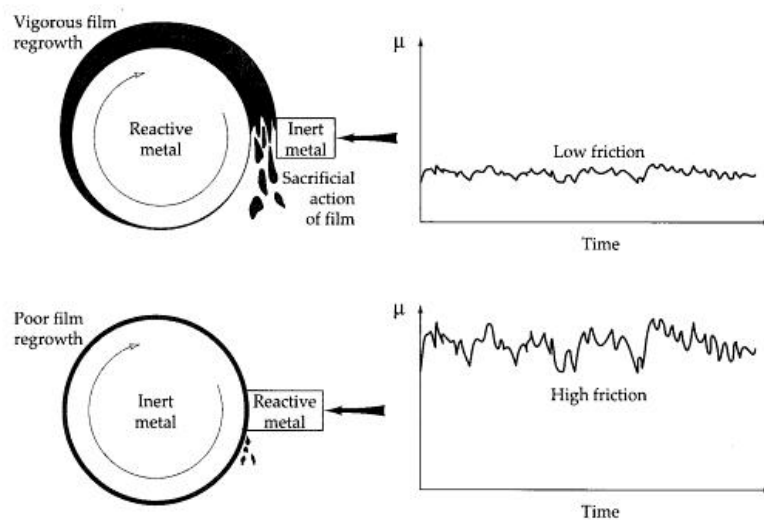


Fig 6. 4 Shaeffler diagram- modified after Schneider (1960))

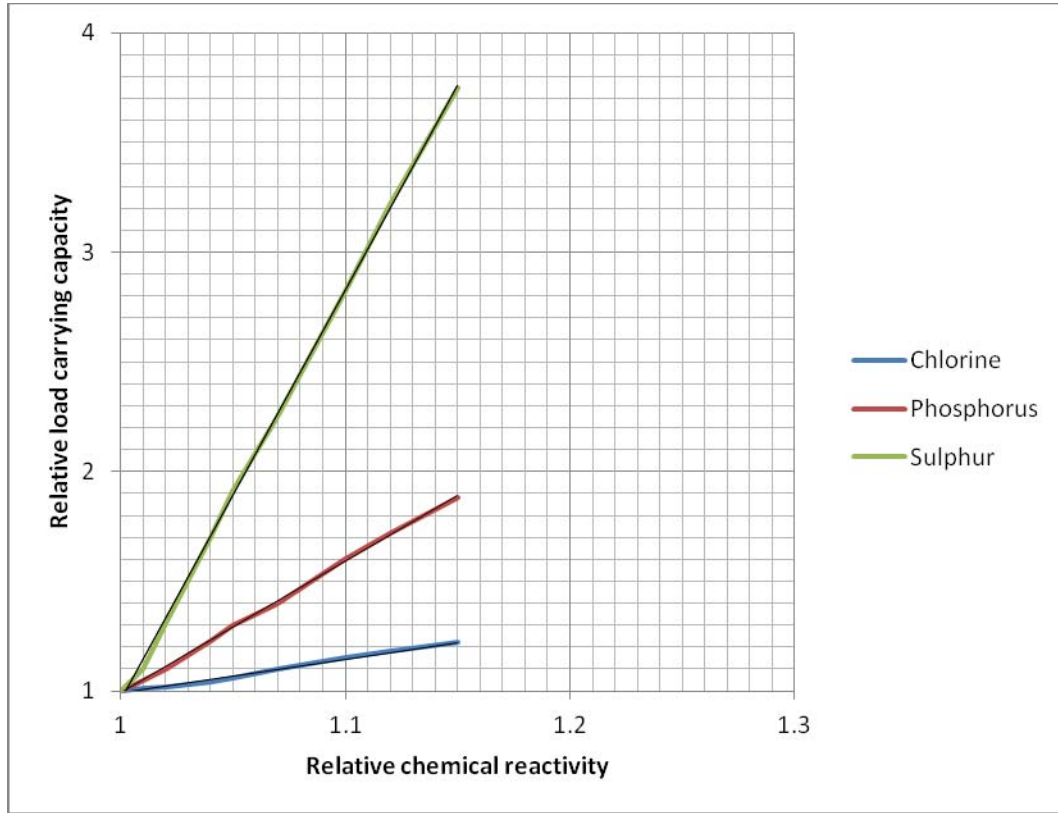
- Machinability of a material is an important factor which also influences surface roughness. High machinability of a material leads to fine surface finish. The percentage of sulphur content in an alloy steel is proportional to the machinability. From Table 6.3 the sulphur content in this material is 0.001% which is much lower compared to the other materials. This could be the reason why the material has low machinability and high surface roughness.
- During turning, the amount of friction between the tool insert and the work piece depends on the sacrificial film formed. The existence of this film is difficult to demonstrate as it is thought to be continuously destroyed and reformed during the wear process but it was indirectly proved about the existence of the film (Gwidon and Andrew, 2005). A model of film formation is schematically illustrated as shown in Fig 6. 5. If the material is reactive i.e. with more sulphur and phosphorous percentage, the sacrificial film is formed between the insert and the metal work piece. The adhesion between opposing asperities covered with these films is much less than for nascent metallic

surfaces and this forms the basis for lubricating effect by reducing the friction. The asperities are able to slide past each other with minimum of damage and wear while the film material is destroyed by the shearing that inevitably occurs. If the material is inert and the tool insert is reactive, then this mechanism will fail and asperity adhesion and severe wear occur due to mixed lubrication and scuffing. In ST 17-4PH the percentage of sulphur and phosphorous are less as compared to the other two materials. As the material is almost inert and the tool insert material (carbide tool insert) is also non reactive, a poor sacrificial film growth will occur and the friction will be high between the metals and surface roughness is also high.



**Fig 6. 5 Favorable and unfavorable conditions for sacrificial film formation (Gwidon and Andrew, 2005)**

- From the previous point it is evident that ST 17-4PH is not a reactive material with vegetable oil as a coolant. The performance of a coolant (also as a lubricant) with respect to corrosivity is shown in Fig 6.6. This reveals that performance of lubricant is proportional to its corrosivity or film formation rate. For the same film formation rate, sulphur's load carrying capacity is greater as compared to phosphorous and chlorine. Hence, it is recommended that sulphur can be added as an additive to the coolant for reducing the friction and to increase the surface finish of this material. To conform this, experiments were conducted with sulphur additive and the results showed that surface roughness had reduced from 4.9 $\mu\text{m}$  to 3  $\mu\text{m}$ .



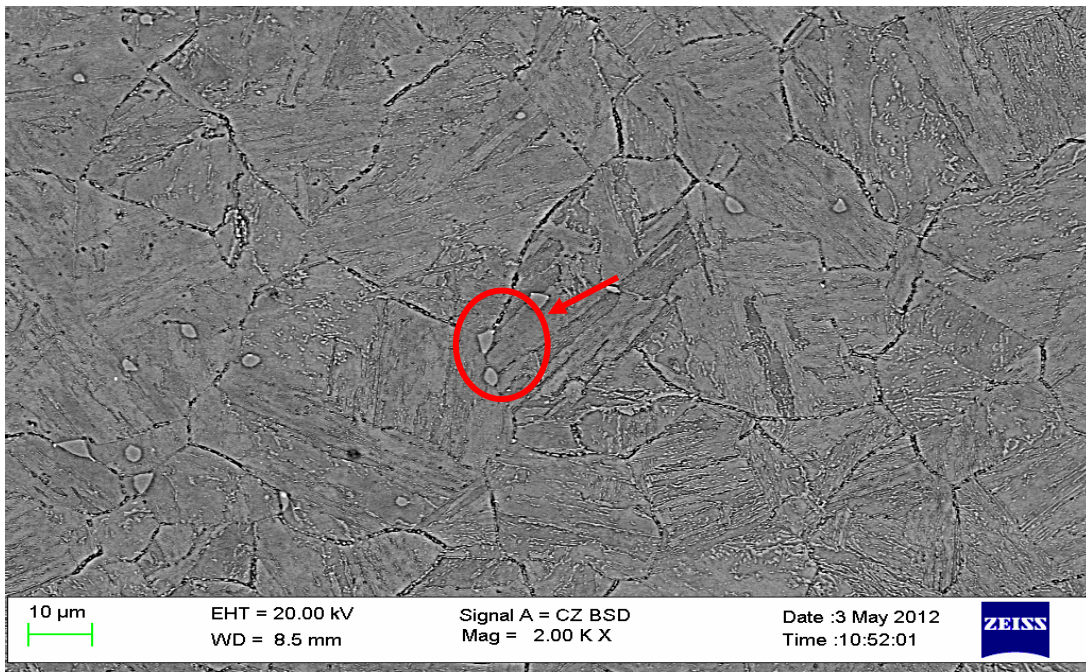
**Fig 6. 6** The relationship between corrosivity and lubricating effect of some EP lubricants (Heshmat and Dill, 1992)

- To test the relative hardness of each material, the hardness test was conducted and this material registered a hardness of 100.9 HRB, which was slightly higher than that of the other two materials (77 and 97.7HRB). The indentation made during the hardness test was observed under the microscope and at the boundary of the indentation shows small cracks which indicated that the relative hardness of the material was greater. The cracks are indicated in the Fig 6.7 using the arrows. This image was observed under a microscope (KOWA) at a focal length between 1-5.5 mm and at magnification of 100x.

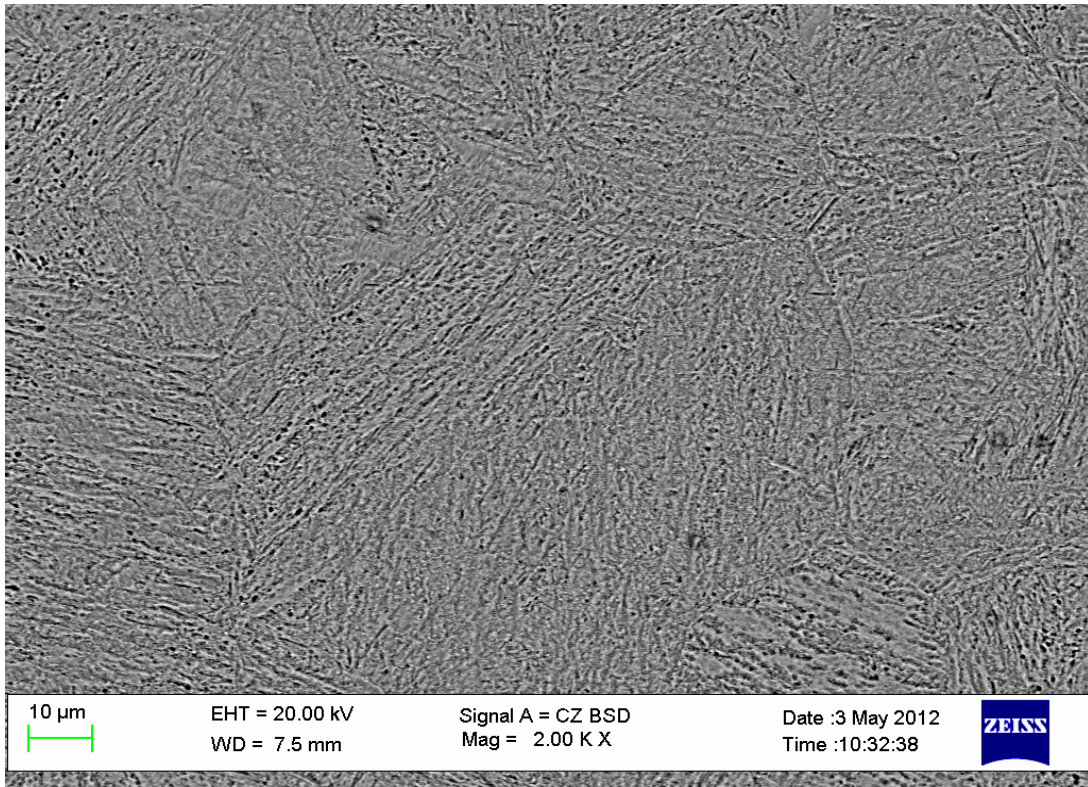


**Fig 6. 7** Photograph of indentation observed under microscope for the material ST 17-4PH

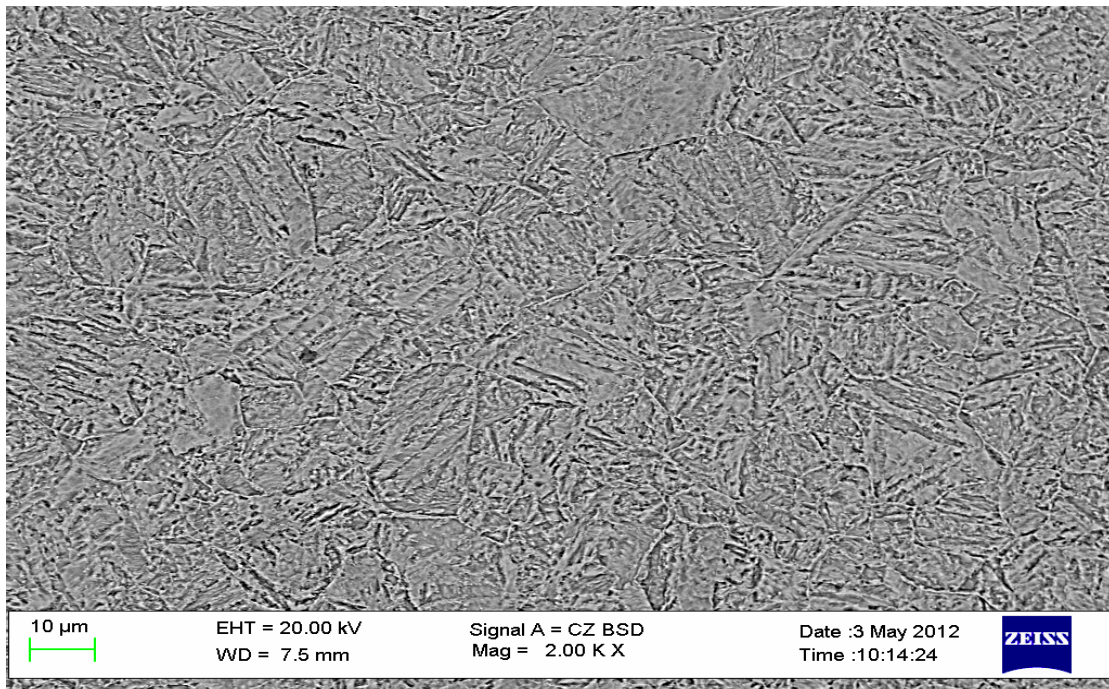
- To analyze the microstructure influence on the hardness, all the three samples were analyzed using scanning electron microscope (SEM) and the results obtained are shown in Fig 6.8 to 6.10. To maintain uniformity, all the three samples were observed at the same magnification (2000X) and the focal length was maintained constant (10  $\mu\text{m}$ ). The microstructure of the material ST 17-4PH was found to have precipitants of copper containing phase alloy and other martensite like structures at the grain boundaries. These precipitants may be responsible for the hardness of the material which in turn, would reduce its machinability. This observation also corroborated with the results given by Liu and Yan (2010).



**Fig 6. 8 SEM microstructure of material ST 17-4PH**






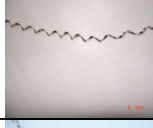


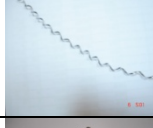







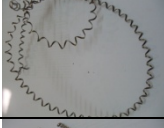



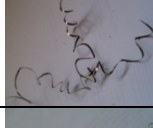
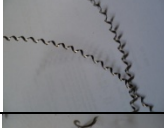
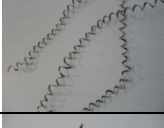



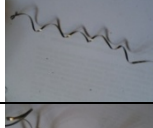



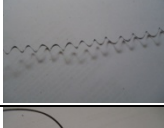


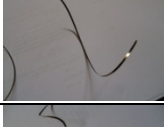

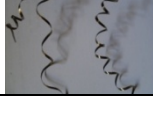
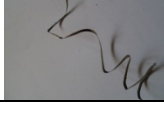

**Fig 6. 9 SEM microstructure of material ST 12TE**







**Fig 6. 10 SEM microstructure of material ST 17/13W**



Table 6. 8 Experimental results  $R_a$  in ( $\mu\text{m}$ )

St d. Or de r	ST 12TE	Chip quality	Chip quality	ST T17/13 W	Chip quality	Chip quality	ST 17-4 PH	Chip quality	Chip quality
1	1.514		Continuous	1.2030		Continuo us	2.13		Continuo us
2	0.910		Continuous	1.1000		Continuo us	0.513		Continuo us
3	0.613		Continuous	0.9540		Continuo us	1.576		Continuo us
4	0.414		Brittle fracture	0.7740		Continuo us	2.561		Brittle fracture
5	0.850		Continuous	1.6420		Continuo us	4.942		Continuo us
6	0.253		Continuous	0.7440		Continuo us	1.958		Continuo us
7	1.284		Continuous	1.5870		Continuo us	3.35		Continuo us
8	0.815		Continuous	0.8960		Continuo us	2.366		Continuo us
9	1.810		Continuous	1.5800		Continuo us	4.541		Continuo us
10	0.743		Continuous	0.6520		Continuo us	0.831 6		Continuo us
11	0.475		Continuous	0.7400		Continuo us	1.46		Continuo us
12	0.592		Continuous	0.7500		Continuo us	1.657		Brittle fracture

13	0.576		Continuous	1.3520		Continuous	1.178		Continuous
14	0.727		Continuous	1.5300		Continuous	4.323		Continuous
15	0.670		Continuous	0.8060		Continuous	1.946		Continuous
16	0.712		Continuous	0.8120		Continuous	1.838		Continuous
17	0.758		Continuous	0.8500		Continuous	1.866		Continuous
18	0.640		Continuous	0.8200		Continuous	1.858		Continuous
19	0.588		Continuous	0.8030		Continuous	1.855		Continuous
20	0.600		Continuous	0.8025		Continuous	1.826		Continuous

The approximation of the response was developed based on either first-order or second-order model as given in the equations (6.1) and (6.2) respectively.

$$y = \beta_0 + \beta_1 x_1 + \beta_2 x_2 + \dots + \beta_k x_k + \varepsilon \quad (6.1)$$

$$y = \beta_0 + \sum_{i=1}^k \beta_i x_i + \sum_{i=1}^k \beta_{ii} x_i^2 + \sum_{i < j=2}^k \sum_{j=2}^k \beta_{ij} x_i x_j + \varepsilon \quad (6.2)$$

From the results obtained, the second order regression equation was postulated in order to derive the relation between the surface roughness and cutting parameters. The respective equations of materials St 17-4PH, St T17/13 W, and St 12TE are given by equation (6.3), (6.4) and (6.5) respectively.

$$R_{a(ST17-4PH)} = 3.5032 - 0.0481 \times V + 0.01356 \times f + 0.00012 \times V^2 + 0.00013 \times f^2 + 0.0307 \times V \times a - 1.668e-04 \times V \times f - 0.0178 \times a \times f \quad (6.3)$$

$$R_{a(ST12TE)} = 4.6901 - 0.02828 \times V + 8.7098E - 05 \times V^2 + 0.0036 \times V \times a + 0.01595 \times a \times f \quad (6.4)$$

$$R_{a(ST17-13W)} = 2.7939 - 0.0041 \times V - 0.01757 \times f + 3.2301E - 05 \times V^2 + 7.826E - 05 \times f^2 - 0.3585 \times a^2 - 6.530E - 05 \times V \times f + 0.00448 \times a \times f \quad (6.5)$$

The regression equation formulated for the ST 17-4PH was verified with the surface roughness results available in the literature. The work of Chien and Tsai, 2003 and Liu and Yan, 2010 were found to be in close agreement with the equation (6.3) derived herein. The equations for the materials ST 12TE and ST 17 13/W were verified by conducting the confirmatory experiments and are discussed in a later section.

### 6.2.1 ANOVA

The analysis of variance (ANOVA) was carried out at 5% level of significance to decide the extent of significance of process variables and interactions on the  $R_a$  values. ANOVA of the RSM model for the material ST 17-4PH, ST 12TE and St T17/13 W are shown in Table 6.9, 6.10 and 6.11 respectively.

**Table 6.9 Analysis of Variance for the regression model of ST 17-4PH**

Source	DF	Seq SS	Adj SS	Adj MS	F	P
Regression	9	25.5791	25.5791	2.84212	25.11	0.000
Linear	3	17.6947	17.6947	5.89824	52.11	0.000
Square	3	2.9495	2.9495	0.98318	8.69	0.004
Interaction	3	4.9349	4.9349	1.64496	14.53	0.001
Residual Error	10	1.1319	1.1319	0.11319		
Pure Error	5	0.0090	0.0090	0.00179		
Total	19	26.7110	$R^2=95.76\%$	$Adj.R^2=91.95\%$	$R^2(Pred)=67.75\%$	

**Table 6. 10 Analysis of Variance for the regression model of ST 12TE**

Source	DF	Seq SS	Adj SS	Adj MS	F	P
Regression	9	2.49885	2.49885	0.277650	28.51	0.000
Linear	3	0.98644	0.98644	0.328814	33.76	0.000
Square	3	0.75276	0.75276	0.250922	25.76	0.000
Interaction	3	0.75964	0.75964	0.253215	26.00	0.000
Residual Error	10	0.09740	0.09740	0.009740		
Pure Error	5	0.02158	0.02158	0.004316		
Total	19	2.59625	R <sup>2</sup> =96.25%	Adj.R <sup>2</sup> =92.87%	R <sup>2</sup> (Pred)=76.04%	

**Table 6. 11 Analysis of Variance for the regression model of ST T17/13W**

Source	DF	Seq SS	Adj SS	Adj MS	F	P
Regression	9	1.93471	1.93471	0.214967	27.01	0.000
Linear	3	0.97312	0.97312	0.324373	40.76	0.000
Square	3	0.68982	0.68982	0.229941	28.90	0.000
Interaction	3	0.27177	0.27177	0.090588	11.38	0.001
Residual Error	10	0.07958	0.07958	0.007958		
Pure Error	5	0.04174	0.04174	0.008347		
Total	19	2.01428	R <sup>2</sup> =96.05%	Adj.R <sup>2</sup> =92.49%	R <sup>2</sup> (Pred)=81.96%	

Tables 6.9 to 6.11 show that the linear, square and interactions are significant for all the three materials. From this it may be concluded that the quadratic model is suitable for this material. The suitability of the regression model was decided based on the value of R<sup>2</sup>. As the value of R<sup>2</sup> approaches 1 it is the best suitable regression model and if it moves towards 0 then

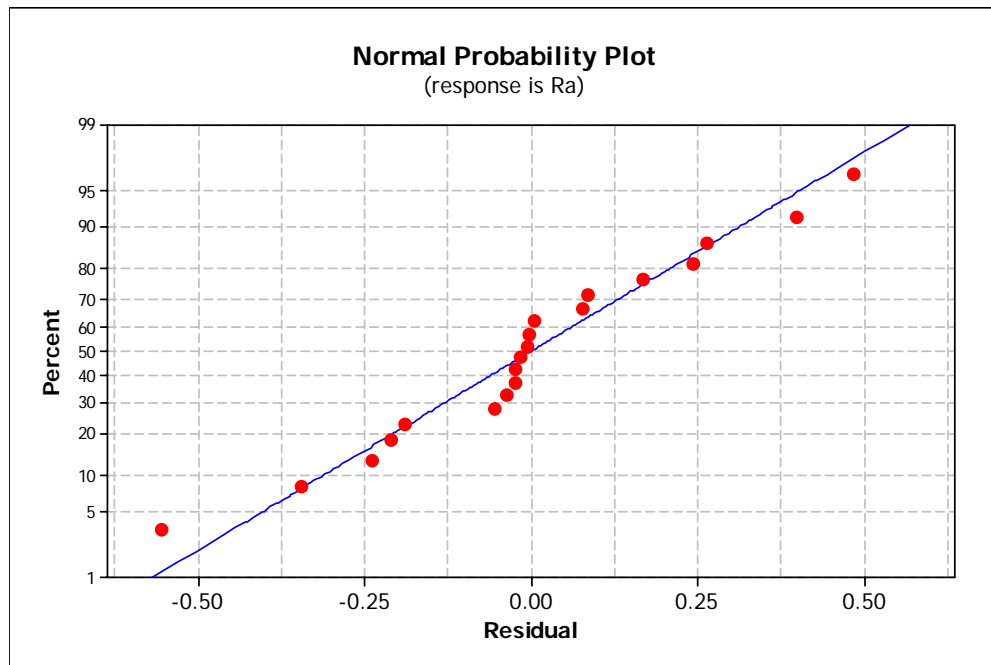
the value of the residuals increase. With increase in the number of variables, the value of residuals decrease and the coefficient of determination  $R^2$  increases. To achieve a more precise comparison  $Adj.R^2$  is used, which is adjusted for the degrees of freedom.  $Adj.R^2$  is used for comparing the range of predicted values at the design points to the average prediction error. It is like signal to noise ratio used in Taguchi method. All the materials had  $R^2$  values greater than 95% (and  $Adj.R^2$  is approximately 92%). In each of the three cases, the predicted  $R^2$  value was in reasonable agreement with the  $Adj. R^2$  value. The value of  $R^2$  was closer to 1, which was desirable. Based on these ANOVA results, the contribution of individual interactions to the mean was studied, and the results are shown in Table 6.12.

For the material ST 17-4PH the main effects were speed and feed and interaction effects (speed\*speed, feed\*feed, speed\*depth of cut, speed\*feed, depth of cut\*feed) were significant in formulating the regression equation. On the other hand, depth of cut and its quadratic effect were insignificant. For the material ST 12TE, the results showed that the main effects depth of cut and feed were insignificant and speed was significant. In the interaction effects speed\*speed and depth of cut\*feed were significant. Though depth of cut and feed were insignificant as individual factors, they were significant when varied simultaneously. ANOVA results of the material ST T17/13W shows that for this material speed and feed were significant main effects.

**Table 6. 12 ANOVA for the coefficients in regression equation**

	<b>ST 17-4PH</b>	<b>ST 12TE</b>	<b>ST T17/13 W</b>
Term	Probability (P)	Probability (P)	Probability (P)
Constant	0.000	0.000	0.000
speed	0.000	0.000	0.000
doc	0.617	0.589	0.192
feed	0.000	0.990	0.006
speed*speed	0.006	0.000	0.006
doc*doc	0.310	0.115	0.058
feed*feed	0.004	0.906	0.000
speed*doc	0.001	0.085	0.618
speed*feed	0.006	0.369	0.000
doc*feed	0.018	0.000	0.024

The adequacy of the model was also checked with the help of a normal probability plot between the residuals and the predicted values. This plot should form a straight line if the model is adequate (Noodin et al, 2004). The normal probability plot and the residuals vs fits for the material ST 17-4PH are shown in Fig. 6.11 and Fig. 6.12 respectively. Fig. 6.11 reveals that residuals fall on a straight line and the errors are distributed normally. Fig. 6.12 reveals that most of the residuals fall closer to the zero residual line, therefore giving minimum error in fitting regression equation. From these two plots also it could be concluded that the model proposed was adequate. The normal probability plot and residual graph for the material ST 12TE are shown in Figures 6.13 and 6.14 respectively and in Figures 6.15 and 6.16 respectively for the material ST T17/13W. These graphs also formed the straight line pattern and from these plots it could be concluded that the proposed regression model was adequate.



**Fig 6. 11 Normal probability plot for the Ra response of St 17-4PH material**

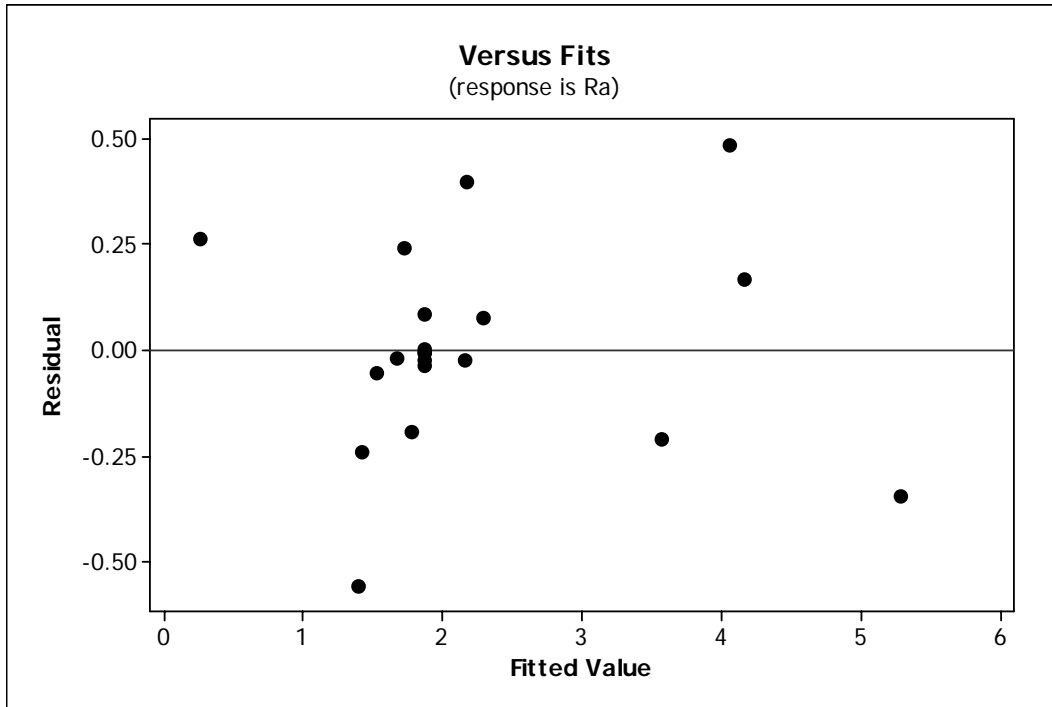


Fig 6.12 Residual vs Fits for the Response Ra of St 17-4PH

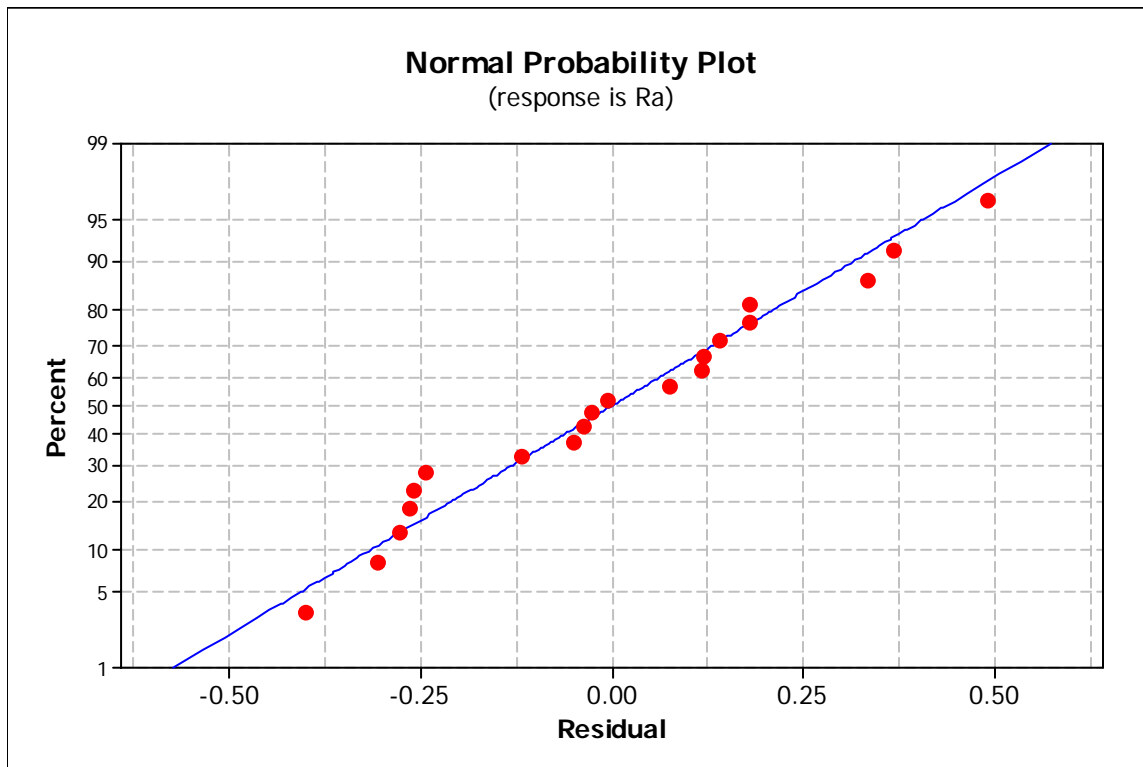


Fig 6.13 Normal probability plot for the Ra response of material ST 12TE

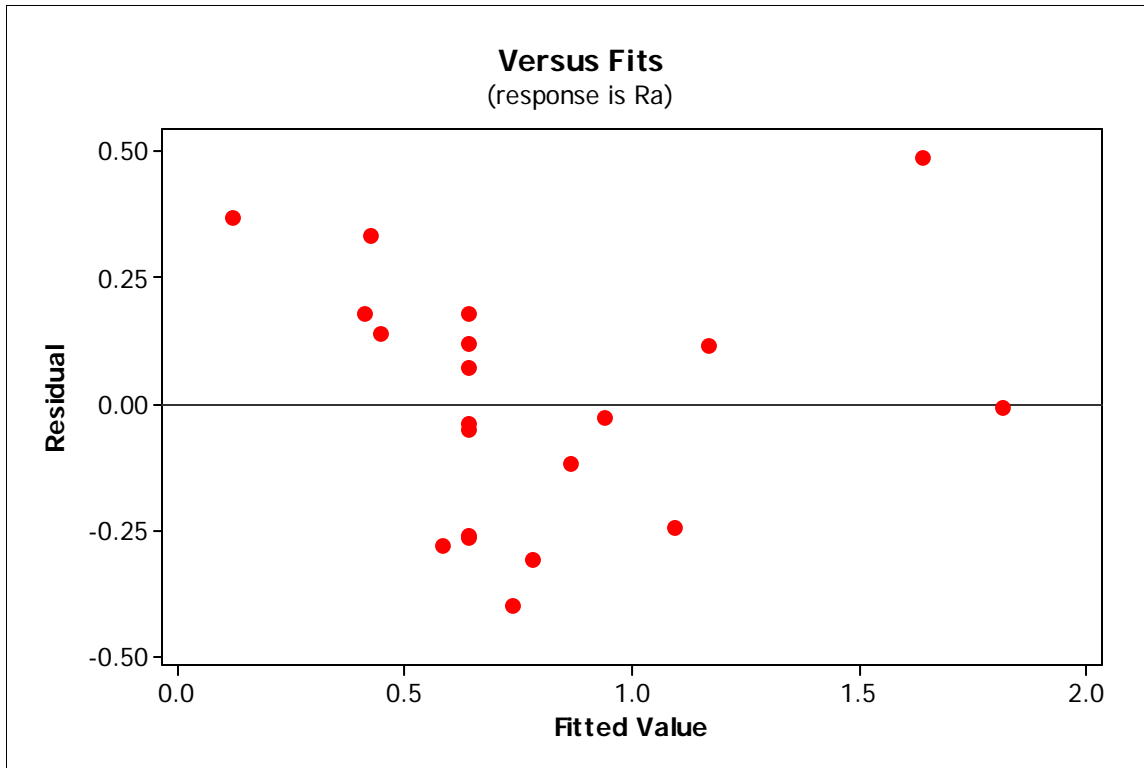


Fig 6. 14 Residual plot for the Ra response of material ST 12TE

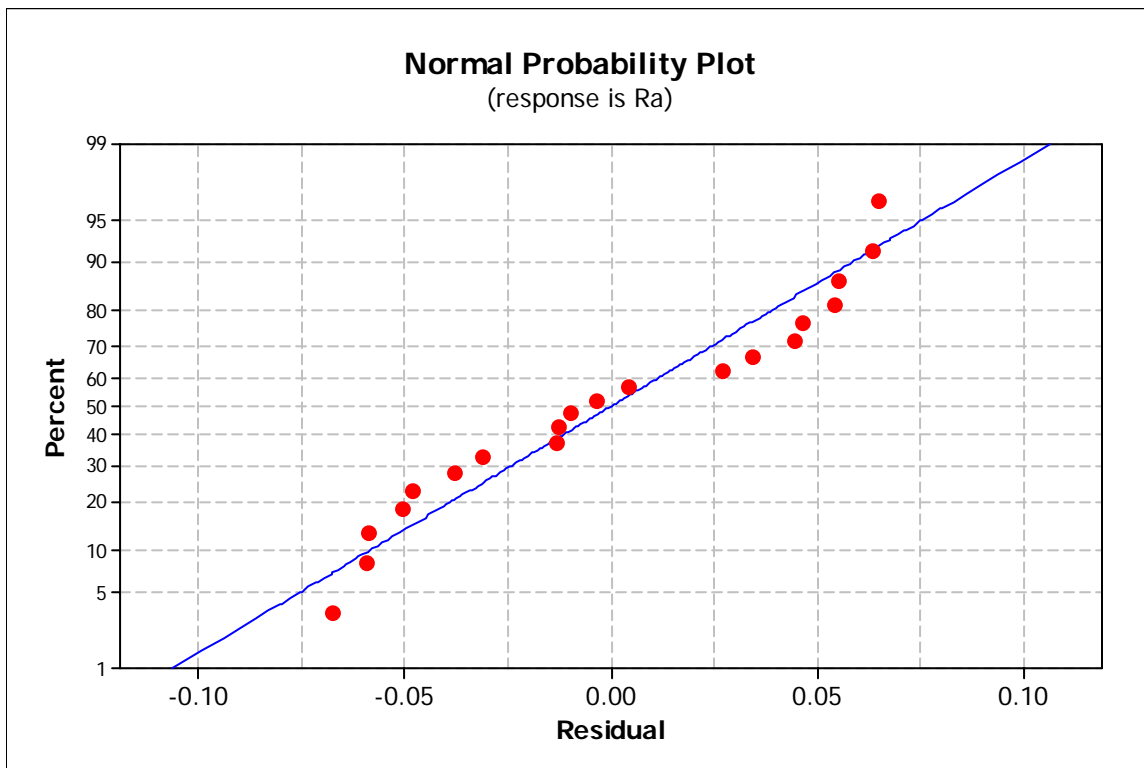


Fig 6. 15 Normal probability plot for the Ra response of material ST T17/13W



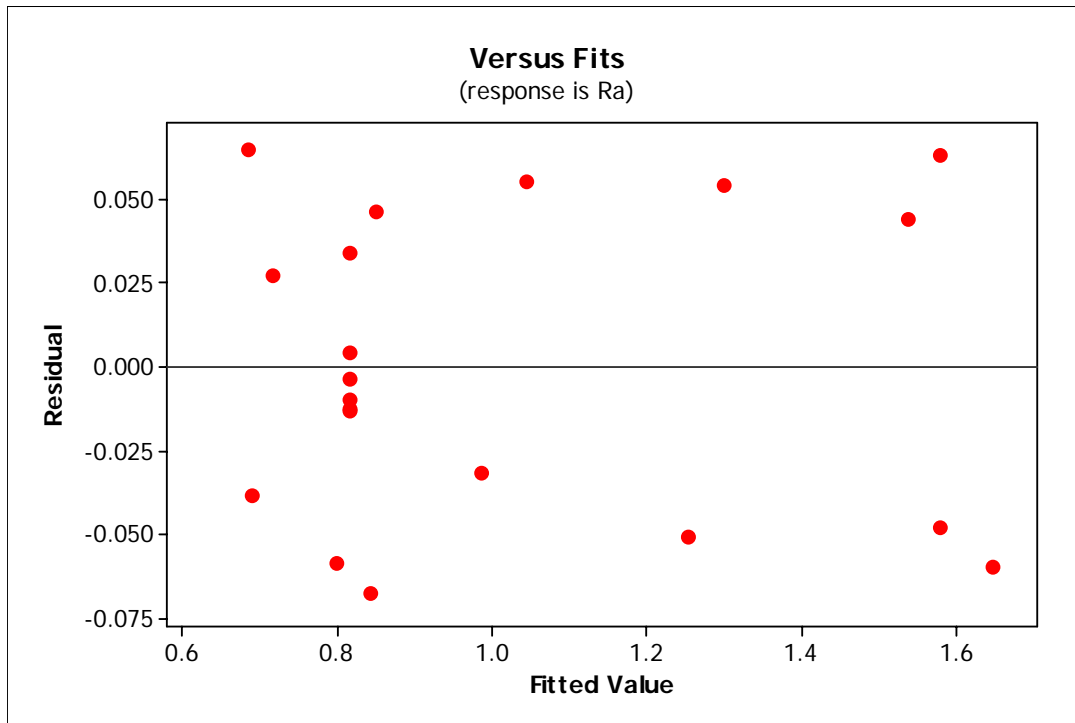


Fig 6. 16 Residual plot for the Ra response of material ST T17/13W

### 6.2.2 Contour plots and response surface graphs

Using Minitab 15.0 software, contour plots and 3D graphs for the cutting parameters with respect to surface roughness were generated in order to find the responsible parameters or combinations of these. A contour plot is a graphical technique used for representing a three dimensional surface by plotting constant  $z$  slices called contours on a 2-dimensional format.

A surface graph provides a three dimensional view, which gives a clear picture of the response surface. The contour and surface plots for all the materials are shown in Fig 6.17, 6.18 and 6.19. Fig 6.17(a) and 6.17(b) represent the contour and surface plots for the material ST 17-4PH. Fig 6.17(a) revealed that when speed and feed vs  $R_a$  was considered, the lowest surface roughness was obtained at highest speed 200 m/min and medium feed rate (145 mm/min), this is shown as red color in the contour plot. It is known from the fundamental theory of machining, that the feed rate and nose radius play an important role in surface roughness of the machined surface when the cutting edge is sharp (Shaw, 1984 metal cutting principles) and is expressed as:

$$R_a = \frac{f^2}{32r} \quad (6.6)$$

Where  $f$  is the feed rate and  $r$  is the nose radius. However, if the cutting edge is not sharp or modified, then other factors come into effect and influence the surface roughness.

The 3D surface plot in Fig 6.17(b) showed that the surface roughness was a high peak at lower cutting speed and low to medium feed rate. The surface roughness was less at the higher cutting speeds. Thus, at higher material removal rate, the volume of accumulated material would be more, thereby suppressing the effect of cutting edge radius and feed rate more effectively. Hence, the surface roughness would be less.

Fig 6.17(c) and 6.17(d) respectively represents the contour and surface plots of speed and feed vs  $R_a$  of the material ST 12TE. The contour and surface plots revealed that the surface roughness was highest at the lowest speed (40 m/min) and medium feed rate. As the speed increased, the surface roughness decreased. If both the parameters were varied linearly, then the surface roughness would be reducing with linear variation of both the parameters. Fig 6.17(e) and 6.17(f) respectively represented the contour and surface plots of speed and feed vs  $R_a$  of the material ST T17/13W. The contour plot for this material was similar to the material ST 17-4PH. The difference was ST T17/13W had peaks at several points, for example the surface roughness was highest at the highest feed rate and medium speed.

Fig 6.18(a) revealed that with lower feed rate the surface roughness was less and with the increase in the feed rate the surface roughness also increased. There was not much variation in the surface roughness with increase in value of depth of cut. The Fig 6.18(b) shows the three dimensional variation of the surface roughness w.r.t. to feed and depth of cut. As the feed rate increased from 100 mm/min to 250 mm/min the value of the  $R_a$  was more than doubled, which was also true from the equation (6.6). Figures 6.18(c) and 6.18(d) showed that the surface roughness was highest at lower feed and depth of cut combination and highest feed and depth of cut combination. Figures 6.18(e) and 6.18(f) revealed that irrespective of change in value of the depth of cut the surface roughness was higher at larger feed rates.

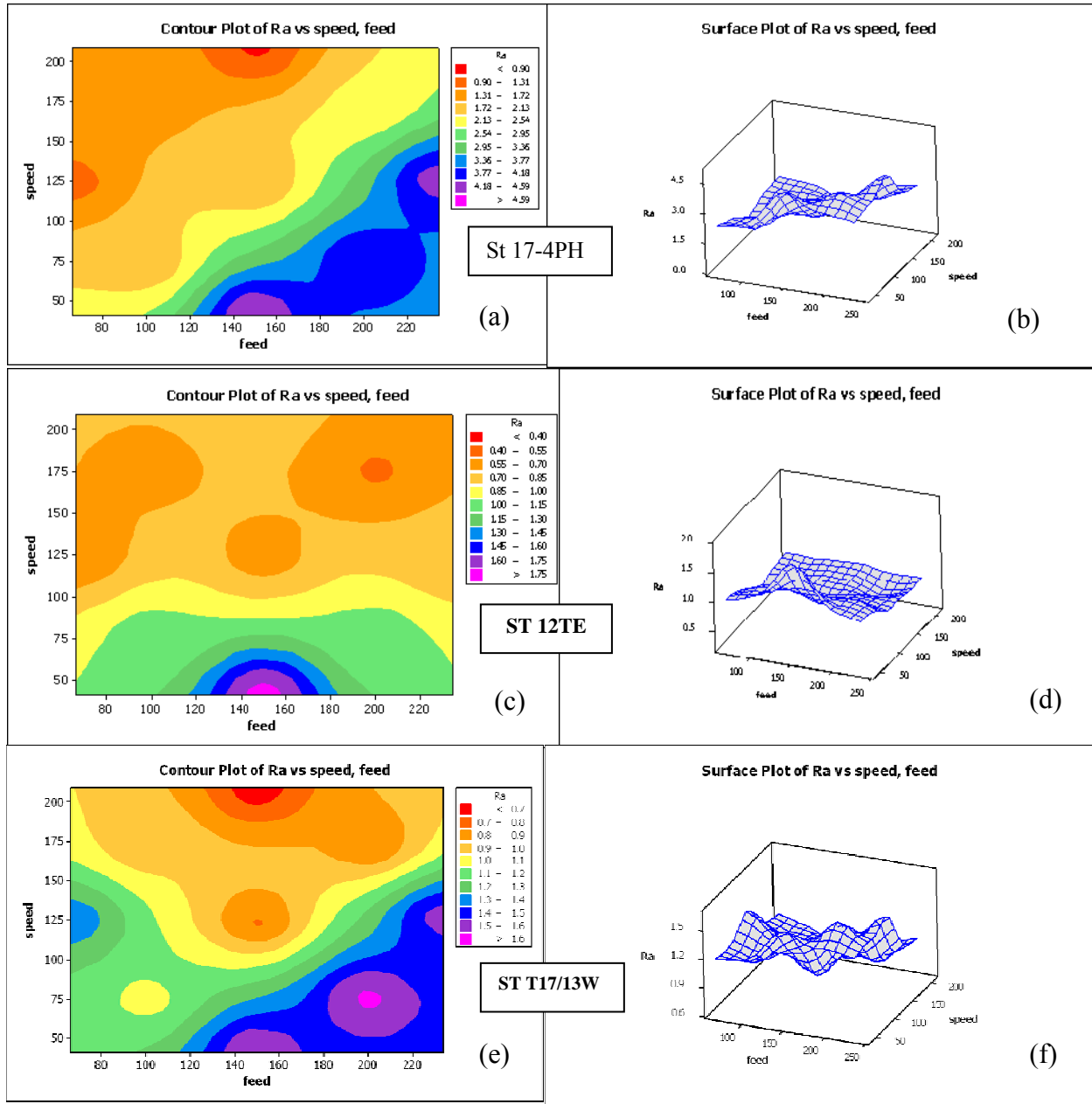
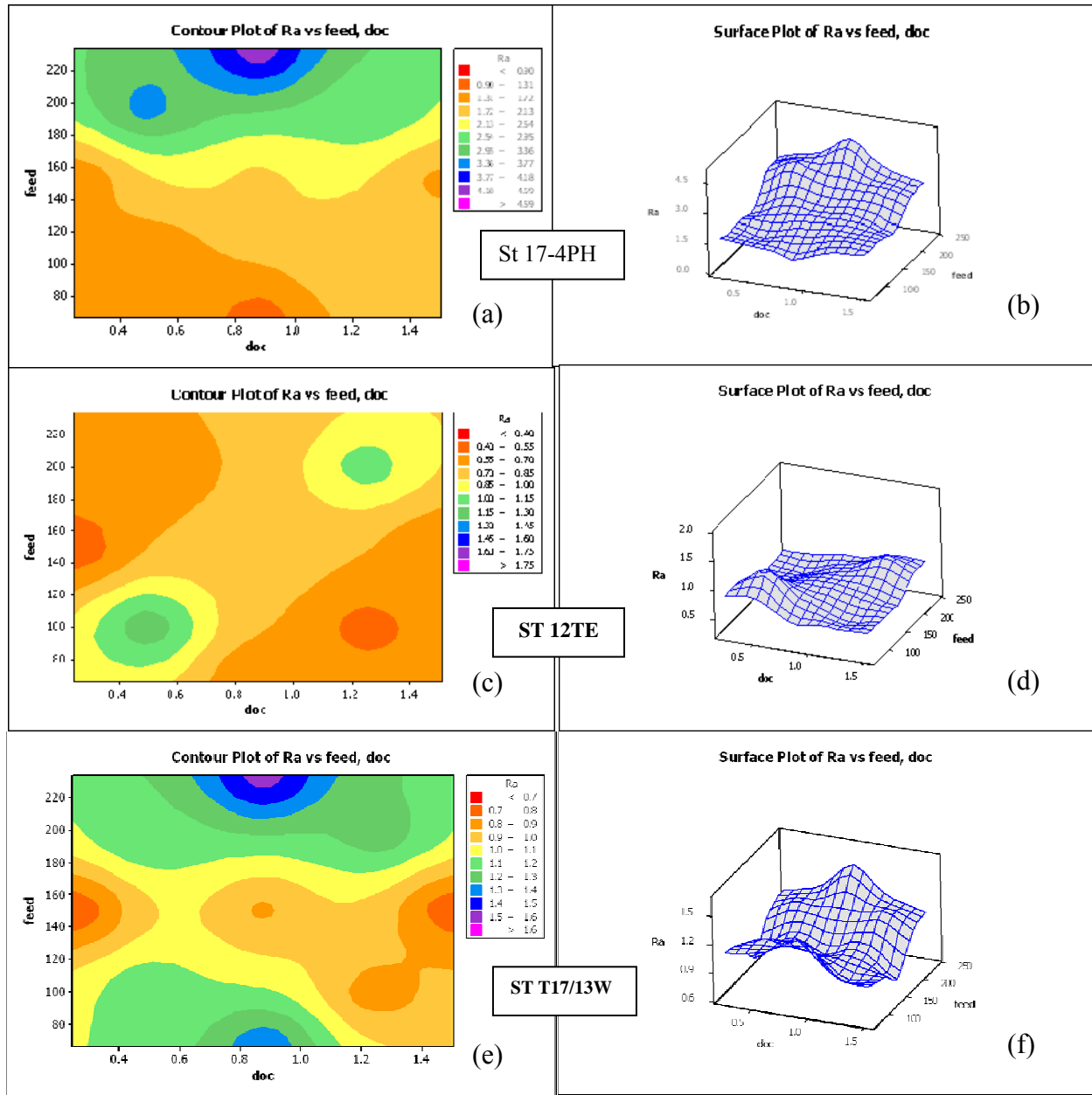


Fig 6. 17 Contour and 3D surface graphs of speed and feed vs surface roughness for the materials



**Fig 6. 18 Contour and 3D surface graphs of feed and depth of cut vs surface roughness for the materials**

Figures 6.19(a) to 6.19(f) showed the variation of  $R_a$  w.r.t. speed and depth of cut. The contour plots for all the three materials had similar pattern. All the three materials had maximum surface roughness at a depth of cut from 0.8-1.0 mm range and at lowest speed. The lowest surface roughness was observed at the highest speed and depth of cut between 0.8-1.0 mm. The value of  $R_a$  was considerably low at the lower speeds irrespective of depth of cut. To reduce the surface roughness the orange color zone is the optimal combination and green, blue and pink colored zones are not recommended.

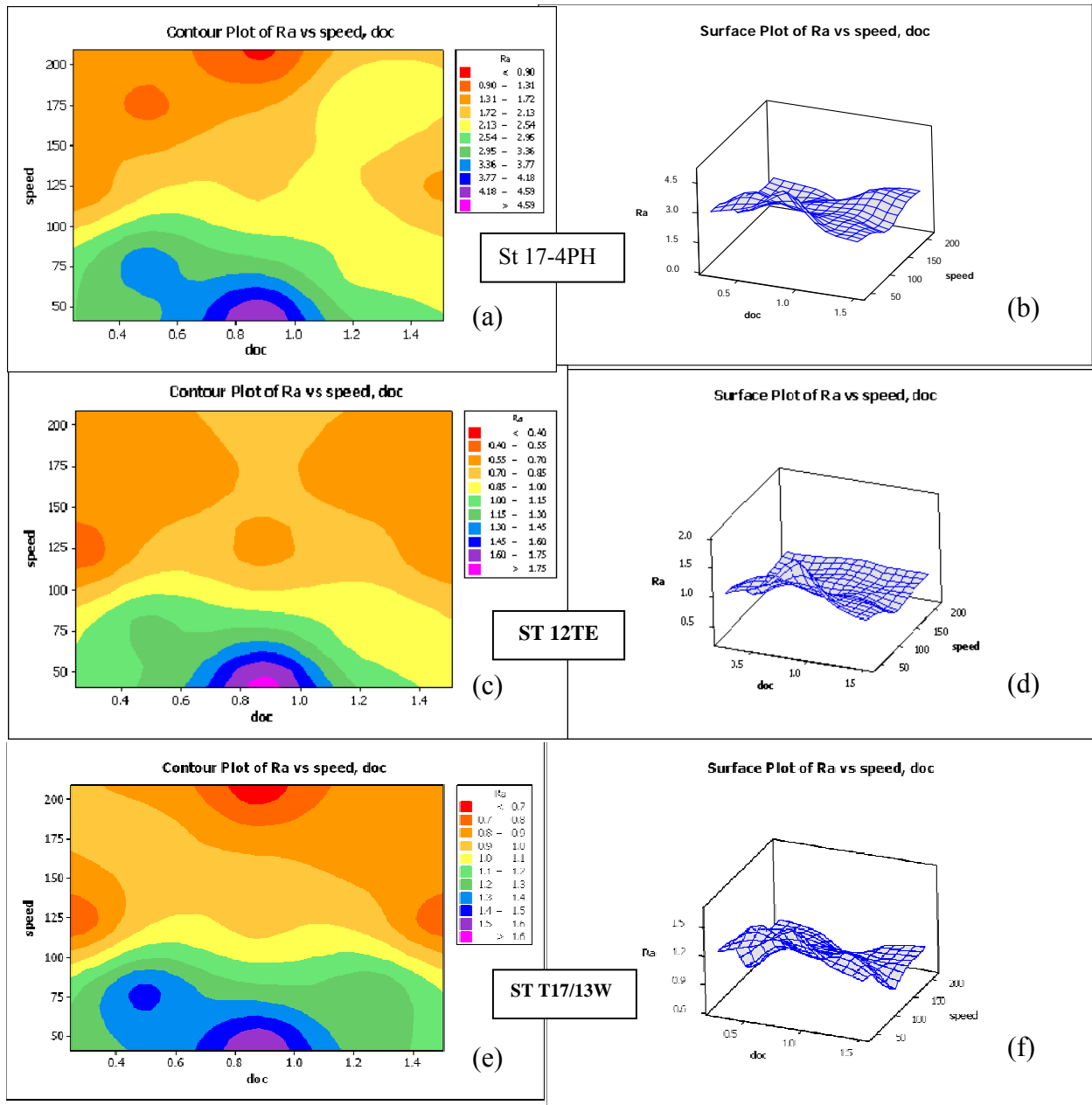
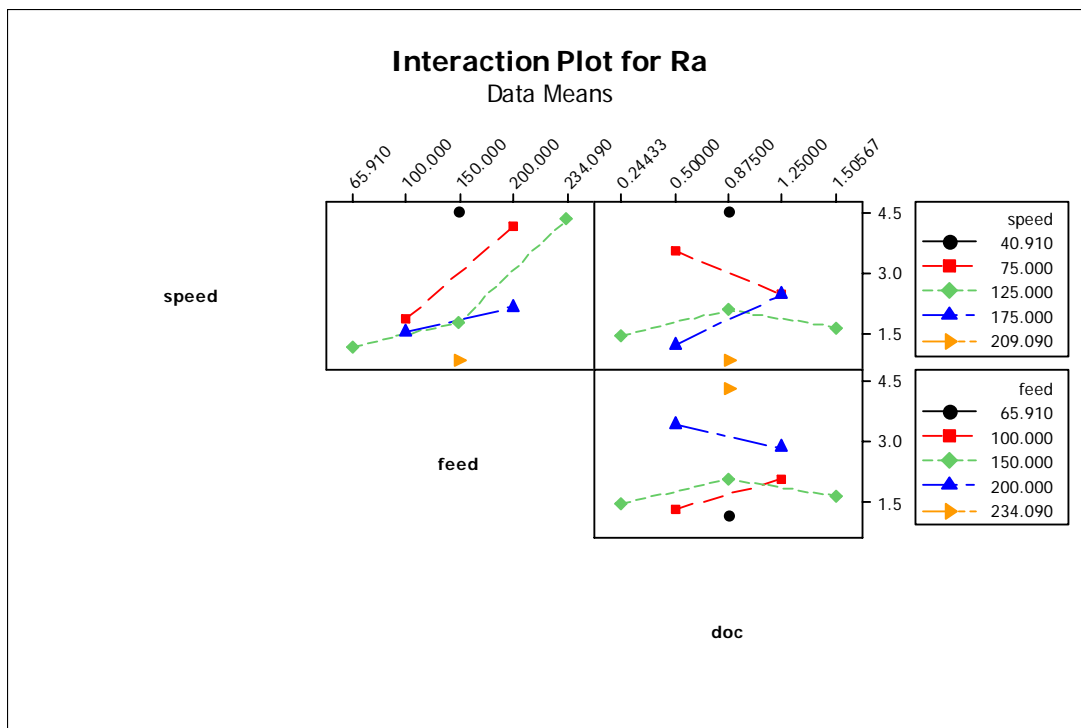


Fig 6. 19 Contour and 3D surface graphs of speed and depth of cut vs surface roughness for the materials

### 6.2.3 Interaction plots

In the contour and surface plots the variation of  $R_a$  with respect to two parameters at a time could be observed. To identifying the interactions effect of all the parameters on  $R_a$ , the interaction plot was generated using Minitab 15.0. The interaction plots for the materials are shown in Fig 6.20, 6.21 and 6.22. In these plots, the variation of surface roughness with respect to the combination of cutting parameters at different levels is represented. The lines which are

parallel to each other, do not have any combine effect on the response. The intersecting lines show that when both the parameters are varied simultaneously, the combined effect will be evident on the response. For example in Fig 6.20, depth of cut alone did not affect the response, when it was varied simultaneously with speed or feed, it would affect the response. For the material ST 17-4PH, at the lower speed (75 m/min) the surface roughness decreased with increase in depth of cut. At the same speed, surface roughness increased if the feed increased from 100 to 200 mm/min. From Fig 6.20, it could be concluded that interaction effects exist between speed, feed and depth of cut.



**Fig 6. 20 Interaction effect of cutting parameters on Ra for the material ST 17-4PH**

Fig 6.21 shows the interaction plots for the material ST 12TE. In this, different lines represent the variation of surface roughness for the parameters combination at different level. The lines are not intersecting for the combination like speed\*feed and depth of cut\*speed and the lines are intersecting for feed\*depth of cut combination. This reveals that the surface roughness is sensitive to simultaneous variation of feed and depth of cut combination.

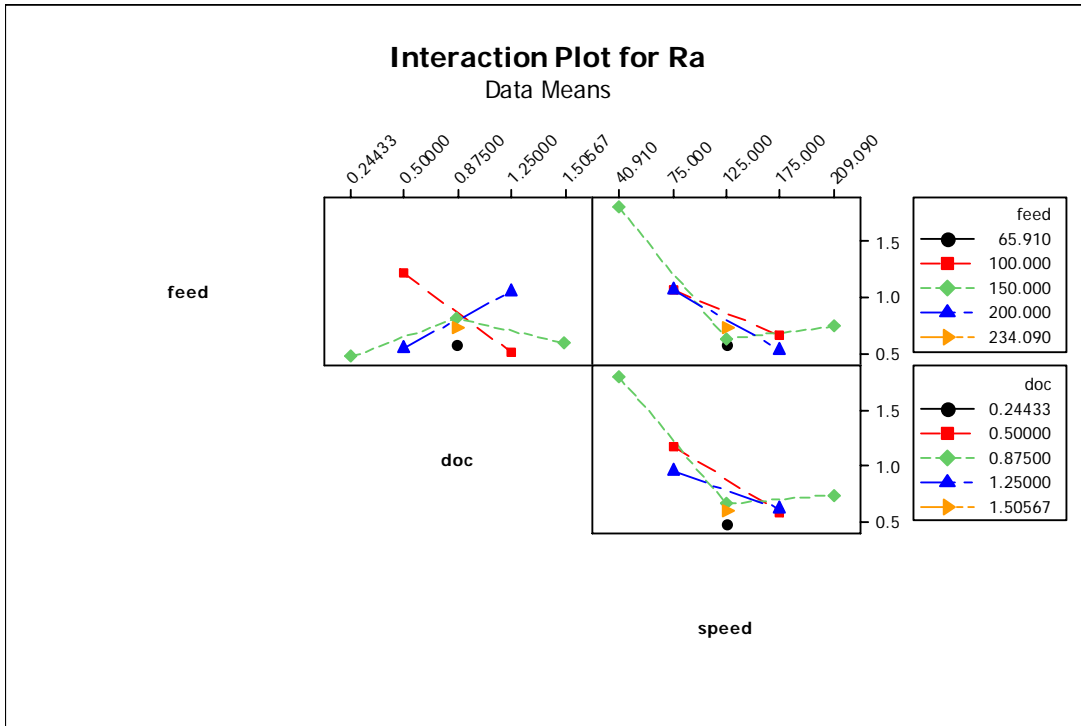


Fig 6. 21 Interaction effect of cutting parameters on Ra for the material ST 12TE

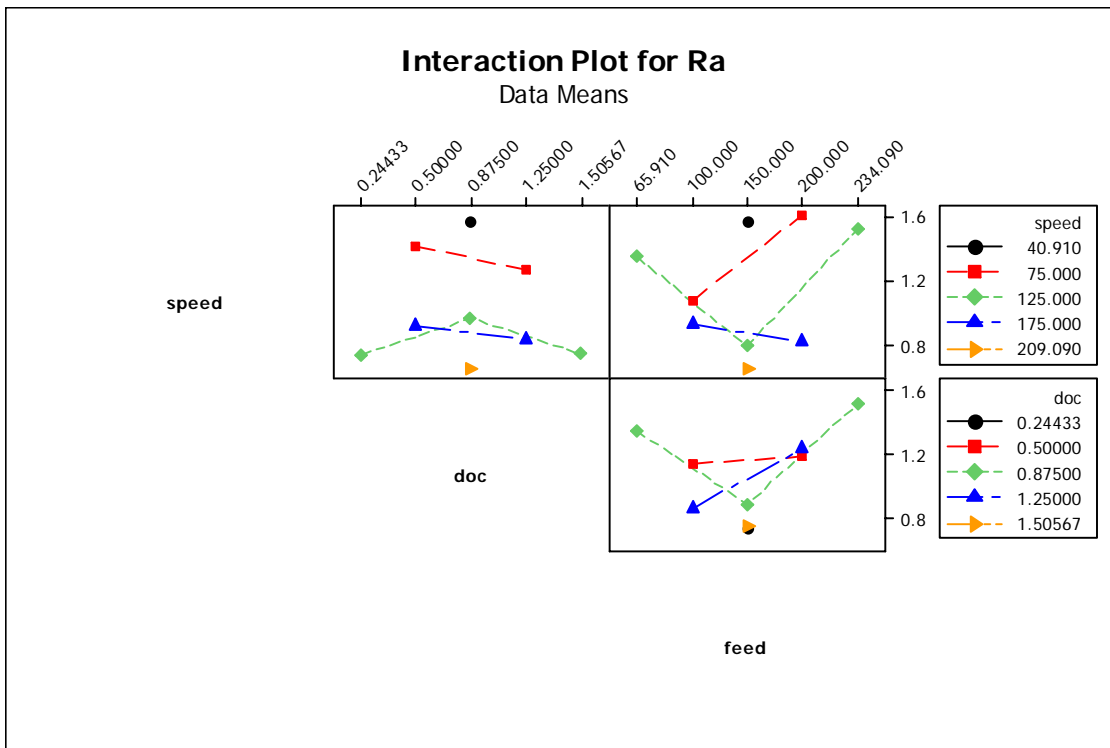


Fig 6. 22 Interaction effect of cutting parameters on Ra for the material ST T17/13W

Fig 6.22 shows the interaction plots for the material ST T17/13W. In this, the top left box represents the variation of surface roughness with the speed and depth of cut combination. In this box all the lines are almost parallel to each other showing that there exists no interaction between these parameters in variation of surface roughness and they are acting independently. In the top right and the bottom box the lines are intersecting meaning there exist interaction effect of speed\*feed and depth of cut\*feed for the response variation.

#### 6.2.4 Confirmatory experiments

To validate the above results, confirmatory experiments were performed with the new set of process parameters. Table 6.13 shows the predicted as well as experimental results. It can be seen that these values were close to each other. The minor deviation between the values could be attributed to uncontrollable parameters like inconsistency in material composition, small deviation in the work piece shape from circular cross section, repeatability of the measuring equipment and entangling of chip around the turned work piece.

**Table 6. 13 Confirmatory experiment results for all the three materials**

Material	Speed (m/min)	Feed (mm/min)	Depth of cut (mm)	Surface roughness ( $\mu\text{m}$ )		
				Predicted	Experimental	% error
ST 12TE	125	150	0.875	0.701	0.670	3.1
ST T17/13W	175	200	1.25	0.8512	0.8960	1.78
ST 17-4 PH	175	100	0.5	0.492	0.513	2.1

#### 6.3 Summary

In this chapter the surface quality evaluation of steels for different combination of cutting parameters in a CNC turning process is presented. The central composite design was used for the design of experiments and 20 experiments for each material were designed and conducted. The trend in the experimental results showed that material ST 17-4PH had the highest surface roughness ( $4.9 \mu\text{m}$ ) and ST 12TE had the lowest surface roughness ( $0.85 \mu\text{m}$ ) for the same combination of parameters. This suggested that ST 17-4PH material would require one more finishing process like grinding to obtain the same surface finish as the other materials. The



reasons proposed for the high surface roughness of machined ST 17-4PH were, Nickel percentage is less than 8%, which prevents forming fully austenitic steel causing increase in hardness, the percentage of sulphur content improves the machinability and is very less (0.001%). In this case, the material was acting inert to the coolant supplied, so the growth rate of sacrificial layer was reduced which lead to increase in friction. It was suggested that coolant additives like sulphur and phosphorous be used to increase the reaction. The regression equation for the response, surface roughness, and the input variables speed, feed and depth of cut was formulated for each material and the insignificant coefficients were eliminated. The equations were verified by conducting confirmatory experiments and the percentage error in all three materials was less than or equal to 3.1. This indicated that formulated regression equations were well in agreement with the literature for the given range of input variables.

The results were analyzed using surface graphs, contour plots and interaction plots. The surface graphs and contour plots revealed that for the materials ST 17-4PH and ST17/13W, feed rate and speed had significant effect on the surface roughness and depth of cut was insignificant. The interaction plots for these two materials showed that speed vs feed and feed vs depth of cut interactions had significant effect on surface roughness. For ST 12TE material, speed and the interaction between depth of cut and feed were significant for the response.

As the machining process discards 75% of the original billet, which is wastage of material, time and shipping cost, it was recommended that ST 17-4PH material should be processed using near net shaped casting in order to save on processes like polishing, machining, etc, and yet retain good surface finish, as well as ensure a defect less product.

# CHAPTER 7

## CONCLUSIONS

### 7.1 Conclusions

The significant contributions made in the present work are as follows:

1. Graph theory, matrix algebra and permanent were applied for quality modeling and evaluation of a CNC turning center. The developed quality index (QI) would be useful for benchmarking, comparison and evaluation of a CNC turning center. The quality based evaluation methodology was applied to a CNC turning center. The calculated QI was 52612, with maximum and minimum possible values of 3281251 and 21 respectively. Using this methodology the areas of improvement for the quality could be identified and improved. For example, if the interaction value of graphical interface (decision making subsystem) with operator (Human subsystem) were improved from 3 to 5, the quality index improved by 10.50% as compared to the original. The evaluation of quality interaction between the cutting tool and the sensor was illustrated using available experimental data and the value was found to be 0.0013. The developed methodology considers all factors influencing the quality evaluation of a CNC turning center including the design, manufacturing and maintenance phases.
2. A concurrent design index (CDI) was derived, which combined all the design aspects/x-abilities and interactions. This would be useful in evaluation and decision making during the conceptual design phase. This index was derived using graph theory, matrix algebra and permanent function. The CDI was applied in DFX based evaluation of turbine blade materials ST 12TE, ST T17/13W and ST17-PH. The x-abilities considered in evaluation of these three alternatives were design for manufacturing (DFM), design for quality (DFQ), design for environment (DFE) and design for cost (DFC). The CDI obtained for these alternative materials showed that ST 12TE had the highest value of 51.12 and would be the most suitable material amongst the three. The highest CDI for ST 12TE could be attributed to lower surface roughness in machining, reduced cutting and thrust forces, low machining costs and milder environment impact.

3. A 3-stage procedure based on MADM approach was proposed. This would be useful in evaluation, comparison and selection of a material for CNC turning process. Several attributes pertinent for the evaluation of a material were identified. The proposed coding scheme considered a collection of 50 attributes that characterize a material and would be useful in differentiating between alternatives. The 3-stage selection procedure included an elimination search, TOPSIS based evaluation and ranking, final decision making and worked on information related to the pertinent attributes. This procedure ranked alternatives based on the Euclidian distance of the alternatives from the hypothetically best and hypothetically worst material. The generated hypothetically best would be useful to industries in setting up the benchmark attribute values for the material. The developed methodology considered the distinction between the two types of possible attributes i.e. larger-the-better and smaller-the-better and gave the ranking accordingly. Only by giving two different matrices, namely, the decision matrix and the relative importance matrix as an input, the user would directly get the ranking of each alternative. It was recommended that the manufacturer should provide information about all the 50 attributes relevant to a material. Evaluation, ranking and selection of a material were applied to turbine blades based on different attributes in turning using a CNC lathe. From the case study, it was found that ST 12TE had the highest  $C_i^*$  index value of 0.5853. This showed that, ST 12TE has the best surface finish, cutting and thrust forces, power consumption, and tool cost, as compared to the other materials considered. The material ST 12TE was the best ranked material among the five materials using MADM-TOPSIS. This result corroborated with that obtained using the DFX based evaluation technique.
4. An experimental investigation study on surface quality evaluation of steels for different combination of cutting parameters in a CNC turning process was conducted. The central composite design was used for the design of experiments and 20 experiments for each material were designed and conducted. The trend in the experimental results showed that the material ST 17-4PH had highest surface roughness (4.9  $\mu\text{m}$ ) and ST 12TE had lowest surface roughness (0.85  $\mu\text{m}$ ) for the same combination of parameters. This indicated that ST 17-4PH material requires one more finishing process like grinding to get the same surface finish as the other materials. Potential reasons for the high surface roughness of machined ST 17-4PH are twofold. Firstly, the nickel percentage is less than the minimum

required (8%) to form fully austenitic structure, thus causing an increase in hardness. Secondly, this material has very low sulphur content (0.001%) thus reducing its machinability. This is because, when the percentage of sulphur is high in a material, it will be reactive to the emulsified water coolant and would form a sacrificial layer which reduces friction and improves the surface finish during machining, but when the sulphur content is low, as in this case, the sacrificial layer is not formed or poorly formed, thus compromising the machinability. The regression equation for the response, surface roughness, and the input variables speed, feed and depth of cut was formulated for each material and the insignificant coefficients were eliminated. The equations were verified by conducting confirmatory experiments and the percentage error in all three materials was found to be less than or equal to 3.1. This indicated that the formulated regression equations were well in agreement for the given range of input variables. The results were analyzed using surface graphs, contour plots and interaction plots. The surface graphs and contour plots revealed that for the materials ST 17-4PH and ST17/13W, the feed rate and speed have a significant effect on the surface roughness and the effect of depth of cut is negligible. The interaction plots for these two materials showed that speed vs feed and feed vs depth of cut interactions had significant effect on surface roughness. For the ST 12TE material, speed and the interaction depth of cut vs feed were significant. The machining process, in general, discards around 75% of the original billet, resulting in wastage of material, time and shipping cost. Hence, it was recommended that ST 17-4PH material should be processed using near net shaped casting in order to save on processes like polishing, machining, etc., and yet retain good surface finish, and to obtain a defect-less product.

5. A step-by-step procedure of this work which is useful for the designer, manufacturer as well as maintenance person, in modeling, analysis and in making key decisions is shown in Fig 7.1.

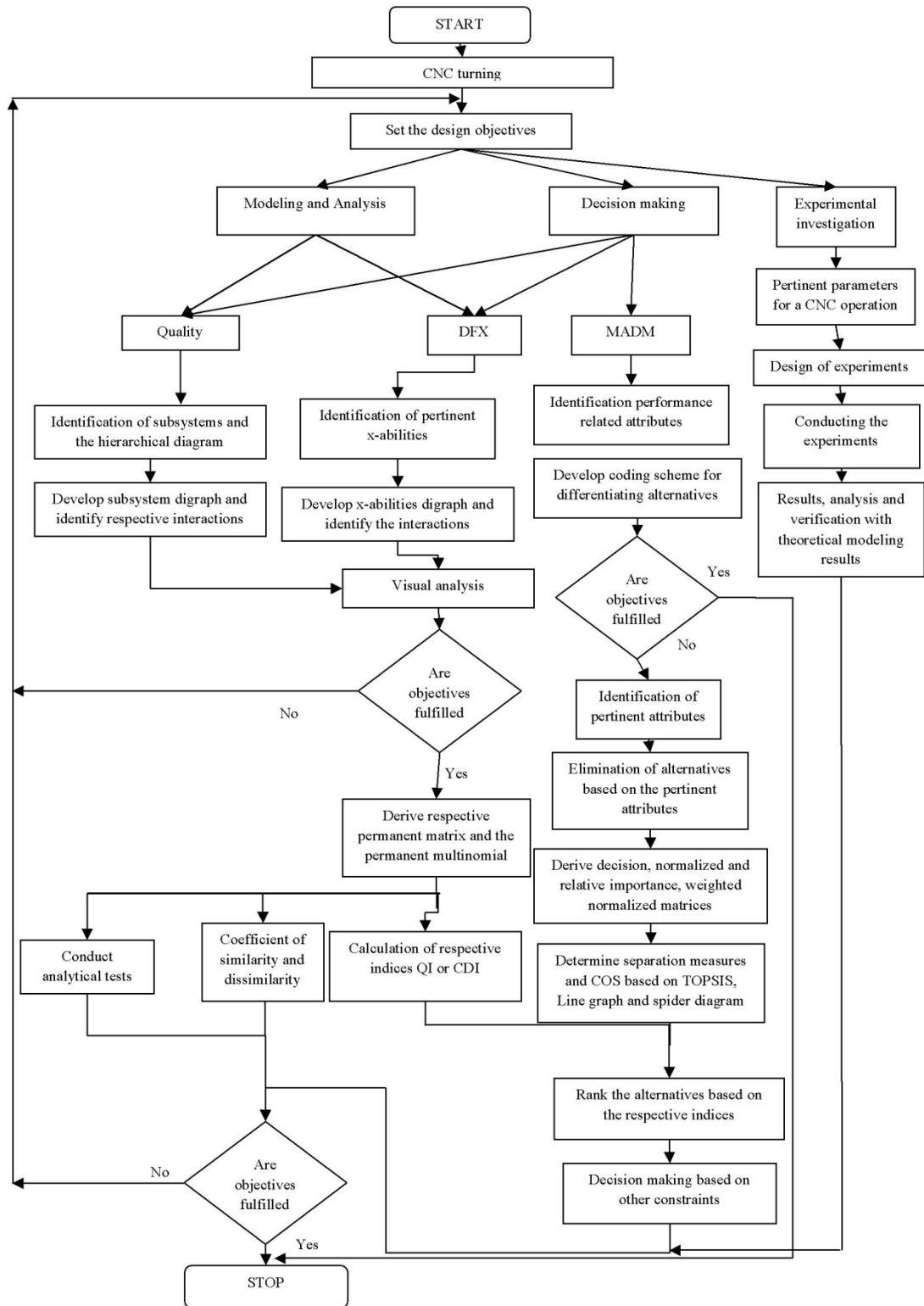


Fig 7.1 Detailed step-by-step procedure

## **7.2 Recommendations for the future work**

The following recommendations are proposed for future work:

1. There is scope for calculating the upper and lower limit values of the performance index QI for all CNC machines in use or to be purchased.
2. A knowledge base of all the materials and their respective CNC machining indices based on CDI and MADM can be developed to help designers in choosing material.
3. There is scope for developing computer codes for evaluating materials by building a data base for quality, DFX, MADM and evaluating against benchmark systems.
4. There is scope for investigations of machining properties of nano-metals, which are not only stronger than the commercially available metals but also, retain the other desirable properties of the metals. For example, nano-copper is four times stronger than the commercially available metal and also retains its original properties like ductility, electric conductivity, thermal conductivity, etc.

## References

Abhishek K. and Agrawal V.P. (2009): Attribute based specification, comparison and selection of electroplating system using MADM approach, *Expert system with applications*, Vol.36, pp.10815-10827.

Aggarwal A., Singh H., Kumar P. and Singh M. (2008a): Optimization of multiple quality characteristics for CNC turning under cryogenic cutting environment using desirability function, *Journal of Materials Processing Technology*, Vol. 205 (1–3), pp.42-50.

Aggarwal A., Singh H., Kumar P. and Singh M. (2008b): Optimizing power consumption for CNC turned parts using response surface methodology and Taguchi's technique—A comparative analysis, *Journal of Materials Processing Technology*, Vol. 200 (1–3), pp.373-384.

Agrawal V.P. and Rao J.S. (1987): Structural classification of kinematic chains and mechanisms. *Mechanisms and machine theory*, Vo. 22, pp. 489-496.

Ahilan C., Kumanan S. and Sivakumaran N. (2010): Application of taguchi based grey relational analysis in multi objective optimization of turning process, *Journal of Advances in Production Engineering and Management*, Vol. 5 (3), pp.171-180.

Ahilan C., Kumanan S., Sivakumaran N. and Dhas J.E.R (2012): Modeling and prediction of machining quality in CNC turning process using intelligent hybrid decision making tools, *Applied Soft Computing* (In press).

Albiñana J.C. and Vila C. (2012): A framework for concurrent material and process selection during conceptual product design stages, *Materials & Design* (Inpress).

Al-Hakim L., Kusiak A. and Mathew J. (2000): A graph-theoretic approach to conceptual design with functional perspectives, *Computer-Aided Design*, Vol.32, pp.867-875.

Alting L. (1995): Life cycle engineering and design, *CIRP Annals - Manufacturing Technology*, Vol. 44, pp. 569-580.

Alting L., Kimura F., Hansen H.N. and Bissacco G. (2003): Micro engineering, *CIRP Annals - Manufacturing Technology*, Vol. 52, pp.635-657.

Altintas Y. and Munasinghe W.K. (1994): A Hierarchical Open-Architecture CNC System for Machine Tools, *CIRP Annals - Manufacturing Technology*, Vol. 43 (1), pp. 349-354.

Aman A., Hari S, Pradeep K, and Manmohan S. (2008): Optimizing power consumption for CNC turned parts using response surface methodology and Taguchi technique-A comparative analysis, *Journal of material processing technology*, Vol.200, pp.373-384.

Amen R. and Vomacka P. (2001): Case-based reasoning as a tool for materials selection, *Mater Des*, Vol.22, pp.353–358.

Amerongen J. (2003): Mechatronic design, *Mechatronics*, Vol.13, pp.1045-1066.

Amitava M. (2008): Fundamentals of quality control and improvement, Prentice Hall India, New Delhi.

Amuthakkannan R., Kannan S.M., Selladurai V. and Vijayalakshmi K. (2008): Software quality measurement and improvement for real-time systems using quality tools and techniques: a case study, *Int. J. of Industrial and systems engineering*, Vol. 3, pp.229-256.

Anandan S. and Summers J.D. (2006): Similarity metrics applied to graph based design model authoring, *Computer-aided design and analysis*, Vol. 3, pp. 297-306.

Ashby M.F. (1995): *Materials selection in mechanical design*, Pergamon Press, New York.

Ashby M.F. and Johnson K. (2002): *Materials and design: the art and science of materials selection in product design*, Butterworth Heinemann, Oxford.

Ashby M.F., Brechet Y.J.M., Cebon D. and Salvo L. (2004): Selection strategies for materials and processes, *Mater Des*, Vol.25, pp.51–67.

Ashby M.F. (1989): Overview No.80- on the engineering properties of materials, *Acta Metall Mater*, Vol.37 (5), pp.1273-1293.

Ashley S. (1992): DARPA initiative in concurrent engineering, *Mechanical Engineering*, Vol. 114, pp. 54-57.



Athani V.V. and Vinod H.N. (1986): A CNC system for a lathe using a low cost PC, *Computers in Industry*, Vol. 7 (5), pp. 427-434.

Audy J. (2006): An appraisal of techniques and equipment for cutting force measurement, *J. Zhejiang Univ. Sci. A*, Vol. 7 (11), pp.1781–1789.

Bahr B., Xiao X. and Krishnan K. (2001): A real-time scheme of cubic parametric curve interpolations for CNC systems, *Computers in Industry*, Vol. 45 (3), pp.309-317.

Balaji G.N.K. and Agrawal V.P. (2008): Concurrent design of a computer network for x-abilities using MADM approach, *Concurrent engineering: research and applications*, Vol. 16, pp. 187-200.

Barschdorff D., Monostori L., Kottenstede T., Warnecke G. and Muller M. (1993): Cutting tool monitoring in turning under varying cutting conditions: an artificial neural network approach, *6th International Conference on Industrial and Engineering Applications of Artificial Intelligence and Expert Systems*, Edinburgh, Scotland, pp. 353–360.

Benardos P.G. and Vosniakos G.C. (2003): Predicting surface roughness in machining: a review, *Int. J. Mach. Tools Manuf.*, Vol.43, pp. 833–844.

Bikramjit P, Pratihar DK, Mondal MS, Joarder R (2002): Prediction of power requirement in turning using a GA-fuzzy approach, *Soft Comput Ind Recent Appl*, pp 167–169.

Bletton O., Duet R. and Pedarre P. (1990): Influence of oxide nature on the machinability of 316l stainless steels, *Wear*, Vol. 139, pp. 179–193.

Boothroyd G. and Alting L. (1992): Design for Assembly and Disassembly, *CIRP Annals - Manufacturing Technology*, Vol. 41, pp. 625-636.

Boothroyd G. and Knight W.A. (1989): *Fundamentals of Machining and Machine Tools*, Marcel-Dekker, New York.

Boothroyd G., Dewhurst P. and Knight W. (2002): Product design for manufacture and assembly, CRC Press, Taylor and Francis group, Florida.

Bralla J.G. (1986): Design for manufacturability handbook, McGraw-Hill, New York.

Brinksmeier E., Lucca D.A. and Walter A. (2004): Chemical Aspects of Machining Processes, *CIRP Annals - Manufacturing Technology*, Vol. 53(2), pp.685-699.

Bruni R., Bucchiarone A., Gnesi S., Hirsch D. and Lafuente A.L. (2008): Graph-based design and analysis of dynamic software architecture, *Concurrency, graph and models*, Vol. 5065, pp. 37-56.

Bruschi S. and Ghiotti A. (2008): Distortions induced in turbine blades by hot forging and cooling, *International Journal of Machine Tools and Manufacture*, Vol. 48 (7–8), pp.761-767.

Campbell M.I., Nair S. and Patel J. (2007): A unified approach to solving graph based design problems, *International Design Engineering Technical Conferences and Computers and Information in Engineering Conference*, 4-7 Sept, Las Vegas, Nevada.

Chan K., King C. and Wright P. (1998): COMPASS: Computer oriented materials, processes, and apparatus selection system, *Journal of Manufacturing Systems*, Vol. 17 (4), pp. 275-286.

Chaudhury S.K. and Bajpai J.B. (2005): Investigation in orthogonal turn-milling to-wards better surface finish, *Journal of Materials Processing Technology*, Vol.170 (3), pp. 487-493.

Chauhan A. and Vaish R. (2012): Magnetic material selection using multiple attribute decision making approach, *Materials & Design*, Vol. 36, pp.1-5.

Chelladurai H. (2008): Cutting tool condition monitoring system for turning process, PhD Thesis, IIT Kanpur, India.

Chelladurai H., Jain V.K. and Vyas N.S. (2008): Development of a cutting tool condition monitoring system for high speed turning operation by vibration and strain analysis, *The International journal of advanced manufacturing technology*, Vol. 37(5-6), pp.471-485.

Chien W.-T. and Tsai C.-S. (2003): The investigation on the prediction of tool wear and the determination of optimum cutting conditions in machining 17-4PH stainless steel, *Journal of Materials Processing Technology*, Vol. 140(1–3), pp.340-345.

Childs T H C, Maekawa K, Obikawa T, and Yamane Y (2001): *Metal Machining Theory and Applications*, Butterworth Heinemann, Oxford.

Chou Y.K. and Evans C.J. (1999): White layers and thermal modeling of hard-turned surfaces, *Int J Mach Tool Manu*, Vol. 39, pp.1863–1868.

Chouchman R.S., Robbins K.E., and Schofield (1997): *GE steam turbine design philosophy and technology program*, GER3705, Schenectady, NY.

Choudhury S.K. and Kishore K.K. (2000): Tool wear measurement in turning using force ratio, *Int. J. Mach. Tools Manuf*, Vol.40, pp.899–909.

Cuenca S., Jimeno-Morenilla A., Martínez A., Maestre R. (2011): Hardware approach to tool path computation for STEP-NC enabled CNC: A case study of turning operations, *Computers in Industry*, Vol. 62 (5), pp. 509-518.

Davim J.P. (2001): A note on the determination of optimal cutting conditions for surface finish obtained in turning using design of experiments, *Journal of Materials Processing Technology*, Vol.116, pp.305–308.

Davim J.P., Gaitonde V.N. and Karnik S.R. (2008): Investigations into the effect of cutting conditions on surface roughness in turning of free machining steel by ANN models, *Journal of Materials Processing Technology*, Vol. 205(1–3), pp.16-23.

de Sam Lazaro A., Zhang J. and Kendall L.A. (1994): Knowledge-based approach for improvement of CNC part programs, *Journal of Manufacturing Systems*, Vol. 13 (1), pp.20-30.

Dedeke A. and Huang K.T. (2010): Simulating the impact of parcel size and barcode quality on the productivity of parcel sorting machines, *Int. J. of Industrial and systems engineering*, Vol. 5, pp.110-128.

Dehnad K. (1989): *Quality control, robust design, and the Taguchi method*, Calif: Wadsworth and books/Cole, Pacific Grove.

Delgado-Friedrichs O. and O'Keeffe M. (2005): Crystal Nets as Graphs: Terminology and Definitions, *Journal of Solid State Chemistry*, Vol. 178, pp. 2480-2485.

Deo N. (2004): Graph Theory with applications to engineering and computer science, Prentice Hall India, New Delhi.

Dhokia V.G., Newman S.T., Crabtree P. and Ansell M.P. (2011): A process control system for cryogenic CNC elastomer machining, *Robotics and Computer-Integrated Manufacturing*, Vol. 27 (4), pp.779-784.

Diaz-Calderon A., Paredis C.J.J. and Khosla P.K. (2000): Automatic Generation of System-Level Dynamic Equations for Mechatronic Systems, *Computer-Aided Design*, Vol. 32, pp.339-354.

Dimla D.E. (2000): Sensors signals for tool-wear monitoring in metal cutting operations - A Review of methods, *Int j mach tools manuf*, Vol. 40, pp.1073–1098.

Dimla D.E. Sr. and Lister P.M. (2000): On-line metal cutting tool condition monitoring: I: force and vibration analyses, *International Journal of Machine Tools and Manufacture*, Vol. 40 (5), pp. 739-768.

Diniz A.E. and Micaroni R. (2002): Cutting conditions for finish turning process aiming: the use of dry cutting, *Int. J. Mach. Tools Manuf.*, Vol. 432, pp. 899–904.

Dornfeld D.A. (1994): In process recognition of cutting states, *JSME International Journal*, (Series C: Dynamics Control), Vol. 37 (4) , pp. 638-650.

Du Z.C., Yang J.G., Yao Z.Q and Xue B.Y. (2002): Modeling approach of regression orthogonal experiment design for the thermal error compensation of a CNC turning center, *Journal of Materials Processing Technology*, Vol. 129 (1–3), pp.619-623.

Duan C. and Wang M. (2005): Some metallurgical aspects of chips formed in high speed machining of high strength low alloy steel, *Scripta Materialia*, Vol. 52(10), pp.1001-1004.

Durai Prabhakaran R.T., Babu B.J.C. and Agrawal V. P. (2006 a): Quality modeling and analysis of polymer composite products, *Polymer Composites*, Vol. 27, pp. 329-340.

Durai Prabhakaran R.T., Babu B.J.C. and Agrawal V.P. (2006 b): Design for 'X' abilities of RTM products-a graph theoretic approach, *Concurrent engineering: research and applications*, Vol. 2, pp. 151-161.

Durai Prabhakaran R.T., Babu B.J.C. and Agrawal V.P. (2006 c): Reliability modeling of a composite product system-a systems approach, *International journal for Manufacturing and science and production*, Vol.7, pp.243-262

Ednic O. and Vayvay O. (2008): Ergonomics interventions improve quality in manufacturing: a case study, *Int. J. of Industrial and systems engineering*, Vol. 3, pp.727-745.

Edwards K.L. (2005): Selecting materials for optimum use in engineering components, *Mater Des*, Vol.26, pp.469-473.

Esteves C. A., and Paulo D. (2011): Surface roughness measurement in turning carbon steel AISI 1045 using wiper inserts, *Measurement*, Vol. 44, pp.1000-1005.

Fang X. D. and Lee N.J. (2001): A new tooling mechanism for CNC lathes, *International Journal of Machine Tools and Manufacture*, Vol. 41 (1), pp.89-101.

Fang X.D. and Safi-Jahanshaki H. (1997): A new algorithm for developing a reference model for predicting surface roughness in finish machining of steels, *International Journal of Production Research*, Vol. 35, pp.179-197.

Feng C.X., Huang C.C., Kusiak A. and Li P.G. (1996): Representation of functions and features in detailed design, *Computer-Aided Design*, Vol.28, pp.961-971

Feng C.X.J. and Wang X. (2002): Development of empirical models for surface roughness prediction in finish turning, *Int. J. Adv. Manuf. Technol.*, Vol. 20, pp. 348-356.

Gandhi O.P., Agrawal V.P. and Shishodia K.S. (1991): Reliability analysis and evaluation of systems, *Reliability engineering and system safety*, Vol. 32, pp.283-305.

Garg R.K., Agrawal V.P. and Gupta, V.K. (2006): Selection of power plants by evaluation and comparison using graph theoretical methodology, *Electrical power and energy systems*, Vol. 28, pp.429-435.

Girvan M. and Newman M.E.J (2002): Community structure in social and biological networks, *Proceedings of National academy of sciences USA*, Vol.99, pp.7821-7826.

Glazebrook B., Coulon R. and Abrassart C. (2000): Towards product life cycle design tool, *IEEE international symposium on electronics and environment*, 8-10May, San Francisco.

Gómez M.P., Hey A.M., Ruzzante J.E. and D'Attellis C.E. (2010): Tool wear evaluation in drilling by acoustic emission, *Physics Procedia*, Vol. 3 (1), pp. 819-825.

Gopalakrishnan B. and Pandiarajan V. (1991): Materials and manufacturing processes selection system for product designs in concurrent engineering, *Journal of Materials Processing Technology*, Vol. 28(1-2), pp. 93-103.

Groover M.P. (1996): *Fundamentals of Modern Manufacturing: Materials, Processes, and Systems*, John Wiley & Sons, USA.

Guerra M.D. and Coelho R.T. (2006): Development of a low cost Touch Trigger Probe for CNC Lathes, *Journal of Materials Processing Technology*, Vol. 179 (1-3), pp.117-123.

Gupta A., Singh H. and Aggarwal A. (2011) Taguchi-fuzzy multi output optimization (MOO) in high speed CNC turning of AISI P-20 tool steel, *Expert Systems with Applications*, Vol. 38 (6), pp.6822-6828.

Gupta N. (2011): Material selection for thin-film solar cells using multiple attribute decision making approach, *Materials & Design*, Vol. 32 (3), pp.1667-1671.

Gurel S. and Akturk M.S. (2007): Considering manufacturing cost and scheduling performance on a CNC turning machine, *European Journal of Operational Research*, Vol. 177 (1), pp.325-343.

Gwidon W.S. and Andrew W.B. (2005): *Engineering tribology*, Elsevier Butterworth-Heinemann publications, Oxford, UK.

Hall L.H. and Kier L.B. (2001): Issues in representation of molecular structure: The development of molecular connectivity. *Journal of Molecular Graphics and Modelling*, Vol. 20, pp. 4-18.

Heinemann R. and Hinduja S. (2012): A new strategy for tool condition monitoring of small diameter twist drills in deep-hole drilling, *International Journal of Machine Tools and Manufacture*, Vol. 52 (1), pp.69-76.

Helle A.S. (1995): *On the interaction between inclusions in steel and the cutting tool during machining*, Acta Polytechnica Scandinavica, Chemical Technology Series No. 228, Helsinki.

Heshmat H. and Dill J.F. (1992): Traction characteristics of high-temperature powder-lubricated ceramics (Su<sub>3</sub>N<sub>4</sub>/αSiC), *Tribology transactions*, Vol.35, pp.360-366.

Hongxiang W., Dan L. and Shen D. (2002): Surface roughness prediction model for ultra-precision turning aluminum alloy with a single crystal diamond tool, *Chinese Journal of Mechanical Engineering*, Vol.15, pp.153–156.

Hsiao C.N., Chiou C.S. and Yong J.R. (2002): Aging reactions in a 17-4PH stainless steel, *Mater Chem Phys*, Vol.42, pp.74:134.

Huang Y. and Liang S.Y. (2005): Effect of cutting conditions on tool performance in CBN hard turning, *Journal of manufacturing process*, Vol.7 (1), pp.10-16.

Huang Y., Chou Y.K. and Liang S.Y. (2007): CBN tool wear in hard turning: a survey on research progresses, *Int J Adv Manuf Technol*, Vol.35, pp.443-453.

Hundal M.S. (1993): Rules and models for low cost design, *Proceeding of ASME Design for Manufacturability Conference*, pp.75–84.

Hwang C.L. and Yoon K. (1982): Multiple attribute decision making-methods and applications- a state of art survey, *Lecture notes in Economics and mathematical systems*, Springer-Verlag, Berlin.

İlhan A. and Akkuş H. (2011): Determining the effect of cutting parameters on surface roughness in hard turning using the Taguchi method, *Measurement*, Vol. 44 (9), pp.1697-1704.

İlhan A. and Süleyman N. (2012): Multi response optimisation of CNC turning parameters via Taguchi method-based response surface analysis, *Measurement*, Vol.45 (4), pp.785-794.

ISO 14649-1: 2003, Data Model for Computerized Numerical Controllers, Part 1. Overview and fundamental principles.

ISO 14649-10: 2003, Data Model for Computerized Numerical Controllers, Part 10. General process data.

ISO 14649-11: 2003, Data Model for Computerized Numerical Controllers, Part 11. Process data for milling.

ISO 14649-111: 2001, Data Model for Computerized Numerical Controllers, Part 111. Tools for milling.

ISO/DIS 14649-12: 2003, Data Model for Computerized Numerical Controllers, Part 12. Process data for turning.

ISO/DIS 14649-121: 2003. Data Model for Computerized Numerical Controllers, Part 12. Tools for turning

Jahan A., Bahraminasab M. and Edwards K.L. (2012): A target-based normalization technique for materials selection, *Materials & Design*, Vol. 35, pp. 647-654.

Jalham I.S. (2006): Decision-making integrated information technology (IIT) approach for material selection, *Int J Comput Appl in Technol*, Vol. 25, pp.65–71.

James M.N., Newby M., Hattingh D.G. and Steuwer A. (2010): Shot-peening of steam turbine blades: Residual stresses and their modification by fatigue cycling, *Procedia Engineering*, Vol. 2 (1), pp.441-451.

Jesweit J. and Hauschild M. (2008): Market forces and need to design for environment, *International journal of sustainable manufacturing*, Vol. 1, pp. 41-57.



Joseph Davidson M., Balasubramanian K. and Tagore G.R.N. (2008): Surface roughness prediction of flow-formed AA6061 alloy by design of experiments, *Journal of Materials Processing Technology*, Vol. 202, pp. 41-46.

Kannatey-Asibu E.Jr., and Dornfeld D.A. (1981): Quantitative relationships for acoustic emissions from orthogonal metal cutting, *Tran ASME*, Vol. 103, pp. 330-340.

Karagöz S. and Fischmeister H.F. (1996): Metallographic observations on the wear process of TiN-coated cutting tools, *Surface Coatings Technol*, Vol. 81(2/3), pp.190–200.

Karayel D. (2009): Prediction and control of surface roughness in CNC lathe using artificial neural network, *Journal of Materials Processing Technology*, Vol. 209 (7), pp.3125-3137.

Kasirolvalad Z., Jahed-Motlagh M.R. and Shadmani M.A. (2006): An intelligent modeling system to improve the machining process quality in CNC machines tools using adaptive fuzzy petri nets, *International Journal of Advanced Manufacturing Technology (UK)*, Vol. 29, pp.1050-1061.

Katayama S. and Hashimura M. (1995): Study on interfacial adhesion between cutting tool and microstructures of free-machining steel, *Int. J. Jpn. Soc. Prec. Eng.*, Vol. 29 (1), pp. 36–41.

Kayani S.A. and Malik M.A.(2007): Automated Design of Mechatronic Systems using Bond-Graph Modeling and Simulation and Genetic Programming, *Proceedings of International Bhurban Conference on Applied Sciences & Technology*, 8th- 11th January, Islamabad, Pakistan.

Kirby E. D., Chen J.C. and Zhang J.Z. (2006): Development of a fuzzy-nets-based in-process surface roughness adaptive control system in turning operations, *Expert Systems with Applications*, Vol. 30 (4), pp.592-604.

Ko T.J. and Cho D.W. (1994): Cutting state monitoring in milling by a neural network, *International Journal of Machine tools and manufacture*, Vol. 34(5), pp 659-676.

Kopac J, Sali S 2001 Tool wear monitoring during the turning process, *J. Mater. Process Technol*, Vol. 113, pp.312–316.

Kumar A. and Agrawal V.P. (2008): Structural modeling and analysis of electroplating system: A graph theoretic systems approach, *Int. J. Surface Science engineering*, Vol. 2, pp.520-540.

Kumar S., Nassehi A., Newman S.T., Allen R.D. and Tiwari M.K. (2007): Process control in CNC manufacturing for discrete components: A STEP-NC compliant framework, *Robotics and Computer-Integrated Manufacturing*, Vol. 23(6), pp.667-676.

Lalwani D.I., Mehta N.K., and Jain P.K. (2008): Experimental investigation of cutting parameters influence on cutting forces and surface roughness in finish hard turning of MDN 250 steel, *Journal of material processing technology*, Vol.206, pp.167-179.

Lan M.S. and Dornfeld D.A. (1984): In process tool fracture detection, *J Eng Mater Technol*, Vol. 106, pp.111–118.

Lan T.S. and Wang M.Y. (2009): Competitive parameter optimization of multi-quality CNC turning, *The International Journal of Advanced Manufacturing Technology*, Vol.41(7), pp.820-826.

Lee S.G. and Xu X. (2005): Design for environment: life cycle assessment and sustainable packaging issues, *International journal of environmental technology and management*, Vol. 5, pp. 14-41.

Li D., Li F., Huang X., Lai Y. and Zheng X. (2010): A model based integration framework for computer numerical control system development, *Robotics and Computer-Integrated Manufacturing*, Vol. 26 (4), pp.333-343.

Li G.-D., Yamaguchi D. and Nagai M. (2007): A grey-based decision making approach to the supplier selection problem, *Mathematical and Computer modeling*, Vol. 46, pp.573-581.

Li P., Gao T., Wang J. and Liu H. (2010): Open architecture of CNC system research based on CAD graph-driven technology, *Robotics and Computer-Integrated Manufacturing*, Vol. 26 (6), pp.720-724.

Liang M., Yeap T., Hermansyah A. and Rahmati S. (2003): Fuzzy control of spindle torque for industrial CNC machining, *International Journal of Machine Tools and Manufacture*, Vol. 43 (14), pp.1497-1508.

Lim H.S., Kumar A. S. and Rahman M. (2002): Improvement of form accuracy in hybrid machining of microstructures, *Journal of Electronic Materials*, Vol. 31(10), pp.1032–1038.

Lim T.-S., Lee C.-M., Kim S.-W. and Lee D.-W. (2002): Evaluation of cutter orientations in 5-axis high speed milling of turbine blade, *Journal of Materials Processing Technology*, Vol. 130–131, pp.401-406.

Liu Q. and Altintas Y. (1999): On-line monitoring of flank wear in turning with multilayered feed-forward neural network, *International Journal of Machine Tools and Manufacture*, Vol. 39 (12), pp.1945-1959.

Liu R.L. and Yan M.F. (2010): The microstructure and properties of 17-4PH martensitic precipitation hardening stainless steel modified by plasma nitrocarburizing, *Surface and Coatings Technology*, Vol. 204(14), pp.2251-2256.

Llewellyn D.T. and Hudd R.C. (2004): *Steels: Metallurgy and Applications*, Butterworth-Heinemann.

Lo K.H., Cheng E.T., Kwok C.T. and Man H.C. (2003): Improvement of cavitation erosion resistance of AISI 316 stainless steel by laser surface alloying using fine WC powder, *Surf Coat Technol*, Vol.67, pp.165:258.

Lu Z.L., Li D.C., Tong Z.Q., Lu Q.P., Traore M.M., Zhang A.F. and Lu B.H. (2011): Investigation into the direct laser forming process of steam turbine blade, *Optics and Lasers in Engineering*, Vol. 49 (9–10), pp.1101-1110.

Ma X.-B, Han Z.-Y., Wang Y.-Z. and Fu H.-Y. (2007): Development of a PC-based Open Architecture Software-CNC System, *Chinese Journal of Aeronautics*, Vol. 20 (3), pp. 272-281.

Maharana M.K. and Swarup K.S. (2010): Graph theoretic approach for preventive control of power systems, *International Journal of Electrical Power & Energy Systems*, Vol.32, pp. 254-261.

Malik M.A. and Khurshid. (2003): Bond graph modeling and simulation of mechatronic systems, *Proceedings of 7<sup>th</sup> IEEE International multi-topic conference*, 9-9 December, Islamabad.

Marcus M. and Minc H. (1965): Permanents, *American Mathematical Monthly*, Vol.72, pp.577-591.

Martin M., Weber S., Izawa C., Wagner S., Pundt A. and Theisen W. (2011): Influence of machining-induced martensite on hydrogen-assisted fracture of AISI type 304 austenitic stainless steel, *International Journal of Hydrogen Energy*, Vol. 36(17), pp.11195-11206.

Masanet E. and Horvath A. (2007): Assessing the benefits of design for recycling of plastics in electronics: A case study of computer enclosures, *Materials and Design*, Vol. 28, pp. 1801-1811.

McDowell D.L., Panchal J.H., Choi H.-J., Seepersad C.C., Allen J.K. and Mistree F. (2010): Chapter 9 - Concurrent Design of Materials and Products—Managing Design Complexity, *Integrated Design of Multiscale, Multifunctional Materials and Products*, Butterworth-Heinemann, Boston, pp.241-311.

Merchant M.E. (1950): Fundamentals of Cutting Fluid Action, *Lubrication Engineering*, Vol.6, pp. 163.

Mondelin A., Valiorgue F., Coret M., Feulvarch E. and Rech J. (2011): Surface integrity prediction in finish turning of 15-5PH stainless steel, *Procedia Engineering*, Vol. 19, pp.270-275.

Montgomery D.C. (2007): Introduction to statistical quality control, Wiley India, New Delhi.

Munson J.C. (1996): Software faults, software failures and software reliability modeling, *Information and Software Technology*, Vol. 38, pp. 687-699.

Nalbant M., Gökaya H., Toktaş I. and Sur G. (2009): The experimental investigation of the effects of uncoated, PVD- and CVD-coated cemented carbide inserts and cutting parameters

on surface roughness in CNC turning and its prediction using artificial neural networks, *Robotics and Computer-Integrated Manufacturing*, Vol. 25 (1), pp.211-223.

Noordin M.Y., Venkatesh V.C., Sharif S., Elting S. and Abdullah A. (2005): Application of response surface methodology in describing the performance of coated carbide tools when turning AISI 1045 steel, *Journal of Materials Processing Technology*, Vol.145, pp. 46-58.

O'Driscoll M. (2002): Design for manufacture, *Journal of Materials Processing Technology*, Vol. 122, pp. 318-321.

Omirou S.L. and Barouni A.K. (2005): Integration of new programming capabilities into a CNC milling system, *Robotics and Computer-Integrated Manufacturing*, Vol. 21(6), pp.518-527.

Park S.H. (1996): *Robust Design and Analysis for Quality Engineering*, Springer International, USA.

Pawade R.S., Suhas S.J., Brahmanekar P.K., and Rahman M. (2007): An investigation of cutting forces and surface damage in high speed turning of Inconel 718, *Journal of material processing technology*, Vol.192-193, pp.139-146.

Petropoulos G.P., Vaxevanidis N.M., Pandazaras C.N. and Antoniadis A.A. (2006): Multi-parameter identification and control of turned surface textures, *Int. J. Adv. Manuf. Technol.*, Vol. 29, pp.118–128.

Portilla-Flores et al (2011): Parametric reconfiguration improvement in non-iterative concurrent mechatronic design using an evolutionary-based approach, *Engineering Applications of Artificial Intelligence*, Vol. 24(5), pp.757-771.

Qi H.S. and Mills B. (2000): Formation of a transfer layer at the tool-chip interface during machining, *Wear*, Vol. 245 (1–2), pp.136-147.

Rahman M., Zhou Q. and Hong G.S. (1995): Application of Kohonen neural network for tool condition monitoring, *International Conference on Intelligent Manufacturing*, Wuhan, China, pp. 422–429.

Rahman M.A., Rahman M., Kumar A. S., Lim H.S. and Asad A.B.M.A. (2003): Fabrication of miniature components using microturning, Proceedings of the Fifth International Conference on Mechanical Engineering, Dhaka, pp. AM-35.

Rao R.V. (2006): A material selection model using graph theory and matrix approach, *Materials Science and Engineering: A*, Vol. 431 (1–2), pp.248-255.

Rao R.V. and Davim J. P. (2008): A decision-making framework model for material selection using a combined multiple attribute decision-making method, *Int J Adv Manuf Technol*, Vol.35, pp.751–760.

Rao R.V. and Patel B.K. (2010): A subjective and objective integrated multiple attribute decision making method for material selection, *Materials & Design*, Vol. 31(10), pp.4738-4747.

Reddy N.S. and Rao P.V. (2005): Selection of optimum tool geometry and cutting conditions using a surface roughness prediction model for end milling, *Int. J. Adv. Manuf. Technol.*, Vol. 26, pp. 1202–1210.

Rehorn A.G., Jiang J. and Orban E. (2005): State-of-the-art methods and results in tool condition monitoring: a review, *Int. J. Adv. Manuf. Tech*, Vol. 26, pp.693–710.

Reinhart G. and Angerer T. (2002): Automated assembly of mechatronic products, *CIRP Annals- Manufacturing technology*, Vol. 51, pp. 1-4.

Remadna M. and Rigal J.F. (2006): Evolution during time of tool wear and cutting forces in the case of hard turning with CBN inserts, *Journal of Materials Processing Technology*, Vol. 178 (1–3), pp.67-75.

Richter C.-H. (2003): Structural design of modern steam turbine blades using ADINA™, *Computers & Structures*, Vol. 81 (8–11), pp.919-927.

Robert H. B. (2002): *The Mechatronics hand book*’, CRC Press, Washington D.C.

Sandstrom R. (1985): An approach to systematic materials selection, *Material Design*, Vol.6, pp. 328-337.

Sapuan S.M. (2001): A knowledge-based system for materials selection in mechanical engineering design, *Mater Des*, Vol.22, pp.687–695.

Schaeffer S.E. (2007): Graph clustering, *Computer science review*, Vol.1, pp. 27-64.

Scheffer C. and Heyns P.S. (2001): Wear monitoring in turning operations using vibration and strain measurements, *Mech. Syst. Signal Process*, Vol. 15 (6), pp.1185–1202.

Scheffer C. and Heyns P.S. (2004): An industrial tool wear monitoring system for interrupted turning, *Mech. Syst. Signal Process*, Vol. 18, pp.1219–1242.

Schneider H. (1960): Foundry trade journal, Vol. 108, pp.562.

Shanian A., Milani A.S., Carson C. and Abeyaratne R.C. (2008): A new application of ELECTRE III and revised Simos' procedure for group material selection under weighting uncertainty, *Knowledge-Based Systems*, Vol. 21 (7), pp.709-720.

Shaw M.C. (1989): *Metal Cutting Principles*, Oxford University Press, New York.

Sick B. (2002): On line and indirect tool wear monitoring in turning with artificial neural networks: A review of more than a decade of research, *Mech syst signal process*, Vol. 16(4), pp.487–546.

Sidjanin L. and Kovac P. (1997): Fracture mechanisms in chip formation processes, *Mater. Sci. Technol.*, Vol.13, pp. 439–444.

Smith S., McFarland J., Assaid T., Tursky D., Barkman W. and Babelay E. (2010): Surface characteristics generated in CNC chip breaking tool paths, *CIRP Annals - Manufacturing Technology*, Vol. 59 (1), pp 137-140.

Sreeram T. R. (2005): Graph theory based parametric influences applied to torsional vibration analysis, *Advances in Engineering Software*, Vol. 36, pp. 209-224.

Suh S.-H., Chung D.-H., Lee B.-E., Shin S., Choi I. and Kim K.-M. (2006): STEP-compliant CNC system for turning: Data model, architecture, and implementation, *Computer-Aided Design*, Vol. 38 (6), pp.677-688.

Suleyman N., Suleyman Y., and Erol T. (2011): Optimization of tool geometry parameters for turning operations based on the response surface technology, *Measurement*, Vol.44, pp.580-587.

Suneel T.S., Pande S.S. and Date P.P. (2002): A technical note on integrated product quality model using artificial neural networks, *Journal of Materials Processing Technology*, Vol. 121(1), pp.77-86.

Taha Z., Gonzales J., Sakundarini N., Ariffin R. and Hanim S (2010): Optimization of Product Design to reduce Environmental Impact of Machining, The 14th Asia Pacific Regional Meeting of International Foundation for Production Research , Melaka, 7 – 10 December.

Tamizharasan T., Selvaraj T. and Noorul Haq A. (2006): Analysis of tool wear and surface finish in hard turning, *Int J Adv Manuf Technol*, Vol.28, pp.671-691.

Tarng Y.S., Lin C.Y. and Nian C.Y. (1995): An optimization approach for the fuzzy control of turning operations, *2nd New Zealand International Two-Stream Conference on Artificial Neural Networks and Expert Systems*, Dunedin, New Zealand, pp. 145–149.

Teti R., Jemielniak K., O'Donnell G. and Dornfeld D. (2010): Advanced monitoring of machining operations, *CIRP Annals - Manufacturing Technology*, Vol. 59 (2), pp.717-739.

Thakker A., Jarvis J., Buggy M. and Sahed A. (2008): A novel approach to materials selection strategy case study: Wave energy extraction impulse turbine blade, *Materials & Design*, Vol. 29 (10), pp.1973-1980.

Tian-Syung L. and Ming-Yung W. (2009): Competitive parameter optimization of multi-quality CNC turning, *Int J Adv Manuf Technol*, Vol.41, pp.820-826.

Trent E M, and Wright P K (2000): *Metal Cutting*, Butterworth Heinemann, Oxford.

Tzeng C.-J., Lin Y.-H., Yang Y.-K. and Jeng M.-C. (2009): Optimization of turning operations with multiple performance characteristics using the Taguchi method and Grey relational analysis, *Journal of Materials Processing Technology*, Vol. 209 (6), pp.2753-2759.



Ueda T, Hosokawa A, and Yamada K (2006): Effect of oil mist on tool temperature in cutting, *Journal of Manufacturing Science and Engineering*, Vol.128, pp. 130–135.

van Luttervelt C.A., Childs T.H.C., et al. (1998): Present situation and future trends in modelling of machining operations, *CIRP Ann*, Vol. 47 (1), pp.1–47.

Venkatasamy R. and Agrawal V.P. (1994): Coding, evaluation and selection of motor vehicles-a MADM approach, *Mobility and vehicle mechatronics*, Vol. 20, pp. 22-41.

Venkatasamy R. and Agrawal V.P. (1995): System and structural analysis of an automobile vehicle-a graph theoretic approach, *Journal of Vehicle Design*, Vol. 16, pp.477-503.

Vichare P., Nassehi A., Kumar S. and Newman S.T. (2009): A Unified Manufacturing Resource Model for representing CNC machining systems, *Robotics and Computer-Integrated Manufacturing*, Vol. 25 (6), pp.999-1007.

Waigaonkar S. (2010): Ph.D. Thesis, BITS-Pilani.

Wang J. and Zou H. (2006): The microstructure evolution of type 17-4PH stainless steel during long-term aging at 350°C, *Nucl Eng Des*, Vol. 6, pp.236:2531.

Wang Y., Jia Y. and Shen G. (2002): Multidimensional force spectra of CNC machine tools and their applications, part one: force spectra, *International Journal of Fatigue*, Vol. 24 (10), pp.1037-1046.

Wang Y., Ma X., Chen L. and Han Z. (2007): Realization Methodology of a 5-axis Spline Interpolator in an Open CNC System, *Chinese Journal of Aeronautics*, Vol. 20 (4), pp. 362-369.

Xavior M. A. and Adithan M. (2009): Determining the influence of cutting fluids on tool wear and surface roughness during turning of AISI 304 austenitic stainless steel, *Journal of Materials Processing Technology*, Vol. 209(2), pp.900-909.

Xu X.W. and Newman S.T. (2006): Making CNC machine tools more open, interoperable and intelligent—a review of the technologies, *Computers in Industry*, Vol. 57(2), pp.141-152.

Xu Z.-L., Park J.-P. and Ryu S.-J. (2007): Failure analysis and retrofit design of low pressure 1st stage blades for a steam turbine, *Engineering Failure Analysis*, Vol. 14 (4), pp. 694-701.

Xue D. and Yang H. (2004): A concurrent engineering-oriented design database representation model, *Computer-Aided Design*, Vol. 36 (10), pp.947-965.

Yao J., Wang L., Zhang Q., Kong F., Lou C. and Chen Z. (2008): Surface laser alloying of 17-4PH stainless steel steam turbine blades, *Optics & Laser Technology*, Vol. 40 (6), pp.838-843.

Yeung C.-H., Altintas Y. and Erkorkmaz K. (2006): Virtual CNC system. Part I. System architecture, *International Journal of Machine Tools and Manufacture*, Vol. 46 (10), pp.1107-1123.

Yih-fong T. and Ming-der j. (2005): Dimensional quality optimisation of high-speed CNC milling process with dynamic quality characteristic, *Robotics and Computer-Integrated Manufacturing*, Vol. 21(6), pp.506-517.

Yuan J. and Ni J. (1998): The real-time error compensation technique for CNC machining systems, *Mechatronics*, Vol. 8 (4), pp.359-380.

Yusof Y. and Case K. (2010): Design of a STEP compliant system for turning operations, *Robotics and Computer-Integrated Manufacturing*, Vol. 26 (6), pp.753-758.

Zadeh L.A., Klir G.J. and Yuan B. (1996): Fuzzy sets, Fuzzy logic, and Fuzzy systems, *Advances in fuzzy systems-applications and theory*, Vol.6, World scientific publishing Co.Pvt.Ltd, Singapore.

Zha X.F. (2005): A web-based advisory system for process and material selection in concurrent product design for a manufacturing environment, *Int J Adv Manuf Technol*, Vol. 25 (3-4), pp. 233-243.

Zhang X., Liu R., Nassehi A. and Newman S.T. (2011): A STEP-compliant process planning system for CNC turning operations, *Robotics and Computer-Integrated Manufacturing*, Vol. 27 (2), pp.349-356.

Zhang Y., Zhang Z. and Han Z. (1995): Detection of tool breakage in turning operations using neural networks, *International Conference on Intelligent Manufacturing*, Wuhan, China, pp 463–468.

Zhou J.M., Andersson M. and Ståhl J.E. (2004): Identification of cutting errors in precision hard turning process, *Journal of Materials Processing Technology*, Vol.153–154, pp.746-750.

Zhu W.-H., Jun M.B. and Altintas Y.(2001): A fast tool servo design for precision turning of shafts on conventional CNC lathes, *International Journal of Machine Tools and Manufacture*, Vol. 41(7), pp.953-965.

## Appendix A

### A.1 Permanent

For an  $n \times n$  matrix  $A = (a_{ij})$  is a scalar number and is defined as

$$\text{per}(A) = \sum_{\sigma \in S_n} \prod_{i=1}^n a_{i, \sigma(i)}$$

The sum here extends over all elements of  $\sigma$  of symmetric group  $S_n$ , that means over all the permutations of number 1, 2, 3, ..., n.

For example the permanent of a (2x2) matrix  $A = \begin{bmatrix} a & b \\ c & d \end{bmatrix}$  is

$$\text{per}(A) = ad + bc$$

#### ***Properties of permanents:***

If  $A$  is a square matrix of size  $n \times n$  then

- $\text{per}(A^T) = \text{per}(A)$
- $|\text{per}(A)|^2 = \text{per}(AA^*)$
- $\text{per}(A) \geq \det(A)$
- [P: permutation matrix]:  $\text{per}(PA) = \text{per}(AP) = \text{per}(A)$
- If  $A$  is an identity matrix then  $\text{per}(A) = 1$
- If all the elements of  $A$  are '1' then  $\text{per}(A) = n!$

### A.2 Determinant

For an  $n \times n$  matrix  $A$ ,  $\det(A)$  is defined as scalar number.

This is the sum of  $n!$  terms each involving the product of  $n$  matrix elements of which exactly one comes from each row and column. Each term is multiplied by the signature (+1 or -1) of the

column-order permutation. The determinant is important because Inverse of matrix  $A$ , exists if  $\det(A) \neq 0$ .

For example the permanent of a (2x2) matrix  $A = \begin{bmatrix} a & b \\ c & d \end{bmatrix}$  is

$$\text{per}(A) = ad - bc$$

***Properties of determinants:***

- $\det(A^T) = \det(A)$
- $\det(cA) = c^n \det(A)$
- $\det(A) \neq 0$  if  $\text{INV}(A)$  exists
- Multiplying any column of a matrix by  $c$  multiplies its determinant by  $c$ .
- $\det(A^k) = (\det(A))^k$ ,  $k$  must be positive if  $\det(A) = 0$ .
- Interchanging any pair of columns of a matrix multiplies its determinant by  $-1$ .

## Appendix B

### B.1 Full form of permanent

The appendix shows the detailed expression of VPQF with reference to the compact form written in the expression (3.2), and is given below

$$\text{VPQF} = \text{Per}(\text{VPQM}) =$$

$$\begin{aligned} & S_1 S_2 S_3 S_4 S_5 S_6 + [(e_{13} e_{31}) S_2 S_4 S_5 S_6 + (e_{15} e_{51}) S_2 S_3 S_4 S_6 + (e_{16} e_{61}) S_2 S_3 S_4 S_6 + (e_{23} e_{32}) S_1 S_4 S_5 S_6 \\ & + (e_{24} e_{42}) S_1 S_3 S_5 S_6 + (e_{34} e_{43}) S_1 S_2 S_5 S_6 + (e_{36} e_{63}) S_1 S_2 S_4 S_5 + (e_{45} e_{54}) S_1 S_2 S_3 S_6 + (e_{56} e_{65}) S_1 S_2 S_3 S_4] \\ & + [(e_{13} e_{36} e_{61}) S_2 S_4 S_5 + (e_{12} e_{23} e_{31}) S_4 S_5 S_6 + (e_{15} e_{56} e_{61}) S_2 S_3 S_4 + (e_{16} e_{63} e_{31}) S_2 S_4 S_5 + \\ & (e_{16} e_{65} e_{51}) S_2 S_3 S_4 + (e_{23} e_{34} e_{41}) S_1 S_5 S_6 + (e_{24} e_{45} e_{52}) S_1 S_5 S_6 + (e_{24} e_{45} e_{52}) S_1 S_3 S_6 + (e_{34} e_{46} e_{63}) S_1 S_2 S_5 \\ & + (e_{46} e_{65} e_{54}) S_1 S_2 S_3] + \{[(e_{34} e_{43})(e_{65} e_{56}) S_1 S_2 + (e_{45} e_{54})(e_{36} e_{63}) S_1 S_2 + (e_{23} e_{32})(e_{65} e_{56}) S_1 S_4 + \\ & (e_{23} e_{32})(e_{45} e_{54}) S_1 S_6 + (e_{24} e_{42})(e_{65} e_{56}) S_1 S_3 + (e_{24} e_{42})(e_{63} e_{63}) S_1 S_5 + (e_{13} e_{31})(e_{24} e_{42}) S_5 S_6 + \\ & (e_{13} e_{31})(e_{45} e_{54}) S_2 S_6 + (e_{13} e_{31})(e_{24} e_{42}) S_5 S_6 + (e_{15} e_{51})(e_{34} e_{43}) S_2 S_6 + (e_{15} e_{51})(e_{36} e_{63}) S_2 S_4 + \\ & (e_{15} e_{51})(e_{23} e_{32}) S_4 S_6 + (e_{15} e_{51})(e_{24} e_{42}) S_3 S_6 + (e_{16} e_{61})(e_{45} e_{54}) S_2 S_3 + (e_{16} e_{61})(e_{34} e_{43}) S_2 S_5 + \\ & (e_{16} e_{61})(e_{23} e_{32}) S_4 S_5 + (e_{16} e_{61})(e_{24} e_{42}) S_3 S_5] + [(e_{34} e_{45} e_{56} e_{63}) S_1 S_2 + (e_{36} e_{65} e_{56} e_{63}) S_1 S_2 + \\ & (e_{23} e_{34} e_{45} e_{52}) S_1 S_6 + (e_{23} e_{36} e_{65} e_{52}) S_1 S_4 + (e_{24} e_{46} e_{63} e_{32}) S_1 S_5 + (e_{24} e_{46} e_{65} e_{52}) S_1 S_3 + \\ & (e_{12} e_{23} e_{36} e_{61}) S_4 S_5 + (e_{12} e_{24} e_{43} e_{31}) S_5 S_6 + (e_{12} e_{24} e_{45} e_{51}) S_3 S_6 + (e_{12} e_{24} e_{46} e_{61}) S_3 S_5 + \\ & (e_{15} e_{54} e_{43} e_{31}) S_2 S_6 + (e_{15} e_{56} e_{63} e_{31}) S_2 S_4 + (e_{15} e_{54} e_{46} e_{61}) S_2 S_3 + (e_{15} e_{52} e_{23} e_{31}) S_4 S_6] \} + \\ & \{[(e_{23} e_{32})(e_{54} e_{46} e_{65}) S_1 + (e_{56} e_{65})(e_{23} e_{34} e_{42}) S_1 + (e_{56} e_{65})(e_{24} e_{43} e_{32}) S_1 + (e_{36} e_{63})(e_{24} e_{45} e_{52}) S_1 + \\ & (e_{56} e_{65})(e_{12} e_{23} e_{31}) S_4 + (e_{45} e_{54})(e_{12} e_{23} e_{31}) S_6 + (e_{13} e_{31})(e_{46} e_{65} e_{54}) S_2 + (e_{45} e_{54})(e_{13} e_{36} e_{61}) S_2 + \\ & (e_{13} e_{31})(e_{24} e_{45} e_{52}) S_6 + (e_{24} e_{42})(e_{13} e_{36} e_{61}) S_5 + (e_{34} e_{43})(e_{15} e_{56} e_{61}) S_2 + (e_{15} e_{51})(e_{63} e_{34} e_{46}) S_2 + \\ & (e_{23} e_{32})(e_{15} e_{56} e_{61}) S_4 + (e_{15} e_{51})(e_{23} e_{34} e_{42}) S_6 + (e_{15} e_{51})(e_{32} e_{24} e_{43}) S_6 + (e_{24} e_{42})(e_{15} e_{56} e_{61}) S_3 + \\ & (e_{45} e_{54})(e_{16} e_{63} e_{31}) S_2 + (e_{43} e_{34})(e_{16} e_{65} e_{51}) S_2 + (e_{23} e_{32})(e_{16} e_{65} e_{51}) S_4 + (e_{16} e_{61})(e_{23} e_{34} e_{42}) S_5 + \\ & (e_{24} e_{42})(e_{16} e_{63} e_{31}) S_5 + (e_{16} e_{61})(e_{43} e_{34} e_{24}) S_5 + (e_{24} e_{42})(e_{16} e_{65} e_{51}) S_3 + (e_{16} e_{61})(e_{52} e_{24} e_{45}) S_3] + \\ & (e_{16} e_{61})(e_{52} e_{24} e_{45}) S_3] + [(e_{23} e_{36} e_{65} e_{54} e_{42}) S_1 + (e_{23} e_{36} e_{65} e_{54} e_{42}) S_1 + (e_{23} e_{43} e_{36} e_{65} e_{52}) S_1 + \\ & (e_{12} e_{23} e_{34} e_{45} e_{51}) S_6 + (e_{12} e_{23} e_{34} e_{46} e_{61}) S_5 + (e_{12} e_{23} e_{36} e_{65} e_{51}) S_4 + (e_{12} e_{24} e_{46} e_{63} e_{31}) S_5 + \\ & (e_{12} e_{24} e_{45} e_{56} e_{61}) S_3 + (e_{12} e_{24} e_{46} e_{65} e_{51}) S_3 + (e_{12} e_{24} e_{43} e_{36} e_{61}) S_5 + (e_{13} e_{34} e_{45} e_{56} e_{61}) S_2 + \\ & (e_{13} e_{34} e_{46} e_{65} e_{51}) S_2 + (e_{13} e_{32} e_{24} e_{45} e_{51}) S_6 + (e_{13} e_{32} e_{24} e_{46} e_{61}) S_5 + (e_{15} e_{54} e_{46} e_{63} e_{31}) S_2 + \\ & (e_{15} e_{52} e_{24} e_{43} e_{31}) S_6 + (e_{15} e_{52} e_{24} e_{46} e_{61}) S_3 + (e_{15} e_{54} e_{46} e_{63} e_{31}) S_2 + (e_{15} e_{52} e_{23} e_{36} e_{61}) S_4 + \\ & (e_{15} e_{52} e_{24} e_{43} e_{31}) S_6 + (e_{16} e_{65} e_{54} e_{43} e_{31}) S_2 + (e_{16} e_{63} e_{34} e_{45} e_{51}) S_2 + (e_{16} e_{65} e_{52} e_{23} e_{31}) S_4] \} + \end{aligned}$$

$$\begin{aligned}
& \{[(e_{45}e_{54})(e_{23}e_{32})(e_{16}e_{61}) + (e_{13}e_{31})(e_{24}e_{42})(e_{56}e_{65}) + (e_{36}e_{63})(e_{24}e_{42})(e_{15}e_{51})] + \\
& [(e_{12}e_{23}e_{31})(e_{46}e_{65}e_{54}) + (e_{13}e_{36}e_{61})(e_{45}e_{52}e_{24}) + (e_{23}e_{34}e_{42})(e_{15}e_{56}e_{61}) + (e_{43}e_{32}e_{24})(e_{15}e_{56}e_{61}) + \\
& (e_{23}e_{34}e_{42})(e_{16}e_{65}e_{51}) + (e_{24}e_{45}e_{52})(e_{16}e_{63}e_{31}) + (e_{32}e_{24}e_{43})(e_{16}e_{65}e_{51})] + [(e_{45}e_{54})(e_{12}e_{23}e_{36}e_{61}) + \\
& (e_{56}e_{65})(e_{12}e_{24}e_{43}e_{31}) + (e_{36}e_{63})(e_{12}e_{24}e_{45}e_{51}) + (e_{13}e_{31})(e_{24}e_{46}e_{65}e_{51}) + (e_{24}e_{42})(e_{13}e_{36}e_{65}e_{51}) + \\
& (e_{23}e_{32})(e_{15}e_{54}e_{46}e_{61}) + (e_{24}e_{42})(e_{15}e_{56}e_{63}e_{31}) + (e_{15}e_{51})(e_{24}e_{46}e_{63}e_{31}) + (e_{16}e_{61})(e_{23}e_{34}e_{45}e_{52})] + \\
& [(e_{12}e_{23}e_{34}e_{45}e_{56}e_{61}) + (e_{12}e_{23}e_{34}e_{46}e_{65}e_{51}) + (e_{12}e_{24}e_{45}e_{56}e_{63}e_{31}) + (e_{12}e_{24}e_{43}e_{36}e_{65}e_{51}) + \\
& (e_{13}e_{32}e_{24}e_{45}e_{56}e_{61}) + (e_{13}e_{32}e_{24}e_{46}e_{65}e_{51}) + (e_{15}e_{52}e_{23}e_{34}e_{46}e_{61}) + (e_{15}e_{54}e_{42}e_{23}e_{36}e_{61}) + \\
& (e_{15}e_{52}e_{24}e_{46}e_{63}e_{31}) + (e_{15}e_{52}e_{24}e_{43}e_{36}e_{61}) + (e_{16}e_{65}e_{54}e_{42}e_{23}e_{31}) + (e_{16}e_{65}e_{52}e_{24}e_{43}e_{31}) + \\
& (e_{16}e_{63}e_{32}e_{24}e_{45}e_{51})] \} \tag{B.1}
\end{aligned}$$

## Appendix C

### C.1 SEM/EDX results of ST 17-4PH

Spectrum processing :

No peaks omitted

Processing option : All elements analyzed (Normalised)

Number of iterations = 4

Standard :

O SiO<sub>2</sub> 1-Jun-1999 12:00 AM

Mg MgO 1-Jun-1999 12:00 AM

Al Al<sub>2</sub>O<sub>3</sub> 1-Jun-1999 12:00 AM

S FeS<sub>2</sub> 1-Jun-1999 12:00 AM

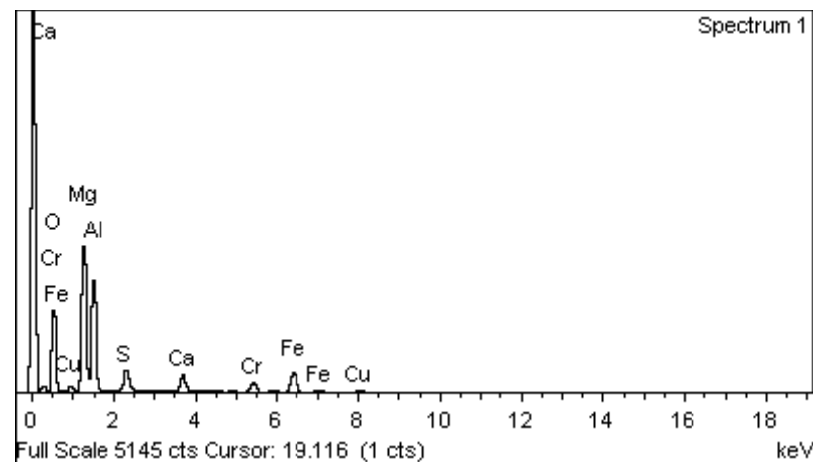
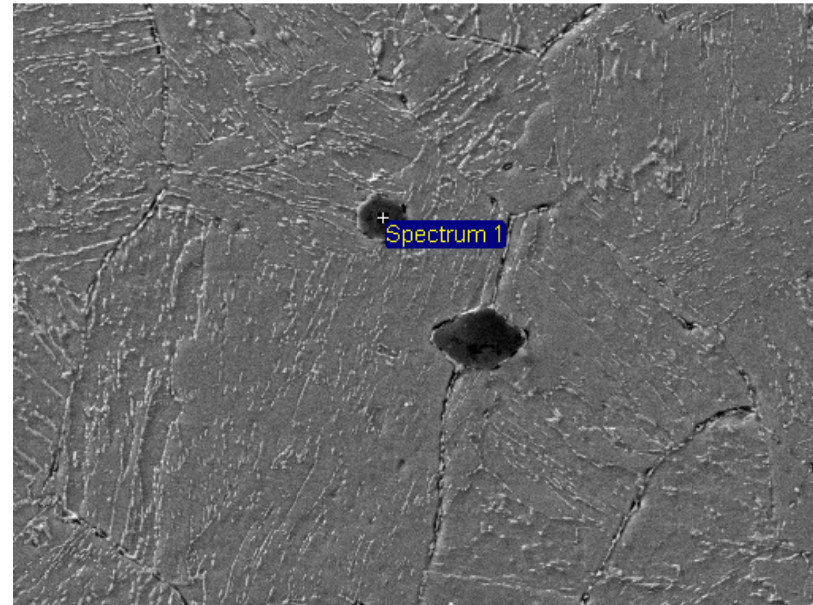
Ca Wollastonite 1-Jun-1999 12:00 AM

Cr Cr 1-Jun-1999 12:00 AM

Fe Fe 1-Jun-1999 12:00 AM

Cu Cu 1-Jun-1999 12:00 AM

Comment:





Element	Weight%	Atomic%
O K	33.27	48.74
Mg K	23.25	22.41
Al K	20.05	17.42
S K	3.52	2.57
Ca K	3.13	1.83
Cr K	3.57	1.61
Fe K	10.91	4.58
Cu K	2.30	0.85
Totals	100.00	

Spectrum processing :

No peaks omitted

Processing option : All elements analyzed (Normalised)

Number of iterations = 5

Standard :

O SiO2 1-Jun-1999 12:00 AM

Mg MgO 1-Jun-1999 12:00 AM

Al Al2O3 1-Jun-1999 12:00 AM

Si SiO2 1-Jun-1999 12:00 AM

S FeS2 1-Jun-1999 12:00 AM

Ca Wollastonite 1-Jun-1999 12:00 AM

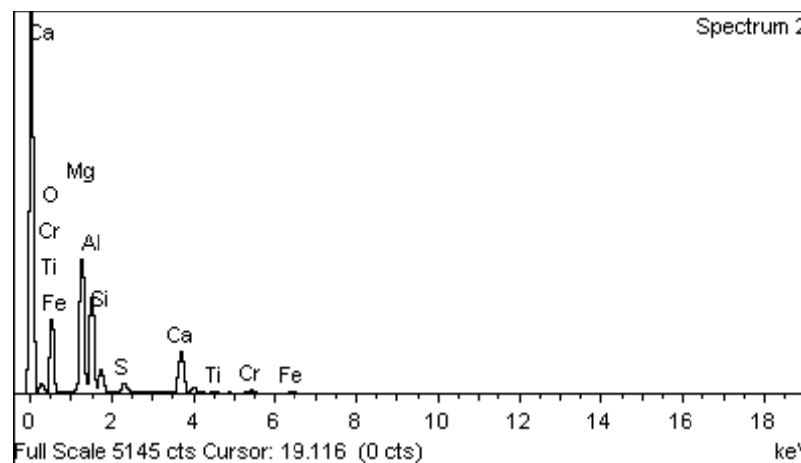
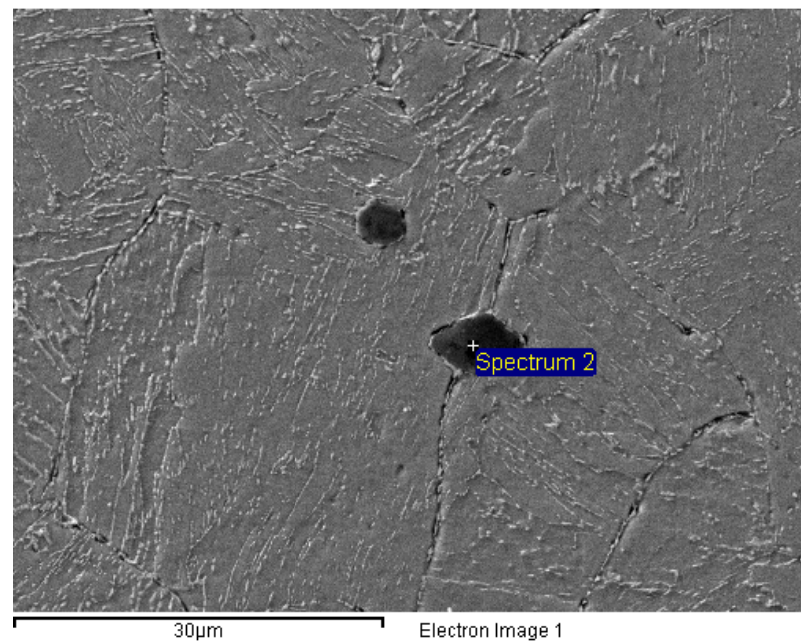
Ti Ti 1-Jun-1999 12:00 AM

Cr Cr 1-Jun-1999 12:00 AM

Fe Fe 1-Jun-1999 12:00 AM

Element	Weight%	Atomic%
O K	43.51	57.58

Comment:



---

Mg K	20.94	18.23
Al K	17.28	13.56
Si K	4.72	3.56
S K	1.69	1.12
Ca K	9.43	4.98
Ti K	0.53	0.24
Cr K	1.01	0.41
Fe K	0.88	0.33
Totals	100.00	

---

Spectrum processing :

No peaks omitted

Processing option : All elements analyzed (Normalised)

Number of iterations = 3

Standard :

Si SiO2 1-Jun-1999 12:00 AM

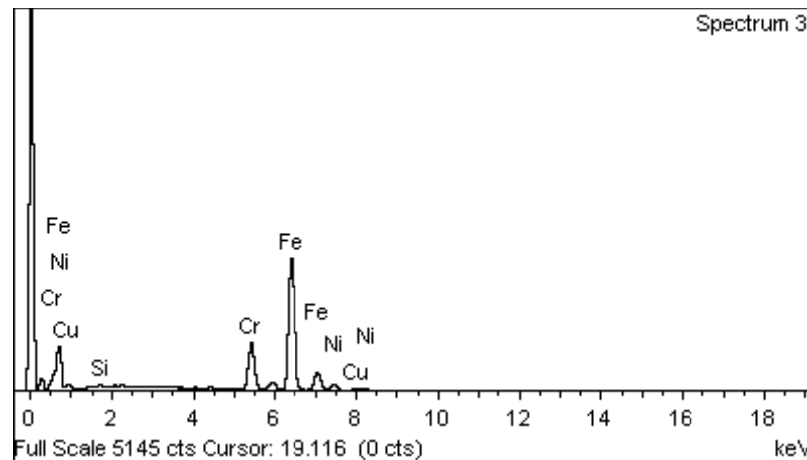
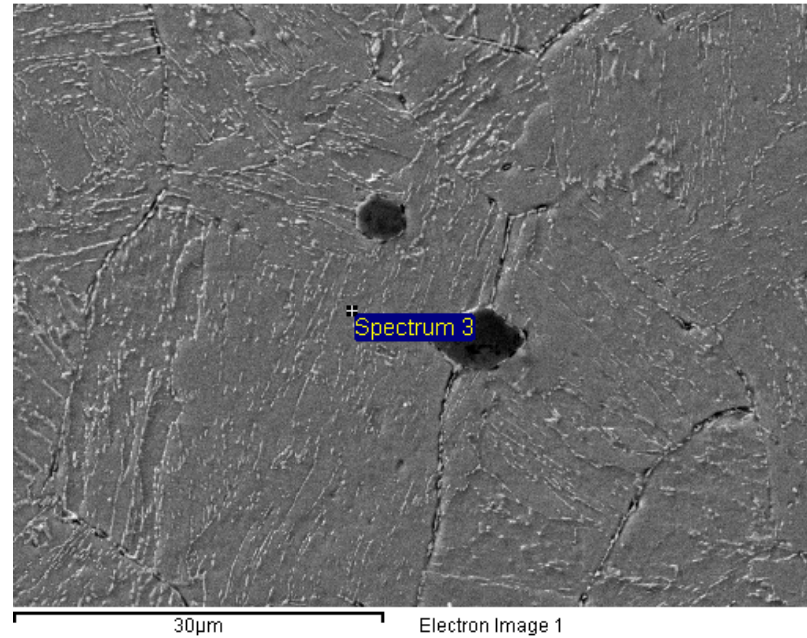
Cr Cr 1-Jun-1999 12:00 AM

Fe Fe 1-Jun-1999 12:00 AM

Ni Ni 1-Jun-1999 12:00 AM

Cu Cu 1-Jun-1999 12:00 AM

Element	Weight%	Atomic%
Si K	0.59	1.15
Cr K	16.39	17.39
Fe K	75.55	74.64
Ni K	4.58	4.30
Cu K	2.89	2.51
Totals	100.00	



Comment:

Spectrum processing :

Peak possibly omitted : 1.740 keV

Processing option : All elements analyzed (Normalised)

Number of iterations = 3

Standard :

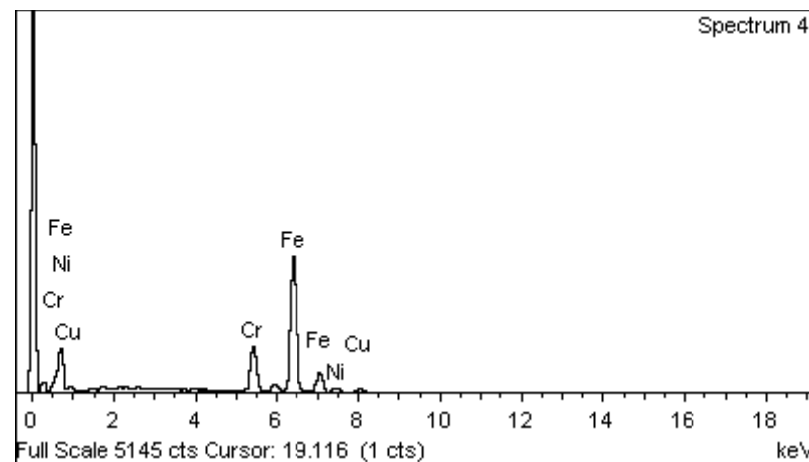
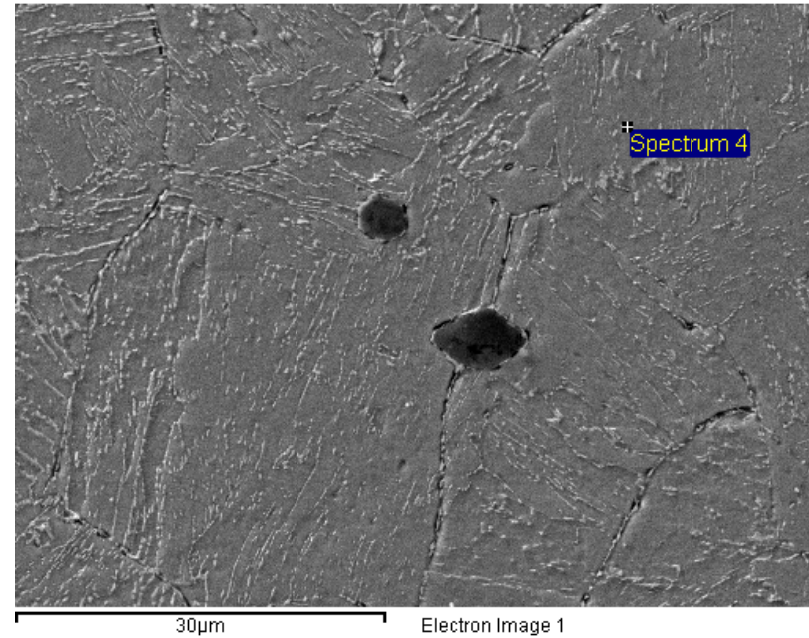
Cr Cr 1-Jun-1999 12:00 AM

Fe Fe 1-Jun-1999 12:00 AM

Ni Ni 1-Jun-1999 12:00 AM

Cu Cu 1-Jun-1999 12:00 AM

Element	Weight%	Atomic%
Cr K	15.83	16.91
Fe K	76.84	76.40
Ni K	4.01	3.79
Cu K	3.32	2.90
Totals	100.00	



Comment:

Spectrum processing :

Peak possibly omitted : 1.740 keV

Processing option : All elements analyzed (Normalised)

Number of iterations = 3

Standard :

C CaCO3 1-Jun-1999 12:00 AM

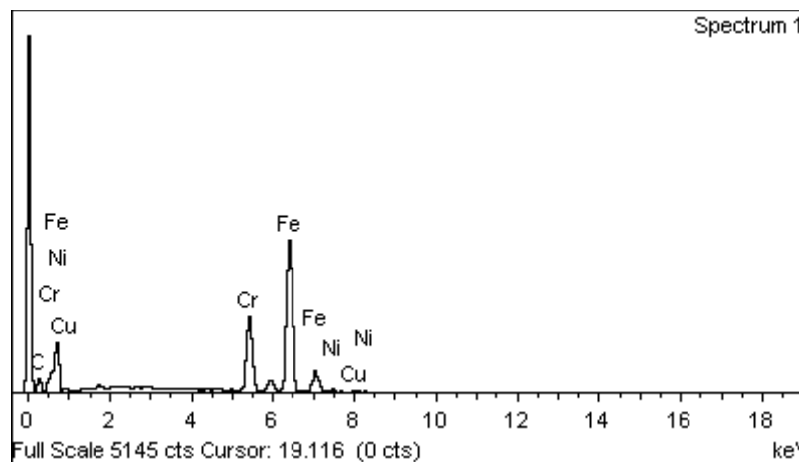
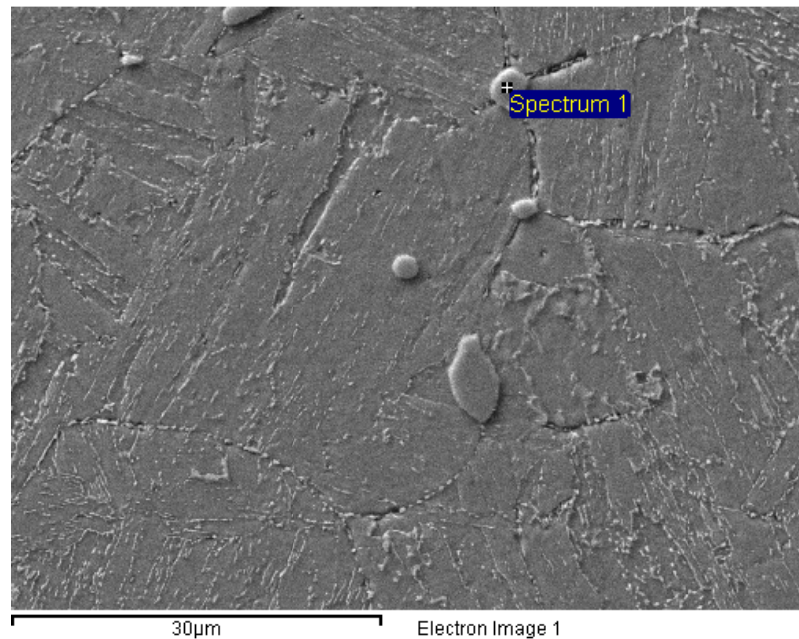
Cr Cr 1-Jun-1999 12:00 AM

Fe Fe 1-Jun-1999 12:00 AM

Ni Ni 1-Jun-1999 12:00 AM

Cu Cu 1-Jun-1999 12:00 AM

Element	Weight%	Atomic%
C K	14.20	43.16
Cr K	19.08	13.39
Fe K	63.78	41.68
Ni K	1.52	0.95
Cu K	1.42	0.81
Totals	100.00	



Comment:

Spectrum processing :

No peaks omitted

Processing option : All elements analyzed (Normalised)

Number of iterations = 3

Standard :

C CaCO3 1-Jun-1999 12:00 AM

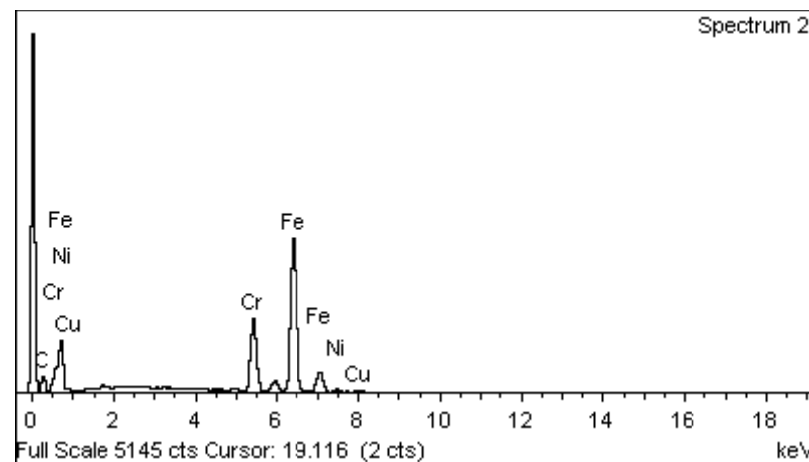
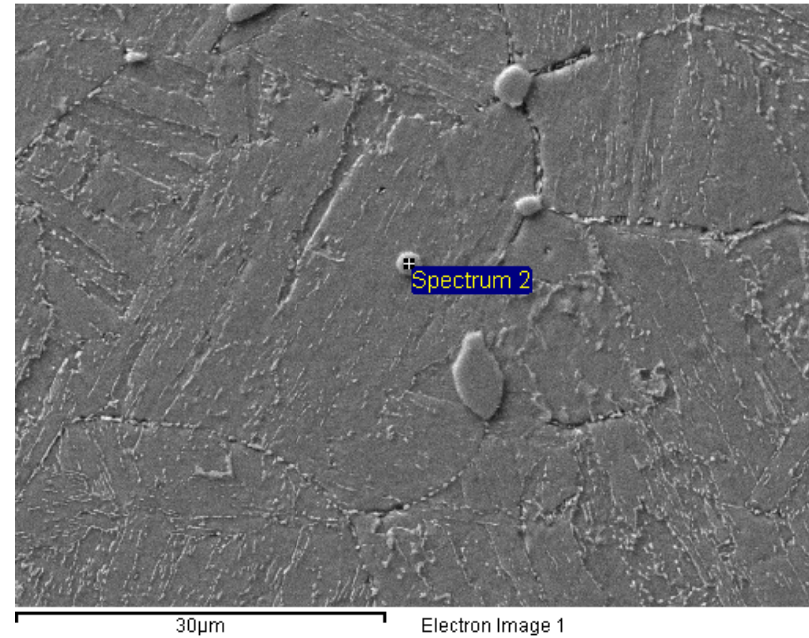
Cr Cr 1-Jun-1999 12:00 AM

Fe Fe 1-Jun-1999 12:00 AM

Ni Ni 1-Jun-1999 12:00 AM

Cu Cu 1-Jun-1999 12:00 AM

Element	Weight%	Atomic%
C K	14.72	44.19
Cr K	18.53	12.84
Fe K	64.39	41.56
Ni K	1.27	0.78
Cu K	1.10	0.62
Totals	100.00	



Comment:

Spectrum processing :

No peaks omitted

Processing option : All elements analyzed (Normalised)

Number of iterations = 3

Standard :

C CaCO3 1-Jun-1999 12:00 AM

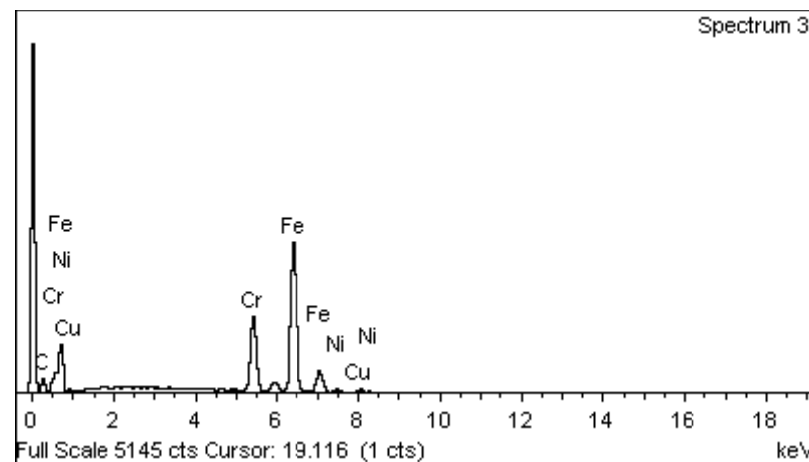
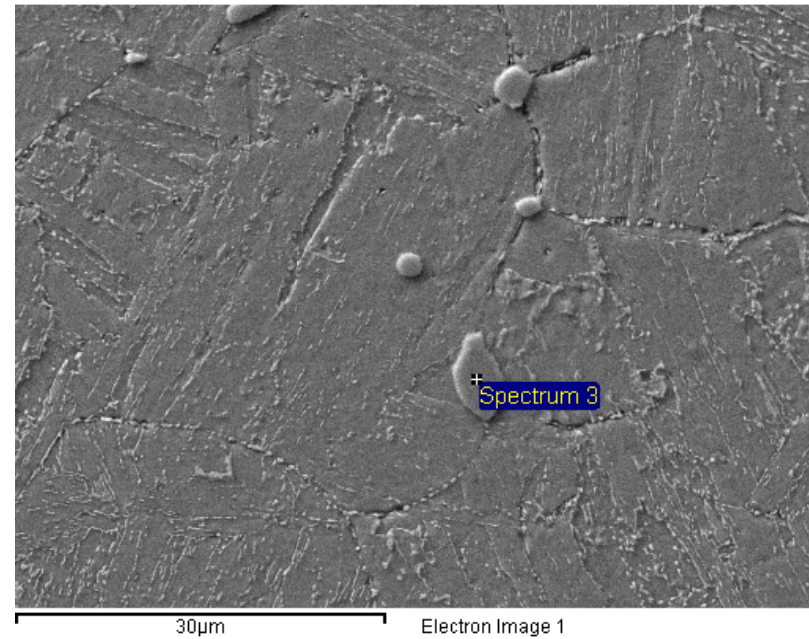
Cr Cr 1-Jun-1999 12:00 AM

Fe Fe 1-Jun-1999 12:00 AM

Ni Ni 1-Jun-1999 12:00 AM

Cu Cu 1-Jun-1999 12:00 AM

Element	Weight%	Atomic%
C K	12.86	40.38
Cr K	19.35	14.03
Fe K	64.20	43.36
Ni K	1.81	1.16
Cu K	1.79	1.07
Totals	100.00	



Comment:



Spectrum processing :

Peak possibly omitted : 1.740 keV

Processing option : All elements analyzed (Normalised)

Number of iterations = 3

Standard :

C CaCO3 1-Jun-1999 12:00 AM

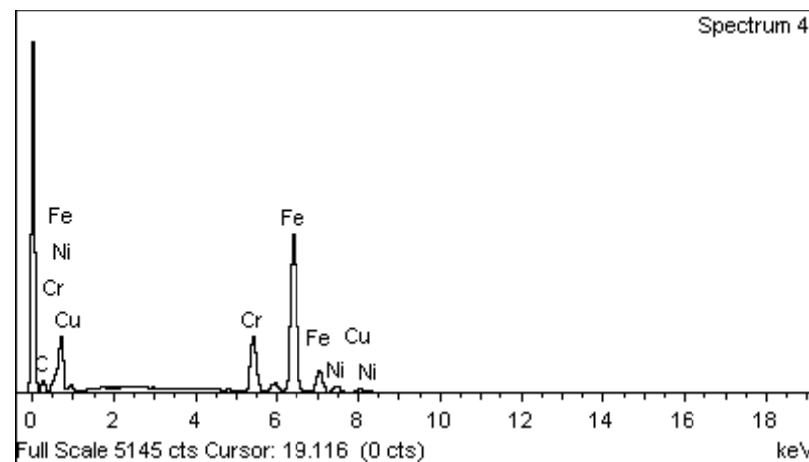
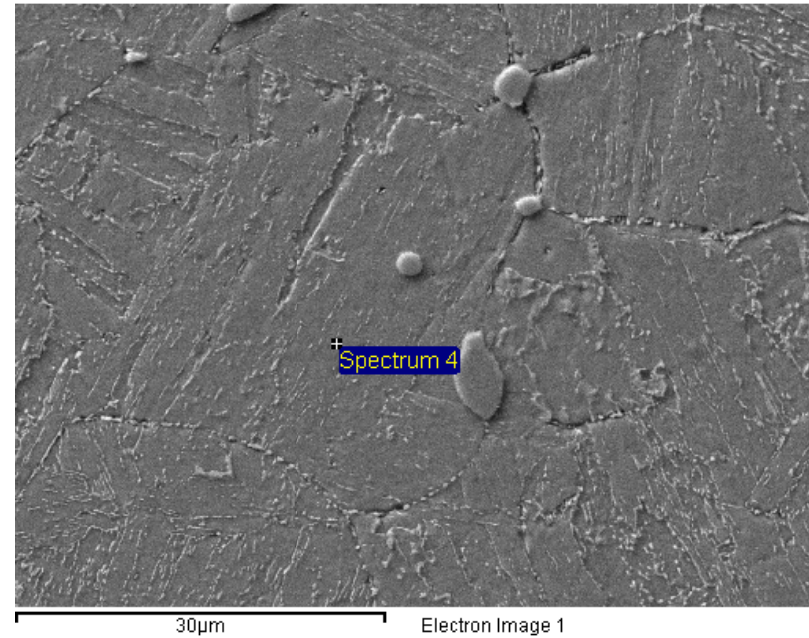
Cr Cr 1-Jun-1999 12:00 AM

Fe Fe 1-Jun-1999 12:00 AM

Ni Ni 1-Jun-1999 12:00 AM

Cu Cu 1-Jun-1999 12:00 AM

Element	Weight%	Atomic%
C K	11.84	38.29
Cr K	14.18	10.59
Fe K	67.70	47.10
Ni K	3.55	2.35
Cu K	2.74	1.68
Totals	100.00	



Comment:

Spectrum processing :

No peaks omitted

Processing option : All elements analyzed (Normalised)

Number of iterations = 3

Standard :

C CaCO3 1-Jun-1999 12:00 AM

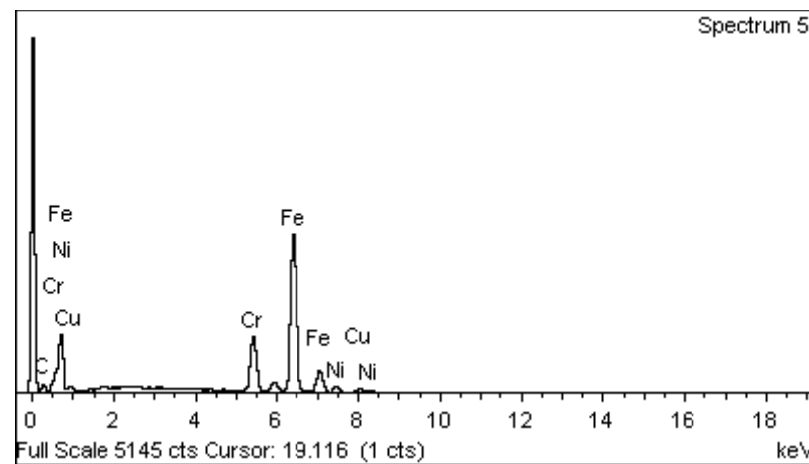
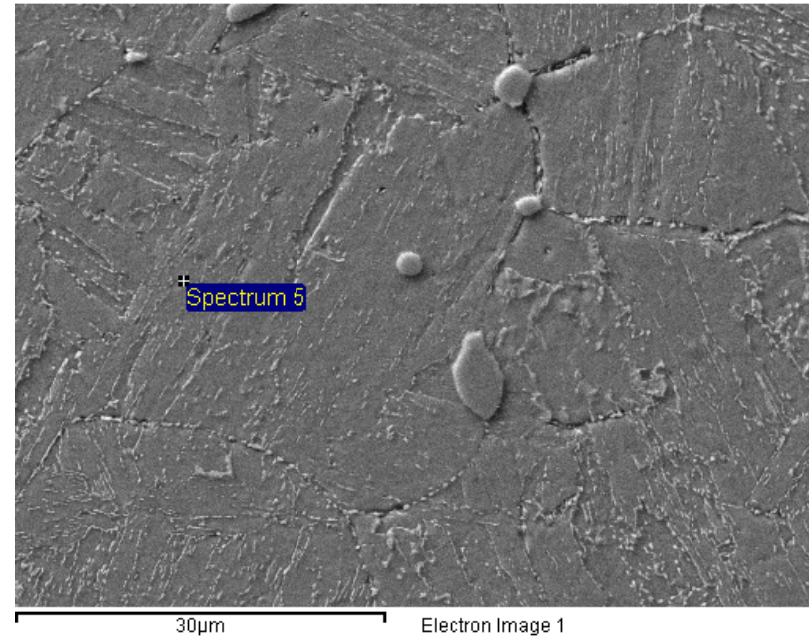
Cr Cr 1-Jun-1999 12:00 AM

Fe Fe 1-Jun-1999 12:00 AM

Ni Ni 1-Jun-1999 12:00 AM

Cu Cu 1-Jun-1999 12:00 AM

Element	Weight%	Atomic%
C K	9.78	33.40
Cr K	14.64	11.55
Fe K	68.43	50.24
Ni K	3.86	2.70
Cu K	3.28	2.12
Totals	100.00	



Comment:

Spectrum processing :

No peaks omitted

Processing option : All elements analyzed (Normalised)

Number of iterations = 3

Standard :

C CaCO3 1-Jun-1999 12:00 AM

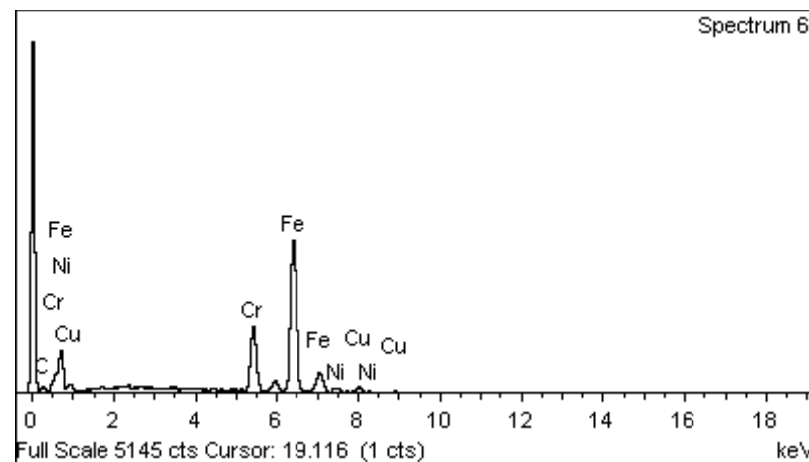
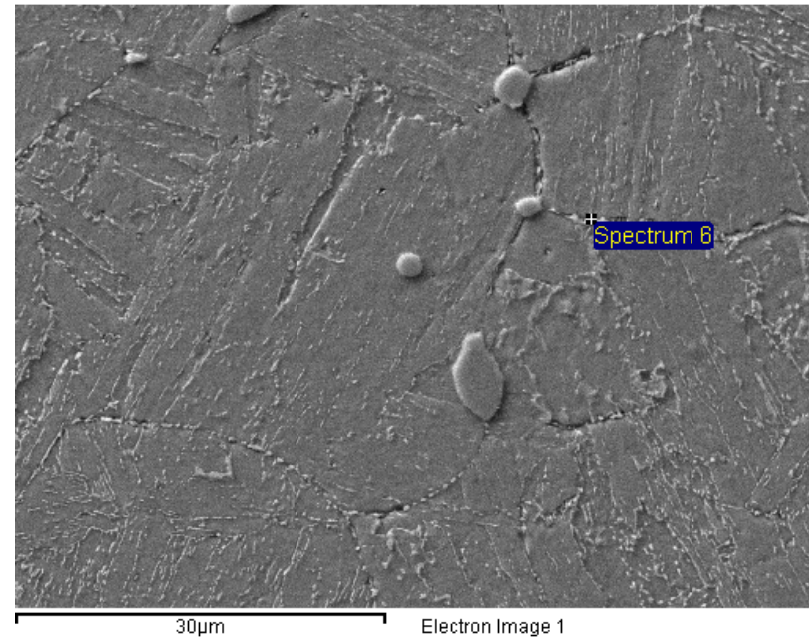
Cr Cr 1-Jun-1999 12:00 AM

Fe Fe 1-Jun-1999 12:00 AM

Ni Ni 1-Jun-1999 12:00 AM

Cu Cu 1-Jun-1999 12:00 AM

Element	Weight%	Atomic%
C K	7.13	26.18
Cr K	17.15	14.55
Fe K	68.74	54.27
Ni K	2.94	2.21
Cu K	4.04	2.80
Totals	100.00	



Comment:

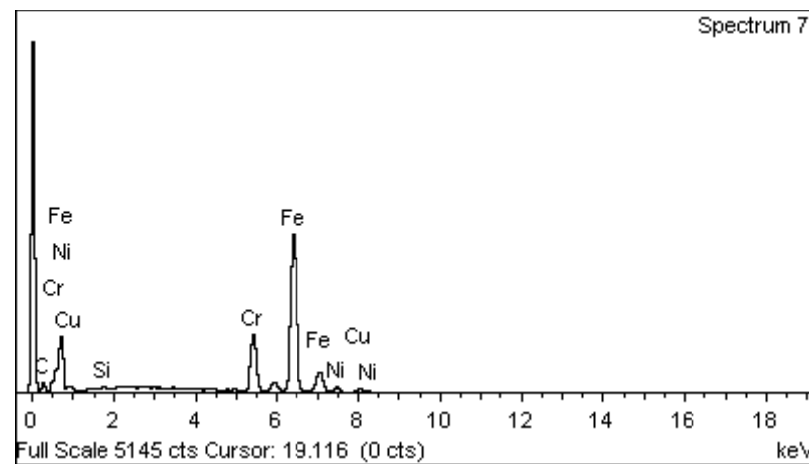
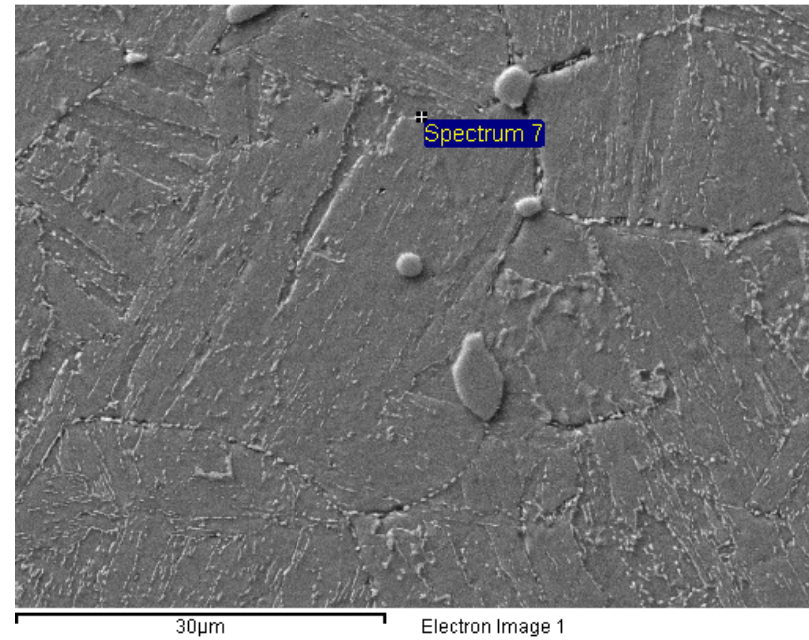
Spectrum processing :

No peaks omitted

Processing option : All elements analyzed (Normalised)

Number of iterations = 3

Element	Weight%	Atomic%
C K	10.82	35.80
Si K	0.44	0.62
Cr K	14.91	11.39
Fe K	67.95	48.33
Ni K	3.55	2.40
Cu K	2.33	1.46
Totals	100.00	



Comment:

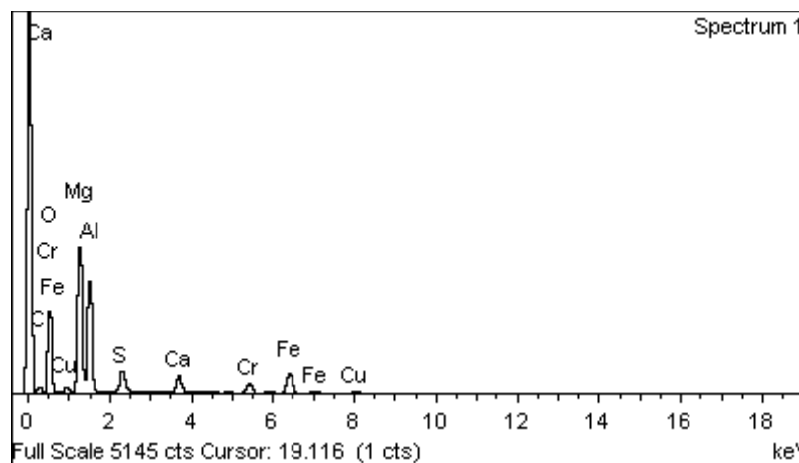
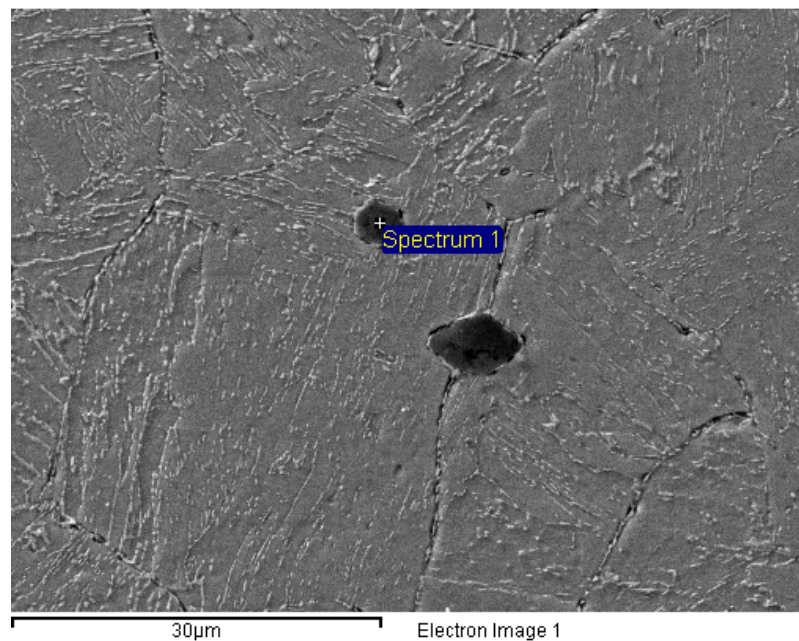
Spectrum processing :

No peaks omitted

Processing option : All elements analyzed (Normalised)

Number of iterations = 5

Element	Weight%	Atomic%
C K	11.35	19.59
O K	32.93	42.67
Mg K	19.59	16.70
Al K	16.22	12.46
S K	2.88	1.86
Ca K	2.64	1.37
Cr K	3.06	1.22
Fe K	9.36	3.48
Cu K	1.97	0.64
Totals	100.00	



Comment:

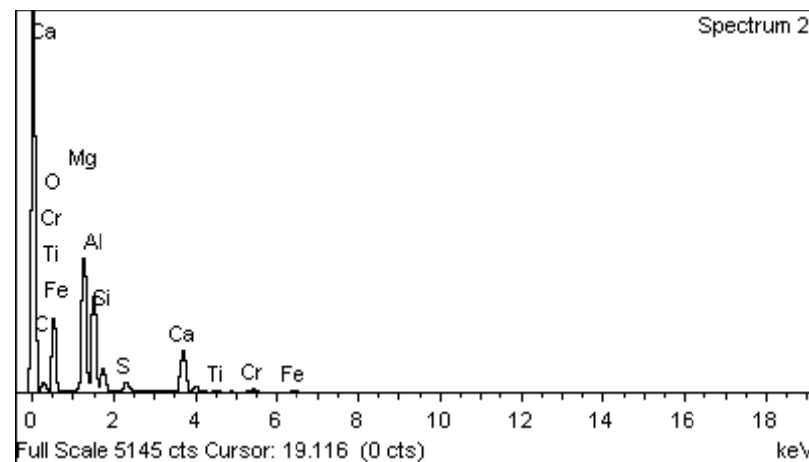
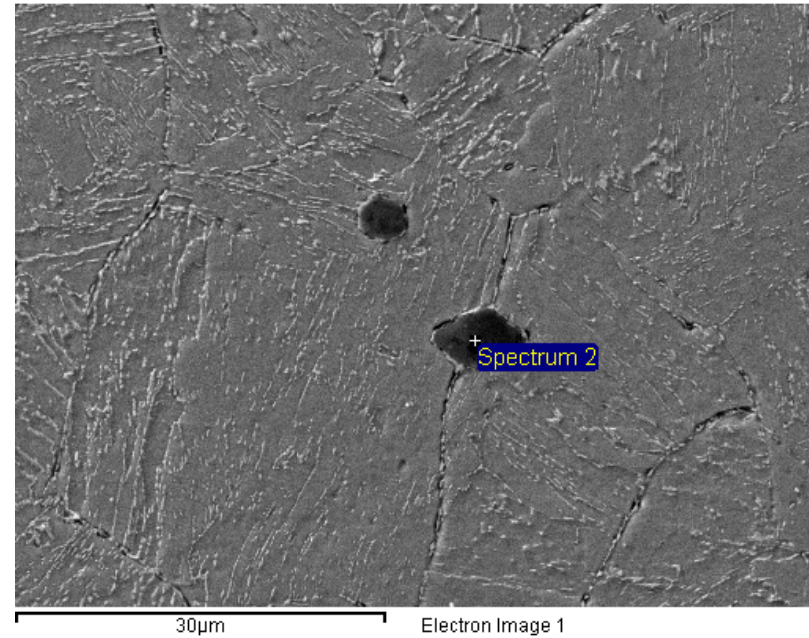
Spectrum processing :

No peaks omitted

Processing option : All elements analyzed (Normalised)

Number of iterations = 5

Element	Weight%	Atomic%
C K	17.87	27.02
O K	40.85	46.37
Mg K	15.86	11.85
Al K	12.19	8.21
Si K	3.21	2.08
S K	1.19	0.68
Ca K	7.00	3.17
Ti K	0.40	0.15
Cr K	0.76	0.27
Fe K	0.66	0.22
Totals	100.00	



Comment:

Spectrum processing : No peaks omitted

Processing option : All elements analyzed (Normalised)

Number of iterations = 3

Standard :

C CaCO3 1-Jun-1999 12:00 AM

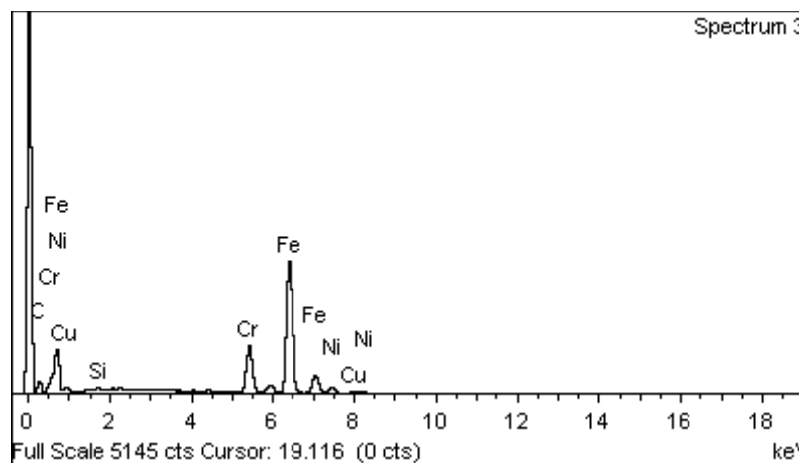
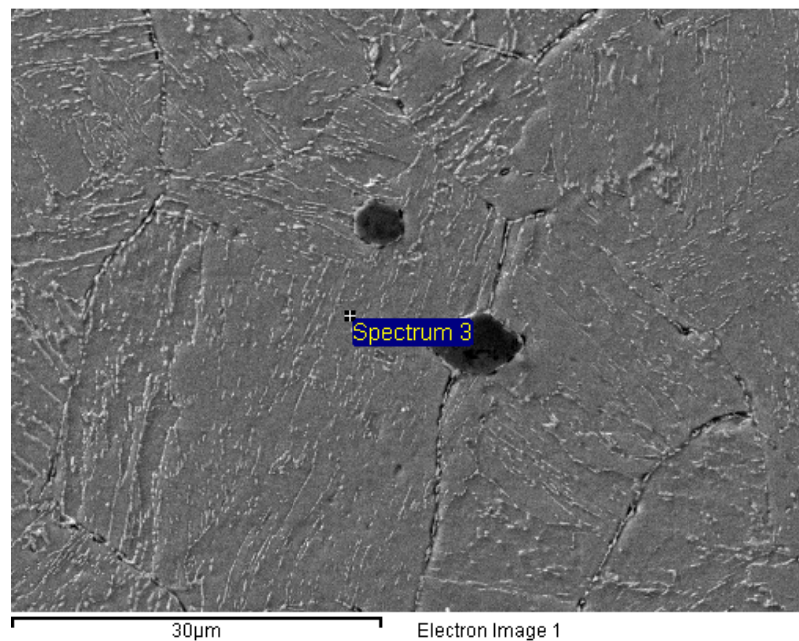
Si SiO2 1-Jun-1999 12:00 AM

Cr Cr 1-Jun-1999 12:00 AM

Fe Fe 1-Jun-1999 12:00 AM

Ni Ni 1-Jun-1999 12:00 AM Cu Cu 1-Jun-1999 12:00 AM

Element	Weight%	Atomic%
C K	14.85	44.48
Si K	0.46	0.58
Cr K	14.03	9.71
Fe K	64.37	41.48
Ni K	3.85	2.36
Cu K	2.45	1.39
Totals	100.00	



Comment:

Spectrum processing :

Peak possibly omitted : 1.740 keV

Processing option : All elements analyzed (Normalised)

Number of iterations = 3

Standard :

C CaCO3 1-Jun-1999 12:00 AM

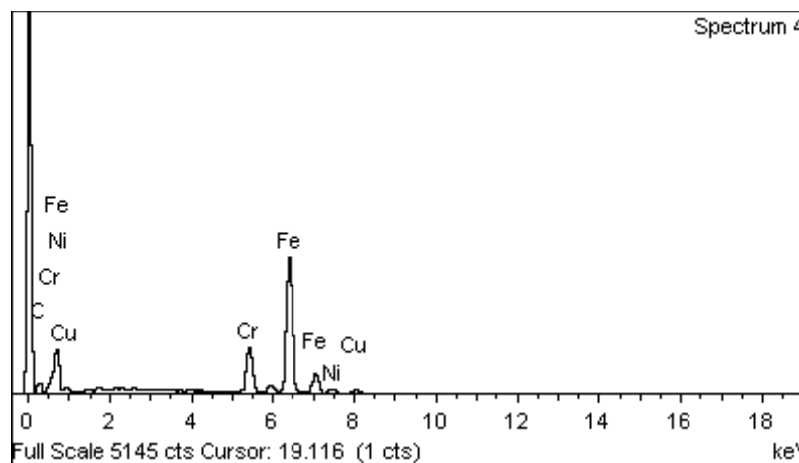
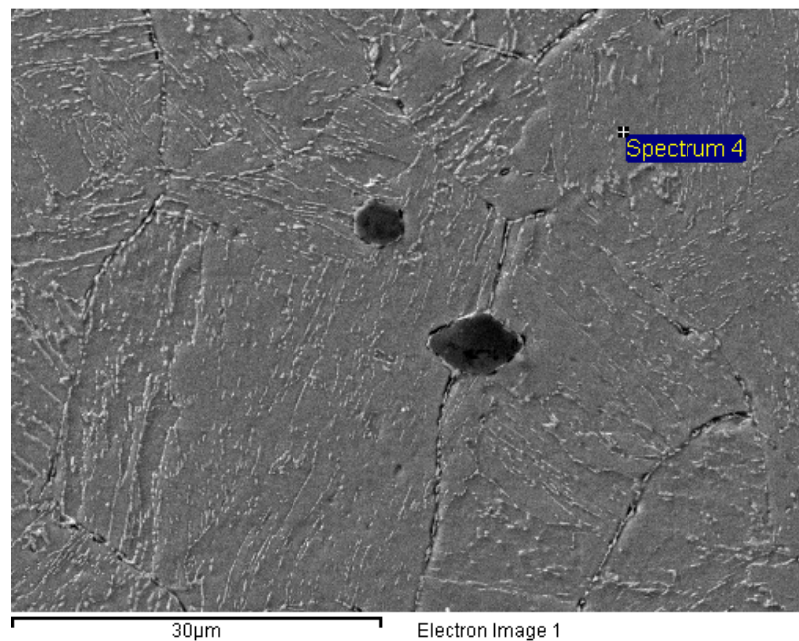
Cr Cr 1-Jun-1999 12:00 AM

Fe Fe 1-Jun-1999 12:00 AM

Ni Ni 1-Jun-1999 12:00 AM

Cu Cu 1-Jun-1999 12:00 AM

Element	Weight%	Atomic%
C K	15.17	45.26
Cr K	13.50	9.30
Fe K	65.18	41.82
Ni K	3.36	2.05
Cu K	2.79	1.57
Totals	100.00	



Comment:



## C.2 Specifications of CNC Lathe

Company: Askar microns (P) Ltd.

Product Name: Compact CNC turning center

Technical specifications

### ***Capacity***

Swing over way covers -350 mm

Admit between centre -375 mm

Maximum turning length (with chuck) -275 mm

Maximum turning diameter -220 mm

### ***Job Holding***

Hydraulic chuck

– Standard- 135 mm (5")

-Optional 165 mm (6")

### ***Slides***

Cross travel X-axis- 130 mm

Longitudinal travel Z-axis 375 mm

Rapid rate X-axis 24 m/min

Z-axis 24 m/min

Ball screw X-axis (dia x pitch) 32 x 10 mm

Z-axis (dia x pitch) 32 x 10 mm

LM guide ways X-axis 35 HSR

Z-axis 35 HSR

### ***Main spindle***

Spindle motor power 7/9 or 5.5/7.5 kW

Spindle bore diameter 40 mm

Spindle front bearing diameter 80 mm

Spindle nose A2-5

Maximum bar capacity	27 mm
Spindle speed - Standard	4000 rpm
- Optional	5000 rpm

***Turret***

No. of stations	Nos.	8
Maximum boring bar capacity		32 mm
Tool cross section		25 x 25 mm

***Tail stock***

Quill diameter	60 mm
Quill stroke	60 mm
Thrust (maximum)	350 Kgf
Quill taper	MT 3

***Coolant***

Tank capacity	100 ltrs
Pump motor capacity	0.25 kW

***Machine size***

Weight (approximate)	3300 kgs
Dimension (L x B x H)	1730 x 2000 x 1500 mm

***Accuracy***

Positioning	+ 0.010 mm
Repeatability	+ 0.003 mm

## Publication based on Present work

1. Kiran C.P, and Agrawal V.P. (2009): Structural modeling and analysis of a mechatronic system: A Graph theoretic Approach, *Journal of mechatronics and intelligent manufacturing*, Vol.1, pp. 24-48
2. Kiran C.P, Shibu Clement and Agrawal V.P.( 2011): X-abilities based concurrent design and evaluation of mechatronic system, *Journal of mechatronics and intelligent manufacturing*, Vol.2, pp.115-127.
3. Kiran C.P., Shibu Clement and Agrawal V.P. (2011): Design for x-abilities of a mechatronic system-a concurrent engineering and graph theoretic approach, *Concurrent engineering- research with applications*, Vol.19, pp.55-69. (**Impact factor: 0.959**)
4. Kiran C.P., Shibu Clement and Agrawal V.P. (2011): Coding, evaluation and selection of a mechatronic system, *Expert system with application*, Vol.38, pp.9704-9712. (**Impact factor: 2.908**)
5. Kiran C.P., Shibu Clement and Agrawal V.P. (2012): Quality modeling and analysis of a mechatronic system, *International Journal of Industrial Systems*, Vol.12, pp.1-28.
6. Kiran C.P., Shibu Clement and Agrawal V.P. (2010): Quality analysis of a mechatronic system using colored graph and Boolean function, National Systems Conference, 10-12 Dec, Suratkal, India, pp. 58-59.
7. Kiran C.P., Shibu Clement and Agrawal V.P. (2011) Mechatronic system reliability modeling and analysis, *International Journal of Reliability and Safety* (under review) Inderscience publishers.
8. Kiran C.P., Shibu Clement and Aneet S.R. (2012): Experimental investigation for surface quality of turbine blade material, *All India Manufacturing Technology, Design Research, AIMTDR 2012* (Abstract accepted).
9. Kiran C.P. and Shibu Clement (2012): Experimental investigation and comparison of surface quality of turbine blade materials for optimal parameters combination of CNC turning. (Under preparation)

## **Brief Biography of the Candidate**

**C.Phaneendra Kiran** is currently serving as Lecturer in Department of mechanical engineering at BITS-Pilani, K.K. Birla Goa campus, Goa. He did his Bachelor degree in Mechanical Engineering from Jawaharlal Nehru Technological University, Hyderabad, India in 2001. During his Bachelor degree he did a three weeks project at Fachhochschule Hochschule für Technik, Esslingen, Germany. He did his Master of Engineering in Manufacturing systems engineering from BITS-Pilani, Pilani Campus, Pilani, India in 2004. During his M.E., he did 6 months practice school at General Motors, Halol, Gurat. In 2004, he chose BITS-Pilani, K.K. Birla Goa campus, Goa to continue his academic pursuit by working towards his PhD. Degree.

He is having eight years of teaching experience. He has taught various courses in Mechanical engineering at BITS-Pilani, K.K. Birla Goa campus, Goa, since 2004. He conducted Practice school program during summer 2005. He was a session chair for one of the IEEE conferences. Also, he has been actively involved in the course and lab development at BITS. He published research articles in various international journals of repute.

## **Brief Biography of the Supervisor**

**Shibu Clement** is working as Assistant Professor of Mechanical Engineering Department at Birla Institute of Technology and Science, Pilani-K.K.Birla Goa Campus, Goa, India. He completed his graduation in 1991, post graduation in 1998, and PhD in 2006 from Bharathiar Univeristy, University of Kerala, and IIT Kanpur respectively. He has published around 12 papers in International journals and conferences. He has guided successfully around 60 BTech, MTech projects, and currently supervising 3 PhD theses. He has been working extensively in the areas of fluid mechanics, aerodynamics, heat transfer and systems approach.